ATMOSPHERIC ACOUSTIC GRAVITY MODES AT FREQUENCIES NEAR AND BELOW LOW FREQUENCY CUTOFF IMPOSED BY UPPER BOUNDARY CONDITIONS

by

Allan D. Pierce, Wayne A. Kinney and Christopher Y. Kapper

School of Mechanical Engineering
Georgia Institute of Technology

Contract No. F19628-74-C-0065
Project No. 7639

SCIENTIFIC REPORT NO. 1

Contract Monitor: Elisabeth F. Iliff
Terrestrial Sciences Laboratory

Prepared for

AIR FORCE CAMBRIDGE RESEARCH LABORATORIES
OFFICE OF AEROSPACE RESEARCH
UNITED STATES AIR FORCE
BEDFORD, MASSACHUSETTS 01730

ABSTRACT

Perturbation techniques are described for the computation of the imaginary part of the horizontal wave number (k_I) for modes of propagation. Numerical studies were carried out for a model atmosphere terminated by a constant sound speed (478 m/sec) half space above an altitude of 125 km. The GR_0 and GR_1 modes have lower frequency cutoffs. It was found that for frequencies less than 0.0125 radian/sec, the GR_1 mode has complex phase velocity; k_I varying from near zero up to a maximum of 3×10^{-4} with analogous results for the GR_0 mode. There is an extremely small frequency gap for each mode for which no poles in the complex k plane corresponding to that mode exist. These mark the transition from undamped propagation to damped propagation. In the complete Fourier synthesis, branch line contributions compensate for the absence of poles in these gaps. Computational procedures are described which facilitate the inclusion of the low frequency portions of these modes in the waveform synthesis.

INTRODUCTION

One of the standard mathematical problems in acoustic wave propagation is that of predicting the acoustic field at large horizontal distances from a localized source in a medium whose properties vary only with height. This problem, as well as its counterpart in electromagnetic theory, has received considerable attention in the literature,[1] is reviewed extensively in various texts[2-7], and, for the most part, may be considered to be well understood.

A typical formulation of, say, the transient propagation problem [8-9] leads (at sufficiently large horizontal distance r) to an intermediate result which may be expressed as a double Fourier integration over angular frequency ω and horizontal wave number k; i.e. for, say, the acoustic pressure, one has

$$p = S(r)\ \mathrm{Re}\left\{\int_0^\infty \hat{f}(\omega)e^{-i\omega t}\int_{-\infty}^{\infty}[Q/D(\omega,k)]e^{ikr}\ dk d\omega\right\} \tag{1}$$

Here S(r) is a geometrical spreading factor, $1/\sqrt{r}$ for horizontally stratified media, $1/[a_e \sin(r/a_e)]^{1/2}$ if the earth curvature (a_e=radius of earth) is to be approximately taken into account. The quantity $\hat{f}(\omega)$ is a Fourier transform of some function characterizing the time dependence of the source; $Q(\omega,k,z,z_o)$ is a function of receiver and source heights z and z_o as well as of ω and k, possibly also of horizontal direction of propagation if, say, winds are included in the formulation, but, in any event, should have no poles in the complex k plane for given real positive ω, and given z and z_o. The denominator $D(\omega,k)$ is independent of z and z_o, may be zero for certain values $k_n(\omega)$ of k, and is termed the <u>eigenmode dispersion function</u>.

Typically, in order to uniquely specify both Q and $D(\omega,k)$ for all complex values of k (given ω real and positive), branch points must be identified and branch cuts must be placed in the complex k plane. The general rule may be taken to be that no branch cut should cross the real axis, and, if a branch point should lie on the real axis (when ω is positive real), the branch cut either extends into the upper or lower half plane depending on whether the branch point moves up or down when ω is given a small positive imaginary part. The integration contour for the k integration goes nominally along the real axis but skirts below or above (see Fig. 1a) those poles lying on the real axis which move up or down, respectively, when ω is given a small positive imaginary part. The placing of the branch cuts and the selection of the contour in this manner is one method of guaranteeing causality in the solution, or, equivalently, of guaranteeing that the solution dies out at large distances if a slight amount of damping (Rayleigh's virtual viscosity) is added in the mathematical formulation. The necessity of branch cuts only occurs if the medium is unbounded either from above or below and a choice of phases can always be made such that (given, say, that the medium is unbounded from above) Q dies out exponentially as $z \to \infty$ when ω has a small positive imaginary part and when k is real.

The so-called guided mode description of the far field waveform arises when the contour for the k integration is deformed (permissible because of Cauchy's theorem and of Jordan's lemma[10]) to one such as is sketched in Fig. 1b. The poles above the initial contour are encircled in the counterclockwise manner. There are also contour segments which encircle each branch cut lying above the real axis in the counterclockwise sense. The integrals around each pole are evaluated by Cauchy's residue theorem and one is left with a sum of residue terms plus branch line integrals. Each residue term may be considered as corresponding to a particular guided mode of propagation. The branch line contributions in some contexts are considered as corresponding to what may be termed lateral waves.[11] (The term may be unappropriate unless there is a

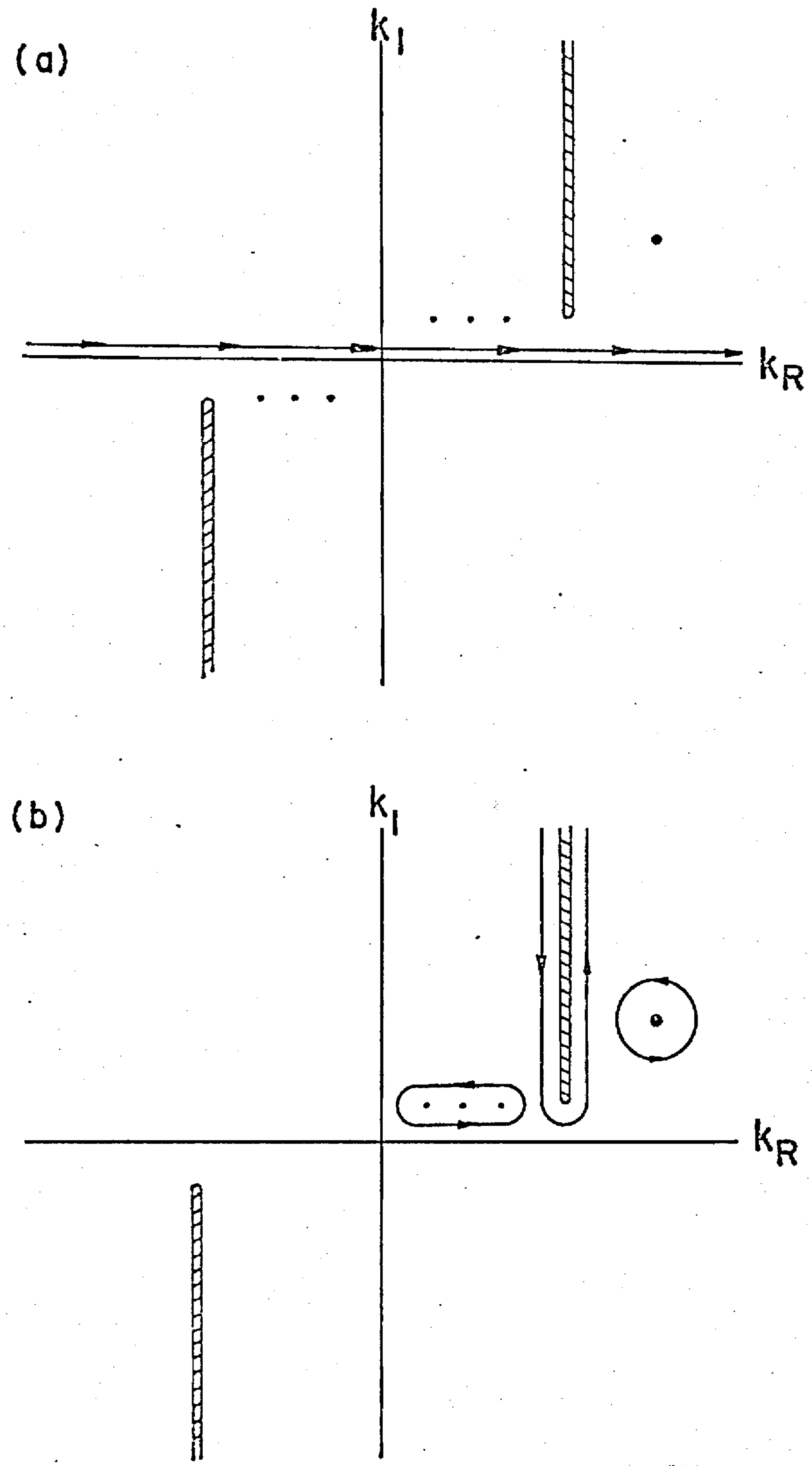

1. Contours in the complex k (wavenumber) plane for evaluation of individual frequency contributions to waveform synthesis. (a) Original contour. (b) Deformed contour.

sharply defined interface separating two types of media, such as a water-muddy bottom interface in shallow water propagation.)

In regards to the guided mode description, one type of approximation frequently made is to neglect all poles (i.e. roots $k_n(\omega)$ of $D(\omega,k)$) which are above the real axis, the argument being that the corresponding e^{ikr} factors in the residues will die out rapidly with increasing r, the bulk of the contribution at large r expected to come from the poles which lie on the real axis. In a similar manner, it is argued that the branch line contour contribution also dies out relatively rapidly (a factor of $1/r^{3/2}$ in addition to the geometrical spreading) so it too may be neglected at large r compared to the terms coming from the real roots. The net result for Eq. (1) would then be

$$p = \sum_n S(r) \int_{\omega_{Ln}}^{\omega_{Un}} A_n(\omega) \cos[\omega t - k_n(\omega) r + \phi_n(\omega)]\, d\omega \tag{2}$$

where $A_n(\omega)$ and $\phi_n(\omega)$ are defined in terms of the magnitude and phase of the residues of the integrand in Eq. (1); the $k_n(\omega)$ being the real roots of $D(\omega,k)=0$, numbered in some order with the index n=1, 2, 3, etc., and it being understood that, for fixed n, $k_n(\omega)$ should be a continuous function of ω over some range of ω from a lower limit ω_{Ln} up to an upper limit ω_{Un}. The remaining integral over ω can then be approximately evaluated by the method of stationary phase or integrated by suitable numerical methods.

In the present paper, a somewhat subtle set of circumstances intrinsic to low frequency infrasound propagation in the atmosphere is discussed for which the arguments leading to the approximation of Eq.(1) by (2) are not wholly valid, even at distances of the order of more than a quarter of the earth's circumference. We suspect that comparable circumstances may arise in other contexts, but the present discussion is, for simplicity, illustrated only by examples from atmospheric infrasound propagation.

I. INFRASOUND MODES

An atmosphere model frequently adopted for infrasound studies is one in which the sound speed c varies continuously with height z in a more or less realistic manner (Fig. 2a) but is constant ($=c_T$) for all heights above some specified height z_T. [If winds are included in the formulation, their velocities are also assumed constant in the upper half space, $z>z_T$.] Conceivably, one has some latitude in the choice of z_T and of the upper halfspace sound speed c_T, although computations of factors such as $Q(\omega,k,z,z_o)$ and $D(\omega,k)$ in Eq. (1) become more lengthy with increasing z_T. Also, it would seem that the most logical choice of c_T would be that which would realistically correspond to height z_T, so the profile c(z) would be continuous with height across z_T, as in Fig. 2a. Another conceivable choice would be one (Fig. 2b) in which $c_T \to \infty$, such that the surface of air nominally at z_T would be a free surface or pressure release surface (corresponding to the model generally adopted for the water-air interface in underwater sound studies). A somewhat intuitive premise which may be adopted is that, if the source and receiver are both near the ground and if the energy actually reaching the receiver travels via propagation modes channeled primarily in the lower atmosphere, then the actual value of the integral in Eq. (1) would be somewhat insensitive to the choices of z_T and c_T. This, however, remains to be justified in any rigorous sense, so we would be somewhat hesitant to take $c_T = \infty$ at the outset. In typical calculations performed in the past, z_T is taken as 225 km, c_T is taken as the sound speed ($\simeq$ 800 m/sec) at that altitude.

Since one is often interested in frequencies (typically corresponding to periods greater than, say, 1 to 5 minutes) at which gravitational effects are important, the formulation leading to the infrasound version of Eq. (1) is based on the fluid dynamic equations with gravitational body forces and the associated nearly exponential decrease of ambient density and pressure with height included.

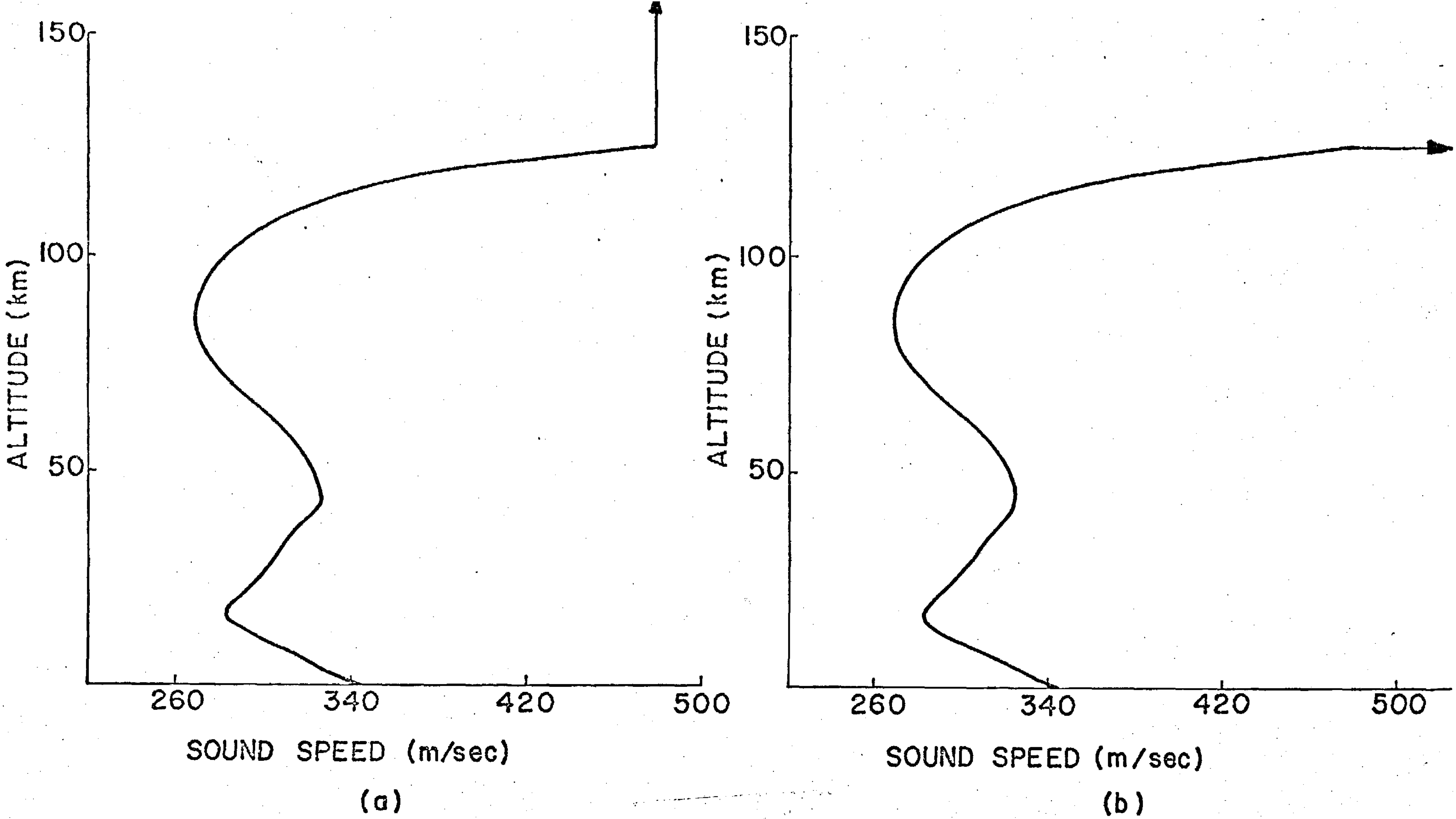

2. Idealizations of model atmospheres (altitude profiles of sound speed) used in acoustic-gravity wave studies. (a) Atmosphere terminated by an upper half space with constant sound speed. (b) Atmosphere temperature formally going to infinity at some finite altitute corresponding to a free surface ($p \simeq 0$) at that altitude.

The incorporation of gravity leads, among other effects, to a somewhat complicated dispersion relation for plane type waves in the upper half space when c_T is finite, i.e. one can have solutions of the linearized fluid dynamics equations for $z > z_T$ of the form[8,9]

$$p/\sqrt{\rho_o} = (\text{Constant})\ e^{-i\omega t}\ e^{ikx}\ e^{ik_z z} \tag{3}$$

where the vertical wave number k_z (alternately written as iG for inhomogeneous plane waves) and the horizontal wave number k are related by the dispersion relation (neglecting winds)

$$k_z^2 = -G^2 = [\omega^2 - \omega_A^2] / c^2 - [\omega^2 - \omega_B^2]\, k^2 / \omega^2 \tag{4}$$

where $\omega_A = (\gamma/2)g/c$, $\omega_B = (\gamma-1)^{\frac{1}{2}} g/c$ are two characteristic frequencies $[\omega_A > \omega_B]$ for wave propagation in an isothermal atmosphere ($g \simeq 9.8\ m/s^2$ is acceleration due to gravity, $\gamma \approx 1.4$ is specific heat ratio). Here, for brevity, the subscript T on c_T has been omitted. For given real positive ω, real k, one can have k_z^2 positive or negative (G^2 negative or positive). The values of k at which k_z^2 or G^2 go to zero turn out, as might well be expected, to be the branchpoints in the k integration in Eq. (1), i.e., synonymous with the branch points of G. Along the real axis, G is either real and positive ($e^{ik_z z}$ or e^{-Gz} dying out with increasing z) or else G is a positive or negative imaginary quantity. In the latter case, the phase of G may be either $\pi/2$ or $-\pi/2$, in accordance with the well known fact that, for acoustic-gravity waves, wavefronts may be moving obliquely downwards (negative k_z) when energy is flowing obliquely upwards. In particular, for $0 < \omega < \omega_B$, one has G real and positive for k in between the two branch points on the real axis, the phase of G is $\pi/2$ ($k_z < 0$) on the remainder of the real axis; the two branch points are, from Eq. (4), at

$$k_{BR}^{+,-}(\omega) = \pm \frac{\omega[\omega_A^2 - \omega^2]^{\frac{1}{2}}}{c[\omega_B^2 - \omega^2]^{\frac{1}{2}}} \tag{5}$$

The branch lines extend upwards and downwards from the positive and negative branch points, respectively. [See Fig. 1.]

The dispersion function $D(\omega,k)$ in the atmospheric infrasound case can be written in the general form

$$D(\omega,k) = A_{12}R_{11} - A_{11}R_{12} - R_{12}G \tag{6}$$

where R_{11} and R_{12} are elements of a transmission matrix [R], these depend on the atmosphere's properties only in the altitude range 0 to z_T, they are independent of what is assumed for the upper half space. In general, their determination requires numerical integration over height of two simultaneous ordinary differential equations (termed the <u>residual equations</u>[8,9,12] in previous literature). They do depend on ω and k (or, alternately, on ω and phase velocity v) but are free from branch cuts, they are real when ω and k are real and are finite for all finite values of ω and k. The other parameters A_{12} and A_{11} depend only on the properties of the upper half space (in addition to ω and k). Specifically, these are given (for the no wind case and with the subscript T omitted on c_T)

$$A_{11} = gk^2/\omega^2 - \gamma g/[2c^2] \tag{7a}$$

$$A_{12} = 1 - c^2k^2/\omega^2 \tag{7b}$$

One may note that, since every quantity in Eq. (6) is necessarily real when ω and k are real (with the possible exception of G), the poles lying on the real k axis (real roots of D) must be in the regions of the (ω,k) plane [or (ω,v) plane] where $G^2 > 0$. Since the integrand of Eq. (1) divided by $\sqrt{\rho_o}$ should vary with z above z_T as e^{-Gz_T} one may call the corresponding modes <u>fully ducted modes</u>. There is no net leakage of energy for such natural modes into the upper halfspace. If one considers D as a function of ω and phase velocity v_p (or simply v), where $v = \omega/k$, the locus of real roots v versus ω (dispersion curves) has (as has been found by numerical calculation) the general form sketched in Fig. 3. The nomenclature for labeling the modes (GR for gravity, S for sound) is due to Press and Harkrider. One may note from Eq. (4) that there are two "forbidden regions" in the v vs. ω plane, i.e.

$$v < c[\omega_B^2 - \omega^2]^{\frac{1}{2}} \;/\; [\omega_A^2 - \omega^2]^{\frac{1}{2}} \tag{8a}$$

for $\omega < \omega_B$ and

$$v > c[\omega^2 - \omega_B^2]^{\frac{1}{2}} \;/\; [\omega^2 - \omega_A^2]^{\frac{1}{2}} \tag{8b}$$

for $\omega > \omega_A$. Within either of these regions G would have to be imaginary and there would accordingly be no real roots for v of $D(\omega,v) = 0$. In the high frequency limit, this simply implies that the phase velocities of propagating modes are always less than the sound speed of the upper halfspace, the branch points in the k plane are simply at $\pm\, \omega/c_T$. The low frequency lower phase velocity "forbidden region" appears to be due to the incorporation of gravity effects into the formulation. However, if c_T is allowed to approach ∞, this lower left hand corner region disappears. We have done numerical studies on the effects of varying c_T on the dispersion curves. Briefly, the result is that the form of the predicted curves for GR_o and GR_1 change very little

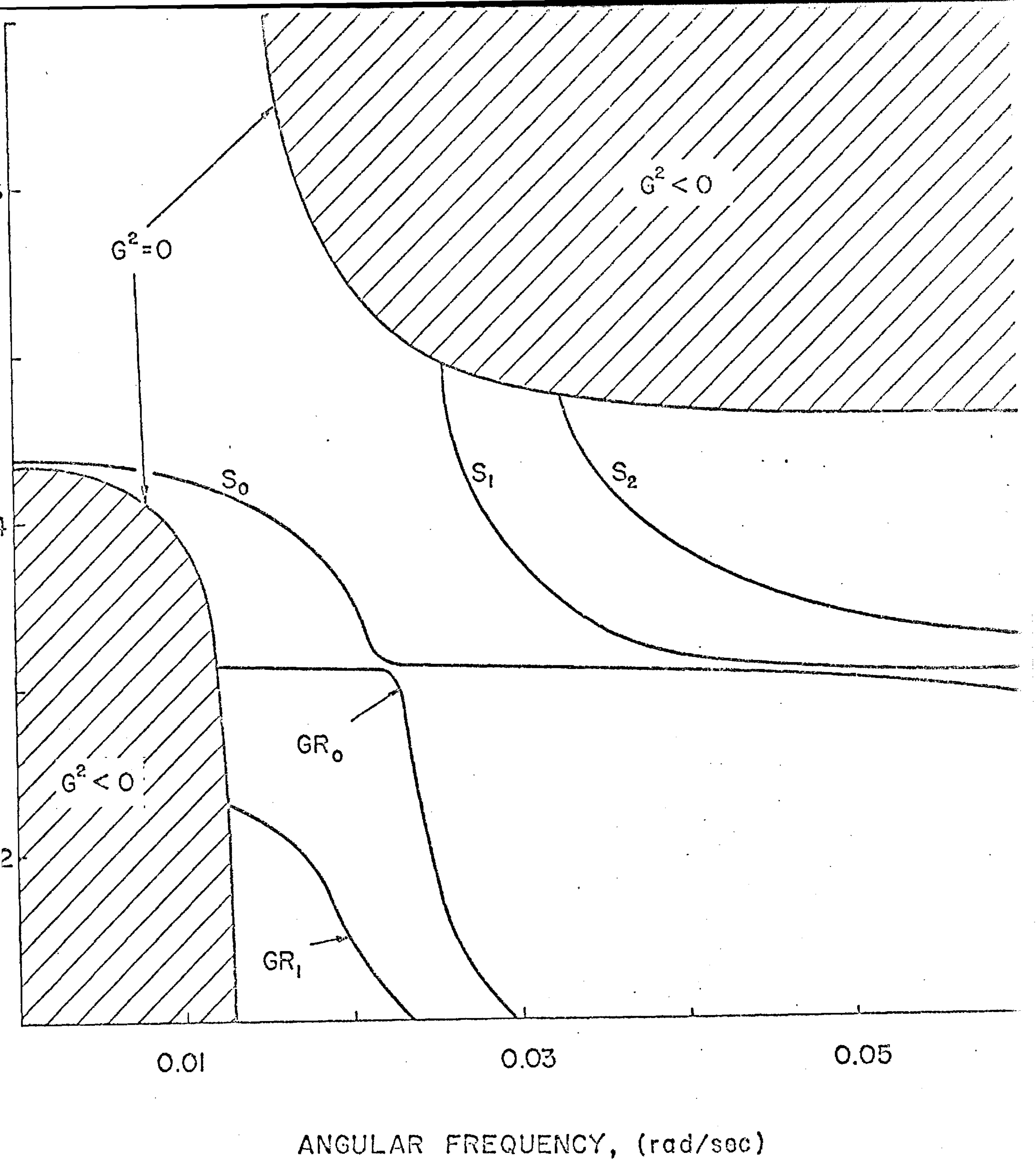

3. Numerically derived plots of phase velocity v versus angular frequency ω for infrasonic modes in a model atmosphere corresponding to Fig. 2. The labeling of modes is with the convention introduced by Press and Harkrider (J. Geophy. Res. 67, 3889-3908 (1962). The lines $G^2=0$ delimit regions of the v versus ω plane where a real root of the eigenmode dispersion function cannot be found.

with increasing c_T; the lower forbidden regions shrink insofar as frequency range is concerned and the curves extend to successively lower frequencies. Thus we see that the fully ducted modes GR_0 and GR_1 both have a lower frequency cutoff [ω_L in Eq. (2)] which depends on c_T. The larger one makes c_T, the smaller is this cutoff frequency.

We thus have the following apparent paradoxes. Given that frequencies below ω_B may be important for the synthesis of the total waveform, an apparently plausible computation scheme based on the reasoning leading to our Eq. (2) will omit much of the information conveyed by such frequencies. Also, in spite of the plausible premise that energy ducted primarily in the lower atmosphere should be insensitive to the choice for c_T, one sees that this choice governs the cutoff frequencies for certain modes and that certain important frequency ranges could conceivably be omitted entirely by a seemingly logical and proper choice for c_T. The resolution of these paradoxes would seem to lie in the nature of the approximations made in going from Eq. (1) to Eq. (2). The latter may not be as nearly correct as earlier presumed and it may be necessary to include contributions from poles off the real axis and from the branch line integrals. Even if r is undisputably large, it may be that the imaginary parts of the complex wavenumbers are sufficiently small that $|e^{ikr}|$ is still not small compared to unity. Also, a branch line integral may be appreciable in magnitude at large r if there should be a pole relatively close to the branch cut.

II. ROOTS OF DISPERSION FUNCTION

In order to understand the manner in which the solution represented by Eq. (2) should be modified in order to remove the apparent artificial low frequency cutoffs of the GR_o and GR_1 modes, we first examine the nature of the dispersion function D at points in the vicinity of a particular mode's dispersion curve. The curve $v_n(\omega)$ of phase velocity v versus ω for a given (n-th) mode is known at points to the right of the lower cutoff frequency ω_L. Given this, one can find analogous curves $v_a(\omega)$ and $v_b(\omega)$ for values of the phase velocity ω/k at which the functions $R_{11}(\omega,v)$ and $R_{12}(\omega,v)$ in Eq. (6), respectively, vanish. Since there may be more than one such curve in each case, we pick $v_a(\omega)$ and $v_b(\omega)$ such that these curves are the closest of all such curves to the curve $v_n(\omega)$ for $\omega > \omega_L$. One may note, however, that one may apparently define and identify $v_a(\omega)$ and $v_b(\omega)$ for frequencies much less than ω_L, simply from analytical continuation.

A premise which we have checked numerically (see Fig. 4) for a specific case is that the curves $v_n(\omega)$, $v_a(\omega)$, $v_b(\omega)$ defined above with reference to a particular given mode all lie substantially closer to each other than to the corresponding curves for a different mode. In retrospect, this is obvious, although it took some time for us to realize that it was so. Briefly, the argument goes that, if the mode is predominantly guided in the lower atmosphere, then there should be a decay of modal height profiles beyond some point substantially lower than z_T. Thus, both the $p/\sqrt{\rho_o}$ and $\rho_o v_z$ profiles for a guided mode would have values at z_T substantially less than their peak values at lower altitudes. The same would be true for the profiles of the auxiliary functions Φ_1 and Φ_2 which satisfy the residual equations. Consequently, if guided waves are excited, the inverse transmission matrix connecting Φ_1 and Φ_2 at the ground to those at height z_T would have to have very small [1,2] and [2,2] components.

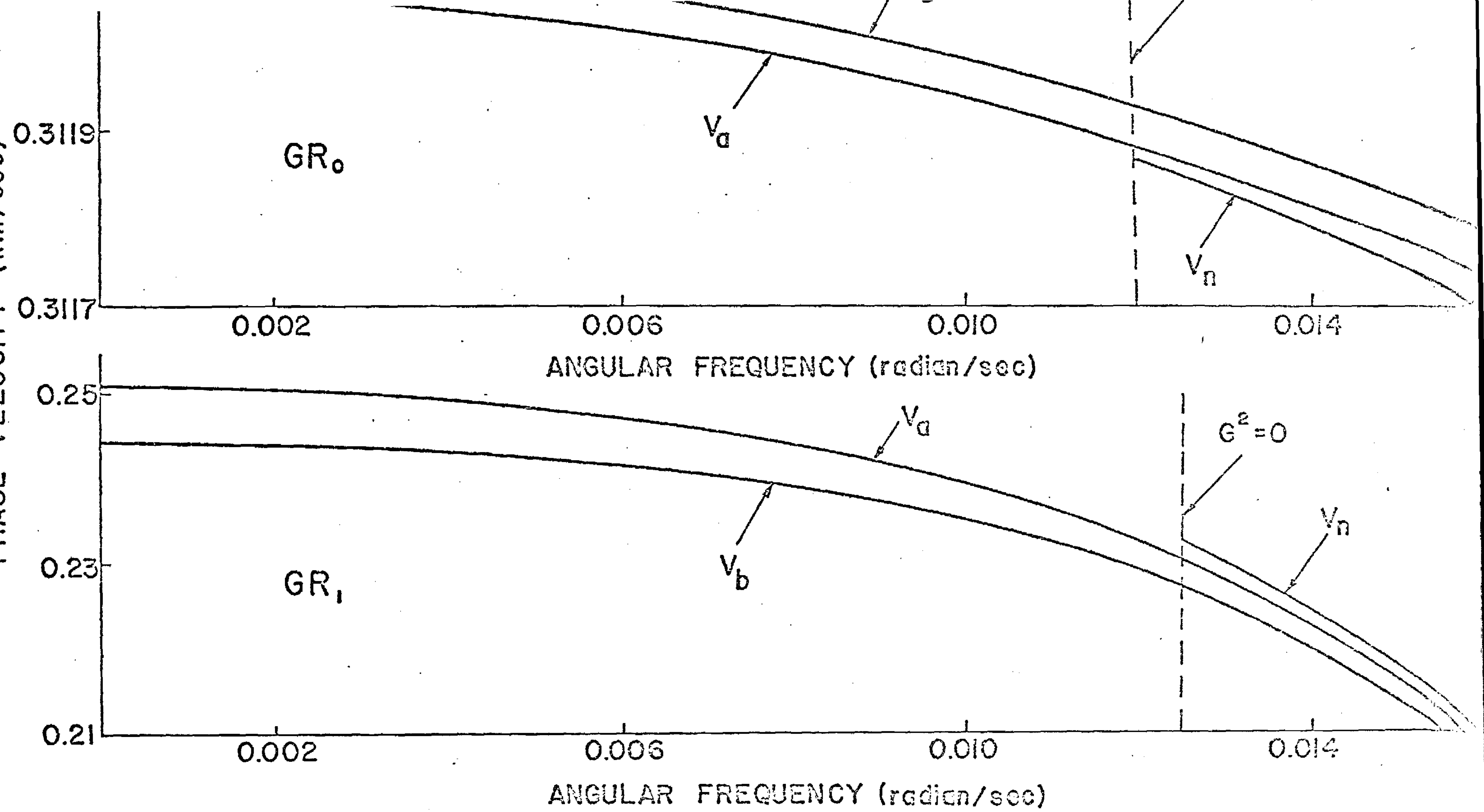

4. Curves in phase velocity (v_n, v_a, v_b) versus angular frequency (ω) plane along which $R_{11}=0$ (giving $v_a(\omega)$), $R_{12}=0$ (giving $v_b(\omega)$), and $D(\omega,k)=0$ (giving $v_n(\omega)$). Curves are shown for (a) the GR_o mode and (b) the GR_1 mode. Note the changes in scale and the relatively close spacing of curves corresponding to the same mode. The lines along which $G^2=0$ are also indicated; $v_n(\omega)$ is not a real quantity for ω values below the indicated lower cutoff frequency.

(Recall that $\Phi_1 = 0$ at the ground.) Since the transmission matrix has unit determinant, it follows that elements R_{12} and R_{11} of the transmission matrix proper [from height Z_T down to the ground and whose elements appear in Eq. (6)] have to be small.

Given the definitions $v_a(\omega)$ and $v_b(\omega)$, the dispersion relation D=0 for a single mode may be written

$$D \approx (A_{12})(\alpha)(v-v_a) - [A_{11} + G](\beta)(v-v_b) = 0 \tag{9}$$

where $\alpha = dR_{11}/dv$, $\beta = dR_{12}/dv$, evaluated at $v = v_a$ and v_b, respectively. (For simplicity, we here consider D as a function of ω and $v = \omega/k$ rather than of ω and k.) The above equation may also equivalently be written in the form

$$v = v_a + (v_a-v_b)X/[1-X] \tag{10a}$$

$$X = (\beta/\alpha)(A_{11} + G)/A_{12} \tag{10b}$$

which may be considered as a starting point for an iterative solution which in essence develops v in a power series in v_a-v_b; G may be considered as a defined function of ω,v. One starts with $v = v_a$ as the zeroth iteration, evaluates the right hand side for the value of v to find the starting point for the next iteration, etc. The considered procedure should converge provided v_a or v_b is not near a point at which G vanishes and providing G in the vicinity of v_a or v_b is not such that the variable X is close to unity. Among other limitations, the iteration scheme would be inappropriate for values of ω in the immediate vicinity of ω_L.

In regards to establishing the general trends represented by the iterative type solutions, two relatively general theorems may be of use. These (whose proof follows along lines previously used by one of the authors[13] in deriving an integral expression for group velocity) are that for real positive ω and v,

$$R_{12}\ \partial R_{11}/\partial v - R_{11}\ \partial R_{12}/\partial v > 0 \tag{11a}$$

$$R_{12}\ \partial R_{11}/\partial \omega - R_{11}\ \partial R_{12}/\partial \omega > 0 \tag{11b}$$

or, alternately, if one inserts $R_{11} = (\alpha)(v-v_a)$, $R_{12} = (\beta)(v-v_b)$, he finds

$$\alpha\beta(v_a - v_b) > 0 \tag{12a}$$

$$(v - v_b)(v - v_a)\ (\beta\alpha'-\beta'\alpha) + \beta\alpha[v_b'\ (v - v_a) - v_a'\ (v - v_b)] > 0 \tag{12b}$$

where the primes represent derivatives with respect to ω. The second of these should hold for arbitary v in the vicinity of v_a and v_b and lead, upon setting $v = v_a$, $v = v_b$, or $v = (v_a v_b' - v_a' v_b)(v_b' - v_a')$, along with the use of Eq. (12a), to

$$v_b' < 0 \tag{13a}$$

$$v_a' < 0 \tag{13b}$$

$$(\alpha/\beta)' > 0 \tag{13c}$$

Equation (12a) implies that as long as α or β do not vanish (which would seem unlikely) the two curves $v_a(\omega)$ and $v_b(\omega)$ do not intersect. If α and β have the same sign the v_a curve lies above the v_b curve; the converse is true if α and β increases with ω.

To demonstrate the general utility of the perturbation approach, a brief table of values ω, v_a, v_b, α, β, $v^{(1)}$, and v_n are given in Table I for the GR_o and GR_1 modes for the case of a U.S. Standard Atmosphere without winds terminated at a height of 125 km by a halfspace with a sound speed of 478 m/sec. Here $v^{(1)}$ is the result of the first iteration for the phase velocity and v_n is the actual numerical result obtained (only if the phase velocity is real) by explicit numerical search for roots of the eigenmode dispersion function. One may note that, for those frequencies where v_n is computed, the agreement between $v^{(1)}$ and v_n is excellent. A more detailed listing of the perturbation calculation results is given in Figs. 5a and b. The plots there give ω/k_R or the reciprocal of the real part of $1/v^{(1)}$ (i.e., ω divided by the real part of the horizontal wave number k) and the imaginary part k_I of $k = \omega/v$ versus angular frequency. Note that k_I is zero above the corresponding cutoff frequencies. The relatively small values of the k_I are commented upon in Sec. IV.

III. TRANSITION FROM NONLEAKING TO LEAKING

The iteration process described by Eqs. (10) in the preceeding section may fail to converge when G is near zero and in any event gives relatively little insight into what happens to a modal dispersion curve in the immediate vicinity of ω_L. To explore this transition region, it would appear sufficient to approximate G in Eq. (9) by

$$G \simeq [(p)(\omega-\omega_L) + (q)(v-v_L)]^{1/2} \tag{14}$$

where p and q are readily identifiable [from Eq. (4)] positive numbers taken independent of ω and v; v_L is the phase velocity on the dispersion curve in the limit as $\omega \to \omega_L$ from above. The bracketed quantity in Eq. (14) may be regarded as a double Taylor series expansion (truncated at first order) of G^2 about the point ω_L, v_L at which G^2 vanishes (hence no zeroth order term). The fact that both p and q are positive follows since G^2 is positive to the upper right of the

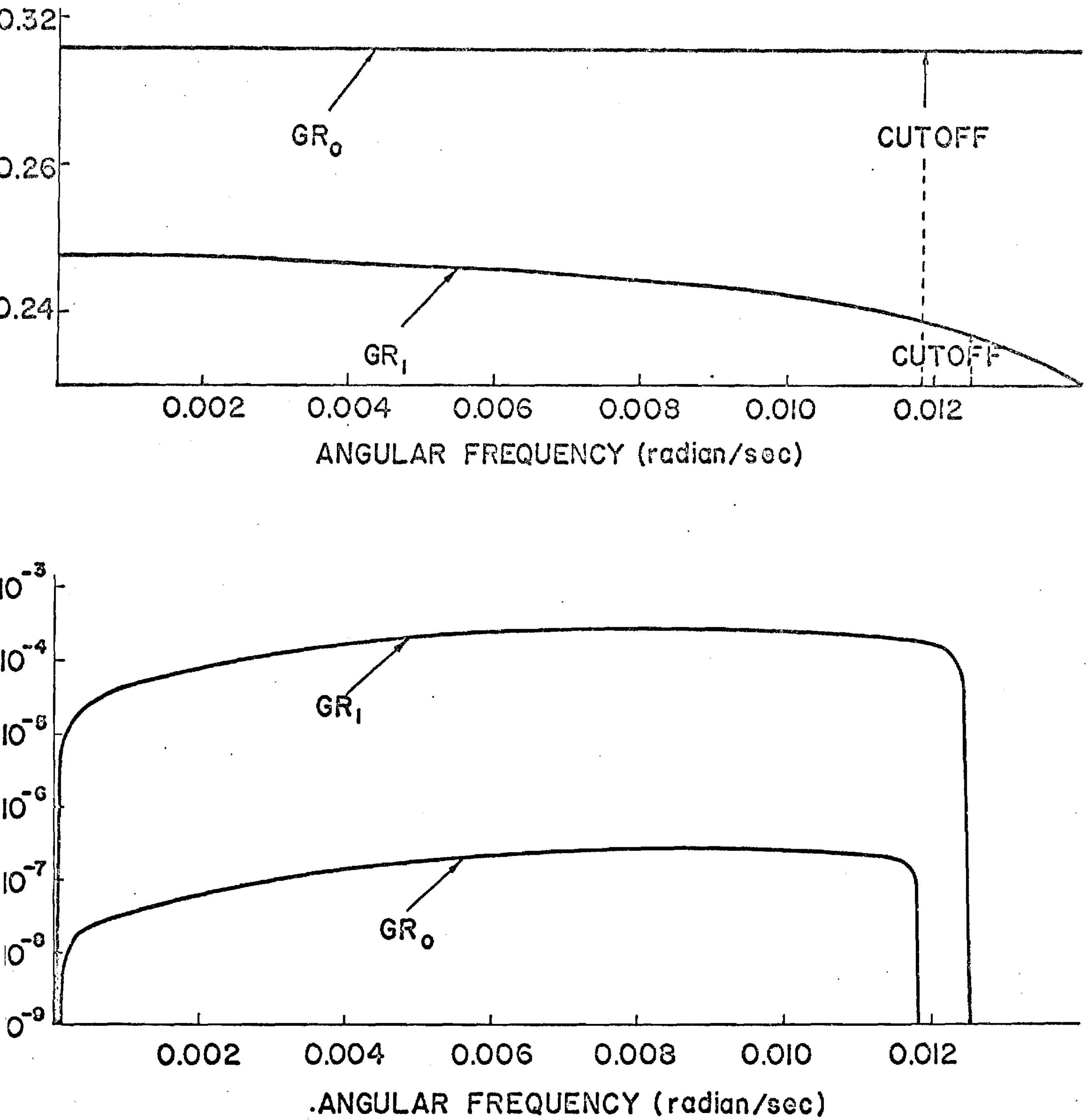

5. Numerically derived plots of phase velocity ω/k_R and of the imaginary part k_I of the complex wavenumber k versus angular frequency for the GR_0 and GR_1 modes. Previous theoretical lower frequency cutoffs for these modes are as indicated. Note that k_I is identically zero above the cutoff frequency.

Mode	ω	v_a	v_b	α	β	$v^{(1)}$	v_η
GR_o	0.0052	0.31203	0.31207	917.4	-2783.7	$0.31202121 + -3.184 \times 10^{-6}i$	
	0.0113	0.31190	0.31194	767.9	-3254.2	$0.31189059 + -1.721 \times 10^{-6}i$	
	0.0155	0.31176	0.31181	621.9	-3644.3	0.31173763	0.31172882
	0.0165	0.31172	0.31177	581.5	-3738.2	0.31167504	0.31167509
	0.0186	0.31162	0.31168	497.5	-3910.1	0.31153369	0.31153394
GR_1	0.0052	0.24229	0.24816	87.8	-3633.0	$0.25267 + -2.715 \times 10^{-3}i$	
	0.0103	0.23433	0.23844	94.7	-3990.0	$0.24218 + -1.337 \times 10^{-3}i$	
	0.0144	0.21842	0.22037	150.7	-5307.0	0.21431	0.22178
	0.0165	0.20252	0.20345	265.0	-7767.3	0.20016	0.20463
	0.0175	0.19058	0.19111	418.9	-10,858.0	0.19226	0.19212

Frequency dependent parameters corresponding to GR_o and GR_1 modes; ω is angular frequency in rad/sec, v_a is phase velocity root of $R_{11}=0$, in km/sec, v_b is analogous root of $R_{12}=0$, α is dR_{11}/dv at $v=v_a$ in sec/km β is dR_{12}/dv at $v=v_b$ in sec, $v^{(1)}$ is first order perturbation solution for phase velocity from equations given in the text (units are km/sec), v_η is the real root determined by direct numerical solution for zeros of eigenmode dispersion function. Note that v_η (defined only when phase velocity is real) agrees exceptionally well with $v^{(1)}$.

line in the ω,v plane where $G^2 = 0$ and also since the $G^2 = 0$ line slopes obliquely downwards. (See Fig. 3).

Let us next note that, in the vicinity of the point ω_L, v_L, the denominator D given by Eq. (9) may be further approximated as

$$D \approx (A_{12}\alpha - A_{11}\beta) \left\{ (\Delta v + \mu\Delta\omega) + \varepsilon(\Delta v + \nu\Delta\omega\ )^{\frac{1}{2}} \right\} \tag{15}$$

where we have abbreviated $\Delta v = v - v_L$, $\Delta\omega = \omega - \omega_L$, $\nu = p/q$; the quantity μ is either $-dv_a/d\omega$ or $-dv_b/d\omega$, the two being assumed to be approximately equal. (The use of the minus sign here assumes that μ be positive.) The remaining quantity ε is

$$\varepsilon = \frac{(q^{\frac{1}{2}})\ (\beta)\ (v - v_b)}{\beta A_{11} - \alpha A_{12}} \tag{16}$$

One should note that ε depends on v, although, for purposes of initial analytical investigation, one may set $v = v_L$ here. All of the above quantities may be considered to be evaluated at $\omega = \omega_L$ and $v = v_L$. Note that μ and ν are both positive quantities. Furthermore, it should also be noted that $\nu > \mu$ since the $G^2 = 0$ curve slopes downwards more rapidly than the lines along which R_{11} or $R_{12} = 0$ in the v vs ω plane. (See Fig. 4.)

The roots of Eq. (15) without regard to the sign of the radical are readily found to be

$$\Delta v = -\mu\Delta\omega + (\tfrac{1}{2})\varepsilon^2 \mp \varepsilon(\nu - \mu)^{\frac{1}{2}}\ [\Delta\omega + \sigma]^{\frac{1}{2}} \tag{17}$$

where

$$\sigma = \varepsilon^2 / [4(\nu - \mu)] \tag{18}$$

Alternately, if $|\Delta\omega| \ll \sigma$, the above may be approximated by the binomial theorem to give

$$\Delta v = -\nu\Delta\omega + [(\nu-\mu)^2/\varepsilon^2](\Delta\omega)^2 \tag{19a}$$

or

$$\Delta v = +\varepsilon^2 - (2\mu - \nu)\ \Delta\omega - [(\nu-\mu)^2/\varepsilon^2](\Delta\omega)^2 \tag{19b}$$

for the upper and lower signs, respectively. The first of these (since $\Delta v = 0$ when $\Delta\omega = 0$) is clearly the description of the disperson curve in the vicinity of $\omega = \omega_L$, $v = v_L$.

Equation (19a) shows that, as $\Delta\omega \to 0$ from above, the dispersion curve becomes tangential to the line $G^2 = 0$. The two curves do not intersect. The general trend is as indicated in Fig. 6. The solution represented by Eq. (19b) is not a proper root of Eq. (15); it corresponds to the wrong sign of the radical and accordingly lies on the second branch. Furthermore, one can readily show that, for values of $\Delta\omega$ slightly less than zero, both roots lie on the second branch. Hence, there must be a gap of finite frequency range in which, for the choice of branch cuts represented by Fig. 1, there are no poles in the k (or v) plane corresponding to the n-th mode.

To determine the order of magnitude of this frequency gap, it is appropriate to consider the trajectory of the second branch roots in some detail and to determine just where one of them should cross the branch cut, reappearing on the first branch. As long as Δv is real and $\Delta v + \nu\Delta\omega > 0$ the criterion for a root to be identified with the first branch is $\Delta v + \mu\Delta\omega > 0$. According to Eq. (17), this would automatically place the second root on the second branch for all $\Delta\omega > -\sigma$ and would place the first root on the second branch for $-\sigma < \Delta\omega < 0$. Consequently, if either root is to reappear on the first branch, it must be at a value of $\Delta\omega < -\sigma$.

One should note from Eq. (17) that at $\Delta\omega = -\sigma$ the two real roots on the second branch coalesce. For values of $\Delta\omega < -\sigma$ the two roots separate again, but

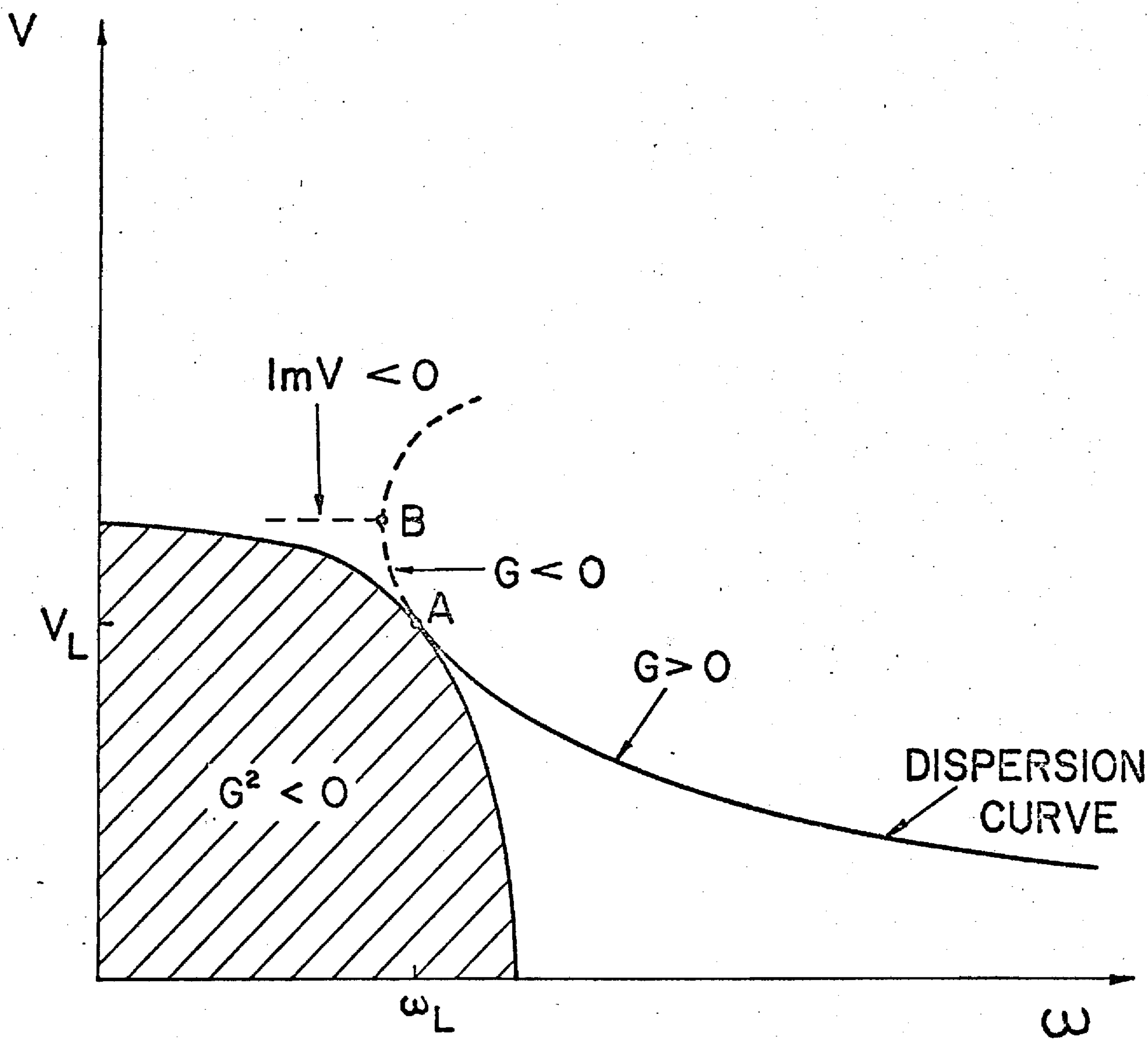

6. Sketch illustrating nature of a single mode's dispersion curve in the vicinity of the $G^2=0$ line. At point A (angular velocity ω_L, phase velocity v_L) the dispersion curve is tangent to the $G^2=0$ line; for frequencies below ω_L down to that corresponding to point B in the sketch there are two real roots for v of the eigenmode dispersion function on the second branch. For frequencies lower than that corresponding to point B, there is a complex root for v on the first branch (which is the complex conjugate of a second root on the second branch).

are now complex conjugates. The root in the upper half of the v plane (lower half of k plane) can never cross the branch cut so it remains on the second branch indefinitely. The one in the lower half of the v plane will cross the branch cut at a point which may be approximately estimated as that where $\mathrm{Re}(\Delta v) = -\nu\Delta\omega$ or where

$$\Delta\omega = \frac{-(\frac{1}{2})\ \varepsilon^2}{(\nu-\mu)} = -2\sigma$$

with a corresponding value of Δv of

$$\Delta v = (\varepsilon^2/2) \left\{[\nu/(\nu-\mu)] - i\right\}$$

For subsequent frequencies successively lower than $\omega_L-2\sigma$ there is a complex root on the first branch with a negative imaginary part which increases with decreasing frequency.

The discussion up to now has assumed that $|\Delta v| << |v_L-v_b|$ and hence that ε may be taken as constant. This would seem appropriate for describing the transition region since all values of Δv of interest in this region are of second order of ε^2. However, if an improved numerical estimate is required, we recommend that one regard Eqs. (16) and (17) as a iterative pair. Successfully computed values of Δv may be used to recalculate ε and the new value of ε may then be used in obtaining the next higher estimate for Δv.

In Table II the values of ω_L, v_L, p, q, μ, ν, ε, and σ are given for the GR_0 and GR_1 modes for the model atmosphere corresponding to Fig. 2a. The extremely small values of σ should be noted. The corresponding plot of Δv versus $\Delta\omega$ (i.e., both branches of Eq.(17)) corresponding to their values for the GR_0 mode is given in Fig. 7. For simplicity, this is plotted in a nondimensional form, i.e.

$$V = -\{\mu/[2(\nu-\mu)]\}\Omega \mp [1 + \Omega]^{1/2} \tag{20}$$

TABLE II

	GR_o	GR_1
ω_L(rad/s)	0.0118	0.0125
v_L(km/s)	0.31188	0.2323
p(s/km^2)	0.14	0.35
q(s/km^3)	1.84×10^{-3}	1.86×10^{-3}
μ(km)	2.94×10^{-2}	4.15
ν(km)	76	190
ε(km$^{1/2}$/s$^{1/2}$)	9.6×10^{-6}	1.02×10^{-3}
σ(rads/s)	3.04×10^{-13}	1.41×10^{-9}

Parameters characterizing the eigenmode dispersion function near points in the phase velocity versus angular frequency plane at which the GR_o and GR_1 modes undergo transition from leaking to non-leaking.

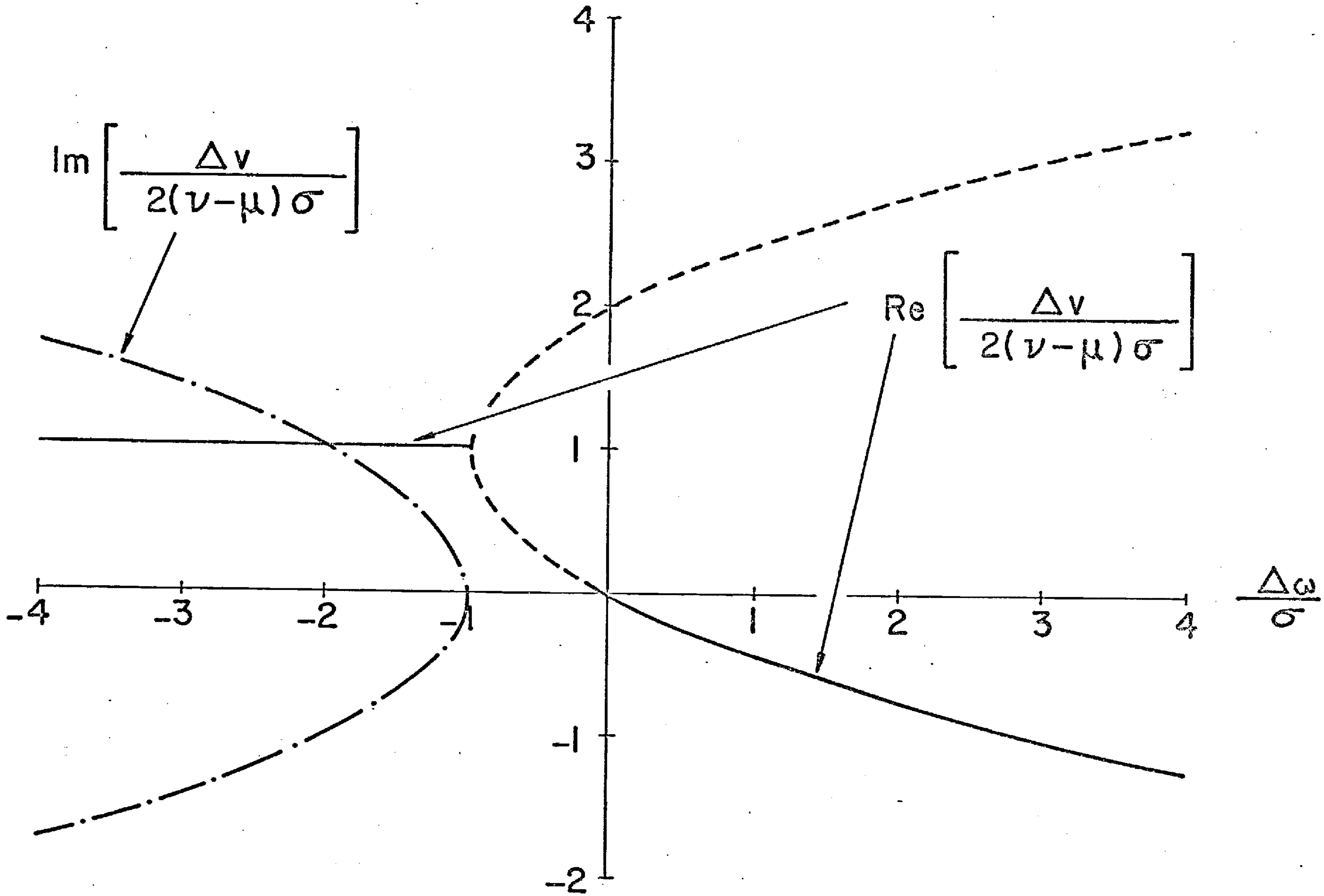

7. Graph of normalized phase velocity versus normalized frequency in the vicinity of the point (v_L, ω_L) for the GR_0 mode. The imaginary and real parts are both plotted. The dashed line corresponds to real roots on the second Riemann sheet.

where $v = \Delta v/[2(\nu-\mu)\sigma]$ and $\Omega=\Delta\omega/\sigma$. Both real and imaginary parts are shown on the same graph. The corresponding plots for the GR_1 mode differ only slightly from those in the Fig. 7 because of a different value of the parameter $\mu/[2(\nu-\mu)]$ in Eq. (20); in both cases this parameter is small compared to unity, i.e. $\mu<<\nu$ as may be seen from Table II.

IV. THE BRANCH LINE INTEGRAL

Since there is a gap in the range of frequencies for which a pole corresponding to a mode may exist, it is evident that evaluation of the k integration in Eq. (1) by merely including residues may be insufficient for certain frequencies. Thus it would seem appropriate in such cases to include a contribution from the branch line integral. It may be anticipated that such branch line integrals are significant at larger values of r only when ω is close to some mode's ω_L (say the n-th mode), in which case the branch point of greatest interest (i.e., that which may have a pole in its immediate vicinity) is at $k=\omega/v_L$. Consequently, it would appear that an adequate approximation to the branch line integral would be

$$\left\{\begin{matrix}\text{Branch line}\\ \text{contribution of}\end{matrix}\right\} \int_{-\infty}^{\infty} [Q/D(\omega,k)]e^{ikr}dk$$

$$= \frac{Q}{A_{12}\alpha-A_{11}\beta} \int_{C_B} \frac{e^{ikr}dk}{x+(\mu-\nu)\Delta\omega+\varepsilon x^{1/2}} \qquad (21)$$

where the denominator $D(\omega,k)$ has been approximated by Eq. (15) with the abbreviation x for $\Delta v+\nu\Delta\omega$. The quantity outside the integral is assumed to be evaluated at $\omega=\omega_L$ and $k=\omega/v_L$. The contour C_B runs down the left side of the branch cut, around the branch point (where $x=0$), and then up the right side. If one next changes the variable of integration from k to x, nothing that for small x/v_L, noting

$$k\approx k_B-(\omega_L/v_L^2)x \qquad (22)$$

he finds approximately that

$$\begin{Bmatrix}\text{Branch line}\\ \text{contribution}\end{Bmatrix} = (\text{Residue})_o \int_{c_B'} \frac{e^{-i(\omega_L/v_L^2)x}}{x+(\mu-\nu)\Delta\omega+\varepsilon x^{\frac{1}{2}}}\, dx \tag{23}$$

where $(\text{Residue})_o$ is that residue which the integrand $(Q/D)e^{ikr}$ would be expected to have at the n-th mode's pole in the k plane were the parameter ε identically equal to zero. The mapped contour c_B' in the x plane may be considered to go up on the right and then down on the left of a branch cut extending vertically downwards from the origin in the x plane. If we set $x=-i\xi$, then, on the right side of the cut, $x^{1/2}$ should be $e^{-i\pi/4}\xi^{1/2}$ while, on the left side, it is $-e^{-i\pi/4}\xi^{1/2}$. Consequently, the total integral combines to

$$\begin{Bmatrix}\text{Branch lines}\\ \text{contribution}\end{Bmatrix} = -(\text{Residue})_o \int_0^\infty \frac{2\varepsilon e^{+i\pi/4} e^{-(\omega_L/v_L^2)\xi r}\sqrt{\xi}\, d\xi}{[-i\xi+(\mu-\nu)\Delta\omega]^2+i\varepsilon^2\xi} \tag{24}$$

This in turn, with an obvious change of integration variable, may be expressed as

$$\begin{Bmatrix}\text{Branch line}\\ \text{contribution}\end{Bmatrix} = (\text{Residue})_o\ 2K \int_0^\infty \frac{e^{i\pi/4} e^{-\eta}\eta^{1/2} d\eta}{(\eta-\eta_1)(\eta-\eta_2)} \tag{25}$$

where

$$K=\varepsilon v_L/(\omega_L r)^{1/2} \tag{26a}$$

$$\eta_1,\ \eta_2 = i(K^2/2)(1+[\Delta\omega/2\sigma]) \pm i(K^2/2)(1+[\Delta\omega/\sigma])^{1/2} \tag{26b}$$

with σ as defined by Eq. (18).

In regards to the η integration, the integral can be expressed in general in terms of Fresnel integrals of complex argument after some considerable mathematical manipulation. One may note, moreover, that $|\eta_1|$ and $|\eta_2|$ are, for most cases of interest, considerably less than unity. In this case, the appropriate approximate result (derivation omitted for brevity) is

$$\int_0^\infty \frac{e^{-\eta}\sqrt{\eta}\, d\eta}{(\eta-\eta_1)(\eta-\eta_2)} = \frac{i\pi}{\eta_1^{1/2}+\eta_2^{1/2}} \tag{27}$$

where the choice of square root should be such that the imaginary part is positive. The net result in this limit then is that the branch line contribution is independent of the parameter κ. (The dependence on range r comes only in the residue.) Thus one may write

$$\left\{\begin{matrix}\text{Branch line}\\ \text{contribution}\end{matrix}\right\} = 2\pi i(\text{Residue})_o\, B_{rh}(\Delta\omega/\sigma) \tag{28}$$

where the function $B_{rh}(\Delta\omega/\sigma)$ is given by

$$B_{rh}(\Omega) = \frac{\sqrt{2}}{[1+(1/2)\Omega+(1+\Omega)^{1/2}]^{1/2}+[1+(1/2)\Omega-(1+\Omega)^{1/2}]^{1/2}} \tag{29}$$

Here any consistent choice may be made for the sign of the inner square roots but the outer square roots should be taken such that the resulting phases are between $-\pi/4$ and $3\pi/4$. The quantities in square brackets turn out to be the squares of $(1/\sqrt{2})[(1+\Omega)^{1/2}\pm1]$, respectively. The phase restriction then gives

$$B_{rh}(\Omega) = (1+\Omega)^{1/2} \quad \text{if } \Omega>0 \tag{30a}$$

$$= 1 \quad \text{if } 0>\Omega>-2 \tag{30b}$$

$$= -i(-\Omega-1)^{-1/2} \quad \text{if } \Omega<-2 \tag{30c}$$

where here all square roots are understood to be positive.

To completely describe the transition it is appropriate to add to Eq. (28) that contribution (which is zero for $0>\Delta\omega>-2\sigma$) from the pole on the first branch in Eq. (21) which lies in the general vicinity of $k=\omega_L/v_L$. If the pole is present, its contribution to the integration over k is $2\pi i$ times the residue (which is not what we have been referring to as $(\text{Residue})_o$ unless ε is identically zero). The evaluation of the residue is moderately straightforward and omitted here for brevity. The net result is that

$$\begin{Bmatrix}\text{Branch line}\\ \text{contribution}\end{Bmatrix}+\begin{Bmatrix}\text{Pole}\\ \text{contribution}\end{Bmatrix}$$

$$= 2\pi i(\text{Residue})_o\left\{B_{rh}(\Delta\omega/\sigma)+P_{o\ell}(\Delta\omega/\sigma)\right\} \tag{31}$$

where the "pole function" $P_{o\ell}(\Delta\omega/\sigma)$ turns out to be given by

$$P_{o\ell}(\Delta\omega/\sigma)=1-B_{rh}(\Delta\omega/\sigma) \; . \tag{32}$$

We accordingly have the remarkable (although, in retrospect, not unexpected) result that

$$\begin{Bmatrix}\text{Branch line}\\ \text{contribution}\end{Bmatrix}+\begin{Bmatrix}\text{Pole}\\ \text{contribution}\end{Bmatrix}= 2\pi i(\text{Residue})_o \tag{33}$$

The above gives one a relatively simple prescription for evaluating a given mode's contribution to the k integration in Eq. (1). First, all branch line integrals are formally neglected. If a pole exists on the first branch, the residue which would normally be utilized is replaced by

$$\text{Res}\left\{\frac{Qe^{ikr}}{D}\right\}\rightarrow\left\{\frac{Qe^{ikr}}{d'D/dk}\right\}_{k=\text{pole}} \tag{34}$$

where

$$\frac{d'D}{dk}=\frac{d}{dk}\left(A_{12}R_{11}-A_{11}R_{12}\right)$$
$$-G\frac{d}{dk}\left(R_{12}\right) \tag{35}$$

i.e. it differs from the actual derivative of D in that G is formally considered as constant. Doing this when ω is somewhat removed from the transition region near ω_L should make very little difference since R_{12} is small at values of k which are poles. Near the transition, this neglect should almost exactly compensate for the neglect of the branch line integral.

REFERENCES

1. J. E. Thomas, A. D. Pierce, E. A. Flinn, and L. B. Craine, "Bibliography on Infrasonic Waves", Geophys. J. R. astr. Soc. 26, 399-426 (1971).

2. C. B. Officer, Introduction to the Theory of Sound Transmission with Application to the Ocean (McGraw-Hill, New York, 1958).

3. J. R. Wait, Electromagnetic Waves in Stratified Media (Pergamon Press, Inc., New York, 1962).

4. L. M. Brekhovskikh, Waves in Layered Media (Academic Press, New York, 1960).

5. K. G. Budden, The Wave-Guide Mode Theory of Wave Propagation (Prentice Hall, Inc., Englewood Cliffs, N.J., 1961).

6. I. Tolstoy and C. S. Clay, Ocean Acoustics (McGraw-Hill, New York, 1966).

7. M. Ewing, W. Jardetzky, and F. Press, Elastic Waves in Layered Media (McGraw-Hill, New York, 1957).

8. A. D. Pierce and J. W. Posey, Theoretical Prediction of Acoustic-Gravity Pressure Waveforms generated by Large Explosions in the Atmosphere, Report AFCRL-70-0134, Air Force Cambridge Research Laboratories, 1970.

9. A. D. Pierce, J. W. Posey, and E. F. Iliff, "Variation of Nuclear Explosion generated Acoustic-Gravity Waveforms with Burst Height and with Energy Yield" J. Geophys. Res. 76, 5025-5042 (1971).

10. E. T. Copson, An Introduction to the Theory of Functions of a Complex Variable (Clarendon Press, Oxford, 1935) p. 137.

11. L. M. Brekhovskikh, loc. cit., pp. 270-280.

12. A. D. Pierce, "The Multilayer Approximation for Infrasonic Wave Propagation in a Temperature and Wind-Stratified Atmosphere", J. Comp. Phys. 1, 343-366 (1967).

13. A. D. Pierce, "Propagation of Acoustic-Gravity Waves in a Temperature and Wind-Stratified Atmosphere", J. Acoust. Soc. Amer. 37, 218-227 (1965).

Appendix B

The 88th Meeting of the Acoustical Society of America

Chase-Park Plaza Hotel • St. Louis, Missouri • 4–8 November 1974

TUESDAY, 5 NOVEMBER 1974 CHASE CLUB, 9:30 A.M.

Session A. Physical Acoustics I: Atmospheric Acoustics

10:45

A5. Asymptotic high-frequency behavior of guided infrasonic modes in the atmosphere. Wayne A. Kinney (School of Mechanical Engineering, Georgia Institute of Technology, Atlanta, Georgia 30332)

Refinement of previous theoretical formulations and numerical computations of pressure waveforms as applied to atmospheric traveling infrasonic waves could include a description of their asymptotic behavior at high frequencies. In the present paper, calculations based on the W.K.B.J. approximation and similar to those introduced by Haskell [J. Appl. Phys. 22, 157–167 (1951)] are performed to describe the asymptotic behavior of infrasonic guided modes as generated by a nuclear explosion in the atmosphere. The results of these calculations are then matched onto numerical solutions which have been given by Harkrider, Pierce and Posey, and others. It is demonstrated that the use of these asymptotic formulas in conjunction with a computer program which synthesizes infrasonic pressure waveforms has enabled the elimination of problems associated with high-frequency truncation of numerical integration over frequency. In this way, small spurious high-frequency oscillations in the computer solutions have been avoided. [Work sponsored by Air Force Cambridge Research Laboratory.]

Recently, Allan D. Pierce, Christopher Y. Kapper and Wayne A. Kinney at the Georgia Institute of Technology have been working to refine a computer program which synthesizes infrasonic pressure waveforms at the ground as generated by large explosions in a wind- and temperature- stratified atmosphere.[1] Shown in Fig. 1 are three such pressure waveforms along with the modal waveforms from which each of the three individual total waveforms has been superposed. Corresponding to each modal waveform is a particular dispersion curve (i.e., a plot of phase velocity versus angular frequency). Any given dispersion curve defines what is referred to as a mode. Fig. 2 shows dispersion curves as they are generated by a portion of the computer program. The labels given to these correspond to the labels given to the modal waveforms in Fig. 1.

Due to temperature stratification, the earth's atmosphere possesses sound speed channels with associated relative sound speed minima. Fig. 3 shows a standard reference atmosphere wherein two such sound speed channels are indicated; one with a minimum occurring at approximately 16 km altitude and the second with a minimum occurring at approximated 86 km altitude. Given the presence of such a channel, an acoustic ducting phenomenon can occur, as is demonstrated in Fig. 4, wherein the energy associated with an acoustic disturbance can become trapped in the region of a relative sound speed minimum.[1] It is this mechanism of propagation only that is of interest here.

In the computer program, the computation of modal waveforms involves the numerical integration over angular frequency of a Fourier transform of acoustic pressure where this integration is truncated at the high-frequency end.[1] It has been speculated that this abrupt truncation leads to the

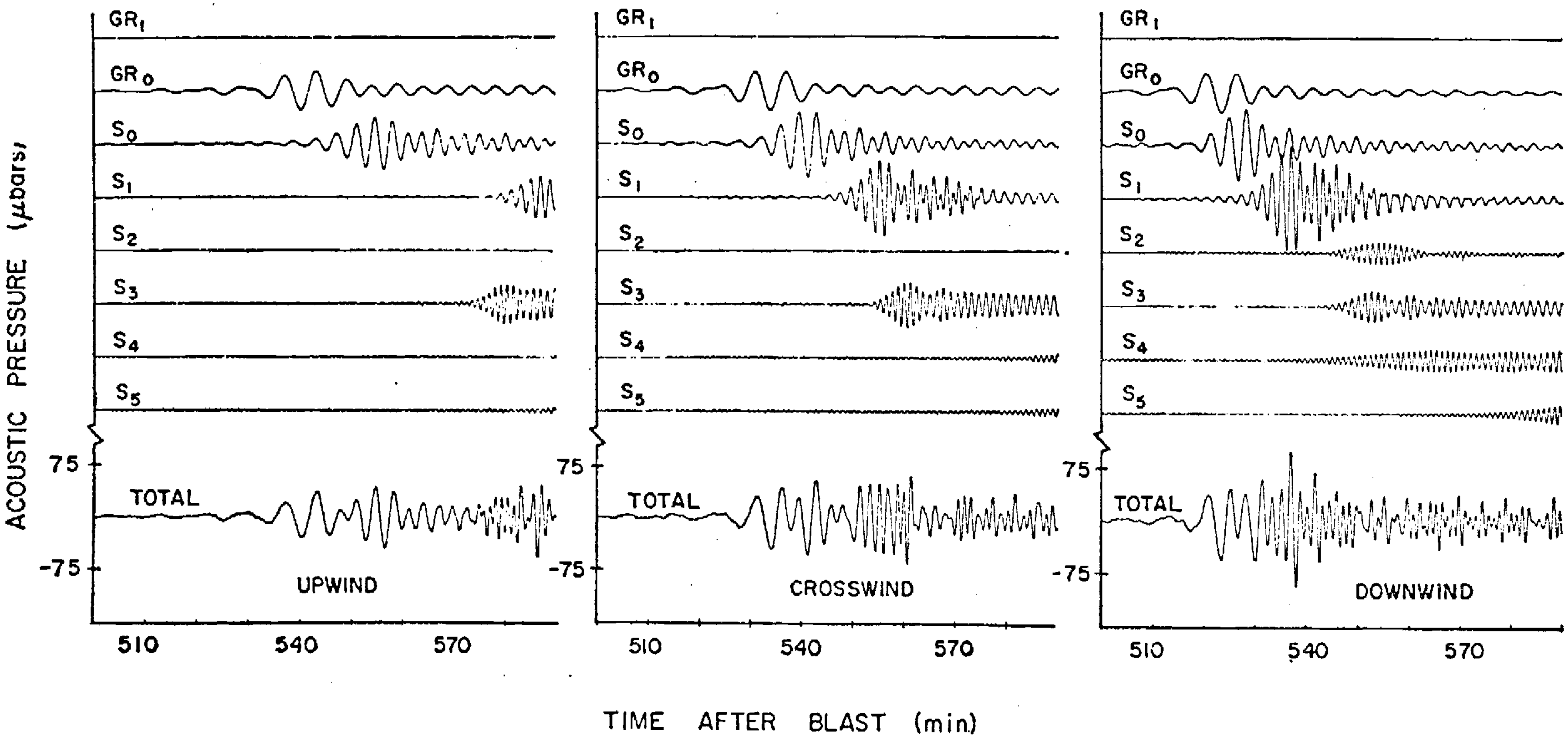

Fig. 1 Superposed infrasonic pressure waveforms (with contributing modal waveforms shown) as generated by the computer model for ground locations 10,000 km upwind, crosswind and downwind from a nuclear explosion.[3]

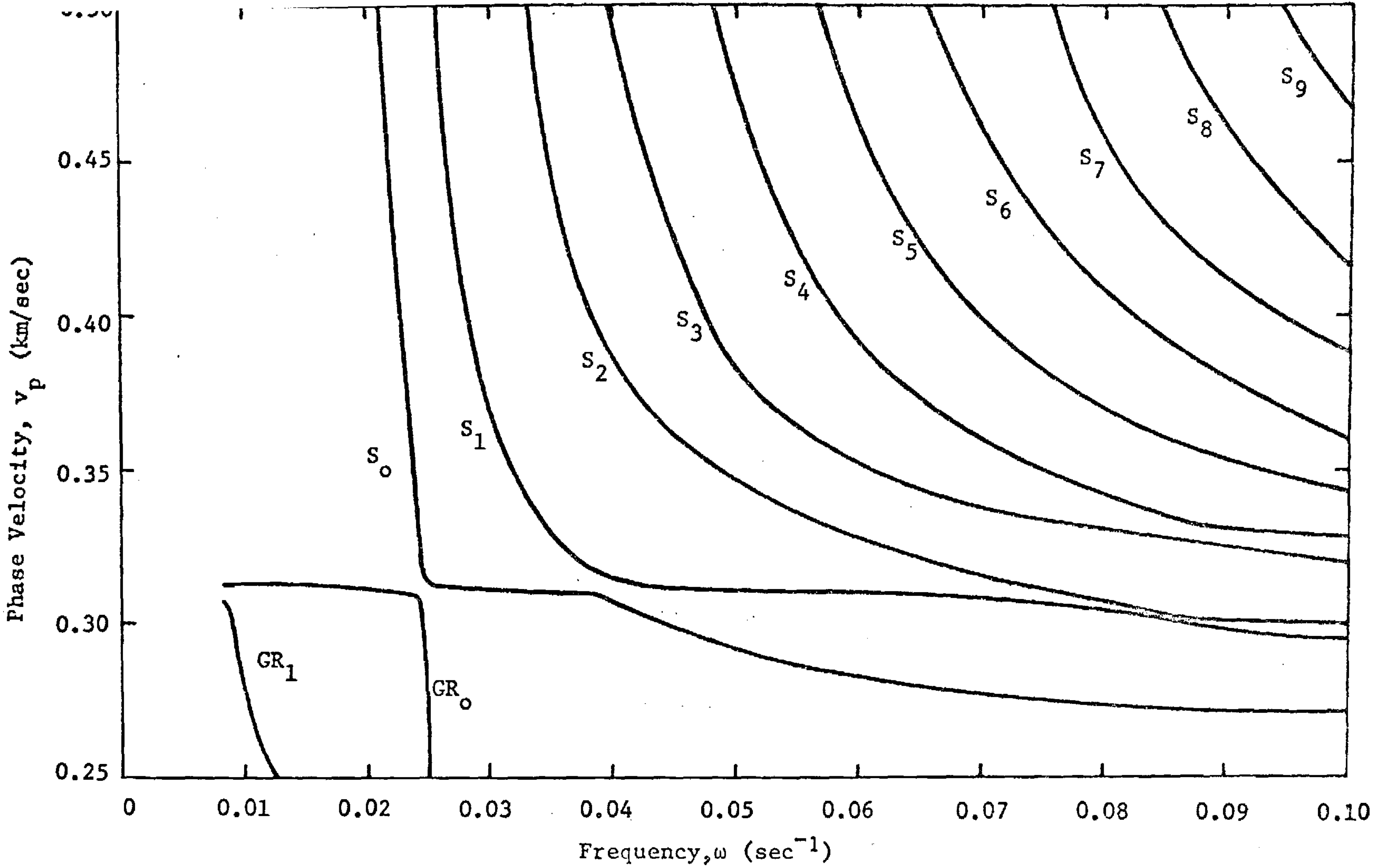

Fig. 2. Dispersion curves generated by the computer model. The labels given these curves correspond to the labels given the modal waveforms of Fig. 1.[4]

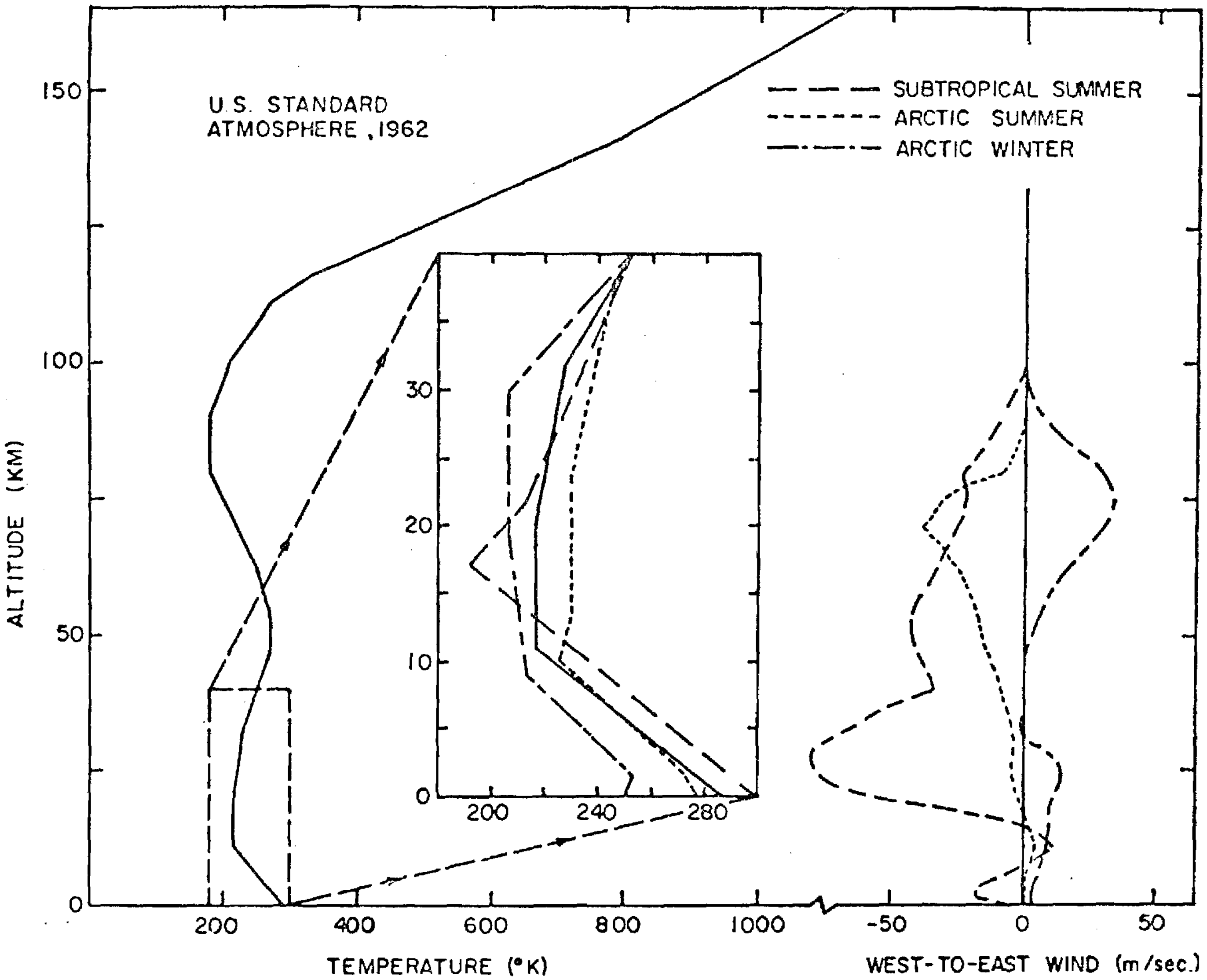

Fig. 3. Standard reference model atmosphere showing two sound speed channels.

SOUND CHANNEL DUCTING

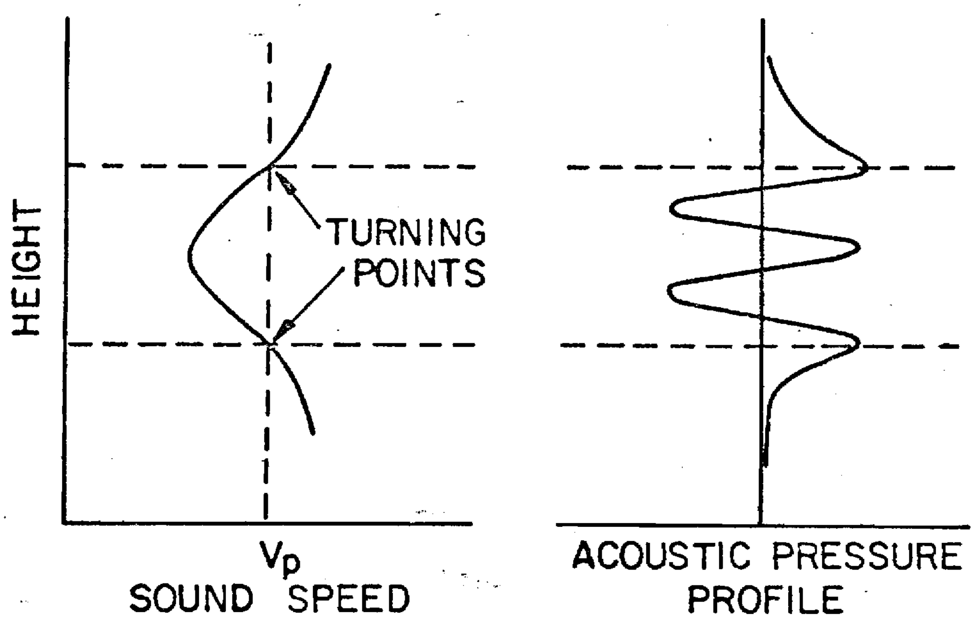

Fig. 4. Graphic illustration of acoustic ducting in a sound speed channel. The energy of an acoustic disturbance can concentrate in the region of a relative sound speed minimum.[1]

generation of what might be called "numerical noise" in the computer output. It was felt useful, therefore, to extend this integration beyond the heretofore upper angular frequency limit by means of some appropriate high-frequency approximation.

The approximations associated with the W.K.B.J. method of solution[2] apply to the analytical model on which the computer program is based at frequencies above approximately 0.1 radian/sec. Below that limit, effects due to density stratification in the atmosphere and gravitational forces cannot be neglected. Such effects therefore are not germaine to the discussion here.

To the best of the authors' present knowledge, the application of the W.K.B.J. method of solution to the problem of describing propagation of acoustic disturbances in an atmosphere that contains two adjacent sound speed channels has not been approached in the literature to date in the manner to be presented. To be specific, the approach taken here is to seek a W.K.B.J. model for each of the sound speed channels separately, then to combine the results rather than to treat the problem with a single model.

The W.K.B.J. model for propagation of acoustic disturbances in a single sound speed channel consists of solving for the acoustic pressure divided by the square root of the ambient density expressed as

$$\frac{P}{\rho_o^{\frac{1}{2}}} = \psi(z)e^{-i\omega t}e^{ikx}$$

where ω is angular frequency, k is the wave number associated with the horizontal dimension x, z is altitude, and where $\psi(z)$ satisfies the reduced wave equation,

$$\frac{d^2\psi}{dz^2} + \left[\frac{\omega^2}{c^2(z)} - k^2\right]\psi = 0$$

where c(z) is sound speed as a function of altitude. The W.K.B.J. approximation as applied to this model would appear to be valid provided

$$\frac{C}{|\nabla C|} << \lambda$$

where λ is some representative wavelength of interest. This approximation states that substantial changes in sound speed should not occur within distances corresponding to a typical wavelength of interest if the model is to apply.

Particular insight into the high-frequency behavior of guided infrasonic modes was gained when the following integral was solved numerically by computer

$$\int_{z_{bottom}}^{z_{top}} \left[\frac{1}{c^2(z)} - \frac{1}{v_p^2}\right]^{\frac{1}{2}} dz = \frac{(n+\frac{1}{2})\pi}{\omega}$$

where v_p is phase velocity, n = 0, 1, 2, 3, ..., and where z_{bottom} and z_{top} identify the lower and upper bounds of the sound speed channel, respectively. This integral is a direct result of the W.K.B.J. method of solution[2], and its numerical solution enabled the plotting of high-frequency dispersion curves.

In the lower portion of Fig. 5 are shown two sets of dispersion curves generated by integrals of the above form; one set (the dashed curves) is appropriate to the W.K.B.J. model for the lower channel and the other set (the solid curves) is appropriate to the W.K.B.J. model for the upper channel.

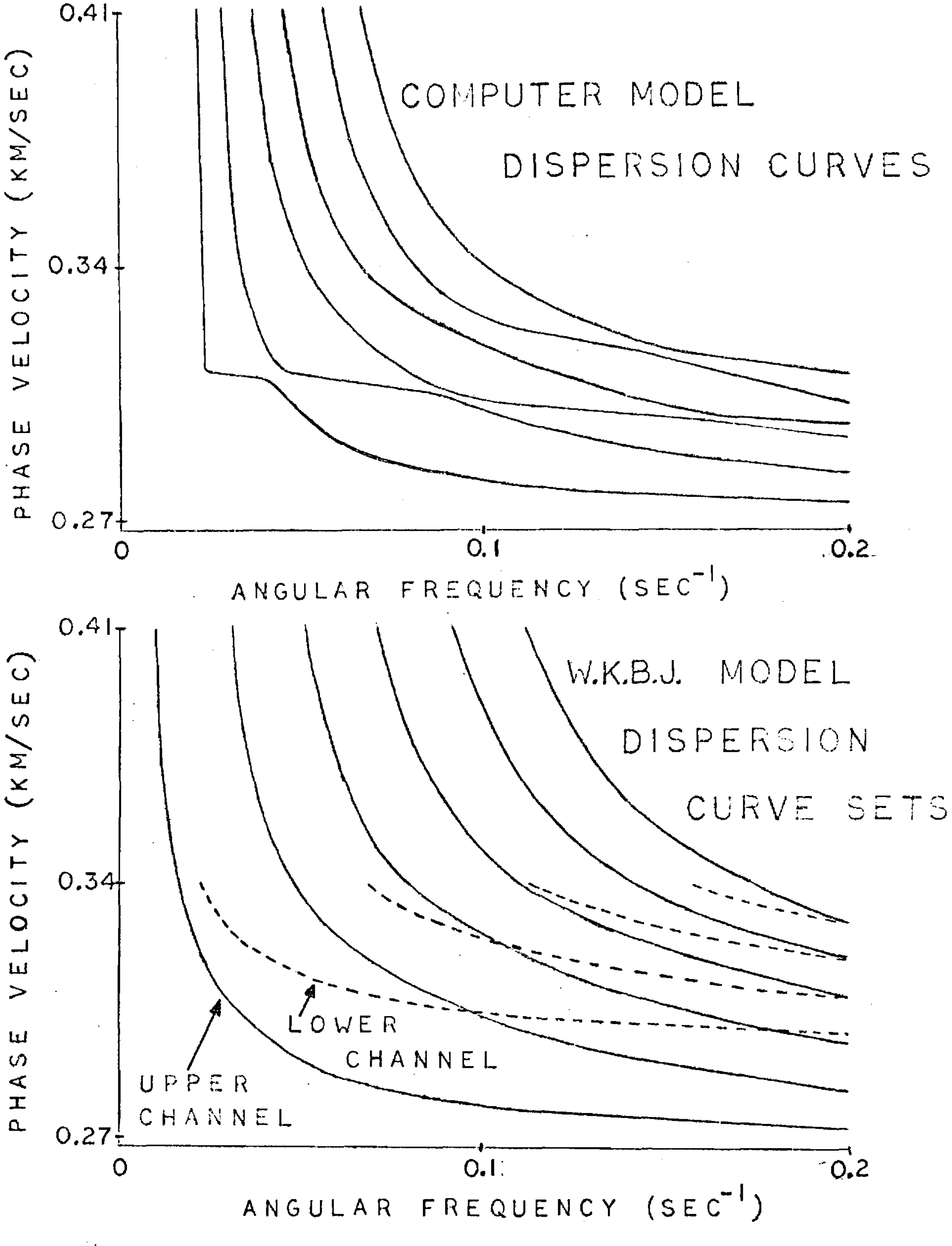

Fig. 5. Comparative dispersion curves as generated by the computer model and the W.K.B.J. models.

In the upper portion of the same figure are shown again dispersion curves as generated by the computer model. It should be mentioned that the computer model solves a more complex problem in the sense that the simplifications inherent in the W.K.B.J. model are not present.

As is illustrated in the lower portion of Fig. 5, the two sets of dispersion curves generated by the W.K.B.J. models intersect with one another at various points. A comparison of the dispersion curves shown in both the upper and lower portions of Fig. 5 reveals that these points of intersection mark regions of resonant interaction in the phase velocity-angular frequency plane between adjacent modes of the computer model. To better illustrate this observation, in the right hand portion of Fig. 6 is shown one such region of interaction with its corresponding point of intersection between two dispersion curves of the W.K.B.J. models shown to the left. It should be mentioned that the dispersion curves of the computer model never intersect with one another. An analytical explanation of this fact is given in reference 1.

The above observation may be stated differently by saying that, for relatively high angular frequencies, the dispersion curve corresponding to a given mode of the computer model is comprised of portions of dispersion curves from both sets of the curves generated by the W.K.B.J. models. Two important inferences about the asymptotic high-frequency behavior of guided infrasonic modes can be drawn from this statement. First, for some frequency ranges, and depending on how dispersion curve portions match between curves of the computer model and the W.K.B.J. models, it can be inferred that the acoustic energy associated with a given mode is comprised of energy associated more with propagation of acoustic disturbances in one sound speed channel than in the other. Also, with increasing frequency, this association alternates back and forth

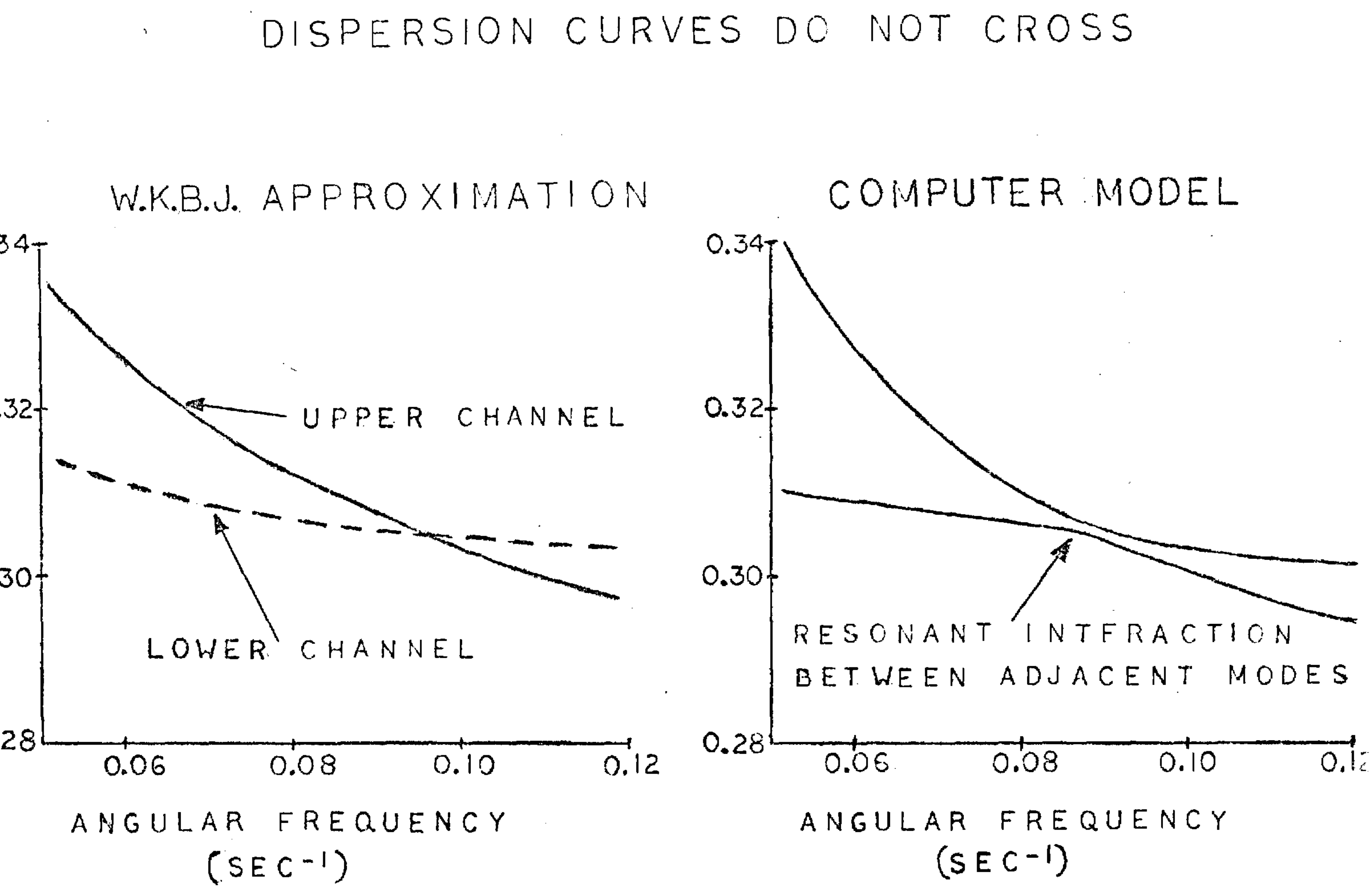

Fig. 6. Blow-up of a section of Fig. 5 showing a region of resonant interaction between two adjacent modes of the computer model. To the left are shown the corresponding intersecting curves of the W.K.B.J. models.

between channels. To illustrate, if for a small range of frequencies a portion of a dispersion curve of the computer model matches (in the phase velocity-angular frequency plane) a portion of one of the W.K.B.J. model curves for the upper channel, then that implies that, for that mode and for that small frequency range, the acoustic energy density associated with that mode is greater in the upper channel than in the lower channel. Secondly, in standard reference atmospheres the sound speed minimum for the upper channel is shown to be less in magnitude than the sound speed minimum for the lower channel. It can be inferred therefore that those acoustic disturbances for which phase velocities are less in magnitude than the sound speed minimum for the lower channel are associated more with acoustic energy trapped in the upper channel than in the lower channel, and thus for this reason do not contribute significantly to the acoustic energy at the ground. This inference implies that care must be taken as to which modes are chosen to superpose in the attainment of the final pressure waveform at the ground, as some may not contribute.

In addition to providing a new analytical tool, the manner in which the W.K.B.J. method of solution has been applied to the two-channel problem has clarified the physical interepretation of a mode as defined in the computer model. It is hoped that the computer program can now be modified accordingly to gain better high-frequency resolution in the pressure waveform output.

REFERENCES

1. Pierce, A. D. and Posey, J. W., "Theoretical Predictions of Acoustic Gravity Pressure Waveforms Generated by Large Explosions in the Atmosphere", Report No. AFCRL-70-0134 (1970), see in particular pp. 32, 38, 41-45, 93-99.

2. Morse, P. M. and H. Feshbach, Methods of Theoretical Physics, McGraw-Hill, New York, 1953, see in particular pp. 1092-1094, 1098-1099.

3. Pierce, A. D., C. A. Moo and J. W. Posey, "Generation and Propagation of Infrasonic Waves", Report No. AFCRL-TR-73-0135 (1973).

4. Posey, J. W., "Application of Lamb Edge Mode Theory in the Analysis of Explosively Generated Infrasound", Ph.D. Thesis, Department of Mechanical Engineering, Mass. Inst. of Tech. (August, 1971).

Appendix C

```
      PROGRAM MAIN (INPUT,OUTPUT,TAPE5=INPUT,TAPE6=OUTPUT)
      DIMENSION ZTS(10)
      COMMON VP,I1,NCS,ZI(100),CI(100),ASOL(100),ZLOW,ZUP
      READ(5,*)NCS,(ZI(I),I=1,NCS),(CI(I),I=1,NCS),VP,ZBL,ZBU,NSCAN
      WRITE(6,*)NCS,(ZI(I),I=1,NCS),(CI(I),I=1,NCS),VP,ZBL,ZBU,NSCAN
      READ*,(ZTS(I),I=1,10)
      WRITE*,(ZTS(I),I=1,10)
      CALL DASOL
      PRINT*,"ASOL=",ASOL
      DO 5 I=1,10
    5 PRINT*,"CSP=",CSP(ZTS(I))
      CALL TNPNT(VP,ZBL,ZBU,NSCAN,NRTS,ZLOW,ZUP)
      PRINT*,"NRTS=",NRTS
      CALL SHIFT(ZLOW,ZUP)
      PRINT*,"ZLOW=",ZLOW,"ZUP=",ZUP
      CALL RANG (RTIME,RLNTH,ZLOW,ZUP)
      PRINT*,"RTIME=",RTIME,"RLNTH=",RLNTH
      I = 1
      Z = ZI(5)
      CALL DRVTNP(I,Z,VP,DXDVPU,DTDVPU,ZLOW,ZUP)
      PRINT*,"DXDVPU=",DXDVPU,"DTDVPU=",DTDVPU
      I =-1
      Z = ZI(3)
      CALL DRVTNP(I,Z,VP,DXDVPL,DTDVPL,ZLOW,ZUP)
      PRINT*,"DXDVPL=",DXDVPL,"DTDVPL=",DTDVPL
      Z1 = ZI(3)
      Z2 = ZI(5)
      CALL MDLINT(Z1,Z2,AMXIN,AMTIN)
      PRINT*,"AMXIN=",AMXIN,"AMTIN=",AMTIN
      CALL DSDVP(I,Z,VP,DXDVP,DTDVP,ZLOW,ZUP,AMXIN,AMTIN,
     1DXDVPT,DTDVPT)
      PRINT*,"DXDVPT=",DXDVPT,"DTDVPT=",DTDVPT
      CALL EXIT
      END
      SUBROUTINE SHIFT(ZLOW,ZUP)
      N = 0
    5 CHKL = CMVP(ZLOW)
      IF(CHKL .LE. 0.0) GO TO 10
      ZLOW = ZLOW + 1.E-8
      N = N+1
      IF(N .GE. 1000) RETURN
      GO TO 5
   10 CHKU = CMVP(ZUP)
      IF(CHKU .LE. 0.0) RETURN
      ZUP = ZUP - 1.E-8
      N = N+1
      IF(N .GE. 1000) RETURN
      GO TO 10
      END
      FUNCTION CMVP(Z)
      COMMON VP
      CMVP = CSP(Z) - VP
      RETURN
      END
      SUBROUTINE TNPNT(VP,ZBL,ZBU,NSCAN,NRTS,ZA,ZB)
      EXTERNAL CMVP
      DIMENSION GUESS(3,1),ANS(1),FANS(1)
      COMMON VPC
      VPC = VP
      DELTA = (ZBU - ZBL)/(NSCAN + 1)
      F1 = CMVP(ZBL)
      Z1 = ZBL
      NRTS = 0
   10 Z2 = Z1 + DELTA
```

```
      F2 = CMVP(Z2)
      TEST = F1*F2
      IF(TEST .GT. 0.0) GO TO 15
      GZ = Z1 - F1*DELTA/(F2 - F1)
      GUESS(1,1) = GZ
      GUESS(2,1) = Z1 - 1.E-6
      GUESS(3,1) = Z2 + 1.E-6
      CALL ZAFUR(1,GUESS,10,1.E-7,1.E-7,CMVP,-1,ANS,FANS)
      NRTS = NRTS + 1
      IF(NRTS .EQ. 1) ZA = ANS(1)
      IF(NRTS .EQ. 2) ZB = ANS(1)
      IF(NRTS .EQ. 2) GO TO 20
   15 Z1 = Z2
      F1 = F2
      IF(ZBU .GE. Z1) GO TO 10
   20 RETURN
      END
      SUBROUTINE RANG (RTIME,RLNTH,ZLOW,ZUP)
      EXTERNAL RDTDZ,RDXDZ
      RTIME = RAINT(RDTDZ,ZLOW,ZUP)
      RLNTH = RAINT(RDXDZ,ZLOW,ZUP)
      RETURN
      END
      SUBROUTINE DASOL
      COMMON VP,I1,NCS,ZI(100),CI(100),ASOL(100)
      N = 1
      DELZ = 1.0
      DELC = 0.0
      AKM2 = 0.0
      ALM2 = 0.0
      AKM1 = 0.0
      ALM1 = 1.0
      NSTP = NCS - 1
   10 DELZP = ZI(N+1) - ZI(N)
      DELCP = CI(N+1) - CI(N)
      ALPHA = DELZ
      GAMMA = DELZP
      BETA = 2.0*(ALPHA + GAMMA)
      DEE = (DELCP/DELZP) - (DELC/DELZ)
      IF(N .EQ. 1) GO TO 30
      AK = (DEE - ALPHA*AKM2 - BETA*AKM1)/GAMMA
      AL = ( - ALPHA*ALM2 - BETA*ALM1)/GAMMA
      IF(N .EQ. NSTP) GO TO 100
      AKM2 = AKM1
      ALM2 = ALM1
      AKM1 = AK
      ALM1 = AL
   30 N = N + 1
      DELZ = DELZP
      DELC = DELCP
      GO TO 10
  .00 ASOL(1) = 0.0
      ASOL(2) = -AK/AL
      DELZ = 1.0
      DELC = 0.0
      N = 1
   10 DELZP = ZI(N+1) - ZI(N)
      DELCP = CI(N+1) - CI(N)
      ALPHA = DELZ
      GAMMA = DELZP
      BETA = 2.0*(ALPHA + GAMMA)
      DEE = (DELCP/DELZP) - (DELC/DELZ)
      IF(N .EQ. 1) GO TO 130
      M = N + 1
```

```
      ASOL(M) = (DEE - ALPHA*ASOL(N-1) - BETA*ASOL(N))/GAMMA
      IF(N .EQ. NSTP) GO TO 200
130   N = N + 1
      DELZ = DELZP
      DELC = DELCP
      GO TO 110
200   RETURN
      END
      FUNCTION CSP(Z)
      COMMON VP,I1,NCS,ZI(100),CI(100),ASOL(100)
      ZL = ZI(1)
      ZP = ZI(NCS)
      IF (Z .LT. ZL) GO TO 50
      IF (Z .GT. ZP) GO TO 60
      I = NCS
10    J = I-1
      ZTEST = ZI(J)
      IF (Z .GT. ZTEST) GO TO 40
      I = J
      GO TO 10
40    CONTINUE
      Z IS BETWEEN ZI(I-1) AND ZI(I)
      DELZ = ZI(I) - ZI(J)
      W = (Z - ZI(J))/DELZ
      WBAR = 1.0 - W
      TERM1 = WBAR*CI(J) + W*CI(I)
      GUT1 = WBAR**3 - WBAR
      GUT2 = W**3 - W
      TERM2 = (DELZ**2)*(ASOL(J)*GUT1 + ASOL(I)*GUT2)
      CSP = TERM1 + TERM2
      RETURN
50    CSP = CI(1)
      RETURN
60    CSP = CI(NCS)
      RETURN
      END
      FUNCTION DCDZ(Z)
      COMMON VP,I1,NCS,ZI(100),CI(100),ASOL(100)
      ZL = ZI(1)
      ZP = ZI(NCS)
      IF(Z .LT. ZL) GO TO 50
      IF(Z .GT. ZP) GO TO 50
      I = NCS
 10   J = I-1
      ZTEST = ZI(J)
      IF(Z .GT. ZTEST) GO TO 40
      I = J
      GO TO 10
 40   CONTINUE
      Z IS BETWEEN ZI(I-1) AND ZI(I)
      DELZ = ZI(I) - ZI(J)
      DELCI = (CI(I) - CI(J))/DELZ
      W = (Z - ZI(J))/DELZ
      WBAR = 1.0 - W
      TRM3A = ASOL(I)*((3.0*(W**2)) - 1.0)
      TRM3B = ASOL(J)*((3.0*(WBAR**2)) - 1.0)
      TRM3 = DELZ*(TRM3A - TRM3B)
      DCDZ = DELCI + TRM3
      RETURN
 50   DCDZ = 0.0
      RETURN
      END
      SUBROUTINE DRVTNP(I,Z,VP,DXDVP,DTDVP,ZLOW,ZUP)
      COMMON VPA,I1,NCS,ZI(100),CI(100),ASOL(100)
```

```
      EXTERNAL FDTDVP,FDXDVP,CMVP
      VPA = VP
      A = ZLOW
      B = Z
      IF(I .LT. 0) GO TO 100
      A = ZUP
      B = Z
      PRINT*,"A=",A
  100 VPSQ = VP**2
      CSPSQ = CSP(B)**2
      DNTR = (CSP(B)*DCDZ(B))*(SQRT(VPSQ - CSPSQ))
      TRMOUT = VP/DNTR
      D = 1.E-6
      CALL QUAD(A,B,D,REL,1,AINTX,FDXDVP,NERR,0)
      IF (I .LT. 0) GO TO 200
      DXDVP = -TRMOUT + AINTX
  200 DXDVP = TRMOUT - AINTX
      CALL QUAD(A,B,D,REL,1,AINTT,FDTDVP,NERR,0)
      IF (I .LT. 0) GO TO 300
      DTDVP = -TRMOUT - AINTT
  300 DTDVP = TRMOUT + AINTT
      RETURN
      END
      SUBROUTINE MOLINT(Z1,Z2,AMXIN,AMTIN)
      EXTERNAL FAMXIN,FAMTIN
      A = Z1
      B = Z2
      D = 1.E-6
      CALL QUAD(A,B,D,REL,0,AMXIN,FAMXIN,NERR,0)
      CALL QUAD(A,B,D,REL,0,AMTIN,FAMTIN,NERR,0)
      RETURN
      END
      SUBROUTINE DSDVP(I,Z,VP,DXDVP,DTDVP,ZLOW,ZUP,AMXIN,AMTIN,
     1DXDVPT,DTDVPT)
      COMMON VPA,I1,NCS,ZI(100),CI(100),ASOL(100)
      EXTERNAL FDTDVP,FDXDVP,FAMXIN,FAMTIN
      I = 1
      Z = ZI(5)
      CALL DRVTNP(I,Z,VP,DXDVPU,DTDVPU,ZLOW,ZUP)
      I = -1
      Z = ZI(3)
      CALL DRVTNP(I,Z,VP,DXDVPL,DTDVPL,ZLOW,ZUP)
      Z1 = ZI(3)
      Z2 = ZI(5)
      CALL MOLINT(Z1,Z2,AMXIN,AMTIN)
      DXDVPT = DXDVPL + AMXIN + DXDVPU
      DTDVPT = DTDVPL + AMTIN + DTDVPU
      RETURN
      END
      FUNCTION FAMXIN(Z)
      COMMON VP,K
      VPSQ = VP**2
      CSPSQ = CSP(Z)**2
      IF (VPSQ .GE. CSPSQ) GO TO 20
      K = 1
   10 TRM1 = 1.E-50
      GO TO 30
   20 K = 0
      TRM1 = (SQRT(VPSQ - CSPSQ))**3
      IF (TRM1 .LT. 1.E-50) GO TO 10
      TRM2 = CSP(Z)*VP
   30 FAMXIN = -TRM2/TRM1
      RETURN
      END
```

```
      FUNCTION FAMTIN(Z)
      COMMON VP,K
      VPSQ = VP**2
      CSPSQ = CSP(Z)**2
      IF (VPSQ .GE. CSPSQ) GO TO 20
      K = 1
   10 TRMA = 1.E-50
      GO TO 30
   20 K = 0
      TRMA = SQRT(VPSQ - CSPSQ)
      IF (TRMA .LT. 1.E-50) GO TO 10
      TRM3 = 1.0/(CSP(Z)*TRMA)
      TRM4 = VPSQ/(CSP(Z)*(TRMA**3))
   30 FAMTIN = TRM3 - TRM4
      RETURN
      END
      FUNCTION DCDZS(Z)
      COMMON VP,I1,NCS,ZI(100),CI(100),ASOL(100)
      ZL = ZI(1)
      ZP = ZI(NCS)
      IF(Z .LT. ZL) GO TO 50
      IF(Z .GT. ZP) GO TO 50
      I = NCS
   10 J = I-1
      ZTEST = ZI(J)
      IF(Z .GT. ZTEST) GO TO 40
      I = J
      GO TO 10
   40 CONTINUE
      Z IS BETWEEN ZI(I-1) AND ZI(J)
      DELZ = ZI(I) - ZI(J)
      W = (Z - ZI(J))/DELZ
      WBAR = 1.0 - W
      DCDZS = 6.0*((WBAR*ASOL(J)) + (W*ASOL(I)))
      RETURN
   50 DCDZS = 0.0
      RETURN
      END
      FUNCTION FDXDVP(Z)
      COMMON VP,K
      CSPSQ = CSP(Z)**2
      VPSQ = VP**2
      DCDZSQ = DCDZ(Z)**2
      IF(VPSQ .GE. CSPSQ) GO TO 50
      K = 1
   40 DN = 1.E-50
      GO TO 60
   50 K = 0
      DN = DCDZSQ*(SQRT(VPSQ - CSPSQ))
      IF(DN .LT. 1.E-50) GO TO 40
   60 FDXDVP = (VP*DCDZS(Z))/DN
      RETURN
      END
      FUNCTION FDTDVP(Z)
      COMMON VP,K
      REAL NMA,NMB,NMC,NM
      CSPSQ = CSP(Z)**2
      VPSQ = VP**2
      DCDZSQ = DCDZ(Z)**2
      CSPCUB = CSP(Z)**3
      IF(VPSQ .GE. CSPSQ) GO TO 70
      K = 1
   60 DN = 1.E-50
      GO TO 80
```

```
70  K = 0
    DN = SQRT(VPSQ - CSPSQ)
    IF(DN .LT. 1.E-50) GO TO 60
    NMA = 1.0/CSP(Z)
    NMB = (2.0*VPSQ)/CSPCUB
    NMC = (VPSQ*DCDZS(Z))/(CSPSQ*DCDZSQ)
    NM = NMA - NMB - NMC
 80 FDTOVP = NM/DN
    RETURN
    END
    FUNCTION RDXOZ(Z)
    COMMON VP,K
    CSPSQ = CSP(Z)**2
    VPSQ = VP**2
    IF (CSPSQ .LE. VPSQ) GO TO 10
    K = 1
  5 DSQ = 1.E-50
    GO TO 20
10  K = 0
    DSQC = 1./CSPSQ
    DSQV = 1./VPSQ
    DSQ = DSQC - DSQV
    IF (DSQ .LT. 1.E-50) GO TO 5
20  RDXOZ = (1./VP)/SQRT(DSQ)
    RETURN
    END
    FUNCTION RDTOZ(Z)
    COMMON VP,K
    CSPSQ = CSP(Z)**2
    VPSQ = VP**2
    IF (CSPSQ .LE. VPSQ) GO TO 30
    K = 1
 20 DSQ = 1.E-50
    GO TO 40
30  K = 0
    DSQC = 1./CSPSQ
    DSQV = 1./VPSQ
    DSQ = DSQC - DSQV
    IF (DSQ .LT. 1.E-50) GO TO 20
40  RDTDZ = (1./CSPSQ)/SQRT(DSQ)
    RETURN
    END
    FUNCTION RAINT(DSDZR,ZLOW,ZUP)
    EXTERNAL DSDZR
    ZAVE = (ZUP + ZLOW)/2.0
    D = 1.E-6
    CALL QUAD(ZLOW,ZAVE,D,REL,1,ANS1,DSDZR,NERR,0)
    CALL QUAD(ZUP,ZAVE,D,REL,1,ANS2,DSDZR,NERR,0)
    RAINT = (ANS1 - ANS2)
    RETURN
    END
```

Bibliography of Related Works

Albers, V. M., Underwater Sound (Dowden, Hutchinson and Ross, Inc., Stroudsburg, Pa., 1972).

Barnes, A. and L. P. Solomon, "Some Curious Analytical Ray Paths for Some Interesting Velocity Profiles in Geometrical Acoustics", J. Acoust. Soc. Am., 53, 148 (1973).

Barry, G., "Ray Tracings of Acoustic Waves in the Upper Atmosphere", J. Atmos. Terrest. Phys., 25, No. 11, 621 (1963).

Bergman, P. G., "The Wave Equation in a Medium with a Variable Index of Refraction", J. Acoust. Soc. Am., 17, 329 (1946).

Brekhovskikh, L. M., "A Limiting Case of Sound Propagation in Natural Wavelengths", Sov. Phys. Acoust., 10, 89 (1964).

Brekhovskikh, L. M., "The Average Field in an Underwater Sound Channel", Sov. Phys. Acoust., 11, 126 (1965).

Brekhovskikh, L. M., Waves in Layered Media (Academic Press, New York, 1960).

Brekhovskikh, L. M., "Possible Role of Acoustics in the Exploring of the Ocean", Rapports du 5e Congrés International d'Acoustique, Vol. II: Conférences Générales, Liége (1965).

Bucker, H. P., "Sound Propagation in a Channel with Lossy Boundaries", J. Acoust. Soc. Am., 48, 1187 (1970).

Budden, K. G., The Waveguide Mode Theory of Wave Propagation (Academic Press, Inc., New York, 1961).

Chen, K. C. and D. Ludwig, "Calculation of Wave Amplitudes by Ray Tracing", J. Acoust. Soc. Am., 54, 431 (1973).

Clark, R. H., "Sound Propagation in a Variable Ocean", J. Sound Vib., 34, (4), 457 (1974).

Clark, R. H., "Theory of Acoustic Propagation in a Variable Ocean", NATO SACLANTCEN Memorandum SM28 (1973).

Davis, J. A., "Extended Modified Ray Theory Field in Bounded and Unbounded Inhomogenious Media", J. Acoust. Soc. Am., 57, 276 (1975).

Deakin, A. S., "Asymptotic Solution of the Wave Equation with Variable Velocity and Boundary Conditions", SIAM J. Appl. Math., 23, No. 1, (1972), and Appl. Mech. Rev., 5417 (No. 7, 1974).

Denham, R. N., "Asymptotic Solutions for the Sound Field in Shallow Water with a Negative Sound Velocity Gradient", J. Acoust. Soc. Am., 45, 365 (1969).

Eby, E. S., "Frenet Formulation of Three-Dimensional Ray Tracing", J. Acoust. Soc. Am., 42, 1287 (1967).

Eby, E. S., "Geometric Theory of Ray Acoustics", J. Acoust. Soc. Am., 47, 273 (1970).

Eby, R. K., A. O. Williams, R. P. Ryan and P. Tamarkin, "Study of Acoustic Propagation in a Two-Layered Model", J. Acoust. Soc. Am., 32, 89 (1960).

Eckart, C., Hydrodynamics of Oceans and Atmospheres (Pergamon Press, New York, 1960).

Ewing, W. M., W. S. Jardetsky and F. Press, Elastic Waves in Layered Media (McGraw-Hill Book Co., New York, 1957).

Fitzgerald, R. M, A. N. Guthrie, D. A. Nutile, and J. D. Shaffer, "Influence of the Subsurface Sound Channel on Long-Range Propagation Paths and Travel Times", J. Acoust. Soc. Am., 55, 47 (1974).

Gossard, E. E. and W. H. Hooke, Waves in the Atmosphere (Elsevier Scientific Publ. Co., New York, 1975).

Gutenberg, B., "Propagation of Sound Waves in the Atmosphere", 14, 151 (1942).

Guthrie, K. M., "Wave Theory of SOFAR Signal Shape", J. Acoust. Soc. Am., 56, 827 (1974).

Guthrie, K. M., "The Connection Between Normal Modes and Rays in Under-Water Sound", J. Sound Vib., 32, No. 2, 289 (1974).

Hale, F. E., "Long-Range Propagation in the Deep Ocean", J. Acoust. Soc. Am., 33, 456 (1961).

Hirsh, P., "Acoustic Field of a Pulsed Source in the Underwater Sound Channel", J. Acoust. Soc. Am., 38, 1018 (1965).

Jacobson, M. J., W. L. Siegman, N. L. Weinberg and J. G. Clark, "Perturbation Method for Determining Acoustic Ray in Two-Dimensional Sound-Speed Medium", J. Acoust. Soc. Am., 57, 843 (1975).

Jobst, W. J., "An application of Poisson Process Models to Multipath Sound Propagation of Sinusoidal Signals", J. Acoust. Soc. Am., 57, 1409 (1975).

Katz, E. J., "Effects of the Propagation of Internal Water Waves on Underwater Sound Transmission", J. Acoust. Soc. Am., 42, 83 (1967).

Krol, H. R., "Intensity Calculations along a Single Ray", J. Acoust. Soc. Am., 53, 864 (1973).

Krol, H. R., "Some Ray and Intensity Solutions in the Compley Plane", J. Acoust. Soc. Am., 54, 96 (1973).

Lysanov, V. P., "Average Decay in a Surface Sound Channel with an Uneven Boundary", Sov. Phys. Acoust. 12, 425 (1967).

Macpherson, J. D. and M. J. Daintith, "Practical Model of Shallow-Water Acoustic Propagation", J. Acoust. Soc. Am., 41, 850 (1966).

McKinnon, R. F., J. S. Partridge and S. H. Tobe, "Calculation of Ray-Acoustic Intensity", J. Acoust. Soc. Am., 52, 1471 (1972).

Mezzino, M. J., "Ray Acoustics Model of the Ocean Incorporating a Sound Velocity Profile with a Continuous Second Derivative", J. Acoust. Soc. Am., 53, 581 (1973).

Milder, D. M., "Ray and Wave Invariant for SOFAR Channel Propagation", J. Acoust. Soc. Am., 46, 1259 (1969).

Miller, M. K., "Calculation of Horizontal Ranges and Sound Intensities by Use of Numerical Integration Techniques", J. Acoust. Soc. Am., 44, 1690 (1968).

Munk, W. H., "Sound Channel in an Exponentially Stratified Ocean, with Applications to SOFAR", J. Acoust. Soc. Am., 55, 220 (1974).

Murphy, E. L., "Modified Ray Theory for Two Turning-Point Problem", J. Acoust. Soc. Am., 47, 899 (1970).

Murphy, E. L., "Modified Ray Theory for Bounded Media", J. Acoust. Soc. Am., 56, 1747 (1974).

Neubert, J. A., "Multipath Summability in Ray Theory Intensity Calculations in the Real Ocean", J. Acoust. Soc. Am., 51, 310 (1972).

Nicholas, N. C., "Perturbation Calculations of Propagation Loss in the Deep Ocean", J. Acoust. Soc. Am., 49, 1621 (1971).

Nomady, V. G. and H. Überall, "Sound Propagation and Attenuation in the Deep Ocean at Very Long Ranges", J. Acoust. Soc. Am., 320 (1975).

Officer, C. B., Sound Transmission, (McGraw-Hill, New York, 1958).

Pedersen, M. A., "Theory of the Axial Ray", J. Acoust. Soc. Am., 45, 157 (1969).

Pedersen, M. A. and DeWayne White, "Ray Theory for Source and Receiver on an Axis of Minimum Velocity", J. Acoust. Soc. Am., 48, 1219 (1970).

Pedersen, M. A. and DeWayne White, "Ray Theory of the General Epstein Profile", J. Acoust. Soc. Am., 44, 765 (1968).

Pedersen, M. A. and D. F. Gordon, "Comparison of Curvilinear and Linear Profile Approximation in the Calculation of Underwater Sound Intensities by Ray Theory", J. Acoust. Soc. Am., 41, 419 (1967).

Pedersen, M. A., "Acoustic Intensity Anomalies Introduced by Constant Velocity Gradients", J. Acoust. Soc. Am., 33, 465 (1961).

Pedersen, M. A., and D. F. Gordon, "Normal-Mode and Ray Theory Applied to Underwater Acoustic Conditions of Extreme Downward Refraction", J. Acoust. Soc. Am., 51, 232 (1972).

Pedersen, M. A. and D. F. Gordon, "Theoretical Investigations of a Double Family of Normal Modes in an Underwater Acoustic Surface Duct", J. Acoust. Soc. Am., 47, 304 (1970).

Pedersen, M. A., "Ray Theory Applied to a Wide Class of Velocity Functions", J. Acoust. Soc. Am., 43, 619 (1968).

Pekeris, C. L., "Theory of Propagation of Sound in a Half-Space of Variable Sound Velocity Under Conditions of Formation of a Shadow Zone", J. Acoust. Soc. Am., 18, 295 (1946).

Pekeris, C. L., "Theory of Propagation of Explosive Sound in Shallow Water," Geol. Soc. Am. Mem., 27, 1 (1948).

Potter, D. S. and S. R. Murphy, "Solution of the Wave Equation in a Medium with a Particular Velocity Variation", J. Acoust. Soc. Am., 34, 963 (1962).

Raphael, D. T., "New Approach to the Determination of Acquiring Rays in Singly and Doubly Layered Oceans", J. Acoust. Soc. Am., 48, 1249 (1970).

Raphael, D. T., "Closed-Form Solutions for SOFAR Ray Acoustics in Media with Bilinear Sound-Speed Profiles", J. Acoust. Soc. Am., 56, 80 (1974).

Shuby, M. T. and R. Halley, "Measurement of the Attenuation of Low-Frequency Underwater Sound", J. Acoust. Soc. Am., 29, 464 (1957).

Silbiger, A., "Phase Shift at Caustics and Turning Points", J. Acoust. Soc. Am., 44, 653 (1967).

Solomon, L. P., D. K. Y. Ai and G. Haven, "Acoustic Propagation in a Continuously Refracting Medium", J. Acoust. Soc. Am., 44, 1121 (1968).

Solomon, L. P., A. Barnes and S. Port, "Fitting Velocity Profiles with Two-Dimensional Cubic Splines", J. Acoust. Soc. Am., 56, 1389 (1974).

Solomon, L. P., W. C. Merx, "Technique for Investigating the Sensitivity of Ray Theory to Small Changes in Environmental Data", J. Acoust. Soc. Am., 56, 1126 (1974).

Solomon, L. P., "Geometric Acoustics with Frequency Dependence", J. Acoust. Soc. Am., 44, 1115 (1968).

Solomon, L. P. and L. Armijo, "Intensity Differential Equation in Ray Acoustics", J. Acoust. Soc. Am., 50, 960 (1971).

Solomon, L. P. and C. Comstock, "Two-Time Methods Applied to Underwater Acoustics", J. Acoust. Soc. Am., 54, 110 (1973).

Stewart, K. R., "Ray Acoustic Model of the Ocean Using a Depth/Sound-Speed Profile with a Continuous First Derivative", J. Acoust. Soc. Am., 38, 339 (1965).

Stickler, D. C., "Normal-Mode Program with Both the Discrete and Branch Line Contributions", J. Acoust. Soc. Am., 57, 856 (1975).

Tolstoy, I., Wave Propagation (McGraw-Hill Book Co, New York, 1973).

Tolstoy, I. and C. S. Clay, Ocean Acoustics (McGraw-Hill, New York, 1966).

Tolstoy, I., "W.K.B. Approximation, Turning Points, and the Measurement of Phase Velocities", J. Acoust. Soc. Am., 52, 356 (1972).

Ugencius, P., "Intensity Equations in Ray Acoustics. I.", J. Acoust. Soc. Am., 45, 193 (1969).

Ugencius, P., "Intensity Equations in Ray Acoustics. II.", J. Acoust. Soc. Am., 45, 206 (1969).

Ugencius, P., "Intensity Equations in Ray Acoustics. III. Exact Two-Dimensional Formulation", J. Acoust. Soc. Am., 47, 339 (1970).

Uride, R. J., "Intensity Sumation of Modes and Images in Shallow-Water Sound Transmission", J. Acoust. Soc. Am., 46, 780 (1969).

Warfield, J. T. and M. J. Jacobson, "Invariance of Geometric Spreading Loss with Changes in Ray Parameterization", J. Acoust. Soc. Am., 50, 342 (1971).

Weinberg, H. and R. Bunidge, "Horizontal Ray Theory for Ocean Acoustics", J. Acoust. Soc. Am., 55, 63 (1974).

Weinberg, H., "Continuous-Gradient Curve-Fitting Technique for Acoustic Ray Analysis", J. Acoust. Soc. Am., 50, 975 (1971).

Weinberg, N. L. and T. Dunderdale, "Shallow Water Ray Tracing with Nonlinear Velocity Profiles", J. Acoust. Soc. Am., 52, 1000 (1972).

Weston, D. E., "Guided Propagation in a Slowly Varying Medium", Proceedings of the Physical Society LXXIII, 3.

White, DeWayne, "Velocity Profiles that Produce Acoustic Focal Points on an Axis of Minimum Velocity", J. Acoust. Soc. Am., 46, 1318 (1969).

Williams, A. O. and W. Horne, "Axial Focusing of Sound in the SOFAR Channel", J. Acoust. Soc. Am., 41, 189 (1967).

Wood, D. H., "Parameterless Examples of Wave Propagation", J. Acoust. Soc. Am., 54, 1727 (1973).

Wood, D. H., "Refraction Correction in Constant Gradient Media", J. Acoust. Soc. Am., 47, 1448 (1970).

Wood, D. H., "Green's Functions for Unbounded Constant Gradient Media", J. Acoust. Soc. Am., 46, 1333 (1969).

Yeh, K. C. and C. H. Liu, Theory of Ionospheric Waves (Academic Press, New York, 1972).

E-25-638

ATMOSPHERIC ACOUSTIC GRAVITY MODES AT FREQUENCIES NEAR AND BELOW LOW FREQUENCY CUTOFF IMPOSED BY UPPER BOUNDARY CONDITIONS

by

Allan D. Pierce, Wayne A. Kinney and Christopher Y. Kapper

School of Mechanical Engineering
Georgia Institute of Technology

Contract No. F19628-74-C-0065
Project No. 7639

SCIENTIFIC REPORT NO. 1

Contract Monitor: Elisabeth F. Iliff
Terrestrial Sciences Laboratory

Prepared for

AIR FORCE CAMBRIDGE RESEARCH LABORATORIES
OFFICE OF AEROSPACE RESEARCH
UNITED STATES AIR FORCE
BEDFORD, MASSACHUSETTS 01730

ABSTRACT

Perturbation techniques are described for the computation of the imaginary part of the horizontal wave number (k_I) for modes of propagation. Numerical studies were carried out for a model atmosphere terminated by a constant sound speed (478 m/sec) half space above an altitude of 125 km. The GR_0 and GR_1 modes have lower frequency cutoffs. It was found that for frequencies less than 0.0125 radian/sec, the GR_1 mode has complex phase velocity; k_I varying from near zero up to a maximum of 3×10^{-4} with analogous results for the GR_0 mode. There is an extremely small frequency gap for each mode for which no poles in the complex k plane corresponding to that mode exist. These mark the transition from undamped propagation to damped propagation. In the complete Fourier synthesis, branch line contributions compensate for the absence of poles in these gaps. Computational procedures are described which facilitate the inclusion of the low frequency portions of these modes in the waveform synthesis.

INTRODUCTION

One of the standard mathematical problems in acoustic wave propagation is that of predicting the acoustic field at large horizontal distances from a localized source in a medium whose properties vary only with height. This problem, as well as its counterpart in electromagnetic theory, has received considerable attention in the literature,[1] is reviewed extensively in various texts[2-7], and, for the most part, may be considered to be well understood.

A typical formulation of, say, the transient propagation problem [8-9] leads (at sufficiently large horizontal distance r) to an intermediate result which may be expressed as a double Fourier integration over angular frequency ω and horizontal wave number k; i.e. for, say, the acoustic pressure, one has

$$p = S(r)\ \mathrm{Re}\left\{\int_0^\infty \hat{f}(\omega)e^{-i\omega t}\int_{-\infty}^{\infty}[Q/D(\omega,k)]e^{ikr}\,dk\,d\omega\right\} \qquad (1)$$

Here S(r) is a geometrical spreading factor, $1/\sqrt{r}$ for horizontally stratified media, $1/[a_e\sin(r/a_e)]^{1/2}$ if the earth curvature (a_e=radius of earth) is to be approximately taken into account. The quantity $\hat{f}(\omega)$ is a Fourier transform of some function characterizing the time dependence of the source; $Q(\omega,k,z,z_o)$ is a function of receiver and source heights z and z_o as well as of ω and k, possibly also of horizontal direction of propagation if, say, winds are included in the formulation, but, in any event, should have no poles in the complex k plane for given real positive ω, and given z and z_o. The denominator $D(\omega,k)$ is independent of z and z_o, may be zero for certain values $k_n(\omega)$ of k, and is termed the <u>eigenmode dispersion function</u>.

Typically, in order to uniquely specify both Q and $D(\omega,k)$ for all complex values of k (given ω real and positive), branch points must be identified and branch cuts must be placed in the complex k plane. The general rule may be taken to be that no branch cut should cross the real axis, and, if a branch point should lie on the real axis (when ω is positive real), the branch cut either extends into the upper or lower half plane depending on whether the branch point moves up or down when ω is given a small positive imaginary part. The integration contour for the k integration goes nominally along the real axis but skirts below or above (see Fig. 1a) those poles lying on the real axis which move up or down, respectively, when ω is given a small positive imaginary part. The placing of the branch cuts and the selection of the contour in this manner is one method of guaranteeing causality in the solution, or, equivalently, of guaranteeing that the solution dies out at large distances if a slight amount of damping (Rayleigh's virtual viscosity) is added in the mathematical formulation. The necessity of branch cuts only occurs if the medium is unbounded either from above or below and a choice of phases can always be made such that (given, say, that the medium is unbounded from above) Q dies out exponentially as $z \to \infty$ when ω has a small positive imaginary part and when k is real.

The so-called guided mode description of the far field waveform arises when the contour for the k integration is deformed (permissible because of Cauchy's theorem and of Jordan's lemma[10]) to one such as is sketched in Fig. 1b. The poles above the initial contour are encircled in the counterclockwise manner. There are also contour segments which encircle each branch cut lying above the real axis in the counterclockwise sense. The integrals around each pole are evaluated by Cauchy's residue theorem and one is left with a sum of residue terms plus branch line integrals. Each residue term may be considered as corresponding to a particular guided mode of propagation. The branch line contributions in some contexts are considered as corresponding to what may be termed lateral waves.[11] (The term may be unappropriate unless there is a

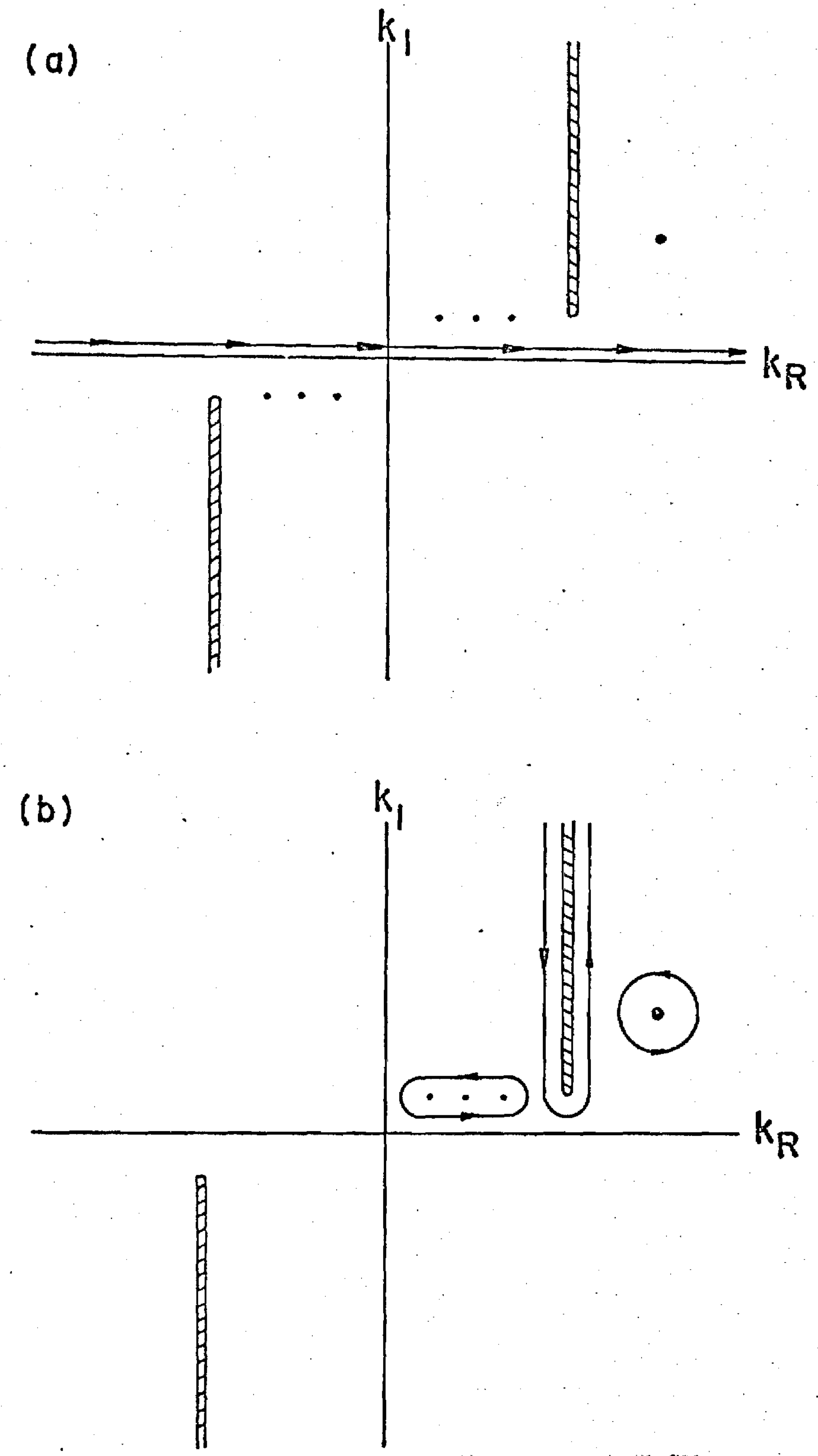

1. Contours in the complex k (wavenumber) plane for evaluation of individual frequency contributions to waveform synthesis. (a) Original contour. (b) Deformed contour.

sharply defined interface separating two types of media, such as a water-muddy bottom interface in shallow water propagation.)

In regards to the guided mode description, one type of approximation frequently made is to neglect all poles (i.e. roots $k_n(\omega)$ of $D(\omega,k)$) which are above the real axis, the argument being that the corresponding e^{ikr} factors in the residues will die out rapidly with increasing r, the bulk of the contribution at large r expected to come from the poles which lie on the real axis. In a similar manner, it is argued that the branch line contour contribution also dies out relatively rapidly (a factor of $1/r^{3/2}$ in addition to the geometrical spreading) so it too may be neglected at large r compared to the terms coming from the real roots. The net result for Eq. (1) would then be

$$p = \sum_n S(r) \int_{\omega_{Ln}}^{\omega_{Un}} A_n(\omega) \cos[\omega t - k_n(\omega) r + \phi_n(\omega)]\, d\omega \tag{2}$$

where $A_n(\omega)$ and $\phi_n(\omega)$ are defined in terms of the magnitude and phase of the residues of the integrand in Eq.(1); the $k_n(\omega)$ being the real roots of $D(\omega,k)=0$, numbered in some order with the index n=1, 2, 3, etc., and it being understood that, for fixed n, $k_n(\omega)$ should be a continuous function of ω over some range of ω from a lower limit ω_{Ln} up to an upper limit ω_{Un}. The remaining integral over ω can then be approximately evaluated by the method of stationary phase or integrated by suitable numerical methods.

In the present paper, a somewhat subtle set of circumstances intrinsic to low frequency infrasound propagation in the atmosphere is discussed for which the arguments leading to the approximation of Eq.(1) by (2) are not wholly valid, even at distances of the order of more than a quarter of the earth's circumference. We suspect that comparable circumstances may arise in other contexts, but the present discussion is, for simplicity, illustrated only by examples from atmospheric infrasound propagation.

I. INFRASOUND MODES

An atmosphere model frequently adopted for infrasound studies is one in which the sound speed c varies continuously with height z in a more or less realistic manner (Fig.2a) but is constant ($=c_T$) for all heights above some specified height z_T. [If winds are included in the formulation, their velocities are also assumed constant in the upper half space, $z>z_T$.] Conceivably, one has some latitude in the choice of z_T and of the upper halfspace sound speed c_T, although computations of factors such as $Q(\omega,k,z,z_o)$ and $D(\omega,k)$ in Eq. (1) become more lengthy with increasing z_T. Also, it would seem that the most logical choice of c_T would be that which would realistically correspond to height z_T, so the profile c(z) would be continuous with height across z_T, as in Fig. 2a. Another conceivable choice would be one (Fig. 2b) in which $c_T \to \infty$, such that the surface of air nominally at z_T would be a free surface or pressure release surface (corresponding to the model generally adopted for the water-air interface in underwater sound studies). A somewhat intuitive premise which may be adopted is that, if the source and receiver are both near the ground and if the energy actually reaching the receiver travels via propagation modes channeled primarily in the lower atmosphere, then the actual value of the integral in Eq. (1) would be somewhat insensitive to the choices of z_T and c_T. This, however, remains to be justified in any rigorous sense, so we would be somewhat hesitant to take $c_T = \infty$ at the outset. In typical calculations performed in the past, z_T is taken as 225 km, c_T is taken as the sound speed ($\simeq$ 800 m/sec) at that altitude.

Since one is often interested in frequencies (typically corresponding to periods greater than, say, 1 to 5 minutes) at which gravitational effects are important, the formulation leading to the infrasound version of Eq. (1) is based on the fluid dynamic equations with gravitational body forces and the associated nearly exponential decrease of ambient density and pressure with height included.

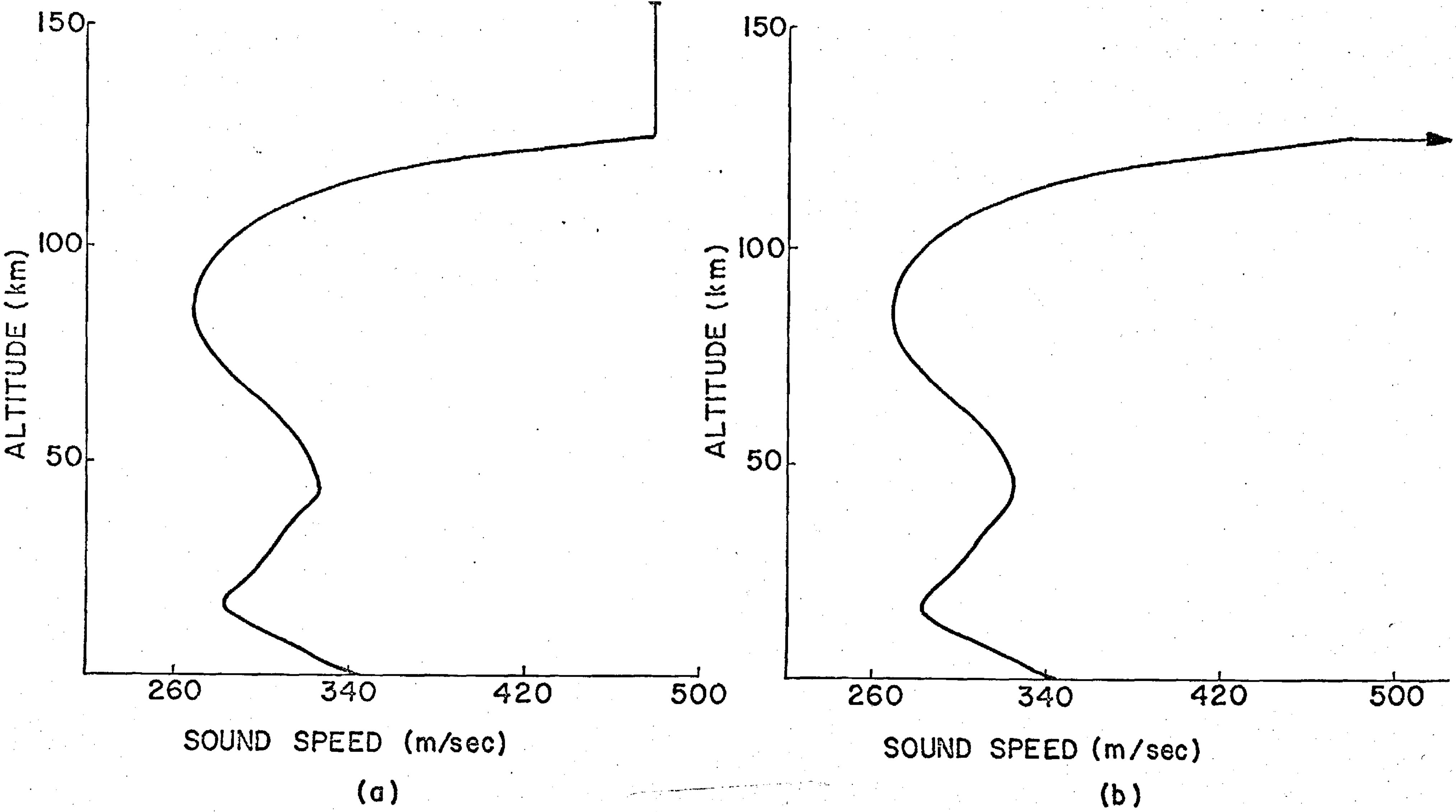

2. Idealizations of model atmospheres (altitude profiles of sound speed) used in acoustic-gravity wave studies. (a) Atmosphere terminated by an upper half space with constant sound speed. (b) Atmosphere temperature formally going to infinity at some finite altitute corresponding to a free surface ($p \simeq 0$) at that altitude.

The incorporation of gravity leads, among other effects, to a somewhat complicated dispersion relation for plane type waves in the upper half space when c_T is finite, i.e. one can have solutions of the linearized fluid dynamics equations for $z > z_T$ of the form[8,9]

$$p/\sqrt{\rho_o} = (\text{Constant})\ e^{-i\omega t}\ e^{ikx}\ e^{ik_z z} \tag{3}$$

where the vertical wave number k_z (alternately written as iG for inhomogeneous plane waves) and the horizontal wave number k are related by the dispersion relation (neglecting winds)

$$k_z^2 = -G^2 = [\omega^2 - \omega_A^2] / c^2 - [\omega^2 - \omega_B^2]\ k^2 / \omega^2 \tag{4}$$

where $\omega_A = (\gamma/2)g/c$, $\omega_B = (\gamma-1)^{1/2}\ g/c$ are two characteristic frequencies $[\omega_A > \omega_B]$ for wave propagation in an isothermal atmosphere ($g \simeq 9.8$ m/s^2 is acceleration due to gravity, $\gamma \approx 1.4$ is specific heat ratio). Here, for brevity, the subscript T on c_T has been omitted. For given real positive ω, real k, one can have k_z^2 positive or negative (G^2 negative or positive). The values of k at which k_z^2 or G^2 go to zero turn out, as might well be expected, to be the branchpoints in the k integration in Eq. (1), i.e., synonymous with the branch points of G. Along the real axis, G is either real and positive ($e^{ik_z z}$ or e^{-Gz} dying out with increasing z) or else G is a positive or negative imaginary quantity. In the latter case, the phase of G may be either $\pi/2$ or $-\pi/2$, in accordance with the well known fact that, for acoustic-gravity waves, wavefronts may be moving obliquely downwards (negative k_z) when energy is flowing obliquely upwards. In particular, for $0 < \omega < \omega_B$, one has G real and positive for k in between the two branch points on the real axis, the phase of G is $\pi/2$ ($k_z < 0$) on the remainder of the real axis; the two branch points are, from Eq. (4), at

$$k_{BR}^{+,-}(\omega) = \pm \frac{\omega[\omega_A^2 - \omega^2]^{1/2}}{c[\omega_B^2 - \omega^2]^{1/2}} \tag{5}$$

The branch lines extend upwards and downwards from the positive and negative branch points, respectively. [See Fig. 1.]

The dispersion function $D(\omega,k)$ in the atmospheric infrasound case can be written in the general form

$$D(\omega,k) = A_{12}R_{11} - A_{11}R_{12} - R_{12}G \tag{6}$$

where R_{11} and R_{12} are elements of a transmission matrix [R], these depend on the atmosphere's properties only in the altitude range 0 to z_T, they are independent of what is assumed for the upper half space. In general, their determination requires numerical integration over height of two simultaneous ordinary differential equations (termed the <u>residual equations</u>[8,9,12] in previous literature). They do depend on ω and k (or, alternately, on ω and phase velocity v) but are free from branch cuts, they are real when ω and k are real and are finite for all finite values of ω and k. The other parameters A_{12} and A_{11} depend only on the properties of the upper half space (in addition to ω and k). Specifically, these are given (for the no wind case and with the subscript T omitted on c_T)

$$A_{11} = gk^2/\omega^2 - \gamma g/[2c^2] \tag{7a}$$

$$A_{12} = 1 - c^2k^2/\omega^2 \tag{7b}$$

One may note that, since every quantity in Eq. (6) is necessarily real when ω and k are real (with the possible exception of G), the poles lying on the real k axis (real roots of D) must be in the regions of the (ω,k) plane [or (ω,v) plane] where $G^2 > 0$. Since the integrand of Eq. (1) divided by $\sqrt{\rho_o}$ should vary with z above z_T as e^{-Gz_T} one may call the corresponding modes <u>fully ducted modes</u>. There is no net leakage of energy for such natural modes into the upper halfspace. If one considers D as a function of ω and phase velocity v_p (or simply v), where $v = \omega/k$, the locus of real roots v versus ω (dispersion curves) has (as has been found by numerical calculation) the general form sketched in Fig. 3. The nomenclature for labeling the modes (GR for gravity, S for sound) is due to Press and Harkrider. One may note from Eq. (4) that there are two "forbidden regions" in the v vs. ω plane, i.e.

$$v < c[\omega_B^2 - \omega^2]^{\frac{1}{2}} / [\omega_A^2 - \omega^2]^{\frac{1}{2}} \tag{8a}$$

for $\omega < \omega_B$ and

$$v > c[\omega^2 - \omega_B^2]^{\frac{1}{2}} / [\omega^2 - \omega_A^2]^{\frac{1}{2}} \tag{8b}$$

for $\omega > \omega_A$. Within either of these regions G would have to be imaginary and there would accordingly be no real roots for v of $D(\omega,v) = 0$. In the high frequency limit, this simply implies that the phase velocities of propagating modes are always less than the sound speed of the upper halfspace, the branch points in the k plane are simply at $\pm\ \omega/c_T$. The low frequency lower phase velocity "forbidden region" appears to be due to the incorporation of gravity effects into the formulation. However, if c_T is allowed to approach ∞, this lower left hand corner region disappears. We have done numerical studies on the effects of varying c_T on the dispersion curves. Briefly, the result is that the form of the predicted curves for GR_o and GR_1 change very little

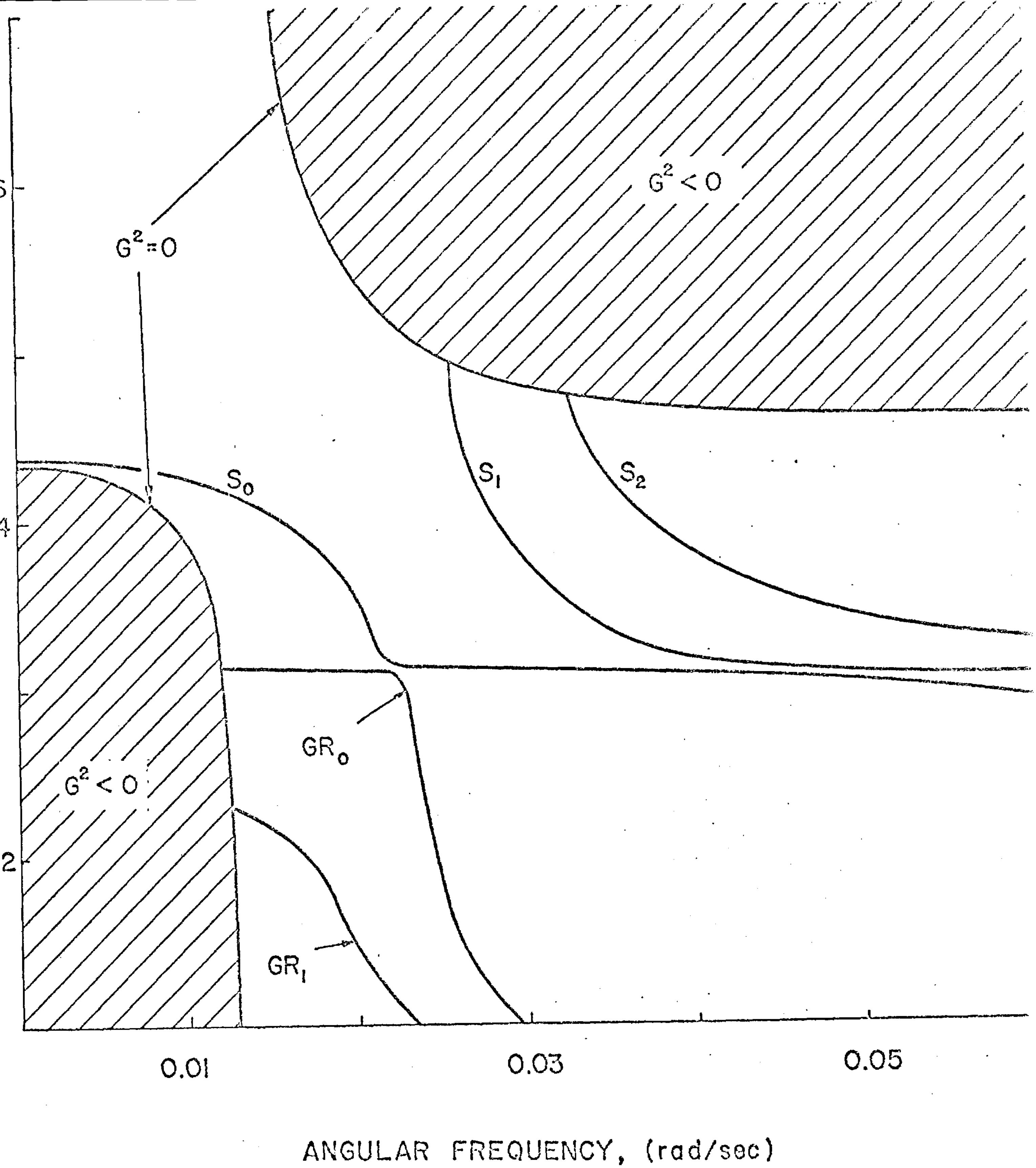

3. Numerically derived plots of phase velocity v versus angular frequency ω for infrasonic modes in a model atmospherc corresponding to Fig. 2. The labeling of modes is with the convention introduced by Press and Harkrider (J. Geophy. Res. 67, 3889-3908 (1962). The lines $G^2=0$ delimit regions of the v versus ω plane where a real root of the eigenmode dispersion function cannot be found.

with increasing c_T; the lower forbidden regions shrink insofar as frequency range is concerned and the curves extend to successively lower frequencies. Thus we see that the fully ducted modes GR_0 and GR_1 both have a lower frequency cutoff [ω_L in Eq. (2)] which depends on c_T. The larger one makes c_T, the smaller is this cutoff frequency.

We thus have the following apparent paradoxes. Given that frequencies below ω_B may be important for the synthesis of the total waveform, an apparently plausible computation scheme based on the reasoning leading to our Eq. (2) will omit much of the information conveyed by such frequencies. Also, in spite of the plausible premise that energy ducted primarily in the lower atmosphere should be insensitive to the choice for c_T, one sees that this choice governs the cutoff frequencies for certain modes and that certain important frequency ranges could conceivably be omitted entirely by a seemingly logical and proper choice for c_T. The resolution of these paradoxes would seem to lie in the nature of the approximations made in going from Eq. (1) to Eq. (2). The latter may not be as nearly correct as earlier presumed and it may be necessary to include contributions from poles off the real axis and from the branch line integrals. Even if r is undisputably large, it may be that the imaginary parts of the complex wavenumbers are sufficiently small that $|e^{ikr}|$ is still not small compared to unity. Also, a branch line integral may be appreciable in magnitude at large r if there should be a pole relatively close to the branch cut.

II. ROOTS OF DISPERSION FUNCTION

In order to understand the manner in which the solution represented by Eq. (2) should be modified in order to remove the apparent artificial low frequency cutoffs of the GR_o and GR_1 modes, we first examine the nature of the dispersion function D at points in the vicinity of a particular mode's dispersion curve. The curve $v_n(\omega)$ of phase velocity v versus ω for a given (n-th) mode is known at points to the right of the lower cutoff frequency ω_L. Given this, one can find analogous curves $v_a(\omega)$ and $v_b(\omega)$ for values of the phase velocity ω/k at which the functions $R_{11}(\omega,v)$ and $R_{12}(\omega,v)$ in Eq. (6), respectively, vanish. Since there may be more than one such curve in each case, we pick $v_a(\omega)$ and $v_b(\omega)$ such that these curves are the closest of all such curves to the curve $v_n(\omega)$ for $\omega > \omega_L$. One may note, however, that one may apparently define and identify $v_a(\omega)$ and $v_b(\omega)$ for frequencies much less than ω_L, simply from analytical continuation.

A premise which we have checked numerically (see Fig. 4) for a specific case is that the curves $v_n(\omega)$, $v_a(\omega)$, $v_b(\omega)$ defined above with reference to a particular given mode all lie substantially closer to each other than to the corresponding curves for a different mode. In retrospect, this is obvious, although it took some time for us to realize that it was so. Briefly, the argument goes that, if the mode is predominantly guided in the lower atmosphere, then there should be a decay of modal height profiles beyond some point substantially lower than z_T. Thus, both the $p/\sqrt{\rho_o}$ and $\rho_o v_z$ profiles for a guided mode would have values at z_T substantially less than their peak values at lower altitudes. The same would be true for the profiles of the auxiliary functions Φ_1 and Φ_2 which satisfy the residual equations. Consequently, if guided waves are excited, the inverse transmission matrix connecting Φ_1 and Φ_2 at the ground to those at height z_T would have to have very small [1,2] and [2,2] components.

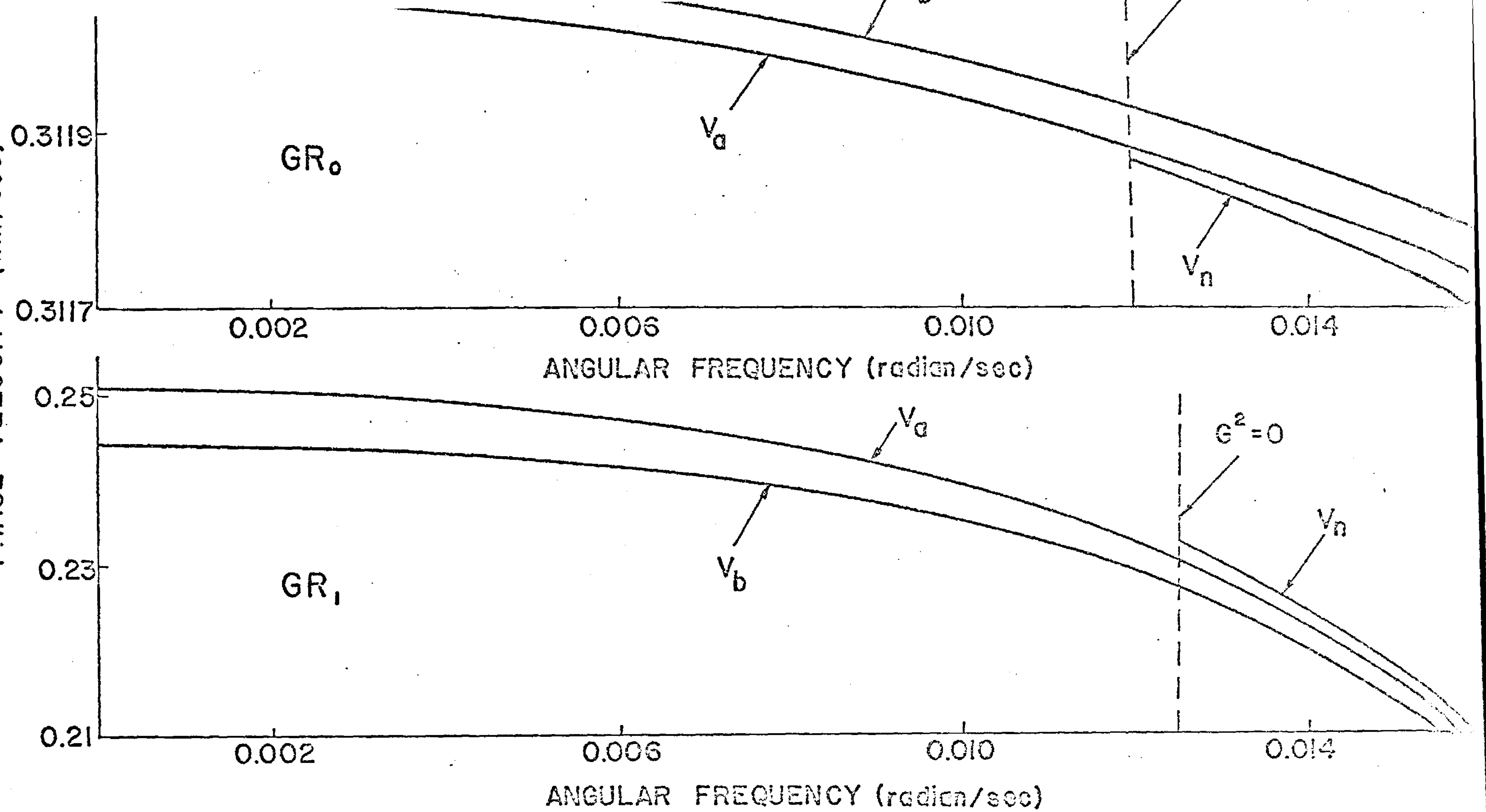

4. Curves in phase velocity (v_n,v_a,v_b) versus angular frequency (ω) plane along which R_{11}=0 (giving $v_a(\omega)$), R_{12}=0 (giving $v_b(\omega)$), and $D(\omega,k)$=0 (giving $v_n(\omega)$). Curves are shown for (a) the GR_o mode and (b) the GR_1 mode. Note the changes in scale and the relatively close spacing of curves corresponding to the same mode. The lines along which G^2=0 are also indicated; $v_n(\omega)$ is not a real quantity for ω values below the indicated lower cutoff frequency.

(Recall that $\Phi_1 = 0$ at the ground.) Since the transmission matrix has unit determinant, it follows that elements R_{12} and R_{11} of the transmission matrix proper [from height Z_T down to the ground and whose elements appear in Eq. (6)] have to be small.

Given the definitions $v_a(\omega)$ and $v_b(\omega)$, the dispersion relation D=0 for a single mode may be written

$$D \approx (A_{12})(\alpha)(v-v_a) - [A_{11} + G](\beta)(v-v_b) = 0 \tag{9}$$

where $\alpha = dR_{11}/dv$, $\beta = dR_{12}/dv$, evaluated at $v = v_a$ and v_b, respectively. (For simplicity, we here consider D as a function of ω and $v = \omega/k$ rather than of ω and k.) The above equation may also equivalently be written in the form

$$v = v_a + (v_a-v_b)X/[1-X] \tag{10a}$$

$$X = (\beta/\alpha)(A_{11} + G)/A_{12} \tag{10b}$$

which may be considered as a starting point for an iterative solution which in essence develops v in a power series in v_a-v_b; G may be considered as a defined function of ω,v. One starts with $v = v_a$ as the zeroth iteration, evaluates the right hand side for the value of v to find the starting point for the next iteration, etc. The considered procedure should converge provided v_a or v_b is not near a point at which G vanishes and providing G in the vicinity of v_a or v_b is not such that the variable X is close to unity. Among other limitations, the iteration scheme would be inappropriate for values of ω in the immediate vicinity of ω_L.

In regards to establishing the general trends represented by the iterative type solutions, two relatively general theorems may be of use. These (whose proof follows along lines previously used by one of the authors[13] in deriving an integral expression for group velocity) are that for real positive ω and v,

$$R_{12}\ \partial R_{11}/\partial v - R_{11}\ \partial R_{12}/\partial v > 0 \tag{11a}$$

$$R_{12}\ \partial R_{11}/\partial \omega - R_{11}\ \partial R_{12}/\partial \omega > 0 \tag{11b}$$

or, alternately, if one inserts $R_{11} = (\alpha)(v-v_a)$, $R_{12} = (\beta)(v-v_b)$, he finds

$$\alpha\beta(v_a - v_b) > 0 \tag{12a}$$

$$(v - v_b)(v - v_a)\ (\beta\alpha' - \beta'\alpha) + \beta\alpha[v_b'\ (v - v_a) - v_a'\ (v - v_b)] > 0 \tag{12b}$$

where the primes represent derivatives with respect to ω. The second of these should hold for arbitary v in the vicinity of v_a and v_b and lead, upon setting $v = v_a$, $v = v_b$, or $v = (v_a v_b' - v_a' v_b)(v_b' - v_a')$, along with the use of Eq. (12a), to

$$v_b' < 0 \tag{13a}$$

$$v_a' < 0 \tag{13b}$$

$$(\alpha/\beta)' > 0 \tag{13c}$$

Equation (12a) implies that as long as α or β do not vanish (which would seem unlikely) the two curves $v_a(\omega)$ and $v_b(\omega)$ do not intersect. If α and β have the same sign the v_a curve lies above the v_b curve; the converse is true if α and β increases with ω.

To demonstrate the general utility of the perturbation approach, a brief table of values ω, v_a, v_b, α, β, $v^{(1)}$, and v_n are given in Table I for the GR_o and GR_1 modes for the case of a U.S. Standard Atmosphere without winds terminated at a height of 125 km by a halfspace with a sound speed of 478 m/sec. Here $v^{(1)}$ is the result of the first iteration for the phase velocity and v_n is the actual numerical result obtained (only if the phase velocity is real) by explicit numerical search for roots of the eigenmode dispersion function. One may note that, for those frequencies where v_n is computed, the agreement between $v^{(1)}$ and v_n is excellent. A more detailed listing of the perturbation calculation results is given in Figs. 5a and b. The plots there give ω/k_R or the reciprocal of the real part of $1/v^{(1)}$ (i.e., ω divided by the real part of the horizontal wave number k) and the imaginary part k_I of $k = \omega/v$ versus angular frequency. Note that k_I is zero above the corresponding cutoff frequencies. The relatively small values of the k_I are commented upon in Sec. IV.

III. TRANSITION FROM NONLEAKING TO LEAKING

The iteration process described by Eqs. (10) in the preceeding section may fail to converge when G is near zero and in any event gives relatively little insight into what happens to a modal dispersion curve in the immediate vicinity of ω_L. To explore this transition region, it would appear sufficient to approximate G in Eq. (9) by

$$G \simeq [(p)(\omega-\omega_L) + (q)(v-v_L)]^{1/2} \tag{14}$$

where p and q are readily identifiable [from Eq. (4)] positive numbers taken independent of ω and v; v_L is the phase velocity on the dispersion curve in the limit as $\omega \to \omega_L$ from above. The bracketed quantity in Eq. (14) may be regarded as a double Taylor series expansion (truncated at first order) of G^2 about the point ω_L, v_L at which G^2 vanishes (hence no zeroth order term). The fact that both p and q are positive follows since G^2 is positive to the upper right of the

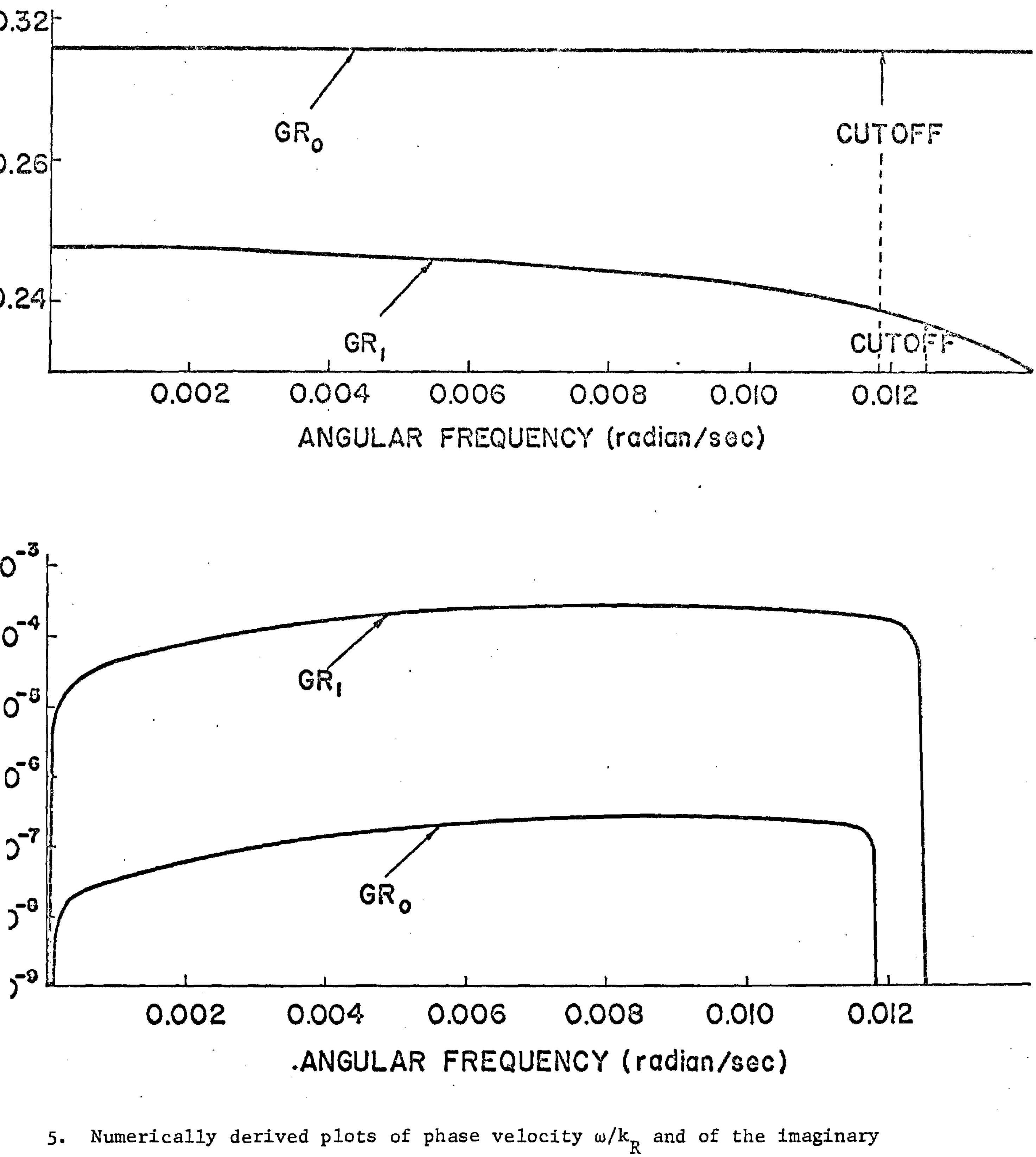

5. Numerically derived plots of phase velocity ω/k_R and of the imaginary part k_I of the complex wavenumber k versus angular frequency for the GR_0 and GR_1 modes. Previous theoretical lower frequency cutoffs for these modes are as indicated. Note that k_I is identically zero above the cutoff frequency.

GR_o	0.0052	0.31203	0.31207	917.4	-2783.7	0.31202121 + $-3.184 \times 10^{-6}i$	
	0.0113	0.31190	0.31194	767.9	-3254.2	0.31189059 + $-1.721 \times 10^{-6}i$	
	0.0155	0.31176	0.31181	621.9	-3644.3	0.31173763	0.31172882
	0.0165	0.31172	0.31177	581.5	-3738.2	0.31167504	0.31167509
	0.0186	0.31162	0.31168	497.5	-3910.1	0.31153369	0.31153394
GR_1	0.0052	0.24229	0.24816	87.8	-3633.0	0.25267 + $-2.715 \times 10^{-3}i$	
	0.0103	0.23433	0.23844	94.7	-3990.0	0.24218 + $-1.337 \times 10^{-3}i$	
	0.0144	0.21842	0.22037	150.7	-5307.0	0.21431	0.22178
	0.0165	0.20252	0.20345	265.0	-7767.3	0.20016	0.20463
	0.0175	0.19058	0.19111	418.9	-10,858.0	0.19226	0.19212

Frequency dependent parameters corresponding to GR_o and GR_1 modes; ω is angular frequency in rad/sec, v_a is phase velocity root of $R_{11}=0$, in km/sec, v_b is analogous root of $R_{12}=0$, α is dR_{11}/dv at $v=v_a$ in sec/km β is dR_{12}/dv at $v=v_b$ in sec, $v^{(1)}$ is first order perturbation solution for phase velocity from equations given in the text (units are km/sec), v_η is the real root determined by direct numerical solution for zeros of eigenmode dispersion function. Note that v_η (defined only when phase velocity is real) agrees exceptionally well with $v^{(1)}$.

line in the ω,v plane where $G^2 = 0$ and also since the $G^2 = 0$ line slopes obliquely downwards. (See Fig. 3).

Let us next note that, in the vicinity of the point ω_L, v_L, the denominator D given by Eq. (9) may be further approximated as

$$D \simeq (A_{12}\alpha - A_{11}\beta) \left\{ (\Delta v + \mu\Delta\omega) + \varepsilon(\Delta v + \nu\Delta\omega)^{\frac{1}{2}} \right\} \tag{15}$$

where we have abbreviated $\Delta v = v - v_L$, $\Delta\omega = \omega - \omega_L$, $\nu = p/q$; the quantity μ is either $-dv_a/d\omega$ or $-dv_b/d\omega$, the two being assumed to be approximately equal. (The use of the minus sign here assumes that μ be positive.) The remaining quantity ε is

$$\varepsilon = \frac{(q^{\frac{1}{2}})\ (\beta)\ (v - v_b)}{\beta A_{11} - \alpha A_{12}} \tag{16}$$

One should note that ε depends on v, although, for purposes of initial analytical investigation, one may set $v = v_L$ here. All of the above quantities may be considered to be evaluated at $\omega = \omega_L$ and $v = v_L$. Note that μ and ν are both positive quantities. Furthermore, it should also be noted that $\nu > \mu$ since the $G^2 = 0$ curve slopes downwards more rapidly than the lines along which R_{11} or $R_{12} = 0$ in the v vs ω plane. (See Fig. 4.)

The roots of Eq. (15) without regard to the sign of the radical are readily found to be

$$\Delta v = -\mu\Delta\omega + (\tfrac{1}{2})\varepsilon^2 \mp \varepsilon(\nu-\mu)^{\frac{1}{2}} [\Delta\omega + \sigma]^{\frac{1}{2}} \tag{17}$$

where

$$\sigma = \varepsilon^2/[4(\nu-\mu)] \tag{18}$$

Alternately, if $|\Delta\omega| << \sigma$, the above may be approximated by the binomial theorem to give

$$\Delta v = -\nu\Delta\omega + [(\nu-\mu)^2/\varepsilon^2](\Delta\omega)^2 \tag{19a}$$

or

$$\Delta v = +\varepsilon^2 - (2\mu - \nu)\ \Delta\omega - [(\nu-\mu)^2/\varepsilon^2](\Delta\omega)^2 \tag{19b}$$

for the upper and lower signs, respectively. The first of these (since $\Delta v = 0$ when $\Delta\omega = 0$) is clearly the description of the disperson curve in the vicinity of $\omega = \omega_L$, $v = v_L$.

Equation (19a) shows that, as $\Delta\omega \to 0$ from above, the dispersion curve becomes tangential to the line $G^2 = 0$. The two curves do not intersect. The general trend is as indicated in Fig. 6. The solution represented by Eq. (19b) is not a proper root of Eq. (15); it corresponds to the wrong sign of the radical and accordingly lies on the second branch. Furthermore, one can readily show that, for values of $\Delta\omega$ slightly less than zero, both roots lie on the second branch. Hence, there must be a gap of finite frequency range in which, for the choice of branch cuts represented by Fig. 1, there are no poles in the k (or v) plane corresponding to the n-th mode.

To determine the order of magnitude of this frequency gap, it is appropriate to consider the trajectory of the second branch roots in some detail and to determine just where one of them should cross the branch cut, reappearing on the first branch. As long as Δv is real and $\Delta v + \nu\Delta\omega > 0$ the criterion for a root to be identified with the first branch is $\Delta v + \mu\Delta\omega > 0$. According to Eq. (17), this would automatically place the second root on the second branch for all $\Delta\omega > -\sigma$ and would place the first root on the second branch for $-\sigma < \Delta\omega < 0$. Consequently, if either root is to reappear on the first branch, it must be at a value of $\Delta\omega < -\sigma$.

One should note from Eq. (17) that at $\Delta\omega = -\sigma$ the two real roots on the second branch coalesce. For values of $\Delta\omega < -\sigma$ the two roots separate again, but

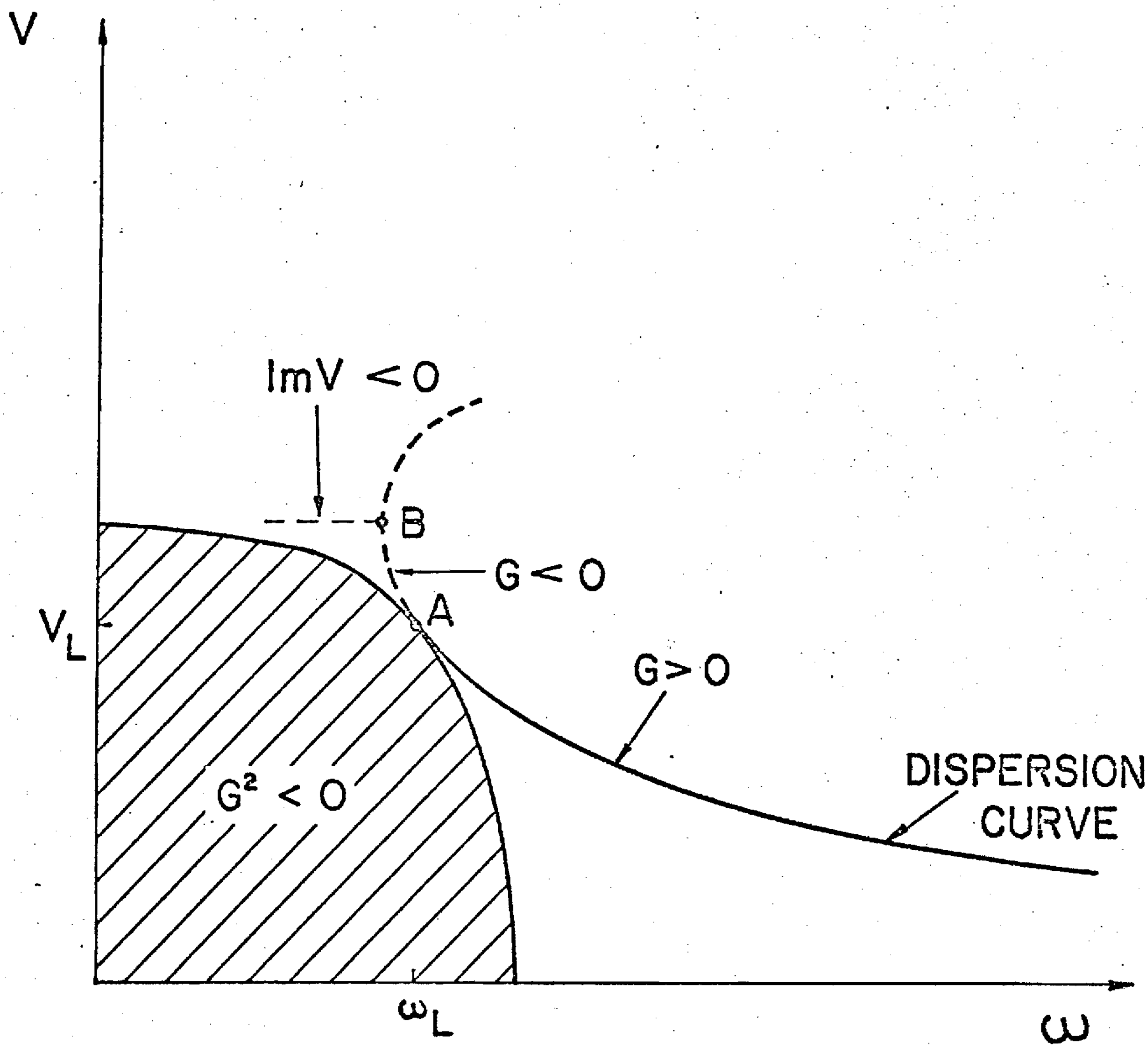

6. Sketch illustrating nature of a single mode's dispersion curve in the vicinity of the $G^2=0$ line. At point A (angular velocity ω_L, phase velocity v_L) the dispersion curve is tangent to the $G^2=0$ line; for frequencies below ω_L down to that corresponding to point B in the sketch there are two real roots for v of the eigenmode dispersion function on the second branch. For frequencies lower than that corresponding to point B, there is a complex root for v on the first branch (which is the complex conjugate of a second root on the second branch).

are now complex conjugates. The root in the upper half of the v plane (lower half of k plane) can never cross the branch cut so it remains on the second branch indefinitely. The one in the lower half of the v plane will cross the branch cut at a point which may be approximately estimated as that where $\mathrm{Re}(\Delta v) = -\nu\Delta\omega$ or where

$$\Delta\omega = \frac{-(\frac{1}{2})\ \varepsilon^2}{(\nu-\mu)} = -2\sigma$$

with a corresponding value of Δv of

$$\Delta v = (\varepsilon^2/2)\ \left\{[\nu/(\nu-\mu)] - i\right\}$$

For subsequent frequencies successively lower than $\omega_L - 2\sigma$ there is a complex root on the first branch with a negative imaginary part which increases with decreasing frequency.

The discussion up to now has assumed that $|\Delta v| << |v_L - v_b|$ and hence that ε may be taken as constant. This would seem appropriate for describing the transition region since all values of Δv of interest in this region are of second order of ε^2. However, if an improved numerical estimate is required, we recommend that one regard Eqs. (16) and (17) as a iterative pair. Successfully computed values of Δv may be used to recalculate ε and the new value of ε may then be used in obtaining the next higher estimate for Δv.

In Table II the values of ω_L, v_L, p, q, μ, ν, ε, and σ are given for the GR_0 and GR_1 modes for the model atmosphere corresponding to Fig. 2a. The extremely small values of σ should be noted. The corresponding plot of Δv versus $\Delta\omega$ (i.e., both branches of Eq.(17)) corresponding to their values for the GR_0 mode is given in Fig. 7. For simplicity, this is plotted in a nondimensional form, i.e.

$$V = -\{\mu/[2(\nu-\mu)]\}\Omega \mp [1 + \Omega]^{1/2} \tag{20}$$

TABLE II

	GR_o	GR_1
ω_L(rad/s)	0.0118	0.0125
v_L(km/s)	0.31188	0.2323
p(s/km^2)	0.14	0.35
q(s/km^3)	1.84×10^{-3}	1.86×10^{-3}
μ(km)	2.94×10^{-2}	4.15
ν(km)	76	190
ε(km$^{1/2}$/s$^{1/2}$)	9.6×10^{-6}	1.02×10^{-3}
σ(rads/s)	3.04×10^{-13}	1.41×10^{-9}

Parameters characterizing the eigenmode dispersion function near points in the phase velocity versus angular frequency plane at which the GR_o and GR_1 modes undergo transition from leaking to non-leaking.

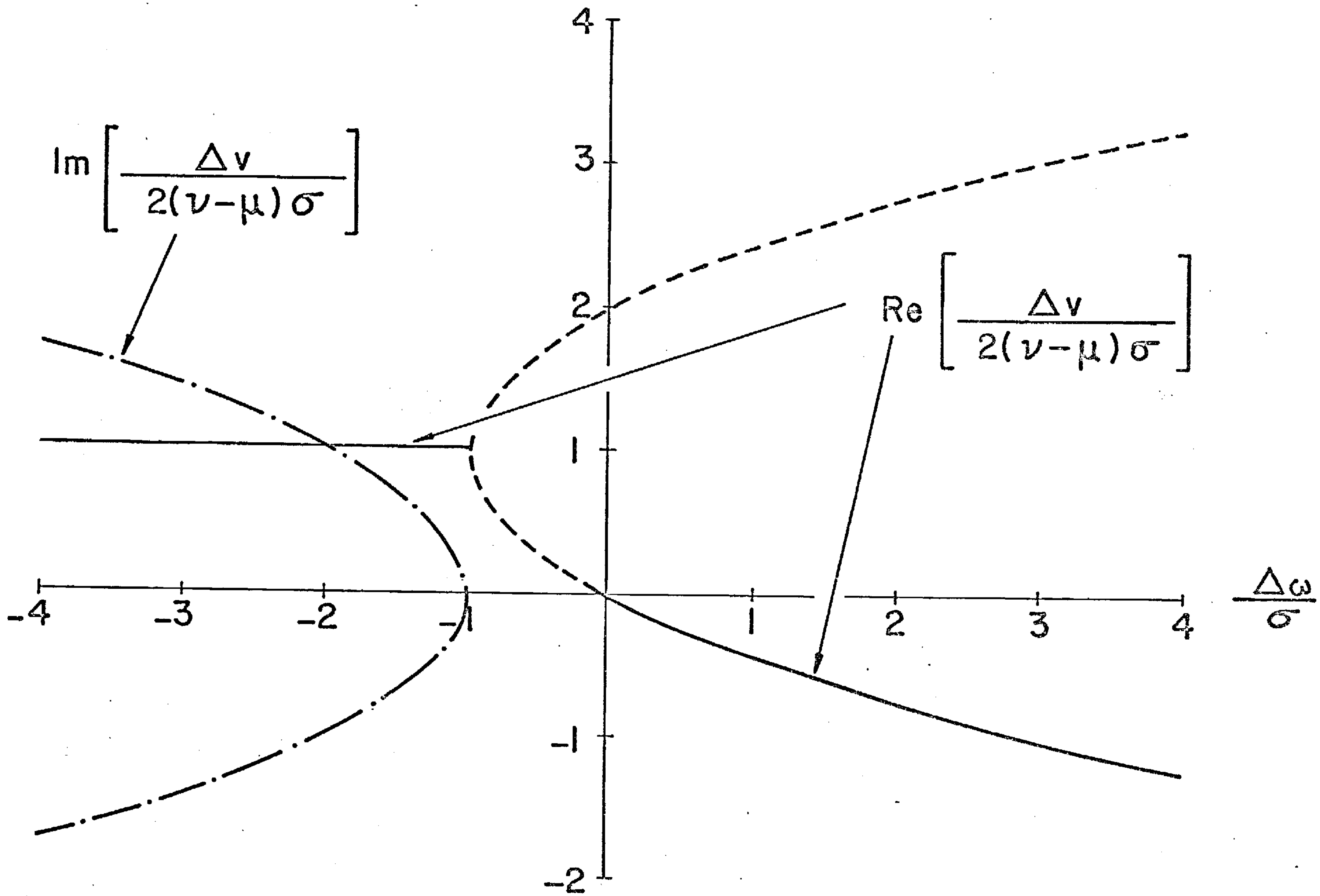

7. Graph of normalized phase velocity versus normalized frequency in the vicinity of the point (v_L, ω_L) for the GR_0 mode. The imaginary and real parts are both plotted. The dashed line corresponds to real roots on the second Riemann sheet.

where $v = \Delta v/[2(\nu-\mu)\sigma]$ and $\Omega=\Delta\omega/\sigma$. Both real and imaginary parts are shown on the same graph. The corresponding plots for the GR_1 mode differ only slightly from those in the Fig. 7 because of a different value of the parameter $\mu/[2(\nu-\mu)]$ in Eq. (20); in both cases this parameter is small compared to unity, i.e. $\mu<<\nu$ as may be seen from Table II.

IV. THE BRANCH LINE INTEGRAL

Since there is a gap in the range of frequencies for which a pole corresponding to a mode may exist, it is evident that evaluation of the k integration in Eq. (1) by merely including residues may be insufficient for certain frequencies. Thus it would seem appropriate in such cases to include a contribution from the branch line integral. It may be anticipated that such branch line integrals are significant at larger values of r only when ω is close to some mode's ω_L (say the n-th mode), in which case the branch point of greatest interest (i.e., that which may have a pole in its immediate vicinity) is at $k=\omega/v_L$. Consequently, it would appear that an adequate approximation to the branch line integral would be

$$\left\{\begin{matrix}\text{Branch line}\\ \text{contribution of}\end{matrix}\right\} \int_{-\infty}^{\infty}[Q/D(\omega,k)]e^{ikr}dk$$

$$= \frac{Q}{A_{12}\alpha-A_{11}\beta}\int_{C_B}\frac{e^{ikr}dk}{x+(\mu-\nu)\Delta\omega+\epsilon x^{1/2}} \qquad (21)$$

where the denominator $D(\omega,k)$ has been approximated by Eq. (15) with the abbreviation x for $\Delta v+\nu\Delta\omega$. The quantity outside the integral is assumed to be evaluated at $\omega=\omega_L$ and $k=\omega/v_L$. The contour C_B runs down the left side of the branch cut, around the branch point (where x=0), and then up the right side. If one next changes the variable of integration from k to x, ~~nothing~~ that for small x/v_L, noting

$$k \approx k_B-(\omega_L/v_L^2)x \qquad (22)$$

he finds approximately that

$$\begin{Bmatrix}\text{Branch line} \\ \text{contribution}\end{Bmatrix} = (\text{Residue})_o \int_{c_B'} \frac{e^{-i(\omega_L/v_L^2)x}}{x+(\mu-\nu)\Delta\omega+\varepsilon x^{1/2}}\, dx \tag{23}$$

where $(\text{Residue})_o$ is that residue which the integrand $(Q/D)e^{ikr}$ would be expected to have at the n-th mode's pole in the k plane were the parameter ε identically equal to zero. The mapped contour c_B' in the x plane may be considered to go up on the right and then down on the left of a branch cut extending vertically downwards from the origin in the x plane. If we set $x=-i\xi$, then, on the right side of the cut, $x^{1/2}$ should be $e^{-i\pi/4}\xi^{1/2}$ while, on the left side, it is $-e^{-i\pi/4}\xi^{1/2}$. Consequently, the total integral combines to

$$\begin{Bmatrix}\text{Branch lines} \\ \text{contribution}\end{Bmatrix} = -(\text{Residue})_o \int_0^\infty \frac{2\varepsilon e^{+i\pi/4} e^{-(\omega_L/v_L^2)\xi r}\sqrt{\xi}\, d\xi}{[-i\xi+(\mu-\nu)\Delta\omega]^2+i\varepsilon^2\xi} \tag{24}$$

This in turn, with an obvious change of integration variable, may be expressed as

$$\begin{Bmatrix}\text{Branch line} \\ \text{contribution}\end{Bmatrix} = (\text{Residue})_o\, 2K \int_0^\infty \frac{e^{i\pi/4} e^{-\eta}\eta^{1/2} d\eta}{(\eta-\eta_1)(\eta-\eta_2)} \tag{25}$$

where

$$K=\varepsilon v_L/(\omega_L r)^{1/2} \tag{26a}$$

$$\begin{aligned}\eta_1,\ \eta_2 &= i(K^2/2)(1+[\Delta\omega/2\sigma]) \\ &\pm i(K^2/2)(1+[\Delta\omega/\sigma])^{1/2}\end{aligned} \tag{26b}$$

with σ as defined by Eq. (18).

In regards to the η integration, the integral can be expressed in general in terms of Fresnel integrals of complex argument after some considerable mathematical manipulation. One may note, moreover, that $|\eta_1|$ and $|\eta_2|$ are, for most cases of interest, considerably less than unity. In this case, the appropriate approximate result (derivation omitted for brevity) is

$$\int_0^\infty \frac{e^{-\eta}\sqrt{\eta}\, d\eta}{(\eta-\eta_1)(\eta-\eta_2)} = \frac{i\pi}{\eta_1^{1/2}+\eta_2^{1/2}} \tag{27}$$

where the choice of square root should be such that the imaginary part is positive. The net result in this limit then is that the branch line contribution is independent of the parameter κ. (The dependence on range r comes only in the residue.) Thus one may write

$$\left\{\begin{matrix}\text{Branch line}\\ \text{contribution}\end{matrix}\right\} = 2\pi i(\text{Residue})_o\, B_{rh}(\Delta\omega/\sigma) \tag{28}$$

where the function $B_{rh}(\Delta\omega/\sigma)$ is given by

$$B_{rh}(\Omega) = \frac{\sqrt{2}}{[1+(1/2)\Omega+(1+\Omega)^{1/2}]^{1/2}+[1+(1/2)\Omega-(1+\Omega)^{1/2}]^{1/2}} \tag{29}$$

Here any consistent choice may be made for the sign of the inner square roots but the outer square roots should be taken such that the resulting phases are between $-\pi/4$ and $3\pi/4$. The quantities in square brackets turn out to be the squares of $(1/\sqrt{2})[(1+\Omega)^{1/2}\pm 1]$, respectively. The phase restriction then gives

$$B_{rh}(\Omega) = (1+\Omega)^{1/2} \quad \text{if } \Omega>0 \tag{30a}$$

$$= 1 \quad \text{if } 0>\Omega>-2 \tag{30b}$$

$$= -i(-\Omega-1)^{-1/2} \quad \text{if } \Omega<-2 \tag{30c}$$

where here all square roots are understood to be positive.

To completely describe the transition it is appropriate to add to Eq. (28) that contribution (which is zero for $0>\Delta\omega>-2\sigma$) from the pole on the first branch in Eq. (21) which lies in the general vicinity of $k=\omega_L/v_L$. If the pole is present, its contribution to the integration over k is $2\pi i$ times the residue (which is not what we have been referring to as $(\text{Residue})_o$ unless ε is identically zero). The evaluation of the residue is moderately straightforward and omitted here for brevity. The net result is that

$$\left\{\begin{matrix}\text{Branch line}\\\text{contribution}\end{matrix}\right\} + \left\{\begin{matrix}\text{Pole}\\\text{contribution}\end{matrix}\right\}$$

$$= 2\pi i(\text{Residue})_o\left\{B_{rh}(\Delta\omega/\sigma)+P_{o\ell}(\Delta\omega/\sigma)\right\} \tag{31}$$

where the "pole function" $P_{o\ell}(\Delta\omega/\sigma)$ turns out to be given by

$$P_{o\ell}(\Delta\omega/\sigma)=1-B_{rh}(\Delta\omega/\sigma)\ . \tag{32}$$

We accordingly have the remarkable (although, in retrospect, not unexpected) result that

$$\left\{\begin{matrix}\text{Branch line}\\\text{contribution}\end{matrix}\right\}+\left\{\begin{matrix}\text{Pole}\\\text{contribution}\end{matrix}\right\}= 2\pi i(\text{Residue})_o \tag{33}$$

The above gives one a relatively simple prescription for evaluating a given mode's contribution to the k integration in Eq. (1). First, all branch line integrals are formally neglected. If a pole exists on the first branch, the residue which would normally be utilized is replaced by

$$\text{Res}\left\{\frac{Qe^{ikr}}{D}\right\} \rightarrow \left\{\frac{Qe^{ikr}}{d'D/dk}\right\}_{k=\text{pole}} \tag{34}$$

where

$$\begin{aligned}\frac{d'D}{dk} &= \frac{d}{dk}\left(A_{12}R_{11}-A_{11}R_{12}\right)\\ &\quad -G\frac{d}{dk}\left(R_{12}\right)\end{aligned} \tag{35}$$

i.e. it differs from the actual derivative of D in that G is formally considered as constant. Doing this when ω is somewhat removed from the transition region near ω_L should make very little difference since R_{12} is small at values of k which are poles. Near the transition, this neglect should almost exactly compensate for the neglect of the branch line integral.

REFERENCES

1. J. E. Thomas, A. D. Pierce, E. A. Flinn, and L. B. Craine, "Bibliography on Infrasonic Waves", Geophys. J. R. astr. Soc. 26, 399-426 (1971).

2. C. B. Officer, Introduction to the Theory of Sound Transmission with Application to the Ocean (McGraw-Hill, New York, 1958).

3. J. R. Wait, Electromagnetic Waves in Stratified Media (Pergamon Press, Inc., New York, 1962).

4. L. M. Brekhovskikh, Waves in Layered Media (Academic Press, New York, 1960).

5. K. G. Budden, The Wave-Guide Mode Theory of Wave Propagation (Prentice Hall, Inc., Englewood Cliffs, N.J., 1961).

6. I. Tolstoy and C. S. Clay, Ocean Acoustics (McGraw-Hill, New York, 1966).

7. M. Ewing, W. Jardetzky, and F. Press, Elastic Waves in Layered Media (McGraw-Hill, New York, 1957).

8. A. D. Pierce and J. W. Posey, Theoretical Prediction of Acoustic-Gravity Pressure Waveforms generated by Large Explosions in the Atmosphere, Report AFCRL-70-0134, Air Force Cambridge Research Laboratories, 1970.

9. A. D. Pierce, J. W. Posey, and E. F. Iliff, "Variation of Nuclear Explosion generated Acoustic-Gravity Waveforms with Burst Height and with Energy Yield" J. Geophys. Res. 76, 5025-5042 (1971).

10. E. T. Copson, An Introduction to the Theory of Functions of a Complex Variable (Clarendon Press, Oxford, 1935) p. 137.

11. L. M. Brekhovskikh, loc. cit., pp. 270-280.

12. A. D. Pierce, "The Multilayer Approximation for Infrasonic Wave Propagation in a Temperature and Wind-Stratified Atmosphere", J. Comp. Phys. 1, 343-366 (1967).

13. A. D. Pierce, "Propagation of Acoustic-Gravity Waves in a Temperature and Wind-Stratified Atmosphere", J. Acoust. Soc. Amer. 37, 218-227 (1965).

K-25-638

AFGL-TR-76-0055

GEOMETRICAL ACOUSTICS TECHNIQUES IN FAR FIELD INFRASONIC WAVEFORM SYNTHESES

by

Allan D. Pierce and Wayne A. Kinney

School of Mechanical Engineering
Georgia Institute of Technology
Atlanta, Georgia 30332

SCIENTIFIC REPORT NO. 2

Approved for public release; distribution unlimited.

March 7, 1976

Prepared for

AIR FORCE GEOPHYSICS LABORATORY
AIR FORCE SYSTEMS COMMAND
UNITED STATES AIR FORCE
HANSCOM AFB, MASSACHUSETTS 01731

SECURITY CLASSIFICATION OF THIS PAGE (When Data Entered)

REPORT DOCUMENTATION PAGE		READ INSTRUCTIONS BEFORE COMPLETING FORM
1. REPORT NUMBER AFGL-TR-76-0055	2. GOVT ACCESSION NO.	3. RECIPIENT'S CATALOG NUMBER
4. TITLE (and Subtitle) GEOMETRICAL ACOUSTICS TECHNIQUES IN FAR FIELD INFRASONIC WAVEFORM SYNTHESES		5. TYPE OF REPORT & PERIOD COVERED Scientific Report No. 2
		6. PERFORMING ORG. REPORT NUMBER
7. AUTHOR(s) Allan D. Pierce Wayne A. Kinney		8. CONTRACT OR GRANT NUMBER(s) F19628-74-C-0065
9. PERFORMING ORGANIZATION NAME AND ADDRESS School of Mechanical Engineering Georgia Institute of Technology Atlanta, Georgia 30332		10. PROGRAM ELEMENT, PROJECT, TASK AREA & WORK UNIT NUMBERS 62101F 76390102
11. CONTROLLING OFFICE NAME AND ADDRESS Air Force Geophysics Laboratory Hanscom AFB, Massachusetts 01731 Monitor: Elisabeth F. Iliff, LWW		12. REPORT DATE 7 March 1976
		13. NUMBER OF PAGES 68
14. MONITORING AGENCY NAME & ADDRESS(if different from Controlling Office)		15. SECURITY CLASS. (of this report) Unclassified
		15a. DECLASSIFICATION/DOWNGRADING SCHEDULE

16. DISTRIBUTION STATEMENT (of this Report)

Approved for public release; distribution unlimited.

17. DISTRIBUTION STATEMENT (of the abstract entered in Block 20, if different from Report)

18. SUPPLEMENTARY NOTES

19. KEY WORDS (Continue on reverse side if necessary and identify by block number)

Acoustics	Ray Acoustics
Geometrical Acoustics	Guided waves
Infrasound	Atmospheric Acoustics
Wave Propagation	Waves in inhomogeneous media
Caustics	

20. ABSTRACT (Continue on reverse side if necessary and identify by block number)

A ray acoustic computational model for the prediction of long range infrasound propagation in the atmosphere is described. A cubic spline technique is used to approximate the sound speed versus height profile when values of sound speed are input for discrete height intervals. Techniques for finding ray paths, travel times, ray turning

DD FORM 1 JAN 73 1473 EDITION OF 1 NOV 65 IS OBSOLETE

SECURITY CLASSIFICATION OF THIS PAGE (When Data Entered) points, and rays connecting source and receiver are described. A parameter characterizing the spreading of adjacent rays (or ray tube area) is defined and methods for its computation are given. A method of determining the number of times a given ray touches a caustic is also described. Formulas are given for the computation of acoustic amplitudes and waveforms which involve a superposition of contributions from individual rays connecting source and receiver and which incorporate phase shifts at caustics. The possibility of a receiver being in the proximity of a caustic is considered in some detail and distinction is made between cases where the receiver is on the illuminated or shadow sides of a caustic. It is shown that a knowledge of parameters characterizing two rays at a point in the vecinity of a caustic provides sufficient information concerning the caustic to allow one to give a relatively accurate description of the acoustic field in its vicinity. The resulting theory involves Airy functions and uses concepts extrapolated from a theory published in 1951 by Haskell. The net result is a detailed computational scheme which should accurately cover the contingency of the receiver being near a caustic in the calculation of amplitudes and waveforms. A number of FORTRAN subroutines illustrating the method are given in an apprendix. Limitations of the theory and suggestions for future developments are also given.

I. INTRODUCTION

The present report is concerned with the development of a computational model for the prediction of long range infrasound propagation in the atmosphere. The computational model discussed here is one which is partly based on ray acoustic concepts; it should be applicable to wave periods less than three minutes and is intended to complement the guided mode model of acoustic gravity wave propagation which has been extensively discussed in previous reports and papers.[1-5]

The ray acoustic method has a sizable literature pertaining to it; most of the published work is concerned with applications to underwater sound. (A brief bibliography of relevant papers is given in Appendix A.) Discussions of ray acoustics which are particularly germane to infrasound propagation in the atmosphere are an article published in 1951 by N. Haskell[6], a 1966 AFCRL report by Pierce[7], and a 1973 AFCRL report by Pierce, Moo, and Posey.[4] In the present report, the details of the pertinent theory are assumed to be already known; the emphasis is on the computational implementation of the theory. Particular innovations discussed here, not generally included in ray acoustic models, are (1) the presence of many rays which connect source and receiver, (2) a method of computing ray amplitudes based on analytical differentiation of ray formulas appropriate to a stratified medium, (3) the inclusion of caustics into the formulation, and (4) the inclusion of Lamb's atmospheric edge mode.

The general model used as a starting point may be taken (Fig. 1) as a height stratified atmosphere above a flat rigid ground. The sound speed $c(z)$ and ambient density $\rho_0(z)$ are assumed to be continuous functions of height z above the ground. For simplicity, winds are not included in the present formulation, although we believe that this limitation can easily be overcome with only a modest degree of effort. The pertinent governing equations are taken as the linearized equations of atmospheric compressible fluid dynamics (gravity included).[3] Nonlinear effects are neglected other than in the selection of a source term. How such a source term appropriate to nuclear explosions may be selected has previously been discussed in some detail by Pierce, Posey,

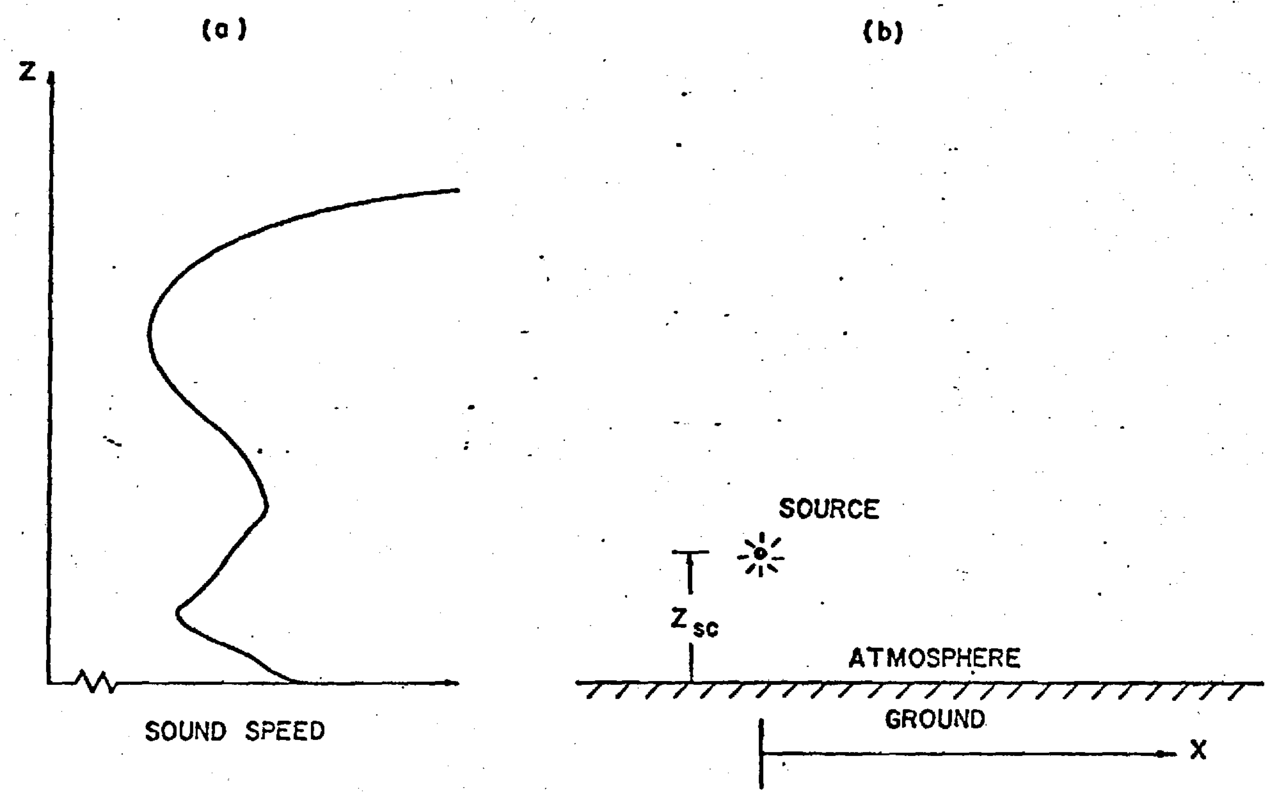

Figure 1.

Sketches illustrating general model used in the analysis. (a) Typical sound speed versus height profile. (b) Sketch of point source above a flat rigid ground, with a height stratified atmosphere.

and Iliff.[8] It suffices here to only state that the source is assumed localized at a point whose coordinates may be taken as $x = 0$, $y = 0$, $z = ZSC$

A modest analysis of the governing equations suggests that the wave portion with periods less than approximately three minutes may be described at moderate distances from the source (greater than, say, 50 kilometers) by an acoustic pressure which is separable as follows

$$p(\vec{r},t) \quad = \quad \{\text{Lamb mode portion}\} \quad + \quad \{\text{ordinary acoustic portion}\} \tag{1.1}$$

where the Lamb mode portion may be computed by techniques such as discussed by Pierce and Posey[9] and by Posey.[10] The ordinary acoustic portion (which is the only portion considered here) may be taken as the ray acoustic (excluding the edge mode) solution of the wave equation

$$\nabla^2(p/\sqrt{\rho_o}) - (1/c^2)\partial^2(p/\sqrt{\rho_o})/\partial t^2 \quad = \quad -4\pi f(t)\delta(\vec{r} - \vec{r}_{SC}) \tag{1.2}$$

where the function $f(t)$ is characteristic of the source. In addition, $p/\sqrt{\rho_o}$ satisfies approximately the boundary condition $\partial p/\partial z + (g/c^2)p = 0$ at the ground ($z=0$). The justification for separating out the Lamb mode portion at the outset follows from a 1963 paper by Pierce[11] which may be construed as showing, for the special case of an isothermal atmosphere, that such a separation is possible at the frequencies of interest here.

The rays proceeding from the source are lines, each of which lies in a vertical plane including the source (Fig. 2). Since the geometry is circularly symmetric, we may limit our consideration to rays which lie in the x, z plane. A typical ray path passes through the source, bends downwards when the ray is proceeding up and the sound speed is increasing with height, bends upwards when the sound speed is decreasing, etc. This phenomenon of ray bending is known as refraction and makes it possible for more than one ray to pass

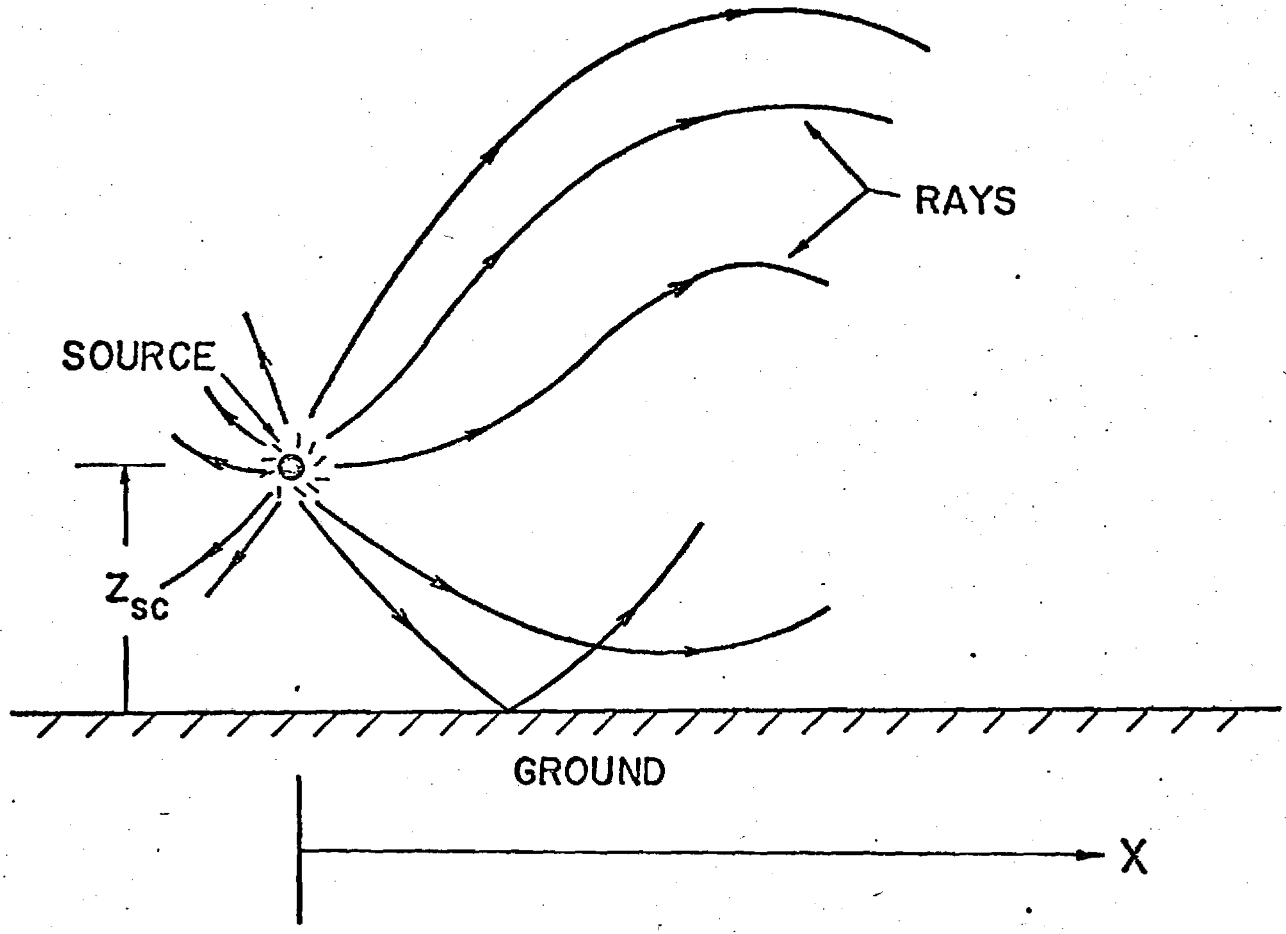

Figure 2.

Sketch of acoustic ray paths emanating from a source in an atmosphere in which the sound speed varies with height.

through a given far field point. For distances and receiver locations of interest, one may regard this possibility of multi-ray arrivals as typical rather than the exception. The equations for computing such ray paths are well known and are discussed in particular in the 1966 report by Pierce.[7] Computer programs which compute such paths are also in widespread use, especially in underwater sound studies. However, most such programs do not compute ray amplitudes.

A somewhat lower order (or, strictly speaking, nonuniform) ray acoustic approximation to the solution of Eq. (1.2) is that

$$p = \sum_{\text{rays}} p_{\text{ray}} \tag{1.3}$$

where the sum extends over all rays which connect the source and receiver. Here individual terms have signatures and amplitudes which may be computed from the eikonal approximation[12,13] and from the condition that p reduces to

$$p/\sqrt{\rho_o} \rightarrow f(t - R/c)/R \tag{1.4}$$

in the immediate vicinity of the source. However, the straightforward application of this procedure leads into difficulties if ray tube area, along any ray connecting source and listener, should vanish at any intermediate point along the ray. This difficulty, however, may be largely overcome[14,15] (although this seems to be rarely done) by simply adding a phase shift of $\pi/2$; ie.

$$f(t) = \mathrm{Re} \int_o^\infty \hat{f}(\omega)\, e^{-i\omega t}\, d\omega \tag{1.5}$$

is replaced by

$$f_{\text{Shift}}(t) = \mathrm{Re} \int_o^\infty e^{-i\pi/2}\, \hat{f}(\omega)\, e^{-i\omega t}\, d\omega \quad . \tag{1.6}$$

this shift being applied each time the ray tube area goes to zero along the ray. This is in addition to the normal shift due to travel time along the ray from source to listener. The successive shifting of phase by intervals of $\pi/2$ is a relatively simple matter; the principal challenge in the application is that of determining the number of such phase shifts to be applied.

There are two further modifications to Eq. (1.3) which, if incorporated into a computational model, should guarantee that results be good approximations down to relatively low frequencies and for large propagation distances of the order of 1000-18,000 km. These modifications include the explicit taking into account of caustics and lacunae (voids, skip zones, shadow zones, etc.) in the vicinity of the receiver. A caustic is a surface formed by a locus of points at which ray tube areas vanish or, alternately, at which adjacent rays intersect. The eikonal approximation breaks down at any point on a caustic and should be suspect near a caustic. The manner in which the computational method may be revised to incorporate an accurate theoretical model valid near caustics is one of the central topics in the present report.

Examples of lacunae (see Fig. 3) occur whenever two adjacent rays split. The splitting leaves a shadow zone or a region in which there is one less ray than in adjacent regions. Lacunae occur in particular if there is a maximum in the profile of sound speed versus height. They also occur near the ground when the sound speed near the ground decreases with height. (The consideration of an image source and an image medium indicates the latter may also be regarded as a case where adjacent rays split.) The present report does not consider the lacuna problem. This is a limitation we hope to overcome in subsequent studies. The inclusion of caustics is regarded as a higher priority and it seems appropriate to thoroughly check out the techniques for including caustics before proceeding to the development of a method for including lacunae. In this regard, it is possible to conceive of a hypothetical model atmosphere in which caustics occur but lacunae do not. This would be a model in which there is no ground, the sound speed has a single minimum but no maxima. This is admittedly

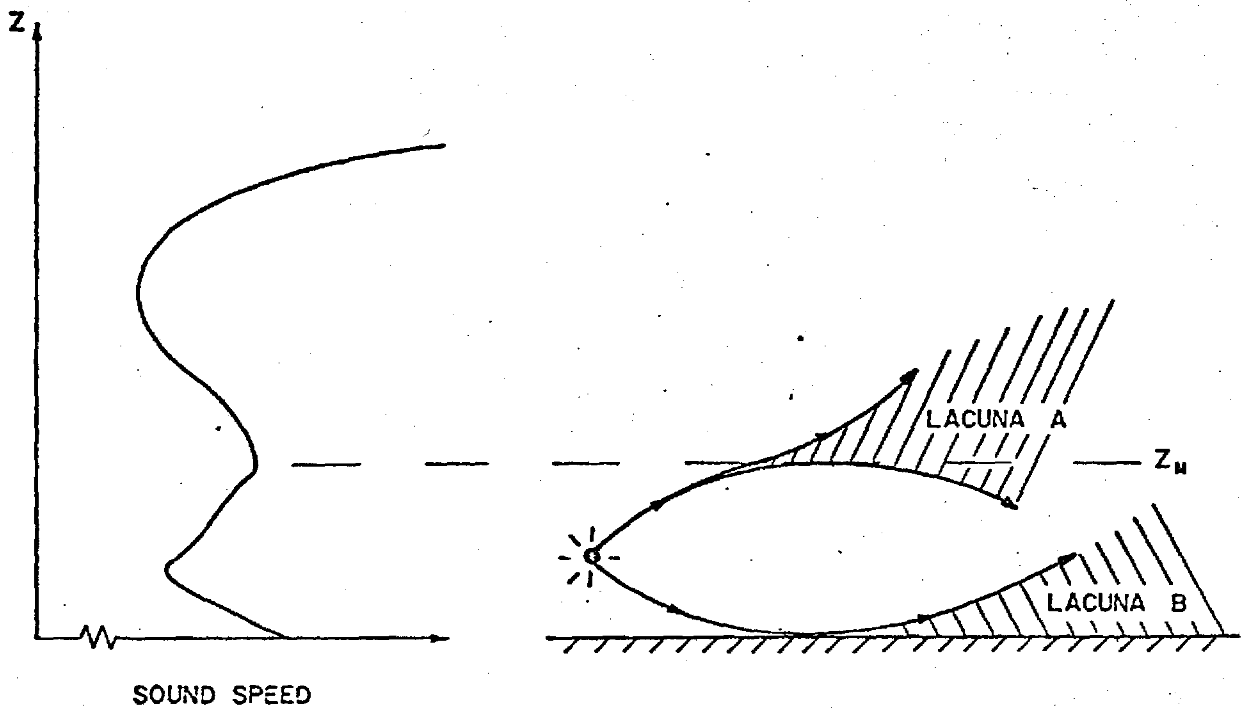

<u>Figure 3.</u>

Examples of the occurrence of lacunae in the propagation of rays from a source in a stratified atmosphere. The lacuna A occurs because of the splitting of ray paths at the height of a sound speed maximum, lacuna B occurs because of the presence of the ground and the fact that the sound speed initially decreases with height.

not a realistic model, but it nevertheless should serve as a vehicle for checking out the computational method.

The present report does not give a complete computer program for the prediction of acoustic waveforms via the ray acoustic model. Such a program is still under development. However, we do include in Appendix B a number of Fortran subroutines which have been developed to date, which may be incorporated into such a program, and which exemplify the computational techniques. The emphasis in our discussion is on these techniques.

II. SOUND SPEED PROFILE

Sound speed data typically supplied in any computation scheme takes the form of individual values c_i ($i=1,2,\ldots,NCS$) at heights z_i ($i=1,2,\ldots, NCS$). However, in the types of calculations pertinent to geometrical acoustical predictions, one needs to know values of $c(z)$, dc/dz, and d^2c/dz^2 at heights not necessarily coinciding with one of the z_i. To this purpose, we use an interpolation scheme known as cubic splines and which was recently introduced into the underwater sound propagation literature by Moler and Solomon[16]. In these authors' notation, one lets

$$\Delta z_i = z_i - z_{i-1} \tag{2.1a}$$

$$\Delta c_i = (c_i - c_{i-1})/\Delta z_i \qquad i=1,\ldots,NCS \tag{2.1b}$$

$$w = (z - z_{i-1})/\Delta z_i \tag{2.1c}$$

$$\bar{w} = 1 - w \tag{2.1d}$$

and takes the sound speed $c(z)$ for z between z_{i-1} and z_i to be of the form of a cubic polynomial

$$c(z) = \bar{w}c_{i-1} + wc_i + (\Delta z_i)^2\left[a_{i-1}(\bar{w}^3 - \bar{w})+a_i(3w^2 - 1)\right] \tag{2.2}$$

where the coefficients a_i are constants chosen as described below. When $z = z_{i-1}$ and $z = z_i$, this automatically reduces to c_{i-1} and c_i, respectively, so continuity of sound speed is automatically provided.

The first, second, third, derivatives of sound speed according to the Moler-Solomon equation above are

$$dc/dz = \Delta c_i + \Delta z_i\left[-a_{i-1}(3\bar{w}^2 - 1) + a_i(3w^2 - 1)\right] \tag{2.3a}$$

$$d^2c/dz^2 = 6(\bar{w}a_{i-1} + wa_i) \tag{2.3b}$$

$$d^3c/dz^3 = 6(a_i - a_{i-1})/\Delta z_i \tag{2.3c}$$

so

$$dc/dz = \Delta c_i - \Delta z_i(a_i + 2a_{i-1}) \quad \text{at } z_{i-1} \tag{2.4a}$$

$$= \Delta c_i + \Delta z_i(2a_i + a_{i-1}) \quad \text{at } z_i \tag{2.4b}$$

$$d^2c/dz^2 = 6a_{i-1} \quad \text{at } z_{i-1} \tag{2.5a}$$

$$= 6a_i \quad \text{at } z_i \tag{2.5b}$$

Thus continuity of d^2c/dz^2 is automatically insured while continuity of dc/dz requires

$$\Delta c_i + \Delta z_i(2a_i + a_{i-1}) = \Delta c_{i+1} - \Delta z_{i+1}(a_{i+1} + 2a_i) \tag{2.6}$$

for all values of i. Continuity of the third derivative is not imposed on the function.

To determine appropriate values of the a_i which insure continuity of the first derivative we note that Eq. (2.6) above implies

$$a_{i+1} = (\Delta c_{i+1} - \Delta c_i)/\Delta z_{i+1} - 2a_i\left[1 + \Delta z_i/\Delta z_{i+1}\right] - a_{i-1}\,\Delta z_i/\Delta z_{i+1} \tag{2.7}$$

and that, given a_1 and a_2, one could in principle generate all of the succeeding a_i's. The linear nature of these difference equations implies furthermore that

$$a_i = K_i + L_i a_2 + M_i a_1 \tag{2.8}$$

for i >2, where

$$K_{i+1} = A_i - B_i K_i - C_i K_{i-1} \tag{2.9a}$$

$$L_{i+1} = -B_i L_i - C_i L_{i-1} \tag{2.9b}$$

$$M_{i+1} = -B_i M_i - C_i M_{i-1} \tag{2.9c}$$

$$A_i = (\Delta c_{i+1} - \Delta c_i)/\Delta z_{i+1} \tag{2.10a}$$

$$B_i = 2\left[1 + \Delta z_i/\Delta z_{i+1}\right] \tag{2.10b}$$

$$C_i = \Delta z_i/\Delta z_{i+1} \tag{2.10c}$$

$$K_2 = 0; \qquad K_3 = A_2; \qquad K_4 = A_3 - B_3 A_2 \tag{2.11a}$$

$$L_2 = 1; \qquad L_3 = -B_2; \qquad L_4 = B_3 B_2 - C_3 \tag{2.11b}$$

$$M_2 = 0; \qquad M_3 = -C_2; \qquad M_4 = B_3 B_2 \tag{2.11c}$$

Thus, if one starts with the values K_2 and K_3 given above, he may generate all of the successive K_i, etc.

Boundary conditions on the a_i may be taken as $a_1 = a_{NCS} = 0$. These are somewhat arbitrary but imply that the sound speed profile should be linear above z_{NCS} and below z_1. With this choice, one has

$$a_2 = -K_{NCS}/L_{NCS} \tag{2.12}$$

and the a_i for i=3,....., NCS are then computed according to Eq. (2.7). In this manner all of the a_i may be computed.

The computation just described is realized by a computer subroutine DASOL whose deck listing is given in Appendix B. The c_i and z_i are presumed stored in COMMON when this subroutine is called and the computed a_i (denoted ASOL) are stored in COMMON after this subroutine returns. The number of points is denoted by NCS (number of c's).

The sound speed at an arbitrary value of z is computed by a function subroutine CSP(Z). Given the value of z, this uses the values of the a_i, the c_i and the z_i (stored in COMMON) in Eq. (2.2) to compute the sound speed. (The deck listing is also given in Appendix B.) Analogous function subroutines are DCDZ(Z) and DCDZS(Z) which compute the dc/dz and d^2c/dz^2 at a given value of z according to Eqs. (2.3a) and (2.3b).

III. RAY PARAMETERS

For a height stratified atmosphere without winds, the ray equations of geometrical acoustics predict that

$$dx/dz = \pm c/(v_p^2 - c^2)^{1/2} \qquad (3.1)$$

where x is horizontal distance of the ray, z is vertical distance. Here, v_p, the horizontal phase velocity of the ray, is a constant for any given ray. Snell's law (a corollary of the ray equations) predicts that

$$v_p = c/(\sin\theta) = \text{constant} \qquad (3.2)$$

where c is the local sound speed, θ is the angle between the momentary ray direction and the vertical. The choice of sign in Eq. (3.1) above depends on whether the ray is presently moving obliquely upwards or obliquely downwards.

In a similar manner, the ray tracing equations predict that the rate of change of net travel time t along a ray with respect to height is

$$dt/dz = \pm (v_p/c)/(v_p^2 - c^2)^{1/2} \tag{3.3}$$

The magnitudes $|dx/dz|$ and $|dt/dz|$ are computed by function subroutines RDXDZ(Z) and RDTDZ(Z). Both of these use the subroutine CSP(Z) to find the sound speed at height z. The phase velocity v_p is assumed to be stored in COMMON.

A turning point for a ray is a value of z at which $c(z) = v_p$. In general if the sound speed profile has a minimum then there is an upper z_U and a lower turning point z_L. These are found by calling a subroutine TNPNT. This subroutine takes as inputs the phase velocity VP and the lower and upper bounds ZBL and ZBU for the search. The search proceeds by dividing the interval (ZBU,ZBL) into NCS+4 intervals, each of width

$$\Delta = (ZBU - ZBL)/(NSCAN + 1) \tag{3.4}$$

It successively examines the sign of the function CMVP(Z) = CSP(Z)-VP at points ZBU, ZBU + Δ, ZBU + 2Δ, etc., until an interval is found at which the signs at the two intervals are opposite, suggesting that a root is bracketed in that interval. The actual value of the root is found by a library subroutine ZREAL2. The search then goes on to succeeding intervals until a maximum of two roots is found. Output is NRTS the number of roots (0,1, or 2) and the values ZA and ZB of the roots; ZA is the first root (smallest z) and ZB is the second root (larger z). Typically, we would expect ZA to correspond to the lower turning point, ZB to the upper turning point.

In successive applications of integration between limits, one or both of which are turning points, it is important that one not overshoot a turning point since then the square root in the denominator in Eqs. (3.1)and (3.3) would be imaginary. For this reason we have devised another subroutine called SHIFT which adjusts the values

ZLOW and ZUP corresponding to a numerical approximation for the actual turning points to values which are in the immediate neighborhood of the input values but which are such that CSP(ZLOW) < VP and CSP(ZUP) < VP The adjustments are carried out in units of 10^{-8} until these criteria are satisfied.

Integrals of $|dx/dz|$ and $|dt/dz|$ (or of any other z dependent quantity) between arbitrary values ZLOW and ZUP (not necessarily turning points) are accomplished by an integration function subroutine RAINT. This performs such that

$$\mathrm{RAINT(RDXDZ,ZLOW,ZUP)} = \int_{\mathrm{ZLOW}}^{\mathrm{ZUP}} |dx/dz| \, dz \qquad (3.5)$$

$$\mathrm{RAINT(RDTDZ,ZLOW,ZUP)} = \int_{\mathrm{ZLOW}}^{\mathrm{ZUP}} |dt/dz| \, dz \qquad (3.6)$$

In the execution of this integration, the range of integration is broken into integrals from ZLOW to ZAVE and from ZAVE to ZUP where ZAVE = (1/2)(ZLOW + ZUP), i.e.

$$\mathrm{INTEGRAL} = \int_{\mathrm{ZLOW}}^{\mathrm{ZAVE}} \mathrm{(INTEGRAND)}\, dz - \int_{\mathrm{ZUP}}^{\mathrm{ZAVE}} \mathrm{(INTEGRAND)}\, dz \qquad (3.7)$$

The reason for this is that the library subroutine QUAD used to perform the integration is most efficient when it integrates away from a singularity and we anticipate the possibility that the integrand may be singular at either ZLOW or ZUP; these could be ray turning points.

The integrals of $|dx/dz|$ and $|dt/dz|$ between lower and upper turning points are performed by a subroutine named RANG. The values of z corresponding to the turning point values are supplied as inputs, the other information needed is presumed stored in COMMON. Outputs are RTIME and RLNTH for the integrals over $|dt/dz|$ and $|dx/dz|$ respectively. The significance of these parameters is that the rays are periodic in path. The time required to go N half ray cycles is just

(N)(RTIME) while the horizontal distance traveled is (N)(RLNTH).

Ray paths going from a given source location to a far field point may be characterized by (1) the horizontal phase velocity VP, (2) an index parameter IT which is 1 if the ray is proceding initially obliquely upwards, -1 if proceding initially obliquely downwards, (3) another index parameter JT whose values +1 or -1 give the sign of dx/dz at the final point on the ray, (4) the number NUP of upper turning points which the ray passes through, (5) the number NDOWN of lower turning points, (6) the initial height ZSC of the ray, and (7) the final height ZLIS of the ray. These parameters are further explained in Fig. 4. One should note that, if IT=JT, then NUP=NDOWN, if IT=1, JT=-1, then NDOWN=NUP-1; if IT=-1, JT=1 then NUP=NDOWN-1. The total horizontal distance R which the ray travels is

$$R = (N)(RLNTH) + RST + REND \qquad (3.8)$$

where N is the number of complete half cycles the ray makes, given by

$$N = NUP + NDOWN - 1 \qquad (3.9)$$

while

$$RST = \int_{ZSC}^{ZUP} |dx/dz|\, dz \qquad IT = 1 \qquad (3.10a)$$

$$= \int_{ZLOW}^{ZSC} |dx/dz|\, dz \qquad IT = -1 \qquad (3.10b)$$

$$REND = \int_{ZLIS}^{ZUP} |dx/dz|\, dz \qquad JT = -1 \qquad (3.11a)$$

$$= \int_{ZLOW}^{ZLIS} |dx/dz|\, dz \qquad JT = 1 \qquad (3.11b)$$

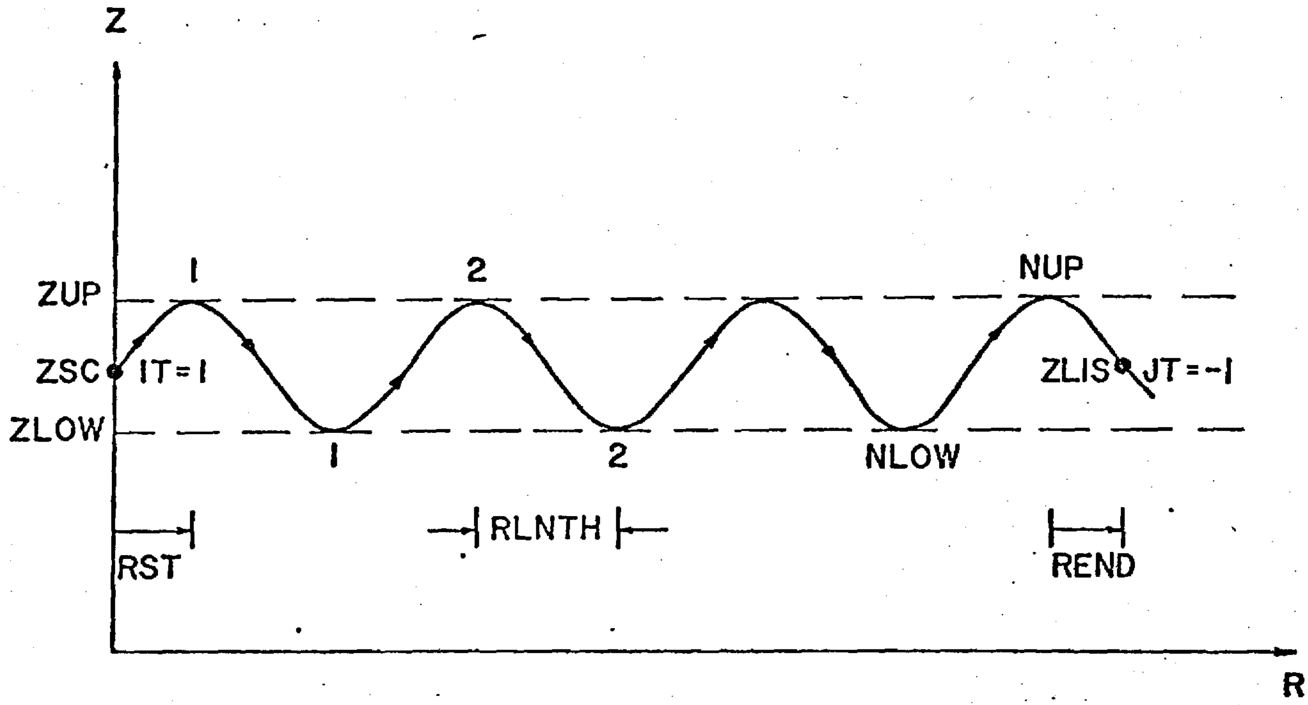

Figure 4.

Parameters describing a guided ray's path through the atmosphere; RLNTH is the half cycle ray repetition length, IT=1 or -1 if the ray is initially proceeding obliquely upwards or obliquely downwards, respectively, JT=1 or -1 describes slope at end point, ZUP and ZLOW are heights of upper and lower turning points, NUP is the number of upper turning points, NLOW is the number of lower turning points, RST is horizontal distance to first turning point, REND is corresponding distance from last turning point to receiver, ZSC is height of source, ZLIS is height of receiver.

The above formulas hold even should both NUP and NDOWN be zero, the computation giving for, say, IT=JT=1

$$R = \left[\int_{ZSC}^{ZUP} + \int_{ZLOW}^{ZLIS} - \int_{ZLOW}^{ZUP}\right] |dx/dz|\ dz$$

$$= \int_{ZSC}^{ZLIS} |dx/dz|\ dz \qquad (3.12)$$

The computation of total range with the above listed inputs is accomplished by a subroutine named TOTRAN. It calls TNPNT first to find the turning points, then SHIFT to adjust the turning points so that the integrands exist throughout the integration range, then RANG to determine the ray half cycle length RLNTH and uses the library subroutine QUAD to find the initial and final integrals RST and REND.

The above computation algorithms implicitly assume the lower point on any given ray is a lower turning point rather than the ground. The method may be easily extended to include ground reflections although we have not yet done so.

IV. RAYS CONNECTING SOURCE AND LISTENER

Of pertinent interest in any ray acoustic calculation is the tabulation of rays which connect given source and listener (receiver) locations. Let us denote source and listener heights by ZSC and ZLIS, the horizontal distance of listener from source by RANGE. Then, given a ray type denoted by parameters IT, JT, NUP, NDOWN as defined previously, and given a phase velocity VP we may define a function RMRAYD(VP) as the difference between actual range R and the range which would correspond to the given values VP, ZSC, ZLIS, IT, JT, NUP, and NDOWN. If this function is zero, then the ray being considered does pass through the listener location. Otherwise, it does not. The function subroutine RMRAYD computes this difference, VP is an input, the remaining necessary parameters are stored in COMMON.

To find the values of VP at which

$$\text{RMRAYD(VP)} = 0 \tag{4.1}$$

given fixed ZSC, ZLIS, IT, JT, NUP, and NDOWN, a subroutine FNDVP is used. This scans values of VP between VPHST and VPHEND at intervals of SDELT until an interval is bracketed within which RMRAYD changes sign. Once such an interval is found, a library subroutine ZREAL2 is used to find the precise value of the root. Up to NMAX such roots are found, the number actually found is denoted NFND, the roots being denoted VPFND(1), VPFND(2), ... , VPFND(NFND).

By use of FNDVP, one can, in principle, find all rays of a given type which connect source and listener. A systematic variation of ray types (IT, JT, NUP, and NDOWN) will in this manner give all the rays connecting source and listener.

V. RAY SPREADING

Two coplanar rays, both proceeding initially either obliquely upwards or obliquely downwards, may be characterized by phase velocities v_{p1} and v_{p2}. Assuming that v_{p2} is arbitrarily close (but not identically equal to) v_{p1} we may characterize the separation of the rays by a parameter Δs which (see Fig. 5) is the perpendicular distance from a point on the first ray to the second ray. We consider Δs as positive if the second ray lies above the first, negative if below the first. The parameter Δs may be considered a function of horizontal distance x and also of the phase velocity. The limit

$$ds/dv_p = \lim_{v_{p2} \to v_{p1}} \left\{ \Delta s/(v_{p2}-v_{p1}) \right\} \tag{5.1}$$

may be considered a uniquely defined function of range x, phase velocity v_p, ray type (IT=1 or -1) and ray initial height ZSC. We term this derivative the <u>ray spreading function.</u> One may note that within any

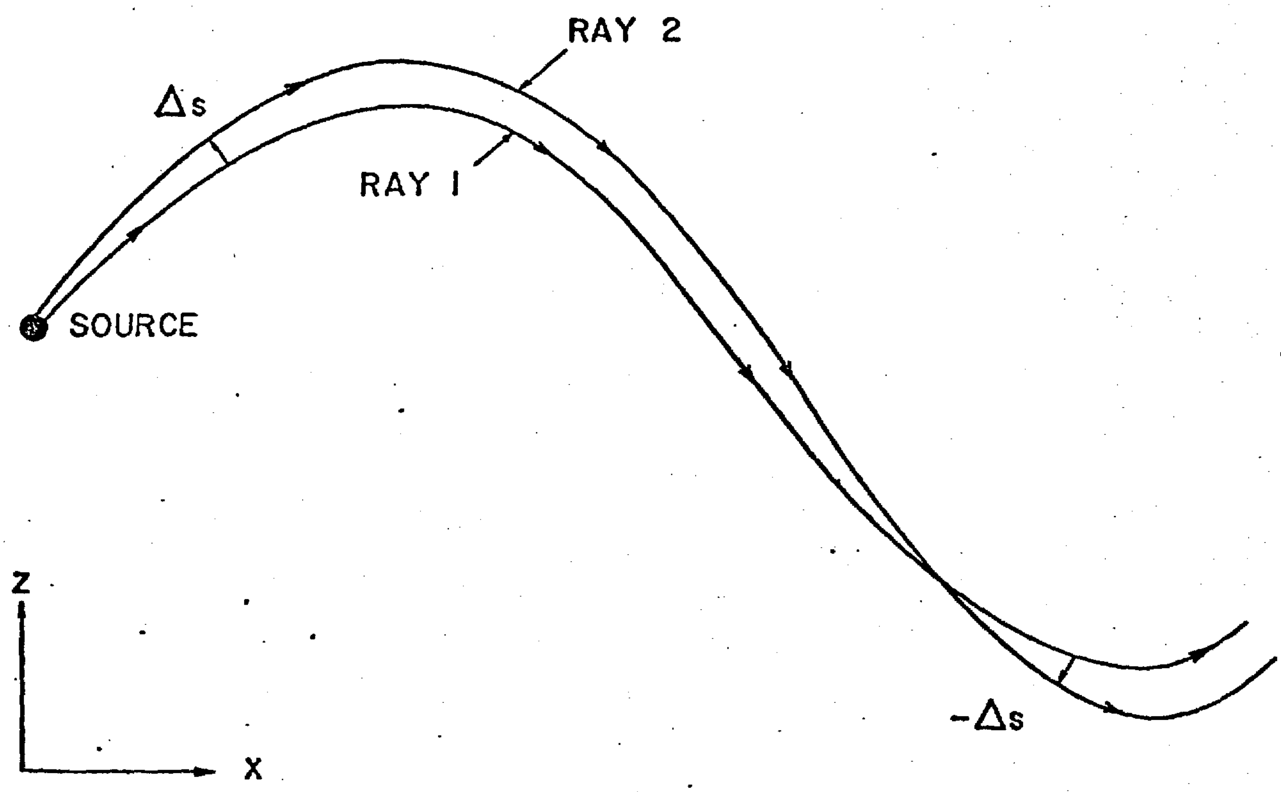

Figure 5.

Definition of parameter Δs characterizing two adjacent rays with horizontal phase velocities v_{p1} and v_{p2}. Note that Δs changes sign when the rays cross.

ray segment (i.e. between turning points)

$$ds/dv_p = \pm(dx/dv_p)/\{1 + (dx/dz)^2\}^{1/2}$$

$$= \pm (dx/dv_p)\{1 - (c/v_p)^2\}^{1/2} \qquad (5.2)$$

where the plus sign applies if the ray is proceeding obliquely downwards (JT=-1), the minus sign if it is proceeding obliquely upwards (JT=1), dx/dv_p is the rate of change of horizontal distance traveled with respect to phase velocity at fixed z and fixed ray initial position.

The derivative dx/dv_p may in turn be calculated if one knows the general ray type. For a ray proceeding initially upwards (IT=1) and going through NUP upper turning points and NDOWN=NUP lower turning points and ending with direction obliquely upwards, one has, for example,

$$x = \int_{ZSC}^{ZUP} |dx/dz|\, dz + N\int_{ZLOW}^{ZUP} |dx/dz|\, dz + \int_{ZLOW}^{Z} |dx/dz|\, dz \qquad (5.3)$$

where N = NUP + NDOWN -1 = 2(NUP) -1. Here the integrand $|dx/dz|$ is given by Eq. (3.1). To differentiate this expression with respect to v_p, one must take into account the fact that ZLOW and ZUP as well as $|dx/dz|$ depend on v_p. A formal application of the rules for differentiating an integral with respect to a parameter leads to singularities and some tricks are required to avoid this. In particular, it is convenient to rewrite the above as

$$x = I(ZSC,ZUI) + (N+1)\, I(ZUI,ZUP) + (N+1)\, I(ZLOW,ZLI)$$

$$+ (N+1)\, I(ZLOW,ZLI) + (N)\, I(ZLI,ZUI) + I(ZLI,Z) \qquad (5.4)$$

where I(Z1,Z2) represents the integral of $|dx/dz|$ between the indicated limits, ZUI is a fixed (v_p independent) value of z slightly less than ZUP, ZLI is slightly larger than ZLOW. (See Fig. 6.) One may also note that

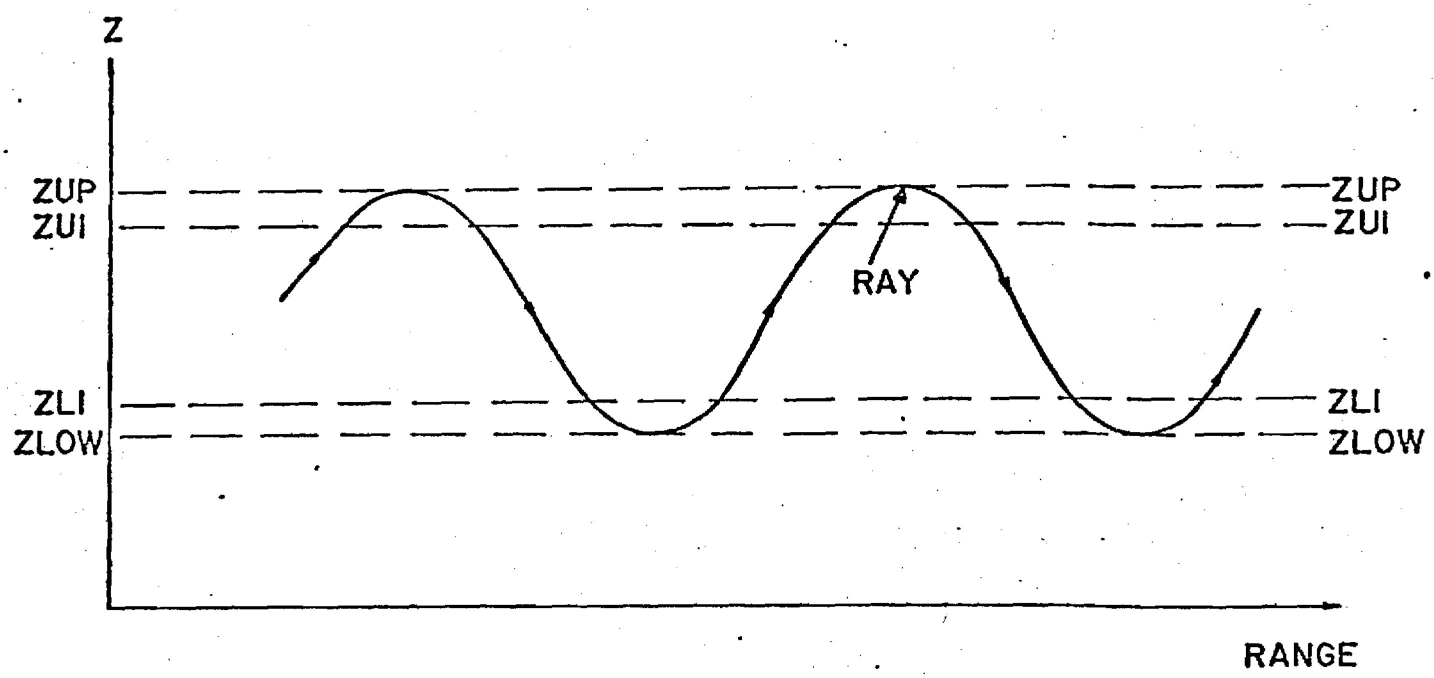

<u>Figure 6.</u>

Definition of parameters ZUI (slightly below upper turning point ZUP) and ZLI (slightly above lower turning point ZLOW) used in the calculation of ray spreading parameter ds/dv_p.

$$I(ZU,ZIP) = \int_{ZU}^{\infty} I(ZIP-z)\,|dx/dz|\,dz \tag{5.5}$$

$$|dx/dz| = -(dc/dz)^{-1}(d/dz)(v_p^2 - c^2)^{1/2} \tag{5.6}$$

so an integration by parts gives

$$I(ZU,ZIP) = \{(dc/dz)^{-1}(v_p^2 - c^2)^{1/2}\}_{ZU} + \int_{ZU}^{\infty} (v_p^2 - c^2)^{1/2}\, I(ZIP-z)(d/dz)(dc/dz)^{-1}\,dz \tag{5.7}$$

and, consequently, one has

$$(d/dv_p)I(ZU,ZP) = \{(v_p/c)(dc/dz)^{-1}|dx/dz|\}_{ZU} + \int_{ZU}^{ZIP} (v_p/c)\,|dx/dz|\,(d/dz)(dc/dz)^{-1}\,dz \tag{5.8}$$

Providing dc/dz does not vanish in the interval between ZU and ZIP, both of these terms should be finite. In a similar manner, one can show that

$$(d/dv_p)I(ZLOW,ZLI) = -\{(v_p/c)(dc/dz)^{-1}|dx/dz|\}_{ZLI} + \int_{ZLOW}^{ZIP} (v_p/c)\,|dx/dz|\,(d/dz)(dc/dz)^{-1}\,dz \tag{5.9}$$

The derivatives of the remaining terms in the expression (5.4) are relatively simple since the integration limits are independent of v_p. In particular one has

$$(d/dv_p)I(ZSC,ZU) = -\int_{ZSC}^{ZU} (v_p\ c)(v_p^2-c^2)^{-3/2}\ dz \qquad (5.10)$$

Thus one obtains the expression (IT=1, JT=1)

$$\begin{aligned} dx/dv_p &= I1(ZSC,ZU) + (N+1)J1(ZU) + (N+1)I2(ZU,ZUP) \\ &\quad - (N+1)J1(ZLI) + (N+1)I2(ZLOW,ZLI) + (N)I1(ZLI,ZU) \\ &\quad + I1(ZLI,Z) \end{aligned} \qquad (5.11)$$

where we have abbveviated

$$I1(ZA,ZB) = -\int_{ZA}^{ZB} cv_p(v_p^2-c^2)^{-3/2}\ dz \qquad (5.12a)$$

$$J1(ZA) = \{(v_p/c)(dc/dz)^{-1}|dx/dz|\}_{z=ZA} \qquad (5.12a)$$

$$I2(ZA,ZB) = \int_{ZA}^{ZB} (v_p/c)|dx/dz|(d/dz)(dc/dz)^{-1}\ dz \qquad (5.12c)$$

In general, for a ray of specified type (IT, JT, NUP,NDOWN), the corresponding expression for dx/dv_p is

$$\begin{aligned} dx/dv_p &= \left\{\begin{matrix} I1(ZSC,ZU) \\ I1(ZLI,ZSC) \end{matrix}\right\} + (2)(NUP)J1(ZU) + (2)(NUP)I2(ZU,ZUP) \\ &\quad - (2)(NDOWN)J1(ZLI) + (2)(NDOWN)I2(ZLOW,ZLI) \\ &\quad + (NUP+NDOWN-1)I1(ZLI,ZU) + \left\{\begin{matrix} I1(ZLI,Z) \\ I1(Z,ZU) \end{matrix}\right\} \end{aligned} \qquad (5.13)$$

The two possibilities for the first term correspond to IT=1 and -1, respectively, while two possibilities for the second term correspond to JT=1 and -1, respectively.

The integrand for the integrals of type I1 is computed by a function subroutine FIRM(Z), while twice the values of those of type I2 are computed by a function subroutine FIRMUL(Z), i.e.

$$\text{I1(ZA,ZB)} = \text{RAYINT(FIRM,ZA,ZB)} \tag{5.14a}$$

$$\text{I1(ZA,ZB)} = \text{RAYINT(FIRMUL,ZA,ZB)/2} \tag{5.14b}$$

Also the quantity 2[J1(Z)] is denoted in the program by TRNPT(Z), i.e.

$$\text{TRNPT}(z) = 2v_p(dc/dz)^{-1}(v_p^2-c^2)^{-1/2} \tag{5.15}$$

so the expression for dx/dv_p becomes

$$\begin{aligned}\text{DXDVP} = {} & \text{TERMST + (NUP)TRNPT(ZUI) + (NUP)RAYINT(FIRMUL,ZUI,ZUP)} \\ & \text{- (NDOWN)TRNPT(ZLI) + (NDOWN)RAYINT(FIRMUL,ZLOW,ZLI)} \\ & \text{+ (NUP+NDOWN-1)RAYINT(FIRM,ZLI,ZUI) + TERMLT}\end{aligned} \tag{5.16}$$

where the first and last terms are

$$\text{TERMST} = \text{RAYINT(FIRM,ZSC,ZUI)} \qquad \text{IT} = 1 \tag{5.17a}$$

$$= \text{RAYINT(FIRM,ZLI,ZSC)} \qquad \text{IT} = -1 \tag{5.17b}$$

$$\text{TERMLT} = \text{RAYINT(FIRM,Z,ZUI)} \qquad \text{JT} = -1 \tag{5.18b}$$

$$= \text{RAYINT(FIRM,ZLI,Z)} \qquad \text{JT} = 1 \tag{5.18b}$$

One may then calculate ds/dv_p from Eq. (5.2), i.e.

$$\text{DSDVP} = -\text{SIGN(JT)(DXDVP)}(1-\{c/v_p\}^2)^{1/2} \tag{5.19}$$

The sequence of computations just described is carried out by a subroutine CDSDVP. The parameters VP, ZSC, Z, IT, JT, NUP, AND NDOWN are inputs, the output is DSDVP. The parameters ZLI and ZUI are computed internally and set to

$$\text{ZLI} = \text{ZLOW} + .01(\text{ZUP}-\text{ZLOW}) \tag{5.20a}$$

$$\text{ZUI} = \text{ZUP} - .01(\text{ZUP}-\text{ZLOW}) \tag{5.20b}$$

The choice of .01 is of course arbitrary. The chief constraint is that dc/dz should not vanish between ZLOW and ZLI and between ZUI and ZUP.

If one considers the variation of ds/dv_p with x along a single ray (say with IT=1) it is apparent that up to the first upper turning point ds/dv_p should be positive since FIRM(Z) is negative; JT is positive. At the turning point one has

$$\begin{aligned} ds/dv_p &= \lim_{z \to \text{ZUP}} \left\{ (1-\{c/v_p\}^2)^{1/2} \int_{\text{ZSC}}^{z} cv_p(v_p^2-c^2)^{-3/2} dz \right\} \\ &= \{1/(dc/dz)\}_{\text{ZUP}} \end{aligned} \tag{5.21}$$

which, interestingly, is independent of ZSC. This follows if one breaks the integral above into integrals from ZSC to ZUI and from ZUI to Z, given ZUI < Z< ZUP, and expands c in a power series about its value v_p at z=ZUP.

Between the first upper turning point and the first lower turning point the function ds/dv_p is given by

$$\begin{aligned} ds/dv_p = \{1-(c/v_p)^2\}^{1/2} \Big\{ & \text{RAYINT(FIRM,ZSC,ZUI)} \\ & + \text{TRNPT(ZUI)} + \text{RAYINT(FIRMUL,ZUI,ZUP)} \\ & + \text{RAYINT(FIRM,Z,ZUI)} \Big\} \end{aligned} \tag{5.22}$$

A brief analysis indicates that this can be put in a form independent of ZUI, i.e.

$$\frac{ds}{dv_p} = \{1-(c/v_p)^2\}^{1/2} \left\{ \frac{(v_p/2)^{1/2}/\alpha^{3/2}}{(ZUP - ZSC)^{1/2}} + \frac{(v_p/2)^{1/2}/\alpha^{3/2}}{(ZUP - Z)^{1/2}} - \int_{ZSC}^{ZUP} Arg^{(1)}(z_o, ZUP)dz_o - \int_{Z}^{ZUP} Arg^{(1)}(z_o, ZUP)dz_o \right\} \tag{5.23}$$

where

$$Arg^{(1)}(z, ZUP) = \frac{cv_p}{(v_p^2 - c^2)^{3/2}} - \frac{v_p^2}{(ZUP-z)^{3/2}(2\alpha v_p)^{3/2}} \tag{5.24}$$

and we have abbreviated α for dc/dz at ZUP. The subtracted term in the arguments insures that the integrals exist. Also, as $Z \to ZUP$, the second term in the brackets dominates and one has

$$\{1 - (c/v_p)^2\}^{1/2} \to (2\alpha/v_p)^{1/2}(ZUP-z)^{1/2} \tag{5.25}$$

and $ds/dv_p \to 1/\alpha$ in accordance with Eq. (5.21). On this basis, we may conclude that the quantity in braces in Eq. (5.22) starts out large and positive for Z close to ZUP, decreases monotonically (since FIRM(Z) is always negative) and eventually goes to $-\infty$ when $Z \to ZDOWN$. Thus there is one and only one point on the ray between the first turning point and the second turning point at which $ds/dv_p=0$. This point is identified as a point on a caustic (where adjacent rays intercept).

At the second turning point (first lower turning point) the same sort of limiting process described above gives

$$ds/dv_p = \{1/(dc/dz)\}_{ZLOW} \tag{5.26}$$

which as mentioned above is a negative number.

Between the first lower (second overall) and second upper (third overall) turning points, one may similarly argue that ds/dv_p goes to zero at one and only one point, etc., before that point ds/dv_p is negative, after that point it is positive, it approaches $[1/(dc/dz)]_{ZUP}$ at the next upper turning point, etc. The general situation is as sketched in Fig. 7.

The number of times ds/dv_P goes to zero along a ray path (i.e., the number of caustics encountered) is just

$$\text{Number of caustics} = (\text{Number of complete half ray cycles}) + (\text{zero or one}) \tag{5.27}$$

The second term is zero if JT=1 (upgoing ray) and the current value of ds/dv_P is negative or if JT=-1 (downgoing ray) and the current value of ds/dv_P is positive. Otherwise, it is one.

The number of complete half ray cycles, one may note, is just NUP + NDOWN -1 if either NUP or NDOWN are greater than one. Thus, it is a simple matter to determine, at a given point on a ray, just how many caustics the ray has encountered in passing from source to that point.

VI. RAY AMPLITUDES

Given that the acoustic pressure in the immediate vicinity of the source is of the form implied by Eq. (1.4), the Fourier transform $\hat{p}(\omega,\vec{r})$, defined such that

$$p(\vec{r},t) = \mathrm{Re}\int_0^\infty \hat{p}(\omega,\vec{r})e^{-i\omega t}\,d\omega, \tag{6.1}$$

of the acoustic pressure may be inferred from the geometrical acoustics model[7] to be (in first approximation) given by a sum over rays. The contribution from any particular ray connecting source and receiver is simply

$$\hat{p}_{ray} = \hat{f}(\omega)\rho_o^{1/2}(z_{SC})\{\text{Atmosphere factor}\}\{\text{Spreading factor}\} \times \{(-i)^{N_c}\}\, e^{i\omega t_{ray}} \tag{6.2}$$

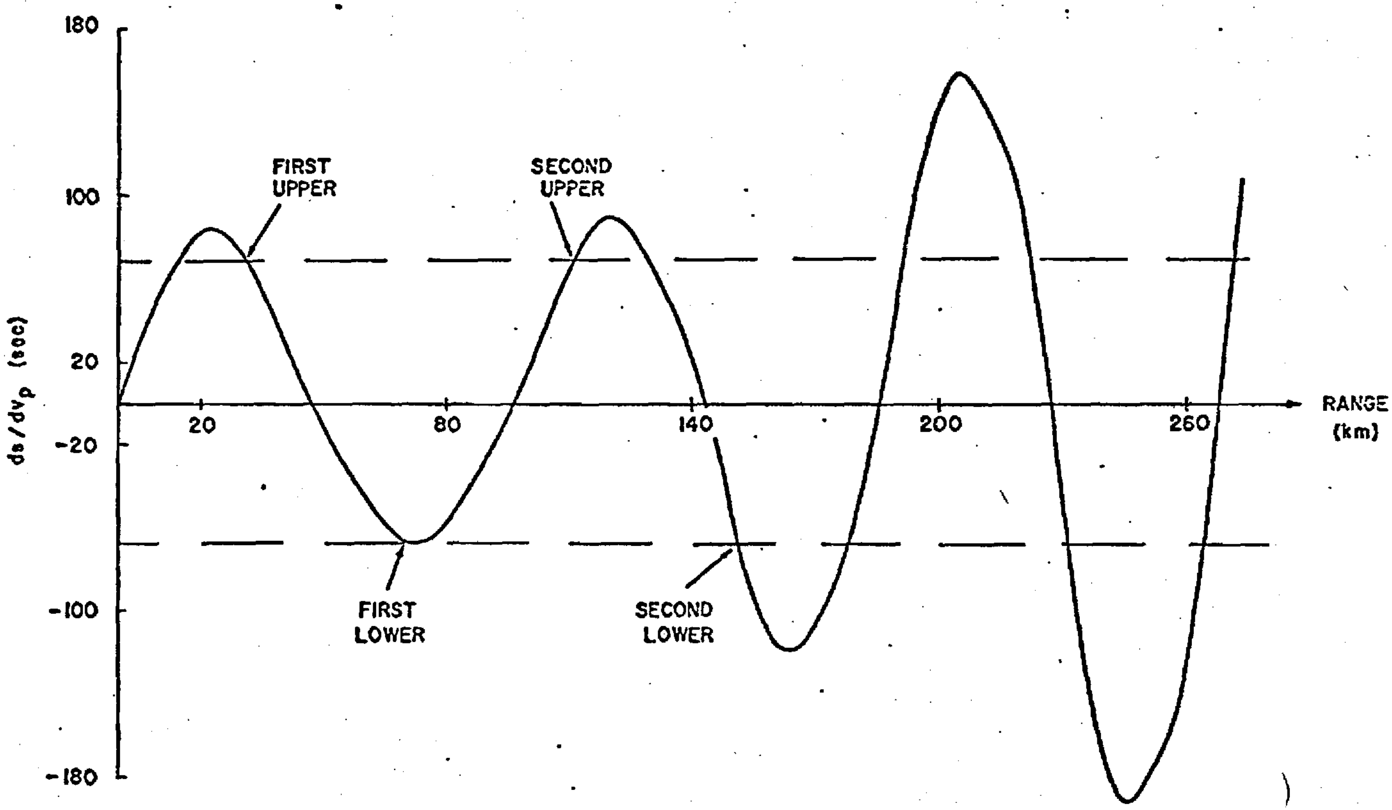

Figure 7.

Values of ds/dv_p along two adjacent guided rays, illustrating the conclusion that the number of caustics encountered is the number of complete half ray cycles traversed plus 0 or 1.

where N_c is the number of times the ray has touched (tangentially) a caustic, t_{ray} is net travel time along the ray. The atmosphere factor is given by

$$\{\text{Atmosphere factor}\} = \{(\rho_o c)_z/(\rho_o c)_{SC}\}^{1/2} \tag{6.3}$$

while the spreading factor is the inverse square root of the ray tube area normalized such that this factor reduces to 1/R near the source (i.e., at the beginning of the ray). The criterion for determination of these factors is that

$$\{|\hat{p}_{ray}|^2/\rho_o c\}\{\text{ray tube area}\} = \text{constant} \tag{6.4}$$

along a ray, that the limit (1.4) be realized and that the net phase change from source to receiver be $-\omega t_{ray} + N_c \pi/2$.

A consideration of a cylindrically symmetric bundle of rays leaving the source at angles between θ and θ+dθ with respect to the vertical leads one to the conclusion that the ray tube area should be a constant times $|(ds/dv_p)r_{Hor}|$ where ds/dv_p is the quantity discussed in the previous section, r_{Hor} is horizontal distance from source to listener. One can also show, by considering a medium in which the sound speed is constant, that near the source

$$r_{Hor}|ds/dv_p| = \frac{R^2 c^2/v_p^3}{\{1-(c/v_p)^2\}^{1/2}} \tag{6.5}$$

so one identifies the spreading factor as the square root of

$$\{\text{Spreading factor}\}^2 = \frac{c^2/v_p^3}{\{1-(c/v_p)^2\}^{1/2}} \frac{1}{r_{Hor}|ds/dv_p|} \tag{6.6}$$

where c is here taken as the sound speed of the source.

One may note that the spreading factor goes to ∞ whenever ds/dv_p goes to zero, i.e., at a caustic. This is one indication that the general formula may not be applicable everywhere. The modification of the method to take into account proximities to caustics is discussed in the remaining portions of the report.

VII. GEOMETRY NEAR CAUSTICS

When viewed in a vertical plane containing the source, caustic surfaces appear locally as arcs of circles, the rays which touch it also appear locally as arcs of circles; the situation is as sketched in Fig. 8. Each caustic has a shadow side and an illuminated side. If a receiver is on the illuminated side, then one may expect in general that two rays touching the caustic tangentially will also pass through a point A on the illuminated side, both of these rays will have approximately the same radius of curvature R_{ray} and will touch the caustic at points B and C, such as indicated in Fig. 9. Parameters of interest here are (1) the radius R_c of curvature of the caustic, (2) the distance δ from point A to the caustic, (3) the arc length $(\Delta\theta)R_c = \ell$ along the caustic between points B and C; and (4) the angle ϕ between the two rays at point A; as well as (5) the radius R_{ray} of curvature of the two rays. These parameters are related and it is a challenging exercise in analytical geometry to determine their interrelationships. Fortunately, the end results are relatively simple in the case of interest where $\delta \ll R_c, \delta \ll R_{ray}$. One finds, in particular

$$\delta = (1/8)(R_c^{-1} + R_{ray}^{-1})\ell^2 \tag{7.1}$$

$$\phi = (R_c^{-1} + R_{ray}^{-1})\ell \tag{7.2}$$

Another quantity of interest is the separation Δs between two rays which touch the caustic at points $\theta = -\Delta\theta/2$ and $\Delta\theta/2$ (Fig. 9). If we interpret Δs as positive if the second ray lies above the first, then

$$\Delta s/(R_c\Delta\theta) \cong -\xi(R_c^{-1} + R_{ray}^{-1}) \tag{7.3}$$

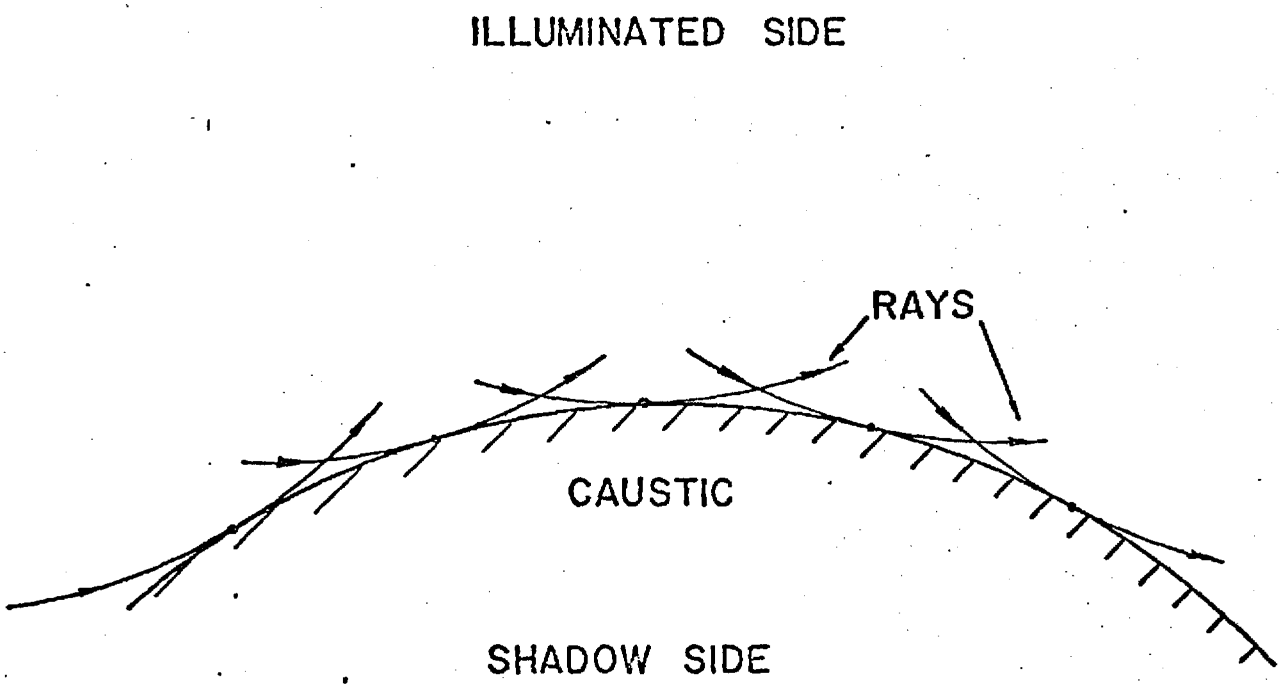

Figure 8.

Sketch of rays in the vicinity of a caustic. The caustic is approximately an arc of a circle, the rays are also locally arcs of circles. Note that the caustic has an illuminated side and a shadow side.

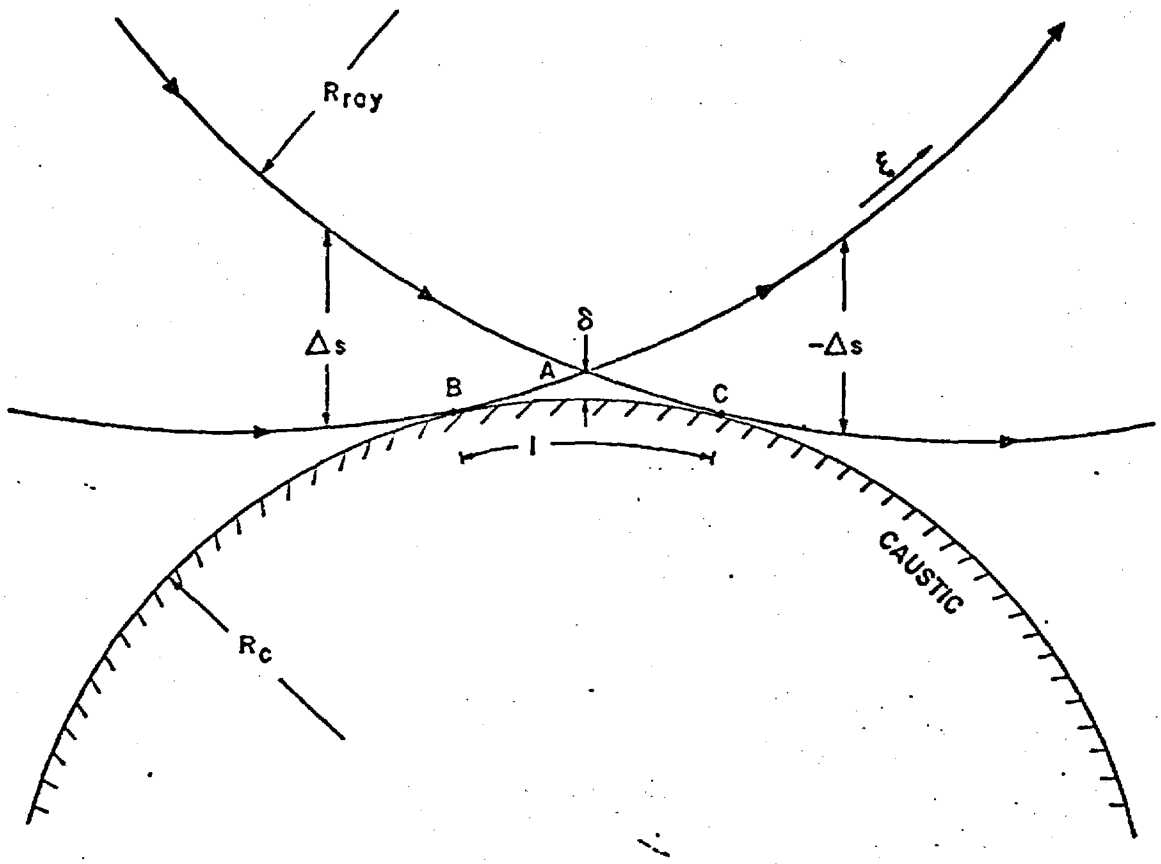

Figure 9.

Detailed sketch of two rays which cross on the illuminated side of a caustic at a point A and which touch the caustic at points B and C respectively; R_c is the radius of curvature of the caustic, R_{ray} is the radius of curvature of either ray; δ is the distance of A from the caustic, ϕ is the angle between the two rays where they cross, ℓ is arc distance along caustic between points B and C, ξ is arc length along either ray, Δs is the separation distance between the two rays.

where ξ is distance along either ray in the positive sense from the caustic. Thus, if the upgoing ray in Fig. 9 is characterized by phase velocity v_{p1}, the downgoing ray by phase velocity v_{p2}, we may characterize their respective ds/dv_p at the point A by

$$(ds/dv_p)_1 = -(d\ell/dv_p)(\ell/2)(R_c^{-1} + R_{ray}^{-1}) \tag{7.4a}$$

$$(ds/dv_p)_2 = (d\ell/dv_p)(\ell/2)(R_c^{-1} + R_{ray}^{-1}) \tag{7.4b}$$

where

$$d\ell/dv_p = \ell/(v_{p2}-v_{p1}) \tag{7.4c}$$

It should be noted that $(ds/dv_p)_1$ is equal and opposite to (ds/dv_p)

In typical applications, such as are discussed in the next section, it may be presumed that the point A is known, the phase velocities and slopes of the two rays and therefore ϕ are known, the ray radius R_{ray} is known, the parameters $(ds/dv_p)_1$ and $(ds/dv_p)_2$ are known and are equal and opposite, but R_c, δ, and ℓ are not known. A successive solution of Eqs. (7.1-4) for the unknowns in terms of the knowns gives

$$\begin{aligned}\delta &= -(1/4)(v_{p2}-v_{p1})(ds/dv_p)_1 = (1/4)(v_{p2}-v_{p1})(ds/dv_p)_2 \\ &= (1/8)(v_{p2}-v_{p1})[(ds/dv_p)_2-(ds/dv_p)_1]\end{aligned} \tag{7.5a}$$

$$\ell = (v_{p2}-v_{p1})[(ds/dv_p)_2-(ds/dv_p)_1]/\phi \tag{7.5b}$$

$$R_c^{-1} + R_{ray}^{-1} = \{(v_{p2}-v_{p1})[(ds/dv_p)_2-(ds/dv_p)_1]\}^{-1} \tag{7.5c}$$

If we wish to characterize the distance of the point A from the caustic by a relevant dimensionless parameter, the natural choice (as explained subsequently) is the <u>caustic proximity parameter</u> whose definition may be taken to be

$$\eta = -2^{1/3}(\omega/c)^{2/3}[(1/R_{ray})+(1/R_c)]^{1/3}\delta \tag{7.6}$$

This is negative on the illuminated side and, as may be noted, depends on the angular frequency ω. In terms of the ray parameters described above, one may state that η for the point A on the illuminated side is

$$\eta = -2^{1/3}(\omega/c)^{2/3}(1/8)\{(v_{p2}-v_{p1})[(ds/dv_p)_2-(ds/dv_p)_1]\}^{2/3} \tag{7.7}$$

which should always be negative (i.e., $[-|f|]^{2/3}=[|f|]^{2/3}$).

VIII. THE SEARCH FOR CAUSTICS

To explore the possibility of the receiver being near but on the illuminated side of a caustic, all of the rays connecting source and receiver are ordered according to increasing phase velocity, those initially going obliquely upwards and obliquely downwards being considered as separate groups. For each successive pair of rays (i,i+1), one computes the corresponding values of ds/dv_p and determines the number of times each ray has touched a caustic according to the prescription in Sec. V. If the signs are the same or if the N_c's differ by a quantity other than one, no action is taken and one proceeds to the next pair ($i+1\to i$, $i+2\to i+1$). Once the above criteria are satisfied, one terms the two rays as a possible caustic pair. They are temporarily reordered such that the one with the larger N_c is called "the first ray" the one with N_c being 1 less is called "the second ray". The slopes of the two rays are determined from Eq. (3.1) and the angle ϕ (which could be negative) is computed in accordance with the correspondence in Fig. 9. One also computes δ from Eq. (7.5a). Then one checks to see if ϕ and δ have the same sign. If not, the process starts over with the next pair. If they do have the same sign, then one computes the caustic proximity parameter η according to Eq. (7.7). If $|\eta|>4$, one would decide that the caustic is too far away for any special modifications. However, if one finds $|\eta|\leq 4$, the contribution to the sum over rays from those two rays is deleted from the sum and replaced by a new composite term involving Airy functions. (The method of doing this is explained in the next section.)

The second possibility is that the receiver lies near a caustic but on its shadow side. The following type of search is contemplated. First one examines the function RMRAYD(VP) described in Sec. IV. If the absolute value of this function has a local minimum (not zero) for some value of the phase velocity, then the possibility of the receiver being near the caustic is indicated. The search for such local minima is similar to that described in the discussion of FNDVP: one scans successive values of RMRAYD until one finds three successive phase velocities such that (1) all three RMRAYD's have the same sign and (2) the magnitude of the middle one is less than either of the two end ones. One then breaks this bracketed interval down into, say, 20 subintervals, calls FNDVP to see if there are any roots in the interval. If FNDVP finds two roots, these are considered as rays connecting source and listener and the process stops. If FNDVP finds only one, the subdivision is made progressively smaller until two roots are found (if there is one, there must be two) and these roots are added to the overall group of rays connecting source and listener. If FNDVP finds no roots, then the local minimum is found by the above scanning process and one continues this iteration until the location of the minimum is accurately bracketed. Its precise location is found by fitting a parabola to the final triplet of points and then finding the minimum of this parabola. The parameters IT, JT, VP, NUP, NDOWN are then considered as defining a <u>near miss ray</u>.

To locate the point on the considered caustic which is closest to the actual receiver location, one considers the two equations

$$x = x(v_p, z) \qquad (8.1a)$$

$$ds/dv_p = F(v_p, z) \qquad (8.1b)$$

with IT, JT, NUP, NDOWN considered fixed. The two indicated functions may be considered as defined by subroutines TOTRAN and CDSDVP. The caustic is the locus of points at which $dx/dv_p=0$. The scheme outlined above gives one such point. Successive points are determined from

$$\partial F/\partial v_p = -(\partial F/\partial z)(dz/dv_p)$$

$$dx/dv_p = (\partial x/\partial v_p) + (\partial x/\partial z)(dz/dv_p)$$

or

$$dz/dv_p = -(\partial F/\partial v_p)/(\partial F/\partial z) \tag{8.2a}$$

$$dx/dv_p = (\partial x/\partial v_p) - (\partial x/\partial z)(\partial F/\partial v_p)/(\partial F/\partial z) \tag{8.2b}$$

One may note that these two functions on the right hand side are easily programed. One now simply numerically integrates these differential equations until he reaches a point at which the distance of (x,z) from the actual receiver location is a minimum. The scanning regime must, however, be restricted to points at which $\partial F/\partial z$ is nonzero, the other quantities on the right hand sides should be finite. The minimum distance is that corresponding to the allowable scanning region. Once this minimum distance point has been found, one varies x and z until a neighboring point is found at which two rays pass through with approximately the same value of v_p as that corresponding to the caustic point. Parameters corresponding to these two rays at this new point are tabulated and one determines the approximate circle which describes the caustic in their vicinity according to the equations given in Sec. VII. The caustic proximity parameter corresponding to the receiver location is then computed according to Eq. (7.6) only with $(1/R_c) + (1/R_{ray})$ replaced by Eq. (7.5c), δ is replaced by the negative of the distance of the receiver location to the caustic circle. The parameter η so computed should be positive, otherwise the search in this instance stops. If η is greater than, say, 5, the presence of the caustic is disregarded.

Otherwise, it is taken into account by the method described in the next section.

IX. FIELD NEAR A CAUSTIC

The method we adopt for incorporating caustics into the computation is based on results derived by Haskell[6] in 1951. While Haskell was primarily concerned with the nature of guided modes near turning points, his analysis may easily be reinterpreted as implying that, near a caustic, the contribution due to the two rays which intersect at a point A on the illuminated side (see Fig. 9) should be replaced by

$$\hat{p} = (G)\exp\{i\omega t_c\}Ai(\eta) \tag{9.1}$$

where

$$\eta = -(3/2)\left\{\int_0^{\delta} k_{\perp}\, d\delta\right\}^{2/3} \tag{9.2}$$

Here $Ai(\eta)$ is the Airy function[17] defined by

$$Ai(\eta) = (1/\pi)\int_0^{\infty} \cos[(s^3/3)+\eta s]\, ds \tag{9.3}$$

Also, t_c is ray travel time from the source to the point on the caustic closest to the receiver point; $k_{\perp}$ is the component, normal to caustic, of either ray's wave number vector (ω/c times unit vector in ray direction); δ is the perpendicular distance from the caustic. The function G is a slowly varying function of position chosen such that Eq. (9.1) matches on to the corresponding ray theory expression when $\eta << -1$.

As regards the matching on, one may note that, if $\eta \ll -1$, the Airy function approaches an asymptotic limit[17]

$$\mathrm{Ai}(-|\eta|) \cong \pi^{-1/2}|\eta|^{-1/4}\sin[(2/3)|\eta|^{2/3}+\pi/4] \tag{9.4}$$

so Eq. (9.1) above approaches

$$\hat{p} \to [G/(2\sqrt{\pi})][e^{i\pi/4}/|\eta|^{1/4}]\{\exp[i\omega t_c - i\int_0^\delta k_\perp d\delta] - i\exp[i\omega t_c + i\int_0^\delta k_\perp d\delta]\} \tag{9.5}$$

the first term is identified, with $k_\perp > 0$, as the contribution from the ray which has not yet touched the caustic, the second from the ray which has already touched the caustic. This follows since the

$$t_{ray} = t_c \mp \int_0^\delta (k_\perp/\omega)d\delta \tag{9.6}$$

correspond to the travel times of the two rays, respectively, to the point under consideration on the illuminated side. A verification of this latter statement may be given from consideration of the fact that the t_{ray} for rays coming into the caustic may be considered as a continuous function of position which satisfies the eikonal equation[7]

$$(\nabla t_{ray})^2 = 1/c^2 \tag{9.7}$$

where t_{ray} reduces to t_c at the caustic. Consequently, if the component of ∇t_{ray} normal to the caustic is $-k_\perp/\omega$ (wave number vector divided by ω is gradient of the eikonal function) then

$$t_{ray} = t_c + \int_0^\delta \nabla t_{ray}\cdot\vec{n}\, d\delta \tag{9.8}$$

which is just Eq. (9.7) with the minus sign. Similar considerations apply for the eikonal function t_{ray} of rays leaving the caustic and the identification corresponding to the plus sign is recovered.

In the vicinity of the caustic, given the respective geometry sketched in Fig. 9, the value of $k_\perp$ may be readily shown to be approximately

$$k_\perp = (\omega/c)\sqrt{2}[(1/R_{ray}) + (1/R_c)]^{1/2}\delta^{1/2} \tag{9.9}$$

this holding to a high relative appsoximation very close to the caustic. Consequently, the value of η is given by

$$\eta = -(\omega/c)^{2/3}2^{1/3}[(1/R_{ray})+(1/R_c)]^{1/3}\delta \tag{9.10}$$

which as might be expected is exactly the same as given in Eq. (7.6) for the caustic proximity parameter

Also, one should note, on eliminating ℓ from Eqs. (7.1) and (7.4), that

$$(ds/dv_p)_1 = -(d\ell/dv_p)\sqrt{2}\,[(1/R_c)+(1/R_{ray})]^{1/2}\delta^{1/2} \tag{9.11a}$$

$$= -(ds/dv_p)_2 \tag{9.11b}$$

so

$$1/|\eta|^{1/4} = (2c/\omega)^{1/6}[(1/R_c)+(1/R_{ray})]^{1/6}|d\ell/dv_p|^{1/2}/|ds/dv_p|^{1/2} \tag{9.12}$$

The fact that the two individual terms in Eq. (9.5) must correspond to Eq. (6.2) allows us to identify the parameter G in the former as

$$G = f(\omega)\rho_o^{1/2}\{\text{Atmosphere factor}\}\{\text{Spreading factor with } |ds/dv_p|^{-1/2}\text{omitted}\}$$

$$(2c/\omega)^{-1/6}[(1/R_c)+(1/R_{ray})]^{-1/6}|d\ell/dv_p|^{-1/2}(2\sqrt{\pi})e^{i\pi/4}(-i)^{N_{pc}} \tag{9.13}$$

where N_{pc} is the number of prior caustics encountered by the two rays.

These formulas developed above give one a straightforward method for incorporating caustic corrections when the receiver lies on the illuminated side of the caustic. Given the parameters describing two rays which touch the caustic, these parameters being appropriate to the receiver location, one first computes η according to Eq. (7.7), computes $1/R_c + 1/R_{ray}$ according to Eq. (7.5c), computes ℓ according to Eq. (7.5b), then $d\ell/dv_p$ from Eq. (7.4c). These numbers are then used to calculate the factor G in Eq. (9.13). The parameter t_c is just the average travel time of the two rays from the source to the receiver location.

As regards the calculation of the Airy function $Ai(\eta)$, subroutines capable of evaluating this function are given by Posey[10] in his thesis, so there is no real computation problem involved.

If the receiver is on the shadow side of the caustic, the process is similar, but one must first find two rays passing through a point (on a line from the receiver normal to the caustic) on the illuminated side in order to determine $d\ell/dv_p$, $[(1/R_c) + (1/R_{ray})]$, and t_c. Once this is done, the parameter η is computed from Eq. (9.10), only with δ replaced by the negative of the distance from the receiver to the caustic. The function G is computed just as described previously. Since the Airy function decreases as

$$Ai(\eta) = (1/2)\pi^{-1/2}\eta^{-1/4}\, e^{-(2/3)\eta^{3/2}} \tag{9.14}$$

for large positive η, we may anticipate the contribution from the caustic on the shadow side to decrease relatively rapidly. Since $Ai(0) = .355$, $Ai(5) \approx 1.1\times10^{-4}$, one can certainly ignore values when η is greater than 5.

X. CONCLUDING REMARKS

The computational method outlined here is still under development and, at present, computer subroutines are available for performing only part of the steps envisioned for the overall waveform synthesis.

The computer subroutines presently available are given in Appendix B along with a sample MAIN program which calls them and which may be used in studying acoustic propagation with the use of these subroutines.

The project is being continued as a Ph.D. dissertation by Mr. Kinney and it is expected that an operational and comprehensive computer program based on the computation method should be available by summer 1976.

It should also be stressed that the overall method described here is expected to avoid many of the limitations one customarily associates with ray theory computations. The fact that the method produces amplitudes and phases rather than merely finding ray paths and travel times is significant. Also the fact that it allows for the possibility of more than one ray connecting source and receiver is important for realistic infrasound applications. The method of taking the presence of caustics into account should extend the applicability of the geometrical acoustics theory down to frequencies formerly considered to be the sole domain of guided mode theory and should be regarded as an important extension of the geometrical acoustics theory.

There are still some unsatisfactory features in the theory which might be given additional attention. One of these is the neglect of lacunae previously mentioned in the Introduction. While some work has been done on propagation into a shadow zone, e.g. by Pekeris[18] and by Ingard and Pridmore-Brown,[19] the results are difficult to interpret in the generalized sense required for incorporation into a computation scheme such as described here. Thus, some considerable intellectual effort probably remains to be exerted before one may satisfactorily handle lacunae.

Closely related to the lacunae problem is the coupling of two adjacent sound channels. The present theory assumes, in particular, that energy trapped in one channel stays in that channel. In reality, there is always some penetration of energy from one channel to the other and one may envision that a satisfactory description may be found by using an extended WKB approximation, matching at turning points on both sides of the barrier comprised of the region where the sound speed is higher than the horizontal phase velocity.

There is also the problem of arêtes[20] formed by the meeting and termination of caustic surfaces. Here the idealization of a caustic having a radius of curvature much larger than a wavelength breaks down and the theory developed here becomes inapplicable. However, we believe arêtes to be so isolated in occurrence that the possibility of a random receiver location being close to an arête or of lying on a ray which touched a caustic close to an arête is relatively small. Thus, there would seem to be little urgency in taking such phenomena into account.

The incorporation of winds, additional dispersion due to gravity, earth curvature, sound absorption due to dissipative processes, and of phase shift on ground reflection would seem to be relatively minor problems since the theory for doing so is relatively well developed and is discussed in particular in previous reports written under this project. We have chosen not to include such effects in the discussion here primarily because of the premise that one may make faster progress in the long run if he first starts out with a simpler model, checks this model out thoroughly, and then adds the embellishments needed for a more nearly accurate simulation of nature in a sequential fashion.

REFERENCES

1. Thomas, J. E., A. D. Pierce, E. A. Flim, and L. B. Craine, "Bibliography on Infrasonic Waves", Geophys. J. Ray. Astr. Soc. 26, 399-426 (1971). (This reference contains an extensive list of papers published prior to 1971. The following references are noted in particular since they describe work done on the same Air Force project of which the present report is a part).

2. Pierce, A. D., and C. A. Moo, "Theoretical Study of the Propagation of Infrasonic Waves in the Atmosphere", Report AFCRL-67-0172, Air Force Cambridge Research Laboratories, Bedford, Mass. (1967).

3. Pierce, A. D., and J. W. Posey, "Theoretical Prediction of Acoustic-Gravity Pressure Waveforms Generated by Large Explosions in the Atmosphere", Report AFCRL-70-0134, Air Force Cambridge Research Laboratories, Bedford, Mass. (April, 1970).

4. Pierce, A. D., Charles A. Moo, and Joe W. Posey, "Generation and Propagation of Infrasonic Waves", Report AFCRL-TR-73-0135, Air Force Cambridge Research Laboratories, Bedford, Mass. (April, 1973).

5. Pierce, A. D., Wayne A. Kinney, and Christopher Y. Kapper, "Atmospheric Acoustic Gravity Modes at Frequencies Near and Below Low Frequency Cutoff Imposed by Upper Boundary Conditions", Report AFCRL-TR-75-0639, Air Force Cambridge Research Laboratories, Hanscom AFB, Mass. (March, 1976).

6. Haskell, N. A., "Asymptotic Approximation for the Normal Modes in Sound Channel Wave Propagation", J. Appl. Phys. 22, No. 2, 157-168 (1951).

7. Pierce, A. D., "Geometric Acoustics' Theory of Waves from a Point Source in a Temperature - and Wind - Stratified Atmosphere", Report AFCRL - 66 - 454, Air Force Cambridge Research Laboratories, Bedford, Mass. (August, 1966).

8. Pierce, A. D., J. W. Posey, and E. F. Iliff, "Variation of Nuclear Explosion Generated Acoustic - Gravity Waveforms with Burst Height and with Energy Yield", J. Geophys. Res. 76, 5025-5042(1971).

9. Pierce, A. D., and J. W. Posey, "Theory of the Excitation and Propagation of Lamb's Atmospheric Edge Mode from Nuclear Explosions", Geophys. J. Roy. Astron. Soc. 26, 341-368 (1971).

10. Posey, J. W., "Application of Lamb Edge Mode Theory in the Analysis of Explosively Generated Infrasound", Ph.D. Thesis, Dept. of Mech. Eng., Mass. Inst. of Tech., (August, 1971).

11. Pierce, A. D. "Propagation of Acoustic -Gravity Waves from a Small Source above the Ground in an Isothermal Atmosphere", J. Acoust. Soc. Amer. 35. 1798-1807 (1963).

12. Sommerfield, A., and J. Runge, Ann. der. Physik 35, 277-298 (1911).

13. Blokhintzev, D., "The Propagation of Sound in an Inhomogeneous and Moving Medium", I., J. Acoust. Soc. Amer. 18, 322-328 (1946), II., J. Acoust. Soc. Amer. 18, 329-334 (1946).

14. Poincare, H., Theorie Analytique de la Lumiere (Georges Carre, Paris, 1889).

15. Tolstoy, I., "Phase Changes and Pulse Deformation in Acoustics," J. Acoust. Soc. Amer. 44, 675-683 (1968).

16. Moler, C. B., and L. P. Solomon, "Use of Splines and Numerical Integration in Geometrical Acoustics," J. Acoust. Soc. Amer. 48, 739-744 (1970).

17. Abramowitz, M. and I. A. Stegun, Handbook of Mathematical Functions with Formulas, Graphs, and Mathematical Tables (Dover, New York, 1965) (see in particular Chapter 10).

18. Pekeris, C. L., "Theory of Propagation of Sound in a Half-Space of Variable Sound Velocity under Conditions of Formation of a Shadow Zone", J. Acoust. Soc. Amer. 18, 295-315 (1946).

19. Pridmore-Brown, D. C. and U. Ingard, "Sound Propagation into the Shadow Zone in a Temperature-Stratified Atmosphere above a Plane Boundary", J. Acoust. Soc. Amer. 27, 36-42 (1955).

20. Pierce, A. D., "Maximum Overpressures of Sonic Booms Near the Cusp of Caustics", Purdue Noise Control Conference Proceedings, July 14-16, 1971, 478-485.

APPENDIX A

BIBLIOGRAPHY OF RELATED WORKS

PERTAINING TO GEOMETRICAL ACOUSTICS

Albers, V. M., Underwater Sound (Dowden, Hutchinson and Ross, Inc., Stroudsburg, Pa., 1972).

Barnes, A. and L. P. Solomon, "Some Curious Analytical Ray Paths for Some Interesting Velocity Profiles in Geometrical Acoustics", J. Acoust. Soc. Am., 53, 148 (1973).

Barry, G., "Ray Tracings of Acoustic Waves in the Upper Atmosphere", J. Atmos. Terrest. Phys., 25, No. 11, 621 (1963).

Bergman, P. G., "The Wave Equation in a Medium with a Variable Index of Refraction", J. Acoust. Soc. Am., 17, 329 (1946).

Brekhovskikh, L. M., "A Limiting Case of Sound Propagation in Natural Wavelengths", Sov. Phys. Acoust., 10, 89 (1964).

Brekhovskikh, L. M., "The Average Field in an Underwater Sound Channel", Sov. Phys. Acoust., 11, 126 (1965).

Brekhovskikh, L. M., Waves in Layered Media (Academic Press, New York, 1960).

Brekhovskikh, L. M., "Possible Role of Acoustics in the Exploring of the Ocean", Rapports du 5e Congrés International d'Acoustique, Vol. II: Conférences Générales, Liége (1965).

Bucker, H. P., "Sound Propagation in a Channel with Lossy Boundaries", J. Acoust. Soc. Am., 48, 1187 (1970).

Budden, K. G., The Waveguide Mode Theory of Wave Propagation (Academic Press, Inc., New York, 1961).

Chen, K. C. and D. Ludwig, "Calculation of Wave Amplitudes by Ray Tracing", J. Acoust. Soc. Am., 54, 431 (1973).

Clark, R. H., "Sound Propagation in a Variable Ocean", J. Sound Vib., 34, (4), 457 (1974).

Clark, R. H., "Theory of Acoustic Propagation in a Variable Ocean", NATO SACLANTCEN Memorandum SM28 (1973).

Davis, J. A., "Extended Modified Ray Theory Field in Bounded and Unbounded Inhomogenious Media", J. Acoust. Soc. Am., 57, 276 (1975).

Deakin, A. S., "Asymptotic Solution of the Wave Equation with Variable Velocity and Boundary Conditions", SIAM J. Appl. Math., 23, No. 1, (1972), and Appl. Mech. Rev., 5417 (No. 7, 1974).

Denham, R. N., "Asymptotic Solutions for the Sound Field in Shallow Water with a Negative Sound Velocity Gradient", J. Acoust. Soc. Am., 45, 365 (1969).

Eby, E. S., "Frenet Formulation of Three-Dimensional Ray Tracing", J. Acoust. Soc. Am., 42, 1287 (1967).

Eby, E. S., "Geometric Theory of Ray Acoustics", J. Acoust. Soc. Am., 47, 273 (1970).

Eby, R. K., A. O. Williams, R. P. Ryan and P. Tamarkin, "Study of Acoustic Propagation in a Two-Layered Model", J. Acoust. Soc. Am., 32, 89 (1960).

Eckart, C., Hydrodynamics of Oceans and Atmospheres (Pergamon Press, New York, 1960).

Ewing, W. M., W. S. Jardetsky and F. Press, Elastic Waves in Layered Media (McGraw-Hill Book Co., New York, 1957).

Fitzgerald, R. M, A. N. Guthrie, D. A. Nutile, and J. D. Shaffer, "Influence of the Subsurface Sound Channel on Long-Range Propagation Paths and Travel Times", J. Acoust. Soc. Am., 55, 47 (1974).

Gossard, E. E. and W. H. Hooke, Waves in the Atmosphere (Elsevier Scientific Publ. Co., New York, 1975).

Gutenberg, B., "Propagation of Sound Waves in the Atmosphere", 14, 151 (1942).

Guthrie, K. M., "Wave Theory of SOFAR Signal Shape", J. Acoust. Soc. Am., 56, 827 (1974).

Guthrie, K. M., "The Connection Between Normal Modes and Rays in Under-Water Sound", J. Sound Vib., 32, No. 2, 289 (1974).

Hale, F. E., "Long-Range Propagation in the Deep Ocean", J. Acoust. Soc. Am., 33, 456 (1961).

Hirsh, P., "Acoustic Field of a Pulsed Source in the Underwater Sound Channel", J. Acoust. Soc. Am., 38, 1018 (1965).

Jacobson, M. J., W. L. Siegman, N. L. Weinberg and J. G. Clark, "Perturbation Method for Determining Acoustic Ray in Two-Dimensional Sound-Speed Medium", J. Acoust. Soc. Am., 57, 843 (1975).

Jobst, W. J., "An application of Poisson Process Models to Multipath Sound Propagation of Sinusoidal Signals", J. Acoust. Soc. Am., 57, 1409 (1975).

Katz, E. J., "Effects of the Propagation of Internal Water Waves on Underwater Sound Transmission", J. Acoust. Soc. Am., 42, 83 (1967).

Krol, H. R., "Intensity Calculations along a Single Ray", J. Acoust. Soc. Am., 53, 864 (1973).

Krol, H. R., "Some Ray and Intensity Solutions in the Compley Plane", J. Acoust. Soc. Am., 54, 96 (1973).

Lysanov, V. P., "Average Decay in a Surface Sound Channel with an Uneven Boundary", Sov. Phys. Acoust. 12, 425 (1967).

Macpherson, J. D. and M. J. Daintith, "Practical Model of Shallow-Water Acoustic Propagation", J. Acoust. Soc. Am., 41, 850 (1966).

McKinnon, R. F., J. S. Partridge and S. H. Tobe, "Calculation of Ray-Acoustic Intensity", J. Acoust. Soc. Am., 52, 1471 (1972).

Mezzino, M. J., "Ray Acoustics Model of the Ocean Incorporating a Sound Velocity Profile with a Continuous Second Derivative", J. Acoust. Soc. Am., 53, 581 (1973).

Milder, D. M., "Ray and Wave Invariant for SOFAR Channel Propagation", J. Acoust. Soc. Am., 46, 1259 (1969).

Miller, M. K., "Calculation of Horizontal Ranges and Sound Intensities by Use of Numerical Integration Techniques", J. Acoust. Soc. Am., 44, 1690 (1968).

Munk, W. H., "Sound Channel in an Exponentially Stratified Ocean, with Applications to SOFAR", J. Acoust. Soc. Am., 55, 220 (1974).

Murphy, E. L., "Modified Ray Theory for Two Turning-Point Problem", J. Acoust. Soc. Am., 47, 899 (1970).

Murphy, E. L., "Modified Ray Theory for Bounded Media", J. Acoust. Soc. Am., 56, 1747 (1974).

Neubert, J. A., "Multipath Summability in Ray Theory Intensity Calculations in the Real Ocean", J. Acoust. Soc. Am., 51, 310 (1972).

Nicholas, N. C., "Perturbation Calculations of Propagation Loss in the Deep Ocean", J. Acoust. Soc. Am., 49, 1621 (1971).

Nomady, V. G. and H. Überall, "Sound Propagation and Attenuation in the Deep Ocean at Very Long Ranges", J. Acoust. Soc. Am., 320 (1975).

Officer, C. B., Sound Transmission, (McGraw-Hill, New York, 1958).

Pedersen, M. A., "Theory of the Axial Ray", J. Acoust. Soc. Am., 45, 157 (1969).

Pedersen, M. A. and DeWayne White, "Ray Theory for Source and Receiver on an Axis of Minimum Velocity", J. Acoust. Soc. Am., 48, 1219 (1970).

Pedersen, M. A. and DeWayne White, "Ray Theory of the General Epstein Profile", J. Acoust. Soc. Am., 44, 765 (1968).

Pedersen, M. A. and D. F. Gordon, "Comparison of Curvilinear and Linear Profile Approximation in the Calculation of Underwater Sound Intensities by Ray Theory", J. Acoust. Soc. Am., 41, 419 (1967).

Pedersen, M. A., "Acoustic Intensity Anomalies Introduced by Constant Velocity Gradients", J. Acoust. Soc. Am., 33, 465 (1961).

Pedersen, M. A., and D. F. Gordon, "Normal-Mode and Ray Theory Applied to Underwater Acoustic Conditions of Extreme Downward Refraction", J. Acoust. Soc. Am., 51, 232 (1972).

Pedersen, M. A. and D. F. Gordon, "Theoretical Investigations of a Double Family of Normal Modes in an Underwater Acoustic Surface Duct", J. Acoust. Soc. Am., 47, 304 (1970).

Pedersen, M. A., "Ray Theory Applied to a Wide Class of Velocity Functions", J. Acoust. Soc. Am., 43, 619 (1968).

Pekeris, C. L., "Theory of Propagation of Sound in a Half-Space of Variable Sound Velocity Under Conditions of Formation of a Shadow Zone", J. Acoust. Soc. Am., 18, 295 (1946).

Pekeris, C. L., "Theory of Propagation of Explosive Sound in Shallow Water," Geol. Soc. Am. Mem., 27, 1 (1948).

Potter, D. S. and S. R. Murphy, "Solution of the Wave Equation in a Medium with a Particular Velocity Variation", J. Acoust. Soc. Am., 34, 963 (1962).

Raphael, D. T., "New Approach to the Determination of Acquiring Rays in Singly and Doubly Layered Oceans", J. Acoust. Soc. Am., 48, 1249 (1970).

Raphael, D. T., "Closed-Form Solutions for SOFAR Ray Acoustics in Media with Bilinear Sound-Speed Profiles", J. Acoust. Soc. Am., 56, 80 (1974).

Shuby, M. T. and R. Halley, "Measurement of the Attenuation of Low-Frequency Underwater Sound", J. Acoust. Soc. Am., 29, 464 (1957).

Silbiger, A., "Phase Shift at Caustics and Turning Points", J. Acoust. Soc. Am., 44, 653 (1967).

Solomon, L. P., D. K. Y. Ai and G. Haven, "Acoustic Propagation in a Continuously Refracting Medium", J. Acoust. Soc. Am., 44, 1121 (1968).

Solomon, L. P., A. Barnes and S. Port, "Fitting Velocity Profiles with Two-Dimensional Cubic Splines", J. Acoust. Soc. Am., 56, 1389 (1974).

Solomon, L. P., W. C. Merx, "Technique for Investigating the Sensitivity of Ray Theory to Small Changes in Environmental Data", J. Acoust. Soc. Am., 56, 1126 (1974).

Solomon, L. P., "Geometric Acoustics with Frequency Dependence", J. Acoust. Soc. Am., 44, 1115 (1968).

Solomon, L. P. and L. Armijo, "Intensity Differential Equation in Ray Acoustics", J. Acoust. Soc. Am., 50, 960 (1971).

Solomon, L. P. and C. Comstock, "Two-Time Methods Applied to Underwater Acoustics", J. Acoust. Soc. Am., 54, 110 (1973).

Stewart, K. R., "Ray Acoustic Model of the Ocean Using a Depth/Sound-Speed Profile with a Continuous First Derivative", J. Acoust. Soc. Am., 38, 339 (1965).

Stickler, D. C., "Normal-Mode Program with Both the Discrete and Branch Line Contributions", J. Acoust. Soc. Am., 57, 856 (1975).

Tolstoy, I., Wave Propagation (McGraw-Hill Book Co, New York, 1973).

Tolstoy, I. and C. S. Clay, Ocean Acoustics (McGraw-Hill, New York, 1966).

Tolstoy, I., "W.K.B. Approximation, Turning Points, and the Measurement of Phase Velocities", J. Acoust. Soc. Am., 52, 356 (1972).

Ugencius, P., "Intensity Equations in Ray Acoustics. I.", J. Acoust. Soc. Am., 45, 193 (1969).

Ugencius, P., "Intensity Equations in Ray Acoustics. II.", J. Acoust. Soc. Am., 45, 206 (1969).

Ugencius, P., "Intensity Equations in Ray Acoustics. III. Exact Two-Dimensional Formulation", J. Acoust. Soc. Am., 47, 339 (1970).

Uride, R. J., "Intensity Summation of Modes and Images in Shallow-Water Sound Transmission", J. Acoust. Soc. Am., 46, 780 (1969).

Warfield, J. T. and M. J. Jacobson, "Invariance of Geometric Spreading Loss with Changes in Ray Parameterization", J. Acoust. Soc. Am., 50, 342 (1971).

Weinberg, H. and R. Burridge, "Horizontal Ray Theory for Ocean Acoustics", J. Acoust. Soc. Am., 55, 63 (1974).

Weinberg, H., "Continuous-Gradient Curve-Fitting Technique for Acoustic Ray Analysis", J. Acoust. Soc. Am., 50, 975 (1971).

Weinberg, N. L. and T. Dunderdale, "Shallow Water Ray Tracing with Nonlinear Velocity Profiles", J. Acoust. Soc. Am., 52, 1000 (1972).

Weston, D. E., "Guided Propagation in a Slowly Varying Medium", Proceedings of the Physical Society LXXIII, 3.

White, DeWayne, "Velocity Profiles that Produce Acoustic Focal Points on an Axis of Minimum Velocity", J. Acoust. Soc. Am., 46, 1318 (1969).

Williams, A. O. and W. Horne, "Axial Focusing of Sound in the SOFAR Channel", J. Acoust. Soc. Am., 41, 189 (1967).

Wood, D. H., "Parameterless Examples of Wave Propagation", J. Acoust. Soc. Am., 54, 1727 (1973).

Wood, D. H., "Refraction Correction in Constant Gradient Media", J. Acoust. Soc. Am., 47, 1448 (1970).

Wood, D. H., "Green's Functions for Unbounded Constant Gradient Media", J. Acoust. Soc. Am., 45, 1333 (1969).

Yeh, K. C. and C. H. Liu, Theory of Ionospheric Waves (Academic Press, New York, 1972).

APPENDIX B

DECK LISTING OF FORTRAN SUBROUTINES

FOR GEOMETRICAL ACOUSTICS COMPUTATIONS

IN A MEDIUM WHERE SOUND SPEED

VARIES WITH HEIGHT

```
      PROGRAM MAIN (INPUT,OUTPUT,TAPE5=INPUT,TAPE6=OUTPUT)
      COMMON VP,I1,NCS,ZI(100),CI(100),ASOL(100)
      DIMENSION ZTS(19)
      READ(5,*)NCS,(ZI(I),I=1,NCS),(CI(I),I=1,NCS),
     1IT,JT,NUP,NDOWN,ZSC,ZLIS,NMAX,RANGE,VPHST,VPHEND,SDELTA,VP
      WRITE(6,*)NCS,(ZI(I),I=1,NCS),(CI(I),I=1,NCS),
     1IT,JT,NUP,NDOWN,ZSC,ZLIS,NMAX,RANGE,VPHST,VPHEND,SDELTA,VP
      READ(5,*)(ZTS(I),I=1,19)
      WRITE(6,*)(ZTS(I),I=1,19)
      CALL DASOL
      DO 5 I=1,19
      ZC = ZTS(I)
      CALL DOSDVP(VP,ZC,ZSC,IT,JT,NUP,NDOWN,DSDVP)
    5 PRINT*,"DSDVP=",DSDVP
      CALL EXIT
      END


      SUBROUTINE TOTRAN(VP,IT,JT,NUP,NDOWN,ZSC,ZLIS,R)
      COMMON VPT
      EXTERNAL RDXDZ
      CALL TNENT(VP,ZBL,ZBU,NSCAN,NRTS,ZLOW,ZUP)
      CALL SHIFT(ZLOW,ZUP)
      CALL RANG(RTIME,RLNTH,ZLOW,ZUP)
      D = 1.E-6
      IF (IT .LT. 0) GO TO 5
      CALL QUAD(ZUP,ZSC,D,REL,1,ANS1,RDXDZ,NERR,0)
      RST = -ANS1
      GO TO 10
    5 CONTINUE
      CALL QUAD(ZLOW,ZSC,D,REL,1,ANS2,RDXDZ,NERR,0)
      RST = ANS2
   10 IF (JT .LT. 0) GO TO 20
      CALL QUAD(ZLOW,ZLIS,D,REL,1,ANS3,RDXDZ,NERR,0)
      REND = ANS3
      GO TO 30
   20 CONTINUE
      CALL QUAD(ZUP,ZLIS,D,REL,1,ANS4,RDXDZ,NERR,0)
      REND = -ANS4
   30 N = NUP + NDOWN - 1
      R = N*RLNTH + RST + REND
      RETURN
      END


      SUBROUTINE FNDVP(NMAX,ZSC,ZLIS,RANGE,IT,JT,NUP,NDOWN,VPHST,
     1VPHEND,SDELTA,NFND,VPFND)
      COMMON VPP,I1,NCS,ZI(100),CI(100),ASOL(100),
     1ZSCC,ZLISC,RANGEC,ITC,JTC,NUPC,NDOWNC
      DIMENSION VPFND(1),X(1)
      EXTERNAL RMRAYD
      ZSCC = ZSC
      ZLISC = ZLIS
      RANGEC = RANGE
      ITC = IT
      JTC = JT
      NUPC = NUP
      NDOWNC = NDOWN
      NFND = 0
      VP1 = VPHST
      F1 = RMRAYD(VP1)
    3 VP2 = VP1 + SDELTA
```

```
   F2 = RMRAYO(VP2)
   IF (F1*F2) 10,5,5
 5 IF (VP2 .GT. VPHEND) RETURN
   VP1 = VP2
   F1 = F2
   GO TO 3
10 GZ = VP1 - F1*SDELTA/(F2 - F1)
   X(1) = GZ
   CALL ZPEAL2(RMRAYO,1.E-5,.01,SDELTA,5,1,X,10,IER)
   NFND = NFND + 1
   VPFND(NFND) = X(1)
   IF (NFND .EQ. NMAX) RETURN
   GO TO 5
   END


   FUNCTION RMRAYO(VPI)
   COMMON VPP,I1,NCS,ZI(100),CI(100),ASOL(100),
  1ZSCC,ZLISC,RANGEC,ITC,JTC,NUPC,NDOWNC
   ZSC = ZSCC
   ZLIS = ZLISC
   RCOM = RANGEC
   IT = ITC
   JT = JTC
   NUP = NUPC
   NDOWN = NDOWNC
   CALL TOTRAN(VPI,IT,JT,NUP,NDOWN,ZSC,ZLIS,R)
   RMRAYO = RCOM - R
   RETURN
   END


   SUBROUTINE SHIFT(ZLOW,ZUP)
SUBROUTINE SHIFT MOVES THE VALUES OF Z (ZLOW,ZUP) FOUND
FOR THE TURNING POINTS (BY TNPNT) SO AS TO AVOID INTEGRATION
THROUGH SINGULARITIES, AS COULD HAPPEN IN THE CALCULATION
OF ALMOST ALL THE QUANTITIES INCLUDED IN THIS PROGRAM.
SHIFT IS CALLED BY MAIN ONLY, AND AFTER TNPNT IS CALLED.
   N = 0
CALCULATE THE DIFFERENCE BETWEEN THE SOUND SPEED AT THE LOWER
TURNING POINT AND THE PHASE VELOCITY.
 5 CHKL = CMVP(ZLOW)
IF THE SOUND SPEED IS LESS THAN VP, WE'RE SAFE, AND WE GO ON TO
CHECK THE UPPER TURNING POINT.  OTHERWISE, WE ADD A TINY AMOUNT
TO ZLOW AND CONTINUE DOING SO UNTIL THE SOUND SPEED IS LESS THAN VP.
   IF(CHKL .LE. 0.0) GO TO 10
   ZLOW = ZLOW + 1.E-8
   N = N+1
IF SHIFT IS UNSUCCESSFUL IN A 1000 TRIES, WE WANT IT TO STOP.
   IF(N .GE. 1000) RETURN
   GO TO 5
WE TRY THE SAME FOR THE UPPER TURNING POINT, AND AGAIN, AS LONG AS
THE SOUND SPEED IS LESS THAN VP, WE'RE SAFE.
10 CHKU = CMVP(ZUP)
   IF(CHKU .LE. 0.0) RETURN
   ZUP = ZUP - 1.E-8
   N = N+1
   IF(N .GE. 1000) RETURN
   GO TO 10
   END
```

```
   FUNCTION CMVP(Z)                                                    CMVP
THIS FUNCTION ROUTINE SIMPLY CALCULATES THE DIFFERENCE                 CMVP
(AS A FUNCTION OF HEIGHT Z) BETWEEN THE PHASE VELOCITY                 CMVP
(WHICH IS INPUT) AND THE SOUND SPEED (WHICH IS A FUNCTION              CMVP
OF HEIGHT Z).                                                          CMVP
   COMMON VP                                                           CMVP
   CMVP = CSF(Z) - VP                                                  CMVP
   RETURN                                                              CMVP
   END                                                                 CMVP
```

```
   SUBROUTINE TNPNT(VP,ZBL,ZBU,NSCAN,NRTS,ZA,ZB)                       TNPNT
SUBROUTINE TNPNT FINDS THE TURNING POINTS (VALUES OF Z                 TNPNT
AT WHICH THE DIFFERENCE BETWEEN THE SOUND SPEED AND THE PHASE          TNPNT
VELOCITY VANISHES) GIVEN THE PHASE VELOCITY (VP).  ZBL AND ZBU         TNPNT
ARE THE LOWER AND UPPER BOUNDS, RESPECTIVELY, BETWEEN WHICH THE        TNPNT
SEARCH FOR THE TURNING POINTS IS CONDUCTED.  NSCAN + 1 IS THE          TNPNT
NUMBER OF SUBINTERVALS INTO WHICH THE INTERVAL OF SEARCH IS            TNPNT
SUBDIVIDED.  NRTS  IS THE NUMBER OF TURNING POINTS FOUND (WE           TNPNT
NORMALLY EXPECT TWO).  ZA IS THE LOWER TURNING POINT (IF FOUND)        TNPNT
AND ZB IS THE UPPER ONE (IF FOUND).                                    TNPNT
   EXTERNAL CMVP                                                       TNPNT
   DIMENSION X(1)                                                      TNPNT
   COMMON VPC,I1,NCS,ZI(100)                                           TNPNT
   VPC = VP                                                            TNPNT
   ZBL = ZI(1)                                                         TNPNT
   ZBU = ZI(NCS)                                                       TNPNT
   NSCAN = NCS + 3                                                     TNPNT
CALCULATE THE WIDTH OF THE SUBINTERVALS                                TNPNT
   DELTA = (ZBU - ZBL)/(NSCAN + 1)                                     TNPNT
CALCULATE CSF(ZBL) - VP                                                TNPNT
   F1 = CMVP(ZBL)                                                      TNPNT
START THE SEARCH AT ZBL                                                TNPNT
   Z1 = ZBL                                                            TNPNT
   NRTS = 0                                                            TNPNT
FIND THE UPPER LIMIT OF THE  SUBINTERVAL                               TNPNT
10 Z2 = Z1 + DELTA                                                     TNPNT
CALCULATE CSF(Z2) - VP                                                 TNPNT
   F2 = CMVP(Z2)                                                       TNPNT
TAKE THE PRODUCT OF F1 AND F2, AND IF IT IS POSITIVE, WE HAVEN'T       TNPNT
FOUND THE SUBINTERVAL WITH A TURNING POINT IN IT YET. SO WE GO TO 15   TNPNT
AND START AT THE BOTTOM OF THE NEXT SUBINTERVAL.                       TNPNT
   TEST = F1*F2                                                        TNPNT
   IF(TEST .GT. 0.0) GO TO 15                                          TNPNT
IF F1*F2 IS NEGATIVE. WE'VE GOT A SUBINTERVAL WITH A TURNING           TNPNT
POINT IN IT.  AT THIS POINT, WE MAKE ONE GUESS  FOR THE                TNPNT
TURNING POINT.                                                         TNPNT
   GZ = Z1 - F1*DELTA/(F2 - F1)                                        TNPNT
   X(1) = GZ                                                           TNPNT
ZREAL2 IS AN INTERNATIONAL MATH SCIENCE LIBRARY ROUTINE FOR            TNPNT
FINDING THE ZEROES OF A SPECIFIED FUNCTION                             TNPNT
   CALL ZREAL2(CMVP,1.E-7,0.01,DELTA,7,1,X,10,IER)                     TNPNT
   NRTS = NRTS + 1                                                     TNPNT
IF WE HAVE GONE THROUGH THIS LOOP SUCCESSFULLY ONCE, THEN WE HAVE      TNPNT
FOUND THE LOWER TURNING POINT.  IF WE HAVE GONE THROUGH TWICE, WE      TNPNT
HAVE FOUND BOTH TURNING POINTS, AND WE'RE DONE.                        TNPNT
   IF(NRTS .EQ. 1) ZA = X(1)                                           TNPNT
   IF(NRTS .EQ. 2) ZB = X(1)                                           TNPNT
   IF(NRTS .EQ. 2) GO TO 20                                            TNPNT
15 Z1 = Z2                                                             TNPNT
   F1 = F2                                                             TNPNT
IF WE HAVE SEARCHED ALL THE WAY TO ZBU, WE'RE DONE.  OTHERWISE, WE     TNPNT
```

```
GO ON TO THE NEXT SUBINTERVAL.
   IF(ZBU .GE. Z1) GO TO 10
20 RETURN
   END


   SUBROUTINE RANG (RTIME,RLNTH,ZLOW,ZUP)
SUBROUTINE RANG PERFORMS THE FINAL STEP IN THE CALCULATION
(BY INTEGRATION OF DT/DZ AND DX/DZ BETWEEN THE TURNING POINTS,
ZLOW & ZUP) OF THE RAY REPETITION TIME AND LENGTH, RTIME AND
RLNTH, RESPECTIVELY.
   EXTERNAL RDTDZ,RDXDZ
   RTIME = RAINT(RDTDZ,ZLOW,ZUP)
   RLNTH = RAINT(RDXDZ,ZLOW,ZUP)
   RETURN
   END


   SUBROUTINE DASOL
SUBROUTINE DASOL CALCULATES THE COEFFICIENTS OF THE CUBIC
SPLINE USED TO APPROXIMATE THE SOUND-SPEED PROFILE, AND AS
DEFINED BY
  DELZ(I)*ASOL(I-1) + 2*(DELZ(I) - DELZ(I+1))*ASOL(I) +
    + DELZ(I+1)*ASOL(I+1) = DELC(I+1) - DELC(I)
WHERE        DELZ(I) = Z(I) - Z(I-1)
             DELC(I) = (C(I) - C(I-1))/DELZ(I).
   COMMON VP,I1,NCS,ZI(100),CI(100),ASOL(100)
   N = 1
   DELZ = 1.0
   DELC = 0.0
   AKM2 = 0.0
   ALM2 = 0.0
   AKM1 = 0.0
   ALM1 = 1.0
   NSTP = NCS - 1
10 DELZP = ZI(N+1) - ZI(N)
   DELCP = CI(N+1) - CI(N)
   ALPHA = DELZ
   GAMMA = DELZP
   BETA = 2.0*(ALPHA + GAMMA)
   DEE = (DELCP/DELZP) - (DELC/DELZ)
   IF(N .EQ. 1) GO TO 30
   AK = (DEE - ALPHA*AKM2 - BETA*AKM1)/GAMMA
   AL = ( - ALPHA*ALM2 - BETA*ALM1)/GAMMA
   IF(N .EQ. NSTP) GO TO 100
   AKM2 = AKM1
   ALM2 = ALM1
   AKM1 = AK
   ALM1 = AL
30 N = N + 1
   DELZ = DELZP
   DELC = DELCP
   GO TO 10
100 ASOL(1) = 0.0
   ASOL(2) = -AK/AL
   DELZ = 1.0
   DELC = 0.0
   N = 1
110 DELZP = ZI(N+1) - ZI(N)
   DELCP = CI(N+1) - CI(N)
   ALPHA = DELZ
   GAMMA = DELZP
```

```
      BETA = 2.0*(ALPHA + GAMMA)
      DEE = (DELCP/DELZP) - (DELC/DELZ)
      IF(N .EQ. 1) GO TO 130
      M = N + 1
      ASOL(M) = (DEE - ALPHA*ASOL(N-1) - BETA*ASOL(N))/GAMMA
      IF(M .EQ. NSTP) GO TO 200
  130 N = N + 1
      DELZ = DELZP
      DELC = DELCP
      GO TO 110
  200 RETURN
      END
```

```
      FUNCTION CSP(Z)

 THIS FUNCTION ROUTINE CALCULATES INTERMEDIATE VALUES OF
 THE SOUND SPEED PROFILE ACCORDING TO THE EQUATION
        CSP(Z) = WBAR*C(I-1) + W*C(I) +
 + ((DELZ(I)**2)*(ASOL(I-1)*(WBAR**3 - WBAR + ASOL(I)*
                                       *(W**3 - W)).

      COMMON VP,I1,NCS,ZI(100),CI(100),ASOL(100)
 DEFINE THE LOWER AND UPPER BOUNDS OF THE SOUND-SPEED PROFILE.
      ZL = ZI(1)
      ZP = ZI(NCS)
 OUTSIDE OF THESE BOUNDS, LET THE SOUND SPEED BE CONSTANT AND EQUAL
 TO THE CORRESPONDING ADJACENT VALUES.
      IF (Z .LT. ZL) GO TO 50
      IF (Z .GT. ZP) GO TO 60
      I = NCS
10    J = I-1
 FOR ANY VALUE Z, WE WANT I SUCH THAT Z IS BETWEEN ZI(I-1) AND ZI(I).
 WE START WITH THE HIGHEST VALUE FOR I AND WORK DOWNWARD UNTIL WE
 FIND THE INTERVAL THAT CONTAINS Z.
      ZTEST = ZI(J)
 IF Z IS BETWEEN ZI(I-1) AND ZI(I), WE GO TO 40 AND CALCULATE CSP(Z).
      IF (Z .GT. ZTEST) GO TO 40
 IF Z IS NOT BETWEEN ZI(I-1) AND ZI(I), WE CHOSE THE NEXT VALUE LOWER
 FOR I AND CONTINUE THE SEARCH.
      I = J
      GO TO 10
40    CONTINUE
      Z IS BETWEEN ZI(I-1) AND ZI(I)
      DELZ = ZI(I) - ZI(J)
      W = (Z - ZI(J))/DELZ
      WBAR = 1.0 - W
      TERM1 = WBAR*CI(J) + W*CI(I)
      GUT1 = WBAR**3 - WBAR
      GUT2 = W**3 - W
      TERM2 = (DELZ**2)*(ASOL(J)*GUT1 + ASOL(I)*GUT2)
      CSP = TERM1 + TERM2
      RETURN
50    CSP = CI(1)
      RETURN
60    CSP = CI(NCS)
      RETURN
      END
```

```
      FUNCTION DCDZ(Z)
 THE FUNCTION DCDZ(Z) CALCULATES THE FIRST DERIVATIVE OF
```

```
THE SOUND SPEED WITH RESPECT TO HEIGHT Z, AND ACCORDING
TO THE EQUATION

DCDZ(Z) = DELC(I) + DELZ(I)*(-ASOL(I-1)*(3*WBAR**2 - 1) +
  + ASOL(I)*(3*W**2 -1))

PLEASE SEE FUNCTION CSP(Z) FOR A MORE DETAILED EXPLANATION OF THE
CALCULATIONAL PROCEDURE THAT FOLLOWS, AS THE TWO PROCEDURES ARE
NEARLY IDENTICAL.
   COMMON VP,I1,NCS,ZI(100),CI(100),ASOL(100)
DEFINE THE LOWER AND UPPER BOUNDS OF THE SOUND-SPEED PROFILE.
   ZL = ZI(1)
   ZP = ZI(NCS)
OUTSIDE OF THESE BOUNDS, LET DC/DZ = 0.
   IF(Z .LT. ZL) GO TO 50
   IF(Z .GT. ZP) GO TO 50
   I = NCS
10 J = I-1
   ZTEST = ZI(J)
   IF(Z .GT. ZTEST) GO TO 40
   I = J
   GO TO 10
40 CONTINUE
   Z IS BETWEEN ZI(I-1) AND ZI(I)
   DELZ = ZI(I) - ZI(J)
   DELCI = (CI(I) - CI(J))/DELZ
   W = (Z - ZI(J))/DELZ
   WBAR = 1.0 - W
   TRM3A = ASOL(I)*((3.0*(W**2)) - 1.0)
   TRM3B = ASOL(J)*((3.0*(WBAR**2)) - 1.0)
   TRM3 = DELZ*(TRM3A - TRM3B)
   DCDZ = DELCI + TRM3
   RETURN
50 DCDZ = 0.0
   RETURN
   END
```

```
   SUBROUTINE COSDVP(VP,ZC,ZSC,IT,JT,NUP,NDOWN,CSDVP)
   COMMON VPT
   EXTERNAL FTRMUL,FTRM
   VPT = VP
   CALL TNPNT(VP,ZBL,ZBU,NSCAN,NRTS,ZLOW,ZUP)
   CALL SHIFT(ZLOW,ZUP)
   D = 1.E-6
   ZIU = ZUP - 0.01*(ZUP - ZLOW)
   ZIL = ZLOW + 0.01*(ZUP - ZLOW)
   CALL QUAD(ZIL,ZIU,D,REL,0,TRMM,FTRM,NERR,0)
   IF (IT .LT. 0) GO TO 10
   CALL QUAD(ZSC,ZIU,D,REL,0,TRMI,FTRM,NERR,0)
   GO TO 15
10 CALL QUAD(ZIL,ZSC,D,REL,0,TRMI,FTRM,NERR,0)
15 IF (JT .LT. 0) GO TO 20
   CALL QUAD(ZIL,ZC,D,REL,0,TRMF,FTRM,NERR,0)
   GO TO 25
20 CALL QUAD(ZC,ZIU,D,REL,0,TRMF,FTRM,NERR,0)
25 CONTINUE
   TRMU1 = TRNPT(ZIU)
   TRML1 = TRNPT(ZIL)
   CALL QUAD(ZUP,ZIU,D,REL,1,TRMU2,FTRMUL,NERR,0)
   CALL QUAD(ZLOW,ZIL,D,REL,1,TRML2,FTRMUL,NERR,0)
   CSDVP = TRMI + NUP*(TRMU1 - TRMU2) + (NUP + NDOWN - 1)*TRMM +
 1  NDOWN*(-TRML1 + TRML2) + TRMF
```

```
   VPSQ = VP**2                                              COSOVP
   CSPZC = CSP(ZC)                                           COSOVP
   CSPZSQ = CSP(ZC)**2                                       COSOVP
   IF (JT .LT. 0) GO TO 30                                   COSOVP
   DSDVP = -(CSPZC*(SQRT(VPSQ - CSPZSQ)/VPSQ))*COXDVP        COSOVP
   GO TO 35                                                  COSOVP
30 DSDVP = (CSPZC*(SQRT(VPSQ - CSPZSQ)/VPSQ))*COXDVP         COSOVP
35 CONTINUE                                                  COSOVP
   RETURN                                                    COSOVP
   END                                                       COSOVP


   FUNCTION FTRM(Z)                                          FTRM
                                                             FTRM
                     -CSP*VP                                 FTRM
FTRM(Z) = ---------------------------                        FTRM
                (VP**2 - CSP**2)**1.5                        FTRM
                                                             FTRM
   COMMON VP,K                                               FTRM
   VPSQ = VP**2                                              FTRM
   CSPSQ = CSP(Z)**2                                         FTRM
   IF (VPSQ .GE. CSPSQ) GO TO 20                             FTRM
   K = 1                                                     FTRM
10 TRM1 = 1.E-50                                             FTRM
   GO TO 30                                                  FTRM
20 K = 0                                                     FTRM
   TRM1 = (SQRT(VPSQ - CSPSQ))**3                            FTRM
   IF (TRM1 .LT. 1.E-50) GO TO 10                            FTRM
   TRM2 = CSP(Z)*VP                                          FTRM
30 FTRM = -TRM2/TRM1                                         FTRM
   RETURN                                                    FTRM
   END                                                       FTRM


   FUNCTION DCDZS(Z)                                         DCDZS
                                                             DCDZS
FUNCTION DCDZS(Z) CALCULATES THE SECOND DERIVATIVE OF THE    DCDZS
SOUND SPEED C WITH RESPECT TO HEIGHT Z, AND ACCORDING TO THE DCDZS
EQUATION                                                     DCDZS
                                                             DCDZS
 DCDZS(Z) = 6*(WBAR*ASOL(I-1) + W*ASOL(I))                   DCDZS
                                                             DCDZS
PLEASE SEE FUNCTION CSP(Z) FOR A MORE DETAILED EXPLANATION OF THE DCDZS
CALCULATIONAL PROCEDURE THAT FOLLOWS, AS THE TWO PROCEDURES ARE DCDZS
NEARLY IDENTICAL.                                            DCDZS
   COMMON VP,I1,NCS,ZI(100),CI(100),ASOL(100)                DCDZS
DEFINE THE UPPER AND LOWER BOUNDS OF THE SOUND-SPEED PROFILE. DCDZS
   ZL = ZI(1)                                                DCDZS
   ZP = ZI(NCS)                                              DCDZS
OUTSIDE OF THESE BOUNDS, LET DCDZS(Z) = 0.                   DCDZS
   IF(Z .LT. ZL) GO TO 50                                    DCDZS
   IF(Z .GT. ZP) GO TO 50                                    DCDZS
   I = NCS                                                   DCDZS
10 J = I-1                                                   DCDZS
   ZTEST = ZI(J)                                             DCDZS
   IF(Z .GT. ZTEST) GO TO 40                                 DCDZS
   I = J                                                     DCDZS
   GO TO 10                                                  DCDZS
40 CONTINUE                                                  DCDZS
   Z IS BETWEEN ZI(I-1) AND ZI(J).                           DCDZS
   DELZ = ZI(I) - ZI(J)                                      DCDZS
   W = (Z - ZI(J))/DELZ                                      DCDZS
```

```
      WBAR = 1.0 - W
      DCDZS = 6.0*((WBAR*ASOL(J)) + (W*ASOL(I)))
      RETURN
   50 DCDZS = 0.0
      RETURN
      END


      FUNCTION FTRMUL(Z)

                       -2.*VP*DCDZS
 FTRMUL(Z) = ----------------------------------
              (DCDZ**2)*(VP**2 -CSP**2)**0.5

      COMMON VP,K
      CSPSQ = CSP(Z)**2
      VPSQ = VP**2
      DCDZSQ = DCDZ(Z)**2
      IF(VPSQ .GE. CSPSQ) GO TO 50
      K = 1
   40 DN = 1.E-50
      GO TO 60
   50 K = 0
      DN = DCDZSQ*(SQRT(VPSQ - CSPSQ))
      IF(DN .LT. 1.E-50) GO TO 40
   60 FTRMUL = -2.*(VP*DCDZS(Z))/DN
      RETURN
      END


      FUNCTION TRNPT(Z)
      COMMON VP,K
      CSPSQ = CSP(Z)**2
      VPSQ = VP**2
      IF (VPSQ .GE. CSPSQ) GO TO 50
      K = 1
   40 DN = 1.E-50
      GO TO 60
   50 K = 0
      DN = DCDZ(Z)*(SQRT(VPSQ - CSPSQ))
      IF (ABS(DN) .LT. 1.E-50) GO TO 40
   60 TRNPT = (2.*VP)/DN
      RETURN
      END


      FUNCTION RDXDZ(Z)

 FUNCTION RDXDZ(Z) CALCULATES THE INTEGRAND USED BY SUBROUTINES
 RANG AND RAINT TO CALCULATE THE RAY REPETITION LENGTH, RLNTH.
 THE EQUATION FOR RDXDZ(Z) IS

                       1/VP
 RDXDZ(Z) = --------------------------
             (1/CSP**2 - 1/VP**2)**0.5

      COMMON VP,K
      CSPSQ = CSP(Z)**2
      VPSQ = VP**2
      IF (CSPSQ .LE. VPSQ) GO TO 10
      K = 1
```

```
 5 DSQ = 1.E-50
   GO TO 20
10 K = 0
   DSQC = 1./CSPSQ
   DSQV = 1./VPSQ
   DSQ = DSQC - DSQV
   IF (DSQ .LT. 1.E-50) GO TO 5
20 ROXOZ = (1./VP)/SQRT(DSQ)
   RETURN
   END
```

```
   FUNCTION ROTOZ(Z)

 FUNCTION ROTOZ(Z) CALCULATES THE INTEGRAND USED BY SUBROUTINES
 RANG AND RAINT TO CALCULATE THE RAY REPETITION TIME, RTIME.
 THE EQUATION FOR ROTOZ(Z) IS

                     1/CSP**2
 ROTOZ(Z) = ---------------------------
             (1/CSP**2 - 1/VP**2)**0.5

   COMMON VP,K
   CSPSQ = CSP(Z)**2
   VPSQ = VP**2
   IF (CSPSQ .LE. VPSQ) GO TO 30
   K = 1
20 DSQ = 1.E-50
   GO TO 40
0  K = 0
   DSQC = 1./CSPSQ
   DSQV = 1./VPSQ
   DSQ = DSQC - DSQV
   IF (DSQ .LT. 1.E-50) GO TO 20
0  ROTOZ = (1./CSPSQ)/SQRT(DSQ)
   RETURN
   END
```

```
   FUNCTION RAINT(DSDZR,ZLOW,ZUP)

 FUNCTION RAINT PERFORMS THE INTEGRATION OF ROXOZ AND ROTOZ
 NECESSARY TO OBTAIN THE RAY REPETITION LENGTH AND TIME, RLNTH
 AND RTIME, RESPECTIVELY.

   EXTERNAL DSDZR
   ZAVE = (ZUP + ZLOW)/2.0
   D = 1.E-6
   CALL QUAD(ZLOW,ZAVE,D,REL,1,ANS1,DSDZR,NERR,0)
   CALL QUAD(ZUP,ZAVE,D,REL,1,ANS2,DSDZR,NERR,0)
   RAINT = (ANS1 - ANS2)
   RETURN
   END
```

```
      SUBROUTINE ZREAL2 (F,EPS,EPS2,ETA,NSIG,N,X,ITMAX,IER)
C
C-ZREAL2--------S--------LIBRARY 3-------------------------------------------
C
C   FUNCTION            - ZREAL2 FINDS THE REAL ZEROS OF A REAL FUNCTION
C                           -- USED WHEN INITIAL GUESSES ARE GOOD
C   USAGE               - CALL ZREAL2(F,EPS,EPS2,ETA,NSIG,N,X,ITMAX,IER)
C   PARAMETERS   F      - A FUNCTION F(X) SUBPROGRAM WRITTEN BY THE USER
C                EPS    - 2ND STOPPING CRITERION. A ROOT X  IS ACCEPTED
C                           IF THE ABSOLUTE VALUE OF F(X)  .LE. EPS
C                           (INPUT)
C                EPS2   - SPREAD CRITERIA FOR MULTIPLE ROOTS. IF THE
C                ETA        ITH ROOT (X(I)) HAS BEEN COMPUTED AND IT IS
C                           FOUND THAT THE ABSOLUTE VALUE OF
C                           X(I)-X(J) .LT. EPS2 WHERE X(J) IS A
C                           PREVIOUSLY COMPUTED ROOT, THEN THE
C                           COMPUTATION IS RESTARTED WITH A GUESS EQUAL
C                           TO X(I) + ETA. (INPUT)
C                NSIG   - 1ST STOPPING CRITERION. A ROOT IS ACCEPTED IF
C                           TWO SUCCESSIVE APPROXIMATIONS TO A GIVEN
C                           ROOT AGREE IN THE FIRST NSIG DIGITS. (INPUT)
C                N      - THE NUMBER OF ROOTS TO BE FOUND (INPUT)
C                X      - ON INPUT X IS AN N-VECTOR OF INITIAL GUESSES
C                           FOR N ROOTS. ON OUTPUT, X CONTAINS THE
C                           COMPUTED ROOTS.
C                ITMAX  - ON INPUT = THE MAXIMUM ALLOWABLE NUMBER OF
C                           ITERATIONS PER ROOT AND ON OUTPUT = THE
C                           NUMBER OF ITERATIONS USED ON THE LAST ROOT.
C                IER    - ERROR PARAMETER (OUTPUT)
C                         WARNING ERROR = 32 + N
C                           N = 1 INDICATES A SINGLE ROOT WAS BYPASSED
C                             BECAUSE ITMAX WAS EXCEEDED FOR THIS ROOT.
C                             X(I) FOR THIS ROOT IS SET TO 111111.
C                           N = 2 INDICATES A SINGLE ROOT WAS BYPASSED
C                             BECAUSE THE DERIVATIVE OF F FOR THIS
C                             ROOT BECOMES TOO SMALL. X(I) FOR THIS
C                             ROOT IS SET TO 222222. NOTE THAT THIS
C                             ERROR CONDITION MAY CAUSE AN OVERFLOW.
C                           N = 3 INDICATES THAT SEVERAL OF THE ABOVE
C                             ERROR CONDITIONS OCCURRED. EACH X(I) IS
C                             SET TO EITHER 111111. OR 222222. AS ABOVE
C   PRECISION           - SINGLE
C   REQD. IMSL ROUTINES - UERTST
C   LANGUAGE            - FORTRAN
C----------------------------------------------------------------------------
C   LATEST REVISION     - OCTOBER 6, 1973
C
      DIMENSION          X(1)
      DATA               P1,P001,ZERO,ONE,TEN/.1,.001,0.0,1.0,10.0/
      IER = 0
      IR=0
      CRIT1 = TEN**(-NSIG)
      DO 30 I=1,N
         IC = 1
         XI = X(I)
```

```
    5   AXI = ABS(XI)
        IF (I .EQ. 1) GO TO 15
        NM1=I-1
        DO 10 J = 1,NM1
           IF (ABS(XI - X(J)) .LT. EPS2) XI = XI + ETA
   10   CONTINUE
   15   FXI = F(XI)
        AFXI = ABS(FXI)
C                                   TEST FOR CONVERGENCE
        IF (AFXI .LE. EPS) GO TO 25
        DI = .0001
        IF (AXI .GE. P1) DI = P001*AXI
        HI = AMIN1(AFXI,DI)
        FXIPHI = F(XI + HI)
        DER = (FXIPHI - FXI)/HI
        IF (DER .EQ. ZERO) GO TO 20
        XIPI=FXI/DER
        IF (LEGVAR(XIPI) .NE. 0) GO TO 20
        XIPI=XI-XIPI
        ERR = ABS(XIPI - XI)
        XI = XIPI
C                                   TEST FOR CONVERGENCE
        IF(AXI.EQ.ZERO) AXI=ONE
        ERR1=ERR/AXI
        IF (LEGVAR(ERR1) .NE. 0) ERR1 = ERR
        IF(ERR1.LE.CRIT1) GO TO 25
        IC = IC + 1
        IF (IC .LE. ITMAX)  GO TO 5
C                                   ROOT NOT FOUND, NO CONVERGENCE
        X(I) = 111111.
        IR=IR+1
        IER=33
        GO TO 30
C                                   ROOT NOT FOUND, DERIVATIVE = 0.
   20   X(I) = 222222.
        IR=IR+1
        IER=34
        GO TO 30
   25   X(I)=XI
   30 CONTINUE
      ITMAX = IC
      IF(IER.EQ.0) GO TO 9005
      IF(IR.LE.1) GO TO 9000
      IER=35
 9000 CONTINUE
      CALL UERTST(IER,6HZREAL2)
 9005 RETURN
      END
```

```
      SUBROUTINE QUAD(A,B,D,REL,N,ANS,FUN,NERR,IMAP)
C     A = LOWER LIMIT OF INTEGRATION  (INPUT)
C     B = UPPER LIMIT OF INTEGRATION (INPUT)
C     D = REQUIRED RELATIVE TOLERANCE (INPUT)
C     REL = ESTIMATE OF RESULTING RELATIVE TOLERANCE  (OUTPUT)
C     N = SINGULARITY FLAG.  SET  N=0  WHEN NO SINGULARITY ALONG PATH.
C             SET  N=1  WHEN ONE OR MORE SINGULARITIES LIE  ON PATH
C     ANS = COMPUTED VALUE OF INTEGRAL  (OUTPUT)
C     FUN = NAME OF FUNCTION GENERATING THE INTEGRAND
C     NERR = ERROR FLAG  (OUTPUT)
C        NERR = -1  STEP SIZE CAN NOT BE MADE SMALL ENOUGH
C        NERR = -2  QUAD INCOMPLETE IN   LIM (200)  TRIES
C        NERR = -3  D HAS BEEN SET TOO SMALL
C        NERR .GT. 0  --SUCCESS--GIVES NUMBER OF TRIES REQUIRED
C     IMAP = PROGRESS MAP FLAG.  SET IMAP=1 WHEN MAP IS DESIRED.
C        SET IMAP=0 WHEN NOT DESIRED
      DIMENSION W4(2),W8(4),W12(6), Z4(2),Z8(4), Z12(6)
      DOUBLE PRECISION YDBLE
      DATA W4(1),W4(2),(W8(I),I=1,4),(W12(I),I=1,6)/.652145154862546,
     1.347854845137454,.362683783378362,.313706645877887,.222381034453337
     15,  .101228536290376,.249147045813403,.233492536538355,
     1.203167426723066,.160078328543346,.106939325995318,
     1.047175336386512/
C     LIM CAN BE CHANGED IF EITHER MORE OR LESS TRIES ARE DESIRED
      LIM=200
      C=D
C     IS  C  SET TOO SMALL
      IF (C.LT. 1.E-13) GO TO  290
   10 IF (IMAP.EQ. 1) PRINT  1
    1 FORMAT ( 2X,14HLEFT END POINT,20X,6HLENGTH,26X,12H8-PT. RESULT
     1  11X,19HREL.ERROR IN 8-PT. ,11X,4H1000 )
      HOP = 0.0
      K = 0
      NONSEK = 0
      NOUT = 1
      ANS = 0.
      F2 = 0.
      NERR=0
      Y = A
      YDBLE = DBLE(Y)
      F = C/200.
      E = 0.
C***********************************************************************
C     FIRST TRY ON FULL SPAN AND ALSO LAST STEP GO THROUGH HERE
   20 H = (B-Y)/2.
      SGN=SIGN(1.,H)
      H=ABS(H)
      LAST = 1
C     ALL INTERMEDIATE STEPS BEGIN HERE
   30 X = Y + H*SGN
C     IS  H  TOO SMALL TO BE SENSED RELATIVE TO  X
      IF(X+.1*H.EQ.X)  GO TO  270
      IF(K.GT.LIM) GO TO  280
C***********************************************************************
C        4 POINT ABSCISSAE
      Z4(1)=.339981043584856*H
      Z4(2)=.861136311594053*H
```

```
C        8 POINT ABSCISSAE
      Z8(1)=.183434642495650*H
      Z8(2)=.525532409916329*H
      Z8(3)=.796666477413627*H
      Z8(4)=.960289856497536*H
C     EVALUATE FUNCTION AND PERFORM WEIGHTED SUM
      G4=H*(W4(1)*(FUN(X+Z4(1))+FUN(X-Z4(1)))+
     1W4(2)*(FUN(X+Z4(2))+FUN(X-Z4(2))))
      G8=0.
      DO 40 I=1,4
      Z1=FUN(X+Z8(I))
      Z2=FUN(X-Z8(I))
   40 G8=G8+W8(I)*(Z1+Z2)
      G8=G8*H
C*********************************************************************
      ABG=ABS(G8)+1.E-260
      TE=ABS(G8-G4)+1.E-14*ABG
C     RE IS THE RELATIVE ERROR IN THE SUBINTERVAL THE 4 PT. RESULT MAKES
C        IF THE 8 PT. RESULT IS EXACT
      RE = 1.E-14 + TE/ABG
      IF(K.EQ.0) P=ABG
C     P IS THE MAX ABS VALUE OF ENTIRE INTEGRAL AS WE KNOW IT UP TO HERE
C     K IS THE COUNTER OF THE NUMBER OF ATTEMPTS
   50 K = K + 1
      EH = F*P
      ER = TE*RE
      Q= EH/ER
      IF(IMAP.NE.1) GO TO  70
   60 XLGNTH=2*H
      ERR=RE**2
      C100=Q*100.0
      PRINT  2 ,Y,XLGNTH,G8  ,ERR,C100
    2 FORMAT (E23.15, 2E30.15, 2E22.5)
   70 Q16 = Q**.0625
      D1 = H/2./RE**.125
      D2 = H/D1*C16
C     D1 IS THE ESTIMATE OF THE DISTANCE "A" TO THE SINGULARITY
C     D2 IS AN IMPORTANCE FACTOR WHICH NORMALLY RANGES FROM ABOUT 10.
C        TO 0.1 .  WHEN THE RESULT IS UNIMPORTANT, D2 IS LARGE.
C
C     THE MAGIC GO-GO OR NO-GO QUANTITY IS  100Q , FOUND AS FOLLOWS.
C     WE REQUIRE THAT THE RELATIVE ERROR IN THE 8 PT. SUBINTERVAL
C     VALUE  (RE**2) TIMES THE IMPORTANCE OF THE SUBINTEGRAL (ABG/P)
C     BE LESS THAN HALF THE REQUIRED TOLERANCE  C .
C     ALTERNATIVELY, (C/2)*(P/ABG)/(RE**2)  MUST BE GREATER THAN 1.0
C     THE ABOVE EXPRESSION, WHEN MULTIPLIED OUT, IS 100Q.
      IF(Q.LE. 0.01) GO TO  120
C     COMPARISON OF 4 PT. AND 8 PT. LOOKS GOOD.
   80 ES = 0.
      IF(N.NE.1) GO TO  200
C*********************************************************************
C     CHECK THE 12 POINT RESULT
C        12 POINT ABSCISSAE
      Z12(1)=.125233408511469*H
      Z12(2)=.367831498998180*H
      Z12(3)=.587317954286617*H
      Z12(4)=.769902674194305*H
```

```
      Z12(5)=.904117256370475*H
      Z12(6)=.981560634246719*H
C     EVALUATE FUNCTION AND PERFORM WEIGHTED SUM
      G12=0
      DO 100 I=1,6
 100  G12=G12+W12(I)*(FUN(X+Z12(I))+FUN(X-Z12(I)))
      G12=G12*H
      ES=ABS(G12-G8)
      G8=G12
      ER=ES
      IF(ES - 100.*ER)  200,200,110
C     NOT GOOD ENOUGH.  TRY AGAIN.
  110 H=H/4.0
      F1 = 0.25
      GO TO  190
C*********************************************************************
C
C     THIS REGION OF THE PROGRAM MODIFIES THE STEP LENGTH WHEN
C        SUBINTERVAL IS NOT SMALL ENOUGH
  120 IF(NCUT .NE. 1) GO TO 130
C     FIRST CUTBACK
      F1 = Q16
      H=AMIN1(.75*H,D1*Q16)
      GO TO 190
C     SUBSEQUENT CUTBACKS IN THIS SERIES.
  130 F1 = F1*Q16
      H = F1*H
  190 NONSEK = 0
      NCUT = 0
      LAST = 0
      GO TO  30
C*********************************************************************
C
C     SUCCESSFUL SUBINTERVAL INTEGRATION
C     INCREASE STEP AS INDICATED
 200  ANS=ANS+G8
      E = E + AMAX1(ER,   ES,1.E-14*ABG)
      IF(LAST.EQ.1) GO TO  300
C     HCP IS AN OLD SUCCESSFUL STEP
  210 IF(HCP)  220,220,230
  220 HCP = H
  230 F2 = 0.50*F2 + ALOG(H/HCP)
      HCP = H
      YDBLE = YDBLE + DBLE(2.0*H*SGN)
      Y = YDBLE
      NONSEK = NONSEK + 1
      IF(NONSEK  .GT. 4 ) GO TO 250
      IF(F2)  240,250,250
C     F2 .LT. 0. SAYS IT HAS NOT FORGOTTEN THE PAST FAILURES YET
  240 HC = D1*D2/(1.+2.*D2)
      GO TO  260
C     F2 .GE. 0. SAYS THE HISTORY HAS BEEN SUCCESSFUL
  250 HC = D2*(D1+2.*H)*Q16
  260 H = HC
      NCUT = 1
      P = AMAX1(P,ABG)
      IF(SGN*Y + 2.0*H - SGN*B) 30,20,20
```

```
C***********************************************************************
C
C      ERROR EXITS
  270 NERR=-1
      WRITE(6, 3 ) H,Y
    3 FORMAT(53H QUAD FAILURE, STEP SIZE CANNOT BE MADE SMALL ENOUGH./
     156H IF YOU WISH TO CONTINUE MOVE SINGULARITY TO THE ORIGIN./
     211H STEP SIZE=,E24.16, 10X,15HLEFT END POINT=,E24.16)
      GO TO   300
  280 NERR=-2
      WRITE(6, 4 ) LIM,Y,H
    4 FORMAT(19H1QUAD INCOMPLETE IN  I4, 7H TRIES.,17H  LEFT END POINT=
     1E24.16,10X,11H STEP SIZE=,E24.16)
      GO TO  300
  290 NERR=-3
      PRINT  5
    5 FORMAT (68H REQUESTED TOLERANCE TOO SMALL, ROUTINE WILL PROCEED US
     1ING 10.0E-14  )
      C=10.0E-14
      GO TO  10
C
C      HERE WE RETURN TO THE MAIN PROGRAM WITH OR WITHOUT AN ANSWER
  300 REL= 2.*E/(ABS(ANS)+1.E-290)
      IF(NERR.GE.0.) NERR=K
      IF(B-A.LT.0.) ANS=-ANS
      RETURN
      END
```

E-25-638

AFCRL-TR-76-

COMPUTATIONAL TECHNIQUES FOR THE STUDY OF INFRASOUND PROPAGATION IN THE ATMOSPHERE

by

Allan D. Pierce and Wayne A. Kinney

School of Mechanical Engineering
Georgia Institute of Technology
Atlanta, Georgia 30332

FINAL REPORT
15 October 1973 to 31 December 1975

13 March 1976

Prepared for

AIR FORCE CAMBRIDGE RESEARCH LABORATORIES
OFFICE OF AEROSPACE RESEARCH
UNITED STATES AIR FORCE
HANSCOM AFB, MASSACHUSETTS 01731

ABSTRACT

A discussion is given of theoretical studies on infrasound propagation through the atmosphere which were carried out under the contract. Topics discussed include (1) the modification and adaptation of a computer program for the prediction of pressure signatures at large distances from nuclear explosions to include leaking guided modes, (2) the nature of guided infrasonic modes at higher infrasonic frequencies and the methods of extending waveform synthesis procedures to include higher frequencies, and (3) the propagation of infrasonic pressure pulses past the antipodes (over halfway around the globe). Summaries are included of all papers, theses, and reports written under the contract and conclusions and recommendations for future studies are given. An updated version of the computer program INFRASONIC WAVEFORMS originally given by Pierce and Posey in the report AFCRL-70-0134 is included as an appendix.

Chapter I

INTRODUCTION

1.1 SCOPE OF THE REPORT

The present report summarizes investigations carried out by the authors during the years 1973-1976 on the propagation of low frequency pressure disturbances under Air Force Contract No. F19628-74-C-0065 with the Air Force Cambridge Research laboratories, Bedford, Massachusetts. The study performed was theoretical in nature.

The central topic of this study was the generation and propagation of infrasonic waves in the atmosphere. The principal emphasis was on waves from man made nuclear explosions although certain aspects of the study pertain to waves generated by natural phenomena including, in particular, severe weather.

Specific topics considered during the study include the following:

1.) The adaptation of the computer program INFRASONIC WAVEFORMS to include leaking modes and to improve its accuracy in synthesizing early long period arrivals. (INFRASONIC WAVEFORMS is a digital computer program for the prediction of pressure signatures as would be detected at large horizontal distances following the detonation of a nuclear device in the atmosphere. The original version of this program was developed by Pierce and Posey[1] under a previous Air Force Contract [F19628-67-C-0217].) The developed theory for this adaptation has already been explained[2] in Scientific Report No. 1 of the present contract; the present report describes the numerical implementation of this theory (Chapter III), and gives some specific numerical examples. The complete current version of INFRASONIC WAVEFORMS is included here as Appendix A.

2.) The development of a ray acoustic model for the synthesis of higher frequency portions of infrasonic waveforms. The theory developed during this study is given[3] in some detail in Scientific Report No. 2 and a discussion of this phase of the work is accordingly not repeated here.

3.) The modification of the multi-modal synthesis method to avoid truncation of upper limits on frequency integration. The method developed is presented here in Chapter IV and represents an extension of the W.K.B.J. technique to the case when the atmosphere has two sound channels. The resulting theory clarifies the problem of selection of modes for inclusion into the synthesis and leads to a relatively simple method for revising the synthesis program. (This revision, however, has not yet been carried out.)

4.) Study of infrasonic waveform synthesis for propagation near and past the antipodes. The method for doing this was briefly mentioned in the 1973 AFCRL report (pages 25 and 26) by Pierce, Moo, and Posey[4]. In Chapter V of the present report the theory underlying this is given and some numerical examples are given.

In Chapter II, we list all of the reports, papers, and theses which were written during the course of this study. The abstracts given there plus the abstract of the present report should be considered as a comprehensive summary of the accomplishments during the contracting period. In subsequent chapters of the present report, detailed discussions are given of some of the topics described above. In Chapter VI, some recommendations are made for future work in the field.

1.2 BACKGROUND OF THE REPORT

The general topics of infrasonic wave propagation, generation, and detection have been of considerable interest to a large segment published bibliography (the existence of which allows us to omit extensive citations here) lists [Thomas, Pierce, Flinn, and Craine, 1971][5] over 600 titles, most of which are directly cncerned with infrasound. Literature pertaining to the infrasonic detection of nuclear explosions constitutes a considerable portion of these. Earlier work by Rayleigh [1890][6], Lamb [1908,1910][7], G. I. Taylor [1929,1936][8], Pekeris [1939, 1938][9] and Scorer [1950][10], among others, which was concerned with waves from the Krakatoa eruption [Symond, 1888][11] and from the great Siberian meteorite [Whipple, 1930][12] is also directly applicable to the understanding and interpretation of nuclear explosion waves.

The present report thus merely summarizes a continuation of a small number of facets of a lengthy pattern of research which has been carried on by a large number of investigators in the past. In a more restricted sense, the work reported here represents a continuation of work done in three previous studies performed under contract for Air Force Cambridge Research Laboratories. The first of these was Air Force Contract No. AF19(628)-3891 with Avco Corporation during 1964-1966; the second was Air Force Contract No. AF19628-67-C-0217 with the Massachusetts Institute of Technology during 1967-1969, the third was AF19628-70-C-0008 (also with M.I.T) during 1970-1972. Summaries of the earlier work may be found in the appropriate final reports by Pierce and Moo [1967][13], by Pierce and Posey [1970][1], and by Pierce, Moo, and Posey [1973][4].

One of the principal results of the first two aforementioned previous contracts was a computer program INFRASONIC WAVEFORMS; the deck listing of the then current version of which is given in the report by Pierce and Posey [1970][1]. This program enables one to compute the pressure waveform at a distant point following the detonation of a nuclear explosion in the atmosphere. The primary limitation on the program's applicability to realistic situations is that the atmosphere is assumed to be perfectly stratified. However, the temperature and wind profiles may be arbitrarily specified. The general theory underlying this program is somewhat similar to that developed by Harkrider [1964][14] but differs from his in that it incorporates background winds and in that it has a different source model for a nuclear explosion.

Chapter II

PAPERS, THESES AND REPORTS

The following gives author, title, and abstract of papers, theses, and reports written during the course of this project.

2.1 A. D. Pierce, "Theory of Infrasound Generated by Explosions," Colloque International sur les Infra-Sons, Proceedings (Centre National de la Recherche Scientifique (CNRS) 15, quai Anatole France, 75700 Paris, September, 1973).

A review is given of recent studies by the author and his colleagues on infrasound generation by explosions and the subsequent propagation through the atmosphere. These studies include (i) development of computer programs for the prediction of pressure signatures at large distances from nuclear explosions, (ii) development of an alternative approximate model for waveform synthesis based on Lamb's edge mode, (iii) development of a geometrical acoustics' theory incorporating nonlinear effects, dispersion, and wave distortion at caustics, and (iv) theoretical models for the mechanisms of wave generation by explosions. The basic theory is briefly outlined in each case and some of the more significant results are explained in terms of simplified physical models. Such results include the predicted dependence of far field waveforms on energy yield and burst height, suggested techniques for estimating energy yield from waveforms, and an explanation of amplitude anomalies in terms of focusing and defocusing of horizontal ray paths.

2.2 W. A. Kinney, C. Y. Kapper, and A. D. Pierce, "Acoustic Gravity Wave Propagation Post the Antipode," J. Acoust. Soc. Amer. 55, S75 (A) (1974).

The previous theoretical formulations and numerical computations of pressure waveforms (such as described by Harkrider, Pierce, and Posey, and others) apply only to atmospheric traveling waves which have traveled less than 1/2 the distance around the earth. In the present paper, a technique resembling that previously introduced by Brune, Nafe, and Alsop [Bull. Seismol. Soc. Am. 51, 247-257 (1961)] for elastic surface waves on the earth is discussed and applied to the acoustic-gravity wave propagation past the antipode problem. The principal modification to the older theory is a shift in phase of $\pi/2$ to the Fourier transform of the wave after it has traveled over halfway round the globe from the source. The source of the wave is presumed to be a nuclear explosion of given energy E. Numerically synthesized waveforms of antipodal arrivals are exhibited and compared with those for direct arrivals. The necessary modifications to the Lambmode model theory of Pierce and Posey [Geophys. J. Roy. Astron. Soc. 26, 341-368 (1971)] are also described.

2.3 C. Y. Kapper, "Leaky Infrasonic Guided Waves in the Atmosphere," J. Acoust. Soc. Amer. 56, S2 (A) (1974).

Prior theoretical formulations and computational techniques for the prediction of pressure waveforms generated by large explosions in the atmosphere have considered only fully ducted modes. In the present paper, a technique for including weakly leaking guided modes in concert with fully ducted modes is developed. Modification of previous theory includes the extension of the boundary condition at the upper halfspace to include a complex horizontal wavenumber. The major alterations to the computer program infrasonic Waveforms (as described in report by Pierce and Posey, 1970) incurred consist of the computation of the imaginary part of the newly incorporated complex wavenumber, extension of the normal-mode dispersion function to lower frequencies, and a second-order correction factor to the phase velocity.

2.4 W. A. Kinney, "Asymptotic High-Frequency Behavior of Guided Infrasonic Modes in the Atmosphere," J. Acoust. Soc. Amer. 56, S2 (A) (1974).

Refinement of previous theoretical formulations and numerical computations of pressure waveforms as applied to atmospheric traveling infrasonic waves could include a description of their asymptotic behavior at high frequencies. In the present paper, calculations based on the W.K.B.J. approximation and similar to those introduced by

Haskell [J. Appl. Phys. 22, 157-167 (1951)] are performed to describe the asymptotic behavior of infrasonic guided modes as generated by a nuclear explosion in the atmosphere. The results of these calculations are then matched onto numerical solutions which have been given by Harkrider, Pierce and Posey, and others. It is demonstrated that the use of these asymptotic formulas in conjunction with a computer program which synthesizes infrasonic pressure waveforms has enabled the elimination of problems associated with high-frequency truncation of numerical integration over frequency. In this way, small spurious high-frequency oscillations in the computer solutions have been avoided.

2.5 C. Y. Kapper, Computational Techniques in Infrasound Waveform Synthesis, M. S. Thesis, School of Mechanical Engineering, Georgia Institute of Technology (December, 1974).

This thesis is concerned with two major theoretical and programming modifications to the digital computer program INFRASONIC WAVEFORMS for the synthesization of acoustic-gravity pressure waveforms generated by large explosions in the atmosphere. The first modification involves the extension of the guided mode approximation for pressure waveforms in the atmosphere into leaking mode regions and a consequent search for the imaginary part of the complex horizontal wave number. Particular results include a plot of phase velocity versus angular frequency showing the extension of the normal mode dispersion function into a leaky mode region for a multilayer atmosphere and a report on the search for the imaginary part of the complex horizontal wave number of a leaky mode for a two layer atmosphere. The second modification involves the extension of the systhesis of acoustic-gravity pressure waveforms to distances beyond the antipode. A phase shift is noted for waves passing through the antipode and a comparison of pre and post antipodal waveforms is presented.

2.6 W. A. Kinney, A. D. Pierce, and C. Y. Kapper, "Atmospheric Acoustic Gravity Modes Near and Below Low Frequency Cutoff Imposed by Upper Boundary Conditions," J. Acoust. Soc. Amer. 58, S1 (A) (1975).

Perturbation techniques are described for the computation of the imaginary part of the horizontal wavenumber (k_I) for modes of propagation. Numerical studies were carried out for a model atmosphere terminated by a constant sound-speed (478 m/sec) half space above an altitude of 125 km. The GR_0 and GR_1 modes have lower-frequency cutoffs. It was found that for frequencies less than 0.0125 rad/sec, the GR_1 mode has complex phase velocity; k_I varying from near zero up to a maximum of 3 X 10^{-4} km^{-1} with analogous results for the GR_0 mode. There is an extremely small frequency gap for each mode for which no poles in the complex k plane corresponding to that mode exist. These mark the transition from undamped propagation to damped propagation. In the complete Fourier synthesis, branch line contributions compensate for the absence of poles in these gaps. Computational procedures are described which facilitate the inclusion of the low-frequency portions of these modes in the waveform sysnthesis.

2.7 A. D. Pierce, and W. A. Kinney, Atmospheric Acoustic Gravity Modes at Frequencies Near and Below Low Frequency Cutoff Imposed by Upper Boundary Conditions, Report AFCRL-TR-75-0639, Air Force Cambridge Research Laboratories, Hanscom AFB, Mass. (March, 1976).

Perturbation techniques are described for the computation of the imaginary part of the horizontal wavenumber (k_I) for modes of propagation. Numerical studies were carried out for a model atmosphere terminated by a constant sound-speed (478 m/sec) half space above an altitude of 125 km. The GR_0 and GR_1 modes have lower-frequency cutoffs. It was found that for frequencies less than 0.0125 rad/sec, the GR_1 mode has complex phase velocity; k_I varying from near zero up to a maximum of 3 X 10^{-4} km^{-1} with analogous results for the GR_0 mode. There is an extremely small frequency gap for each mode for which no poles in the complex k plane corresponding to that mode exist. These mark the transition from undamped propagation to damped propagation. In the complete Fourier synthesis, branch line contributions compensate for the absence of poles in these gaps. Computational procedures are described which facilitate the inclusion of the low-frequency portions of these modes in the waveform sysnthesis.

2.8 A. D. Pierce, and W. A. Kinney, Geometric Acoustics Techniques in Far Field Infrasonic Waveform Synthesis, Report AFCRL-TR-76- , Air

Force Cambridge Research Laboratories, Hanscom AFB, Mass. (1976).

A ray acoustic computational model for the prediction of long range infrasound propagation in the atmosphere is described. A cubic spline technique is used to approximate the sound speed versus height profile when values of sound speed are input for discrete height intervals. Techniques for finding ray paths, travel times, ray turning points, and rays connecting source and receiver are described. A parameter characterizing the spreading of adjacent rays (or ray tube area) is defined and methods for its computation are given. A method of determining the number of times a given ray touches a caustic is also described. Formulas are given for the computation of acoustic amplitudes and waveforms which involve a superposition of contributions from individual rays connecting source and receiver and which incorporate phase shifts at caustics. The possibility of a receiver being in the proximity of a caustic is considered in some detail and distinction is made between cases where the receiver is on the illuminated or shadow sides of a caustic. It is shown that a knowledge of parameters characterizing two rays at a point in the vicinity of a caustic provides sufficient information concerning the caustic to allow one to give a relatively accurate description of the acoustic field in its vicinity. The resulting theory involves Airy functions and uses concepts extrapolated from a theory published in 1951 by Haskell. The net result is a detailed computational scheme which should accurately cover the contingency of the receiver being near a caustic in the calculation of amplitudes and waveforms. A number of FORTRAN subroutines illustrating the method are given in an appendix. Limitations of the theory and suggestions for future developments are also given.

Chapter III

NUMERICAL SYNTHESIS OF WAVEFORMS INCLUDING LEAKING MODES

3.1 INTRODUCTION

The computer program INFRASONIC WAVEFORMS has been modified to allow inclusion of the contribution at low frequencies from leaking modes (specifically the GR_0 and GR_1 modes) to numerically synthesized infrasonic pressure waveforms. The procedure incorporated in this modification involves a partly manual calculation of the imaginary and real parts of the horizontal wavenumber, k_I and k_R, respectively) as discussed in Scientific Report No. 1.[2] That calculation is outlined in more detail here. The numbers presented for illustration are appropriate to the case of observations at 15,000 km distance from a 50 megaton explosion, where the explosion is at 3 km altitude, and where the atmosphere is assumed to contain no winds. (This restriction is just for illustrative purposes, but is not a limitation on the method.)

3.2 CALCULATION OF COMPLEX WAVENUMBERS

The first step in the calculation is to obtain values for the phase velocities $v_n(\omega)$, $v_a(\omega)$, and $v_b(\omega)$ for the GR_0 and GR_1 modes, and to obtain values for the elements $R_{11}(\omega,v)$ and $R_{12}(\omega,v)$ of the transmission matrix [R]. These calculations should be done, in particular, for all frequencies extending below the mode's nominal lower cutoff frequency. As mentioned in the previous report[2], R_{11} and R_{12} depend on the atmospheric properties only in the altitude range 0 to z_T (the bottom of the upper halfspace), and these are independent of what is assumed for the upper halfspace. Also, $v_n(\omega)$ is the phase velocity for a given (n-th) mode for values of ω greater than the lower cutoff frequency ω_L; here $v_a(\omega)$ and $v_b(\omega)$ are values of the phase velocity ω/k at which the functions

```
$NAM1 NSTART=1, NPRNT=1, NPNCH=-1, NCMPL=-1 $END
$NAM2 IMAX=24,
ZI=1.,2.,4.,6.,8.,10.,12.,14.,16.,18.,20.,25.,30.,35.,40.,45.,55.,
    65.,75.,85.,95.,105.,115.,125.,
T=292.,288.,270.,260.,249.,236.,225.,215.,205.,198.,205.,215.,227.,
    237.,249.,265.,260.,240.,205.,185.,184.,200.,250.,400.,570.,
LANGLE=1,
WINDY=25*0.0,
WANGLE=25*0.0
$END
$NAM4
THETKD =35.,
V1 = 0.143, V2 = 0.3318,
OM1 = 0.001,   OM2 = 0.031,
NOMI = 30, NVPI = 80,
MAXMOD = 10
$END
$NAM1 NSTART=6, NPRNT=1, NPNCH=-1, NCMPL=-1  $END
```

Figure 1. Listing of input data required to generate tabulations of R_{11} and R_{12} versus phase velocity and angular frequency in the vicinity of the dispersion curves for the GR_0 and GR_1 modes.

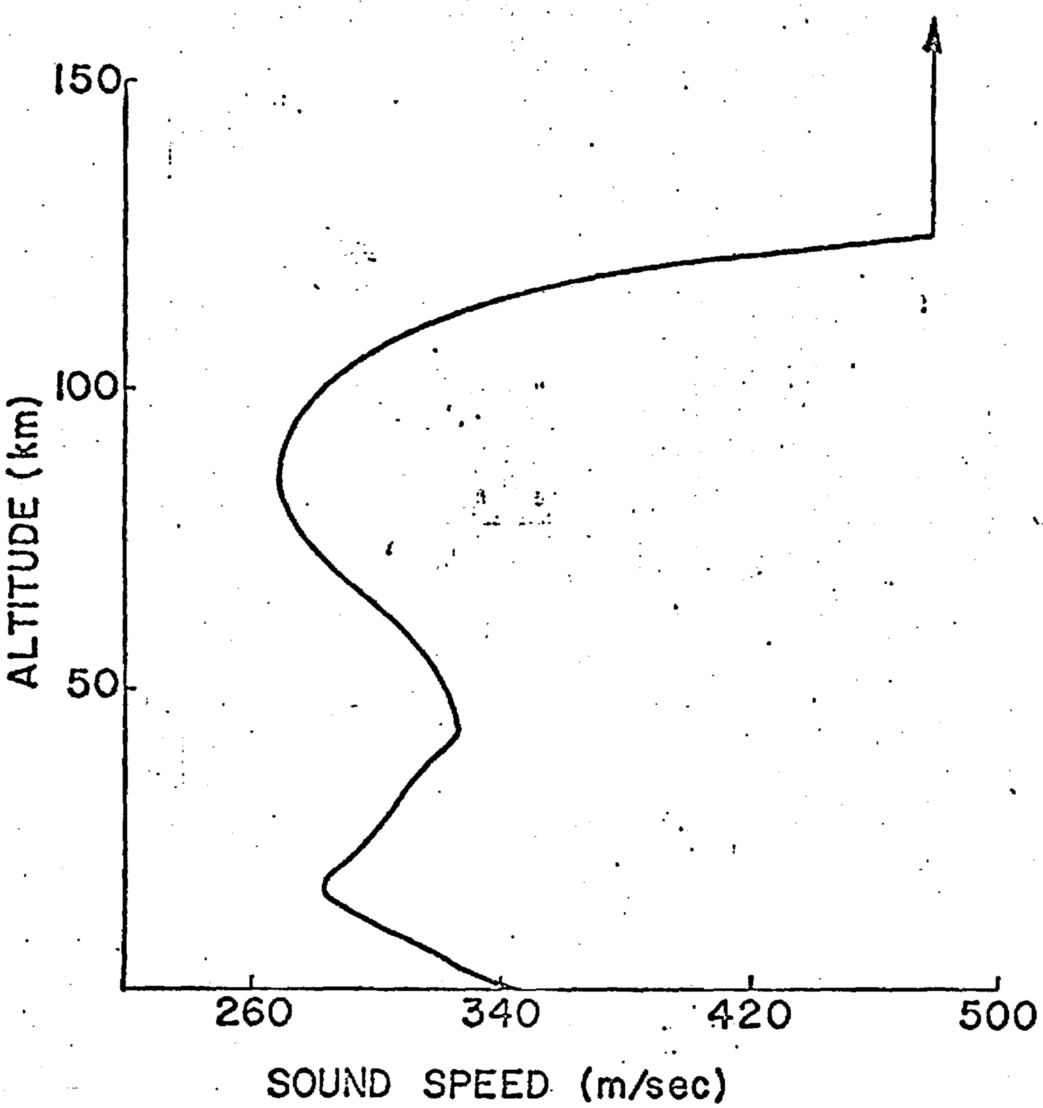

Figure 2. Model atmosphere showing sound speed versus altitude for numerical example treated in the present chapter. The atmosphere is bounded by an isothermal upper half space beginning at 125 km altitude.

R_{11} and R_{12}, respectively, vanish. For a given mode, the values of v_a and v_b chosen are those from the curves $v_a(\omega)$ and $v_b(\omega)$ which lie the closest of all such curves to the curve $v_n(\omega)$ for $\omega>\omega_L$.

As regards the calculation of R_{11} and R_{12}, the computer program INFRASONIC WAVEFORMS may be used, only with an alternate version of the subroutine TABLE. A copy of subroutine TABLE with the appropriate modifications incorporated and indicated is given in Appendix B. A deck listing of all of the input data that is required to obtain R_{11} and R_{12}, and that is appropriate to the running example, follows in Fig. 1. Values for R_{11} and R_{12} need only be calculated for phase velocities between, say, 0.143 and 0.3318 km/sec, and for frequencies between 0.001 rad/sec (as close to zero as would seem necessary and corresponding to a period of 6,283 sec or 1.75 hr) and the value of ω_B for the upper halfspace (.0128 rad/sec in our numerical example). In the calculations reported here, the upper frequency was taken as .031 rad/sec in order to confirm the continuity of the dispersion curves. A sample portion of the printout of R_{11} and R_{12} corresponding to the model atmosphere of Fig. 2 is given in Fig. 3 . The same set of output from a computer run which lists the R_{11} and R_{12} also includes the $v_n(\omega)$ for the GR_0 and GR_1 modes.

Values of $v_a(\omega)$ and $v_b(\omega)$ for these modes are obtained by two successive runs of INFRASONIC WAVEFORMS using in sequence two modified versions of the subroutine NMDFN. These modifications are so minor that the deck listing is omitted and we describe here the nature of the modifications.

To obtain $v_a(\omega)$, one need only change the third from end executable FORTRAN statement of subroutine NMDFN from

```
FPP = RPP(1,1)*A(1,2) - RPP(1,2)*(GU + A(1,1))
```
(3.1)

to

```
FPP = RPP(1,1).
```
(3.2)

v_p	R_{11}	R_{12}
OMEGA=	.30928-02	
.14300+00	.21671+01	-.65152+02
.14539+00	-.72963-01	-.22523+02
.14778+00	-.19992+01	.16898+02
.15017+00	-.34415+01	.49336+02
.15256+00	-.43200+01	.72532+02
.15495+00	-.46324+01	.85619+02
.15734+00	-.44356+01	.88883+02
.15973+00	-.38270+01	.83475+02
.16212+00	-.29260+01	.71114+02
.16451+00	-.18579+01	.53814+02
.16690+00	-.74204+00	.33657+02
.16929+00	.31761+00	.12611+02
.17168+00	.12376+01	-.75995+01
.17407+00	.19579+01	-.25568+02
.17646+00	.24418+01	-.40247+02
.17885+00	.26746+01	-.50952+02
.18124+00	.26605+01	-.57340+02
.18363+00	.24195+01	-.59371+02
.18602+00	.19834+01	-.57261+02
.18841+00	.13917+01	-.51424+02
.19080+00	.68860+00	-.42421+02
.19319+00	-.80574-01	-.30906+02
.19558+00	-.87165+00	-.17582+02
.19797+00	-.16447+01	-.31561+01
.20036+00	-.23637+01	.11690+02
.20275+00	-.29996+01	.26326+02
.20514+00	-.35295+01	.40198+02
.20753+00	-.39379+01	.52832+02
.20992+00	-.42153+01	.63849+02

Figure 3. Sample printout of R_{11} and R_{12} versus phase velocity for various fixed values of angular frequency. Output generated with the input data of Fig. 1.

To obtain $v_b(\omega)$, one need only change the same statement to

$$FPP = RPP(1,2). \tag{3.3}$$

The same limits for phase velocity and angular frequency as are used for the calculation of R_{11} and R_{12} should be used in the calculations for v_n, v_a, and v_b. In our example, when these limits are used, the GR_1 mode corresponds to mode #3, and the GR_0 mode corresponds to mode #4 for the case when $v_n(\omega)$ is calculated. For the cases when $v_a(\omega)$ and $v_b(\omega)$ are calculated, the GR_1 mode corresponds to mode #4 and the GR_0 mode corresponds to mode #6. A sample output listing of $v_n(\omega)$, $v_a(\omega)$ and $v_b(\omega)$ for the two modes is given in Fig. 4. An additional listing of $v_n(\omega)$, $v_a(\omega)$, and $v_b(\omega)$ for the two modes versus various values of ω is given in Table 1.

3.3 CALCULATION OF α AND β

The next step in the procedure is to manually calculate values for the variables α and β which enter into an approximate version [Eq. (9) in Scientific Report No. 1] of the eigenmode dispersion function. These parameters represent the partial derivatives of R_{11} and R_{12}, respectively, with respect to phase velocity v evaluated at $v=v_a$ and $v=v_b$, respectively. Since R_{11} and R_{12} also depend on ω, α and β may be considered as functions of angular frequency (but not of phase velocity).

It may be recalled that $v_a(\omega)$ and $v_b(\omega)$ are values for the phase velocity at which R_{11} and R_{12}, respectively, vanish. From the listing of, say, R_{11} versus v and ω, let the adjacent values R_{111}, R_{211}, R_{311} and R_{411} for R_{11} corresponding to the values for phase velocity v_{11}, v_{21}, v_{31} and v_{41}, respectively (for same chosen ω), such that v_{21} and v_{31} brackett a value for v_a; R_{211} and R_{311} would then be of opposite sign. In the listing of v, R_{11}, R_{12} for various ω, the values for v should all turn out to be equally spaced. Given this fact, it is possible to reasonably approximate α from the listings of R_{11} by the formula

$$\alpha = (1/\Delta v_1)([5/6]e_{11}+[1/12]f_{11}+[1/4]g_{11}h_{11}) \tag{3.4}$$

Table 1. Tabulation of frequency dependent parameters for the GR_0 and GR_1 modes. Tabulation is for frequencies below cutoff; definitions of the various quantities are given in the text and in Scientific Report No. 1.

GR_0 MODE						GR_1 MODE					
ω	v_n	ω	v_a	ω	v_b	ω	v_n	ω	v_a	ω	v_b
12375	.31185608	.001030	.31205939	.001030	.31209836	.013407	.22781499	.001030	.24434330	.001030	.250734
13407	.31181806	.002061	.31205552	.002061	.31209447	.013624	.22664568	.002061	.24409612	.001738	.250544
14438	.31177597	.003093	.31204906	.003093	.31208799	.014040	.22425580	.003093	.24367787	.002061	.250424
15469	.31172882	.004124	.31204001	.004124	.31207393	.014424	.22186593	.003655	.24337478	.003093	.24990
6501	.31167509	.005156	.31202834	.005156	.31206727	.014438	.22177526	.004124	.24307887	.004124	.249150
7532	.31161209	.006187	.31201405	.006187	.31205303	.014778	.21947606	.005156	.24228453	.005156	.248159
8563	.31153394	.007218	.31199710	.007218	.31203620	.015107	.21708619	.006187	.24127431	.005160	.246154
9070	.31148610	.008250	.31197748	.008250	.31201679	.015413	.21469631	.006445	.24098491	.006187	.2460[illegible]
9079	.31148516	.009281	.31195515	.009281	.31199478	.015469	.21423833	.007218	.24001984	.006963	.245764
9595	.31142505	.010312	.31193006	.010312	.31197016	.015699	.21230644	.008181	.23859504	.007218	.245350
9853	.31138841	.011344	.31190215	.011344	.31194291	.015966	.20991657	.008250	.23848240	.008250	.243461
0111	.31134515	.012375	.31187139	.012375	.31191302	.016217	.20752670	.009281	.23660913	.008293	.243374
0626	.31122480	.013407	.31183768	.013407	.31188045	.016453	.20513682	.009479	.23620517	.009281	.241183
1658	.31029529	.014438	.31180093	.014438	.31184518	.016501	.20463309	.010312	.23432708	.009362	.240984
1659	.31029116	.015469	.31176104	.015469	.31180714	.016675	.20274695	.010518	.23381529	.010260	.238595
2005	.30790129	.016501	.31171786	.016501	.31176630	.016886	.20035708	.011344	.23153728	.010312	.238443
2139	.30551142	.017532	.31167120	.017532	.31172258	.017085	.19796721	.011381	.23142542	.011034	.235205
2173	.30475278	.018563	.31162087	.018563	.31167591	.017274	.19557733	.012115	.22903555	.011344	.235148
2240	.30312155	.019595	.31156653	.019595	.31162620	.017454	.19318746	.012375	.22809942	.011712	.233815
2329	.30073168	.020626	.31150781	.020626	.31157334	.017532	.19211887	.012752	.22664568	.012314	.231425
2412	.29834181	.021658	.31144415	.021658	.31151721	.017626	.19079759	.013311	.22425580	.012375	.231168
2490	.29595194	.022689	.31137478	.022689	.31145763	.017790	.18840772	.013407	.22381942	.012855	.229035
2566	.29356207	.023720	.31129855	.023720	.31139444	.017946	.18601784	.013809	.22186593	.013345	.226456
2639	.29117220	.024752	.31121368	.024752	.31132738	.018096	.18362797	.014255	.21947606	.013407	.226325
2689	.28948366	.025783	.31111721	.025783	.31125619	.018240	.18123810	.014438	.21842295	.013790	.224255
2710	.28878233	.026814	.31100382	.026814	.31118049	.018378	.17884823	.014659	.21708619	.014199	.221855
2779	.28639246	.027846	.31086276	.027846	.31109984	.018510	.17645836	.015027	.21469631	.014438	.220366
2846	.28400259	.028877	.31066848	.028877	.31101364	.018563	.17547997	.015364	.21230644	.014575	.219476
912	.28161272	.029909	.31034189	.029909	.31092114	.018638	.17406848	.015469	.21151653	.014922	.217086

Figure 4. A sample output listing of $v_n(\omega)$, $v_a(\omega)$, and $v_b(\omega)$ for the GR_0 and GR_1 modes.

Table 1. Tabulation of frequency dependent parameters for the GR_0 and GR_1 modes. Tabulation is for frequencies below cutoff; definitions of the various quantities are given in the text and in Scientific Report No. 1.

where

$$\Delta v_1 = v_{41} - v_{31} = v_{31} - v_{21} + v_{21} - v_{11} \tag{3.5a}$$

$$e_{11} = R_{311} - R_{211} \tag{3.5b}$$

$$f_{11} = R_{411} - R_{311} + R_{211} - R_{111} \tag{3.5c}$$

$$g_{11} = (R_{211} - R_{311})/e_{11} \tag{3.5d}$$

$$h_{11} = R_{311} + R_{211} - R_{111} - R_{411} \tag{3.5e}$$

In like manner, from the listing of R_{12} versus v and ω, if one lets the adjacent values R_{112}, R_{212}, R_{312}, and R_{412} for R_{12} correspond to the values for phase velocity v_{12}, v_{22}, v_{32}, and v_{42}, respectively (for some chosen ω), such that v_{22} and v_{32} bracket a value for v_b, then one can approximate β by the formula

$$\beta = (1/\Delta v_2)([5/6]e_{12} + [1/12]f_{12} + [1/4]g_{12}h_{12}) \tag{3.6}$$

where Δv_2, e_{12}, f_{12}, g_{12}, and h_{12} are defined by equations analogous to Eqs. (3.5) (last subscript changed from 1 to 2).

Because we use a numerical method (i.e., that described above) to calculate a derivative (it would be preferable to have an explicit formula), there is a small amount of numerical noise in the tabulation versus ω of α and β computed in the above manner. This noise is noticable only for the GR_1 mode and may for all practical purposes be filtered out by plotting α and β versus ω and then drawing smooth curves through the respective sets of points. (See Figs. 5 and 6.) While this procedure is somewhat laborious, it circumvents doing additional runs of the program to get values of R_{11} and R_{12} at more closely spaced values of phase velocity. It also circumvents a somewhat elaborate computer programming chore which would do

Figure 5. A plot of the parameter α versus ω for the G R_1 mode. The parameter α is $\partial R_{11}/\partial v_p$ evaluated at the phase velocity where $R_{11}=0$.

Figure 6. A plot of the parameter β versus ω for the GR_1 mode. The parameter β is $\partial R_{12}/\partial v_p$ evaluated at the phase velocity where $R_{12}=0$.

such steps automatically. (We suspect that the programming time would surpass all time which would ever actually be spent on manual circulations such as described above.) In any event, in view of the relatively small values of k_I which are actually obtained (as described further below) and in view of the recommendations (also given further below) concerning the use of the same k_I in many different types of calculations, the accuracy of the α and β so obtained is more than sufficient.

3.4 CALCULATION OF COMPLEX PHASE VELOCITY

The applicable expression for calculation of a mode's phase velocity (real above cutoff frequency, complex below) is Eq. (10a) in Scientific Report[2] No. 1 (which for brevity is not repeated here). This involves parameters v_a and v_b (whose computation is described in Sec. 3.1), and X, which may be considered as a function of ω and which is defined by Eq. (10b) in the prior report. This latter quantity X depends on β/α, A_{11}, G and A_{12}. The latter three are computed by taking the phase velocity as v_a and using Eqs. (4), (7a), and (7b) of the prior report. These calculations are straight forward, and do not require detailed explanation. Listings of G, A_{11}, A_{12}, and X for various values of ω and for the GR_1 and GR_0 modes are given in Table 1.

As explained in the prior report, below cutoff (that is, below ω_L = 0.0125 rad/sec for GR_1 and below ω_L = 0.0118 rad/sec for GR_0, in the running example) the real part k_R of the horizontal wavenumber is the real part of $\omega/v^{(1)}$, and the imaginary part k_I is of course zero. Finally, the extension by first iteration of the normal mode dispersion curves below cutoff is obtained by simply calculating ω/k_R. Listing of $v^{(1)}$, k_I, k_R, and ω/k_R for various ω for the GR_0 and GR_1 modes are given in Table 1. Plots of k_I and ω/k_R are given in Fig. 7.

3.5 INPUT DATA FOR GR_0 AND GR_1

The present version of INFRASONIC WAVEFORMS allows for the possibility of phase velocity ω/k_R, imaginary component k_I, and source free amplitude AMP to be input as functions of angular frequency ω for any given

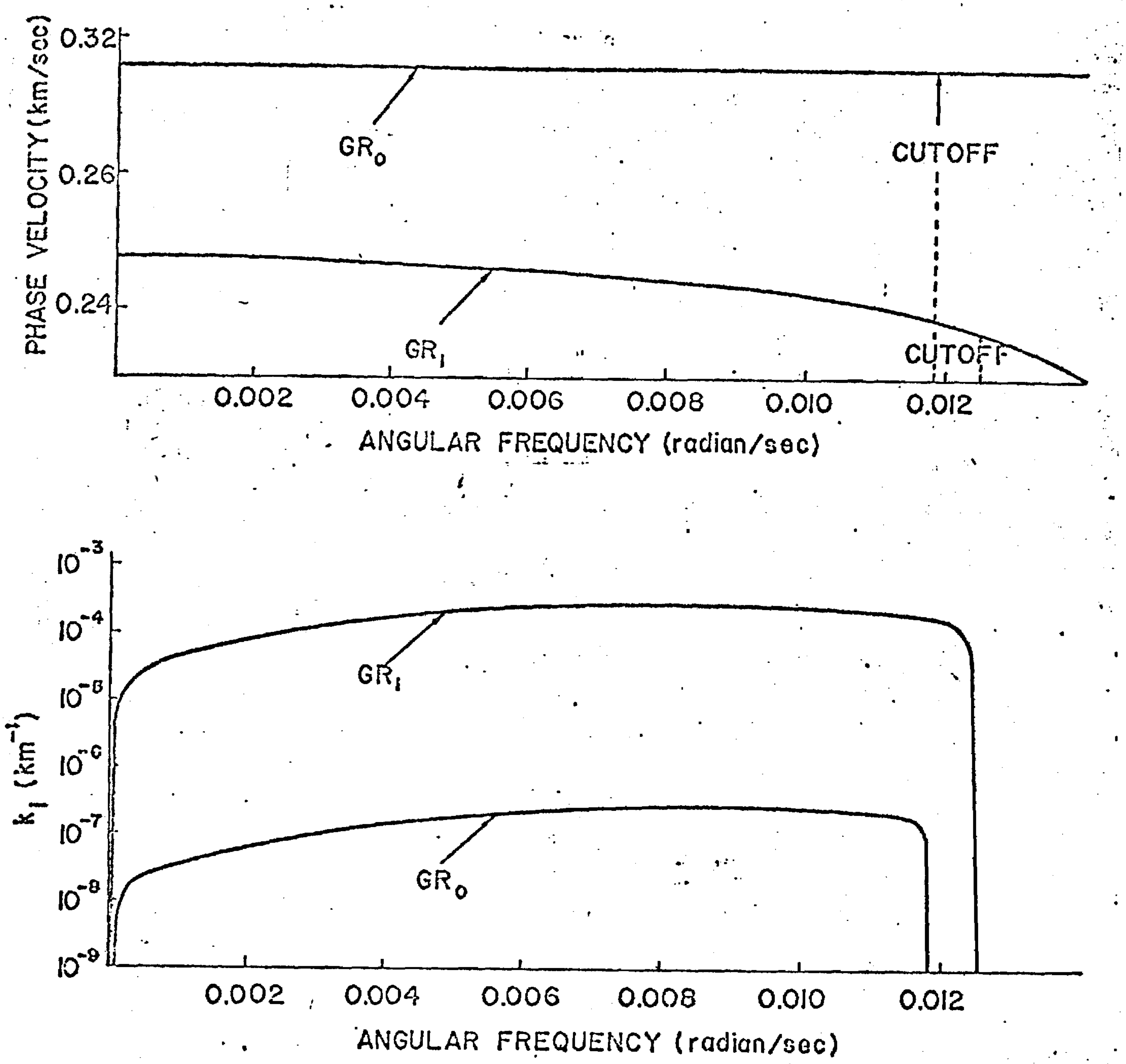

Figure 7. Numerically derived plots of phase velocity ω/k_R and of the imaginary part k_I of the complex horizontal wavenumber k versus angular frequency ω for the GR_0 and GR_1 modes. Nominal lower frequency cutoffs for these modes are as indicated. Note that k_I is identically zero above the cutoff frequency.

mode. The only modes for which this is necessary are GR_0 and GR_1. This input data is partly obtained by the procedure described above. Here we describe how the remaining portion of the input data is obtained.

To obtain values of phase velocity and source free amplitude at frequencies above cutoff one uses the current version of INFRASONIC WAVEFORMS with the variable NCMPL of NAMELIST NAM51 set less than zero. This gives an output essentially identical to what would be obtained with the original version of the program. The input data for this run would be the same as if one were computing waveforms without consideration of leaky modes. A sample listing of such input data is given in Fig. 8. The run will give mode numbers and tabulations of phase velocity VPHSE and amplitude AMP versus angular frequency OMEGA for the GR_0 and GR_1 modes at frequencies, above cutoff. The only output which need be retained for future use are the tabulations of VPHSE versus OMEGA for these two modes, since amplitudes at frequencies above cutoff are computed automatically in the run which utilizes this information as input data. A sample tabulation of the pertinent output (for the running example considered here) is given in Fig. 9.

Input data of phase velocity VPHSE and amplitude AMP for frequencies below cutoff are obtained by a second run of the program, again with NCMPL < 0, only with the original model atmosphere replaced by one which has a thick intermediate layer plus on upper half space replacing the original upper half space. Thus, in the NAM2 input list, IMAX is increased by one, the original ZI and T are unchanged, but one adds a ZI for the new value of IMAX which is, say 100 km larger than the largest ZI for the original model atmosphere; the temperature T for the new IMAX + 1 layer (i.e. for the new upper half space) is set equal to an arbitrarily very large value (say, $2\text{x}10^7$ °K). Doing this will artificially shift the cutoff frequencies for GR_0 and GR_1 down to values which are, for all practical purposes, equal to zero. The input data for this run should include choices of angular frequency and phase velocity limits (V1, V2, OM1, and OM2 of NAM4) which are appropriate for an exploration of the properties of GR_0 and GR_1 at frequencies below their original cutoff frequencies. It is imperative that OM2 not be too large since INFRASONIC WAVEFORMS will

```
$NAM1 NSTART=1, NPRNT=1, NPNCH=-1, NCMPL=-1  $END
$NAM2 IMAX=24,
ZI=1.,2.,4.,6.,8.,10.,12.,14.,16.,18.,20.,25.,30.,35.,40.,45.,55.,
    65.,75.,85.,95.,105.,115.,125.,
T=292.,288.,270.,260.,249.,236.,225.,215.,205.,198.,205.,215.,217.,
    237.,249.,265.,260.,240.,205.,185.,184.,200.,250.,400.,570.,
LANGLE = 1,
WINDY = 25*0.0,
WANGLE = 25*0.0
$END
$NAM4
THETKD = 35.,
V1 = 0.15, V2 = 0.495,
OM1 = 0.005, OM2 = 0.1,
NOMI = 30, NVPI = 30,
MAXMOD = 8
$END
$NAM6  ZSCRCE = 3.0, ZOBS = 0.0  $END
$NAM8  YIELD = 50.E3  $END
$NAM10  ROBS = 15000.,
TFIRST = 46.2E3, TEND = 52.2E3,
DELTT = 15.,
IOPT = 11,
$END
$NAM1 NSTART=6 $END
```

Figure 8. Input data to obtain phase velocity versus angular frequency above cutoff frequency for the GR_0 and GR_1 modes.

GR_0 MODE

OMEGA	V_n
.01482759	.31175833
.01640552	.31167707
.01723448	.31162330
.01810345	.31157130
.01892241	.31150395
.01933190	.31145750
.01974138	.31140492
.02137931	.31079310
.02151639	.31060345
.02178379	.30980225
.02202362	.30762931
.02210359	.30614224
.02214436	.30539871
.02216121	.30502694
.02217751	.30465517
.02219828	.30416532
.02220376	.30391164
.02223357	.30316810
.02229504	.30168103
.02239972	.29870690
.02259055	.29275862
.02293273	.28086207
.02301724	.27771666
.02324256	.26896552
.02353065	.25706897
.02380369	.24517241
.02405701	.23327586
.02432538	.22137931
.02453369	.20948276
.02465517	.20622217
.02484741	.19758621
.02498335	.19163793
.02512335	.18568966
.02526862	.17974138
.02542062	.17379310
.02558111	.16784483
.02566520	.16487069
.02575227	.16189655
.02593679	.15594828
.02613807	.15000000

GR_1 MODE

OMEGA	V_n
.01482759	.21913010
.01601253	.20948276
.01640552	.20500285
.01711598	.19758621
.01723448	.19544661
.01756050	.19163793
.01795598	.18568966
.01810345	.18350434
.01832569	.17974138
.01865292	.17379310
.01892241	.16844746
.01895156	.16784483
.01909212	.16487069
.01922762	.16189655
.01933190	.15953747
.01948594	.15594828
.01973352	.15000000

Figure 9. Sample output of phase velocity versus angular frequency at frequencies above cutoff for the GR_0 and GR_1 modes corresponding to the input data of Fig. 8.

encounter numerical difficulties at higher frequencies when the height of the upper halfspace is as high as considered here. (If it were not for this fact, this run could be used to generate essentially the same information as in the previous run.) For comparison, Fig. 10 indicates the types of atmospheric profiles used in the two runs with NCMPL < 0.

The second run gives values for the source free amplitudes AMP and phase velocities VPHSE for the GR_0 and GR_1 modes for frequencies below cutoff. The latter of these are expected to be virtually identical to the ω/k_R which are obtained by the method described in Sec. 3.4. Also, the source free amplitudes are expected to match on smoothly to those obtained from the prior run for high frequencies even though the two model atmospheres are not identically the same. (This is because the energy transported by the GR_0 and GR_1 modes is predominantly in the lower atmosphere.) Furthermore, we expect these amplitudes to be virtually the same as would be obtained by the modified residue method described in Scientific Report No. 1 for the original model atmosphere. The actual amplitudes should have a small imaginary part, but in view of the relatively small values of the k_I (less than 10^{-3} nepers/km) obtained, we are confident that this imaginary part may be neglected to an excellent approximation. The only aspect of the leaking phenomena which conceivably could be of significance is the accumulative exponential decay represented by the factor $\exp(-k_I r)$, which is retained in subsequent calculations.

Sample input data for this second run with NCMPL < 0 are given in Fig. 11; a listing of the output values for OMEGA, VPHSE, and AMP below the original cutoff frequencies for the GR_0 and GR_1 modes of the running example is given in Fig. 12.

3.6 WAVEFORM SYNTHESIS

The final step in the waveform synthesis is to run the program INFRASONIC WAVEFORMS with input data including the information concerning the GR_0 and GR_1 modes computed as described in the preceding two sections. The essential difference between this run and the first such

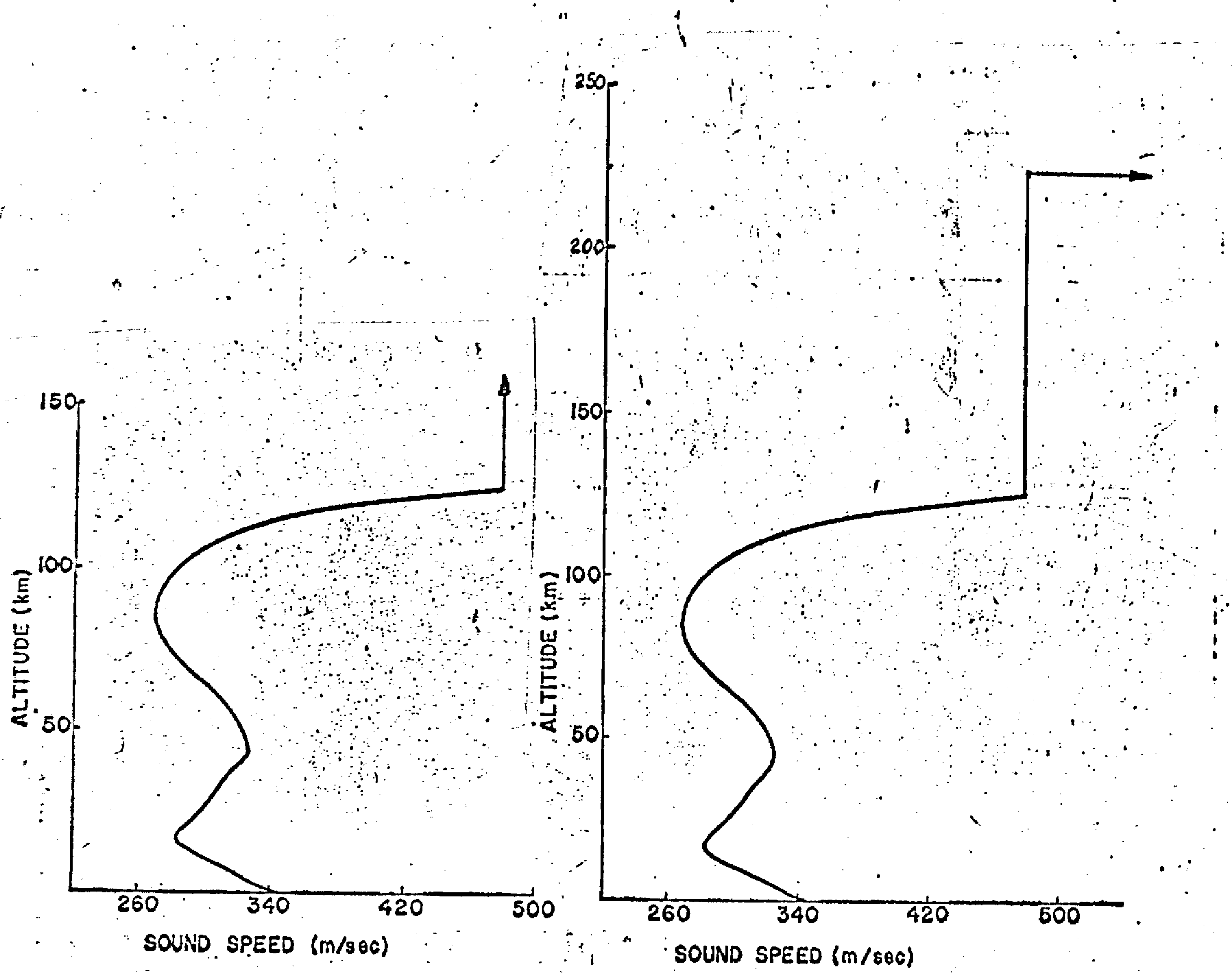

Figure 10. Two model atmosphere profiles; the first is the same as in Fig. 2; the second has the original upper halfspace replaced by a layer of finite but large thickness with a halfspace above it of extremely high temperature and sound speed. Second atmosphere is used to generate phase velocities and source free amplitudes at frequencies below nominal cutoff frequencies.

```
$NAM1 NSTART=1, NPRNT=1, NPNCH=-1, NCMPL=-1  $END
$NAM2 IMAX=25,
ZI=1.,2.,4.,6.,8.,10.,12.,14.,16.,18.,20.,25.,30.,35.,40.,45.,55.,
    65.,75.,85.,95.,105.,115.,125.,225.,
T=292.,288.,270.,260.,249.,236.,225.,215.,205.,198.,205.,215.,227.,
    237.,249.,265.,260.,240.,205.,185.,184.,200.,250.,400.,570.,2.E7,
LANGLE=1,
WINDY=26*0.0,
WANGLE=26*0.0
$END
$NAM4
THETKD= 35.,
V1 = 0.18, V2 = 0.34,
OM1 = 0.001, OM2 = 0.02,
NOMI = 30, NCPI = 30,
MAXMOD = 8
$END
$NAM1 NSTART=6 $END
```

Figure 11. Input data to obtain phase velocity and source free amplitudes below nominal cutoff frequencies for the GR_0 and GR_1 modes.

OMEGA	VPHSE	AMP
.00100	.31206	-.03102934
.00166	.31205	-.03101968
.00231	.31205	-.03100520
.00297	.31205	-.03098589
.00362	.31204	-.03096170
.00428	.31203	-.03093260
.00493	.31203	-.03089855
.00559	.31202	-.03085951
.00624	.31201	-.03081546
.00690	.31200	-.03076637
.00755	.31198	-.03071222
.00821	.31197	-.03065299
.00853	.31196	-.03062146
.00886	.31196	-.03058865
.00952	.31194	-.03051919
.01017	.31192	-.03044457
.01083	.31190	-.03036475
.01148	.31188	-.03027970
.01214	.31186	-.03018936
.01279	.31184	-.03009365
.01345	.31182	-.02999249
.01410	.31179	-.02988574
.01476	.31176	-.02977324
.01541	.31173	-.02965474
.01607	.31170	-.02952988
.01672	.31166	-.02939809
.01738	.31162	-.02925846
.01803	.31158	-.02910932
.01869	.31152	-.02894743
.01934	.31146	-.02876557
.02000	.31136	-.02854424

OMEGA	VPHSE	AMP
.00100	.28308	-.00003660
.00166	.28237	-.00003722
.00231	.28129	-.00003631
.00297	.27983	-.00004009
.00317	.27931	-.00004082
.00362	.27797	-.00004205
.00428	.27567	-.00004754
.00473	.27379	-.00005235
.00493	.27289	-.00005510
.00559	.26958	-.00006619
.00582	.26828	-.00007507
.00624	.26569	-.00009291
.00668	.26276	-.00012320
.00690	.26116	-.00014672
.00740	.25724	-.00024531
.00755	.25596	-.00029472
.00805	.25172	-.00063779
.00821	.25040	-.00084929
.00853	.24780	-.00156605
.00878	.24621	-.00225436
.00886	.24571	-.00249871
.00937	.24395	-.00335025
.00952	.24202	-.00346229
.01017	.24075	-.00365394
.01019	.24069	-.00365562
.01083	.23860	-.00365104
.01148	.23628	-.00358509
.01176	.23517	-.00354504
.01214	.23372	-.00348656
.01279	.23084	-.00336176
.01304	.22966	-.00330833
.01345	.22758	-.00321275
.01406	.22414	-.00305033
.01410	.22387	-.00303760
.01476	.21961	-.00283239
.01490	.21862	-.00278409
.01541	.21469	-.00259141
.01561	.21310	-.00251310
.01607	.20895	-.00230706
.01621	.20759	-.00223902
.01672	.20220	-.00196998
.01674	.20207	-.00196321
.01720	.19655	-.00168722
.01738	.19420	-.00156992
.01761	.19103	-.00141297
.01798	.18552	-.00114281
.01803	.18462	-.00109941
.01831	.18000	-.00087957

Figure 12. Sample output of phase velocity and source free amplitude at frequencies below cutoff for the GR_0 and GR_1 modes corresponding to the input data of Fig. 11.

run described in Sec. 3.5 is that one sets NCMPL > 0, and that one supplies values for the parameters in the input list NAM51. A listing of the input data for the run, allowing for the leaking modes, and appropriate to our running example is given in Fig. 13. The phase velocities input for the GR_0 and GR_1 modes are those derived from the two computer runs described in Sec. 3.5. The source free amplitudes for these modes are supplied only for frequencies below cutoff and these are derived from the second run of Sec. 3.5. The imaginary parts of the wave number are the numbers whose computation is described in Sec. 3.5. The reason we use the phase velocities below cutoff as computed in Sec. 3.5, rather than as in Sec. 3.4, is that both calculations agree to the same order of accuracy as would be expected for the approximations inherent in the method of Sec. 3.4. Consequently, we expect the values from the computer run to be the more nearly accurate. Of course, the values of k_I have to be computed by the method of Sec. 3.4 since the computer program in its present form does not compute these directly.

In Fig.14 we show CALCOMP plots of modal and total waveforms obtained before and after the inclusion of leaking modes. (This is for our running example, 15,000 km from a 50 megaton burst at 3 km altitude, the receiver being on the ground.) One may note that the inclusion of the leaking modes eliminates the spurious precursor in the waveform and raises the amplitude of the first peak. It is also important to note that the waveform with leaking modes included begins with a pressure rise. This is what one would probably expect from intuition alone, and would also appear to be more realistic.

3.7 FURTHER EXAMPLE (HOUSATONIC)

To further explore the effects of inclusion of leaking modes, we chose the case of waveforms observed by Berkeley, California, following the Hausatonic detonation at Johnson Island on October 30, 1962. A previous comparison of theoretical and observed waveforms for this event is given in the Geophysical Journal article by Pierce and Posey.[15] This case is also the central example in the 1970 AFCRL report by Pierce and

Figure 13. Sample input data for synthesis of infrasonic waveform including leaking modes. The data for the NAM51 input list is as derived from previous computations described in the present chapter.

Figure.14. CALCOMP plots of modal and total waveforms before and after inclusion of leaking modes. Example is for the case of a 50 megaton burst at 3 km altitude in the atmosphere of Fig. 2; receiver is at distance of 15,000 km.

Posey[1], and is discussed within the Lamb edge mode theory context in some detail in Posey's thesis.[16]

The model atmosphere assumed for the computation is exactly the same as in Fig. 3-12 of the 1970 report, only we let the upper half space begin at 125 km (IMAX = 24). Rather than repeat the tedious calculations of the k_I for the GR_0 and GR_1 modes for this model atmosphere, we assumed that they would be essentially the same as for the running example in the previous section. Thus the steps in Secs. 3.5 and 3.6 needed only to be carried out to obtain a waveform sysnthesis.

In Fig. 15, we give comparisons of the CALCOMP plots for this event before and after the inclusion of leaking modes. One may note that the first of these does not agree with the comparable CALCOMP plots in Fig. 3-10 of the 1970 AFCRL report. This is of course because we have here taken the upper halfspace to begin at a lower altitude. This choice of where the upper halfspace begins is of little consequence when leaking modes are included, and consequently the agreement of the old computation with the leaking mode included case is quite substantial. Further, the new computation is regarded as an improvement in that the spurious initial pressure drop has been eliminated.

On the basis of the calculations described above, we have redrawn the Fig. 7 in the Geophysical Journal article which compares observed and theoretical pressure waveforms for the Housatonic-Berkeley event. This revised figure is given here as Fig. 16. The only difference is in the center waveform. The precursor is now absent and the first peak to trough amplitude has been changed from 157 μbar to 170 μbar (less than 10% increase); the remanider of the waveform is virtually unchanged. The discrepancy with the edge mode synthesis hasn't been diminished and remains a topic for future study. (It was not addressed during the present study.)

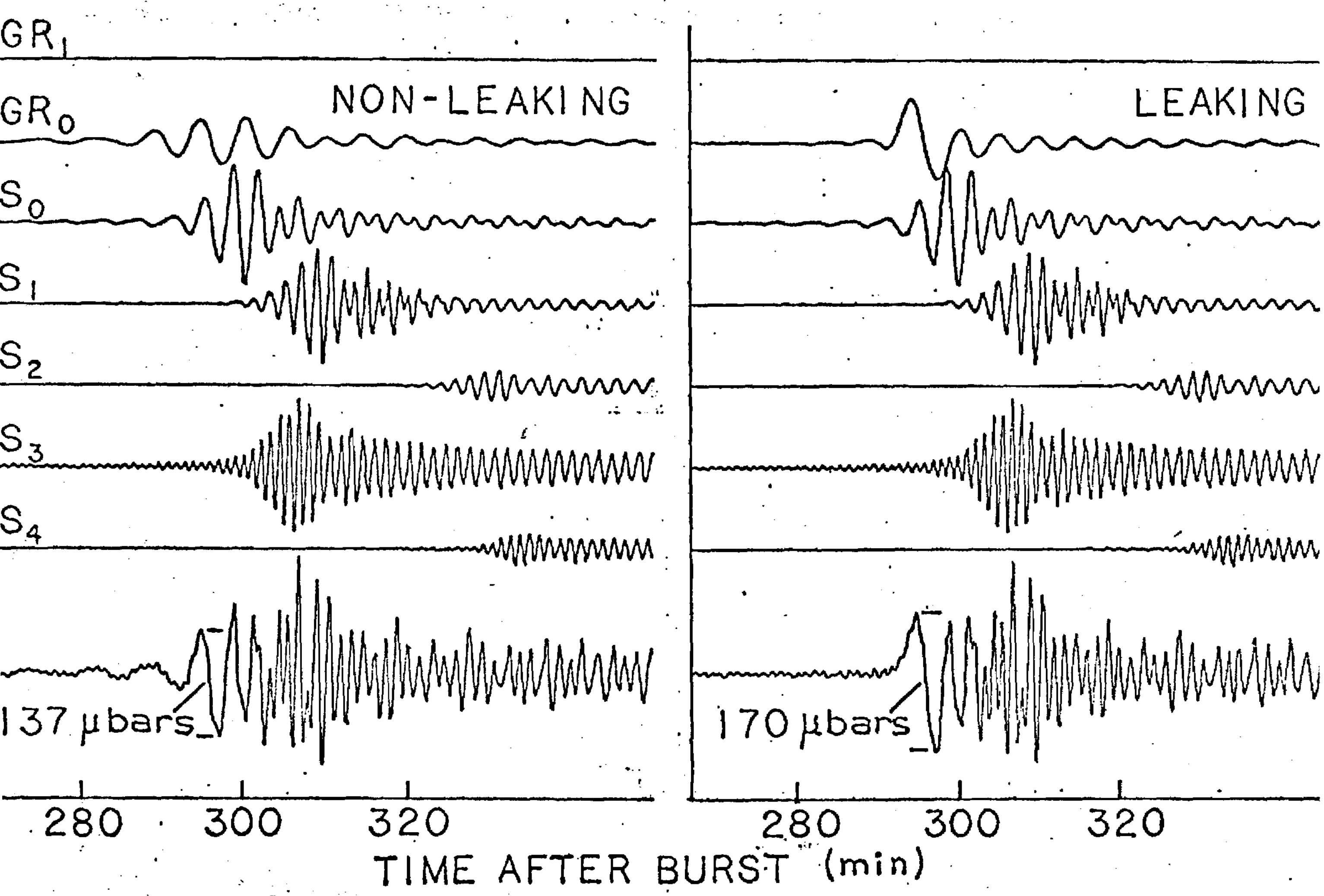

Figure 15. CALCOMP plots of modal and total waveforms before and after the inclusion of leaking modes. The eventis observations at Berkeley, California, following the Housatonic detonation at Johnson Island on 30 October 1962. The energy yield assumed in the theoretical computations was 10 megaton. The model atmosphere is as previously used by Pierce and Posey in AFCRL-70-0134, only the upper halfspace begins at 125 km.

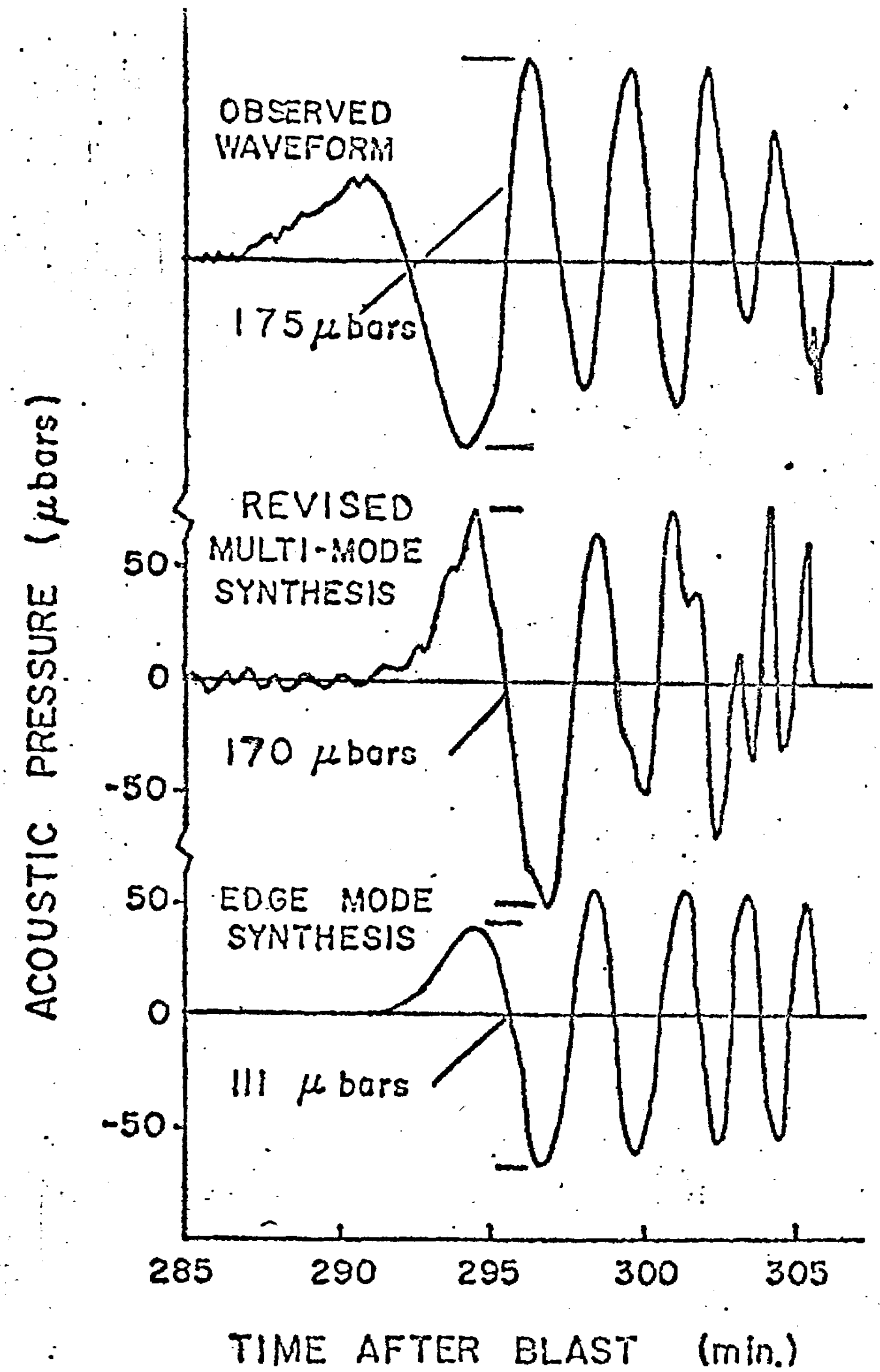

Figure 16. Observed and theoretical pressure waveforms at Berkeley, California, following the Housatonic detonation at Johnson Island on 30 October 1962. The observed waveform is taken from Donn and Shaw (1967). The energy yield assumed in the theoretical computations was 10 megatons. This is a revised version of the Fig. 7 in the 1971 paper by Pierce and Posey (Geophys. J. Roy. Astron. Soc. 26, 341-368). The original multi-mode synthesis figure has been replaced by one including leaking modes.

Chapter IV

ASYMPTOTIC HIGH-FREQUENCY BEHAVIOR OF GUIDED MODES

4.1 INTRODUCTION

Due to temperature and wind stratification, the earth's atmosphere possesses sound speed channels with associated relative sound speed minima. Fig.17 shows a standard reference atmosphere wherein two such sound speed channels are indicated; one with a minimum occurring at approximately 16 km altitude and the second with a minimum occurring at approximately 86 km altitude. Given the presence of such a channel, an acoustic ducting phenomenon can occur, as is demonstrated in Fig.18, wherein the energy associated with an acoustic disturbance can become trapped in the region of a relative sound speed minimum. It is this mechanism of ducting only that is of interest here.

In the computer program INFRASONIC WAVEFORMS, the computation of modal waveforms involves the numerical integration over angular frequency of a Fourier transform of acoustic pressure where this integration is truncated at the high-frequency end. It has been speculated that this abrupt truncation leads to the generation of what might be called "numerical noise" in the computer output. It was felt useful, therefore, to extend this integration beyond the heretofore upper angular frequency limit by means of some appropriate high-frequency approximation. In the case of an atmosphere with just one sound channel, the technique for doing this is well known and dates back to a paper published by N. Haskell[17] in 1951. Haskell's method is the W.K.B.J. (Wentzel, Kramers, Brillouin, Jeffreys) method, then in common use in quantum mechanics, although its invention dates back to Carlini[18] Green[19] in the early 19th century.

The approximations associated with the W.K.B.J. method of solution apply to the analytical model on which the computer program is based at

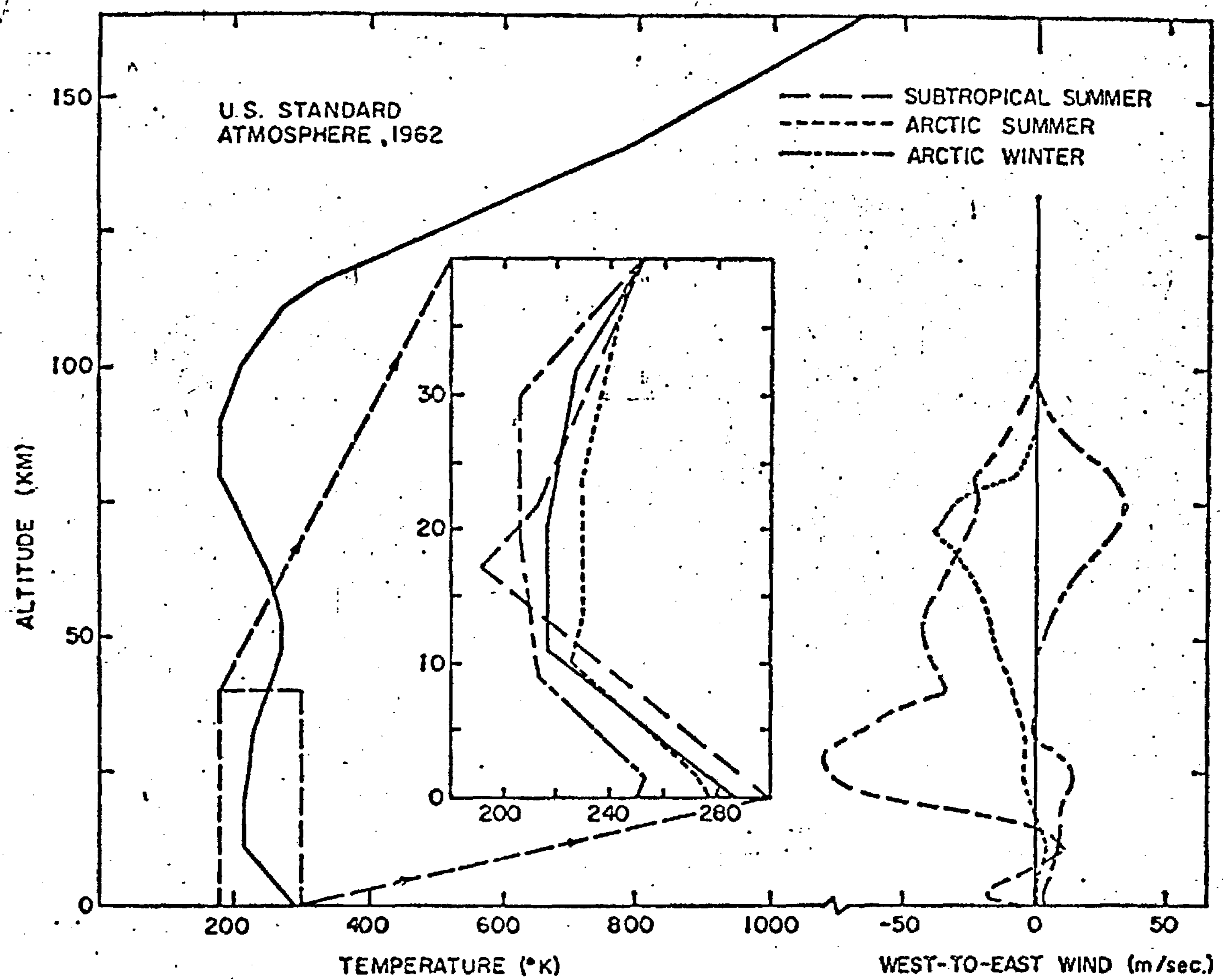

Figure 17. Temperature and wind speed versus height profiles for standard reference atmospheres. Calculations in present chapter are for U. S. Standard Atmosphere 1962 without winds. The presence of two temperature minima indicates two sound speed channels.

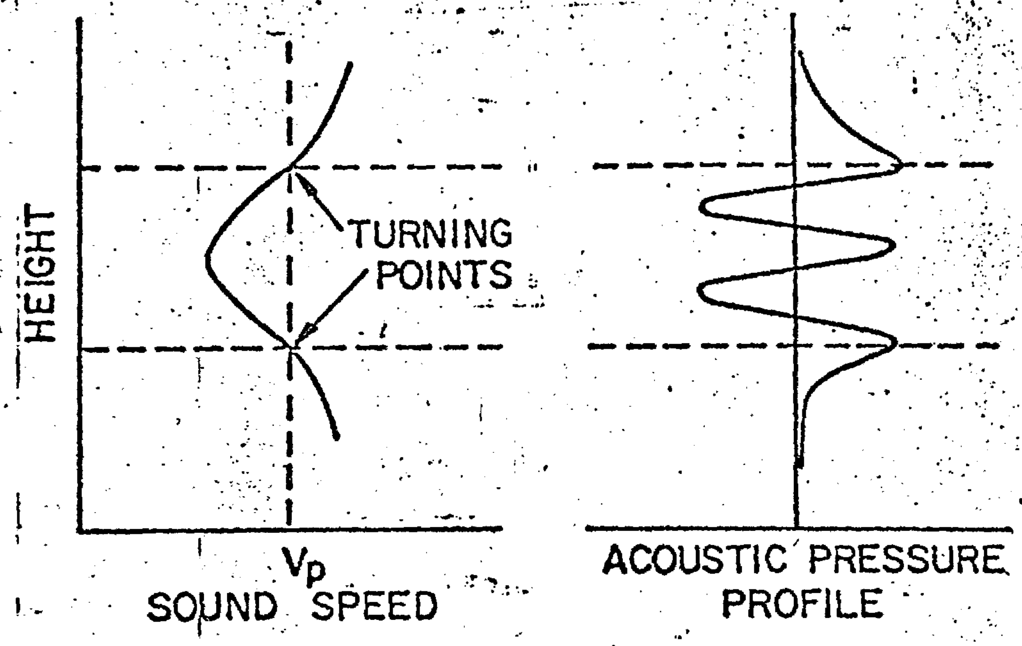

Figure 18. Sketches of sound speed versus height and acoustic pressure amplitude versus height for a guided mode illustrating the mechanism of acoustic ducting in a sound speed channel centered at a region of minimum sound speed. The energy of the disturbance may be considered as concentrated in the height region between turning points.

frequencies above approximately 0.05 radian/sec (periods less than 2 minutes). Below that limit, effects due to density stratification in the atmosphere and gravitational forces cannot be neglected. Such effects therefore are not germane to the discussion here.

The application of the W.K.B.J. method of solution to the problem of describing propagation of acoustic disturbances in an atmosphere that contains two adjacent sound speed channels has previously been discussed in the literature by Eckart,[20] who invented the simple method of seeking a W.K.B.J. model for each of the sound speed channels spearately, then combining the results rather than treating the problem with a single model. In the present chapter, Eckart's method is applied and numerically verified for the case of infrasonic waves in the atmosphere.

4.2 THE W.K.B.J. MODEL

The W.K.B.J. model for propagation of acoustic disturbances in a single sound speed channel may be considered as an approximation for the acoustic pressure divided by the square root of the ambient density, which in general may be expressed as

$$\frac{P}{\sqrt{\rho_o}} = \psi(z)e^{-i\omega t}e^{ikx} \tag{4.1}$$

where ω is angular frequency, k is the wave number associated with the horizontal dimension x, z is altitude. Here $\psi(z)$ satisfies the reduced wave equation,

$$\left[\frac{d^2\psi}{dz^2} + \frac{\omega^2}{c^2(z)} - k^2\right]\psi = 0 \tag{4.2}$$

where c(z) is sound speed as a function of altitude. The W.K.B.J. approximation applies in general to all differential equations of this type if the coeffieient of ψ is sufficiently "slowly varying." It would appear in particular to be valid in the present context provided

$$\frac{c}{|\nabla c|} << \lambda \tag{4.3}$$

where λ is some representative wavelength of interest. This approximation states that substantial changes in sound speed should not occur within distances corresponding to a typical wavelength of interest if the model is to apply.

A particular sesult of the W.K.B.J. approximation is that dispersion curves (v_p vs. ω) of guided modes are given by the equation

$$\int_{z_{bottom}}^{z_{top}} \left[c^{-2} - v_p{}^{-2}\right]^{\frac{1}{2}} dz = \frac{(2n+1)\pi}{2\omega} \tag{4.4}$$

where v_p is phase velocity, $n = 0, 1, 2, 3, \ldots,$ and where z_{bottom} and z_{top} identify the lower and upper bounds of the sound speed channel, respectively. This integral is a direct result of the W.K.B.J. method of solution[21], and its numerical solution enables the plotting of dispersion curves.

4.3 COMPARISON OF DISPERSION CURVES

Particular insight into the high-frequency behavior of guided infrasonic modes was gained when the above integral was solved numerically by computer for both the upper and lower channels, the model atmosphere being that given in Fig.17. The resulting dispersion curves computed in this manner are shown in the lower portion of Fig 19. One set of curves (the dashed curves) is appropriate to the W.K.B.J. model for the lower channel and the other set (the solid curves) is appropriate to the W.K.B.J. model for the upper channel. In the upper portion of the same figure are shown again dispersion curves as generated by the computer model INFRASONIC WAVEFORMS. It should be mentioned that the computer model solves a more complex problem in the sense that the simplifications inherent in the W.K.B.J. model are not present.

As is illustrated in the lower portion of Fig.19, the two sets of dispersion curves generated by the W.K.B.J. models intersect with one another at various points. A comparison of the dispersion curves shown in both the upper and lower portions of Fig. 19 reveals that these points

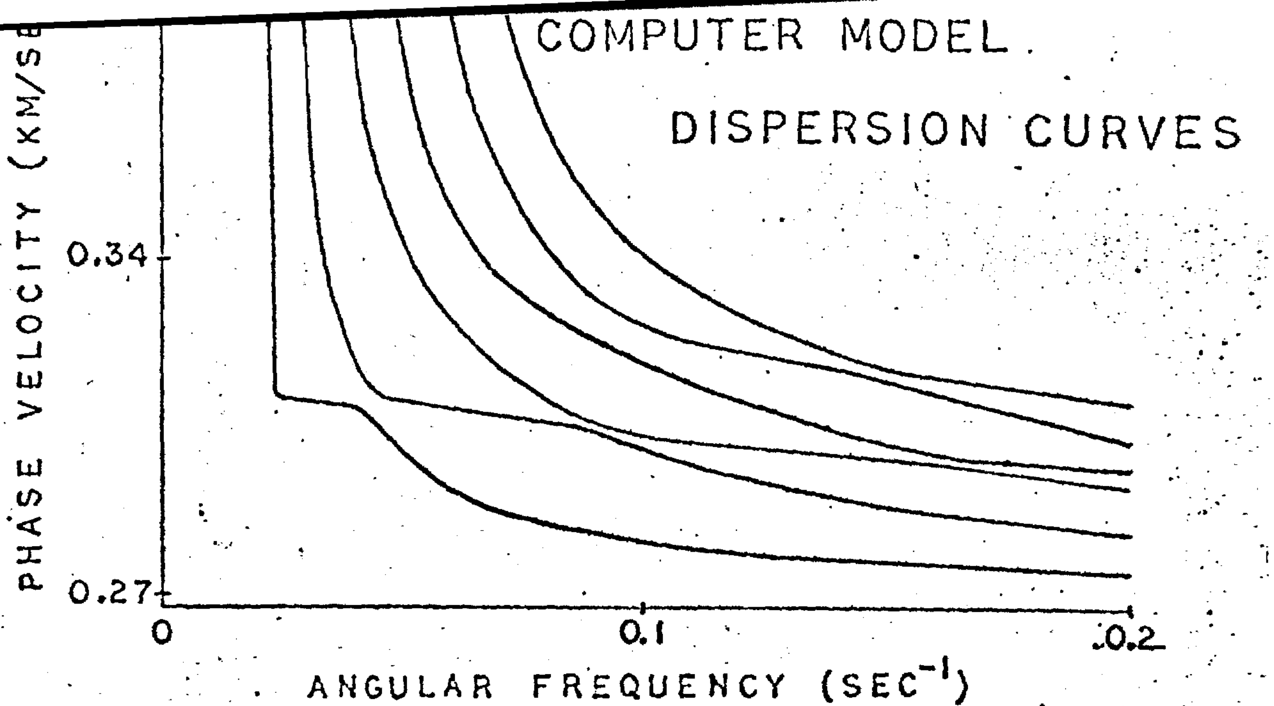

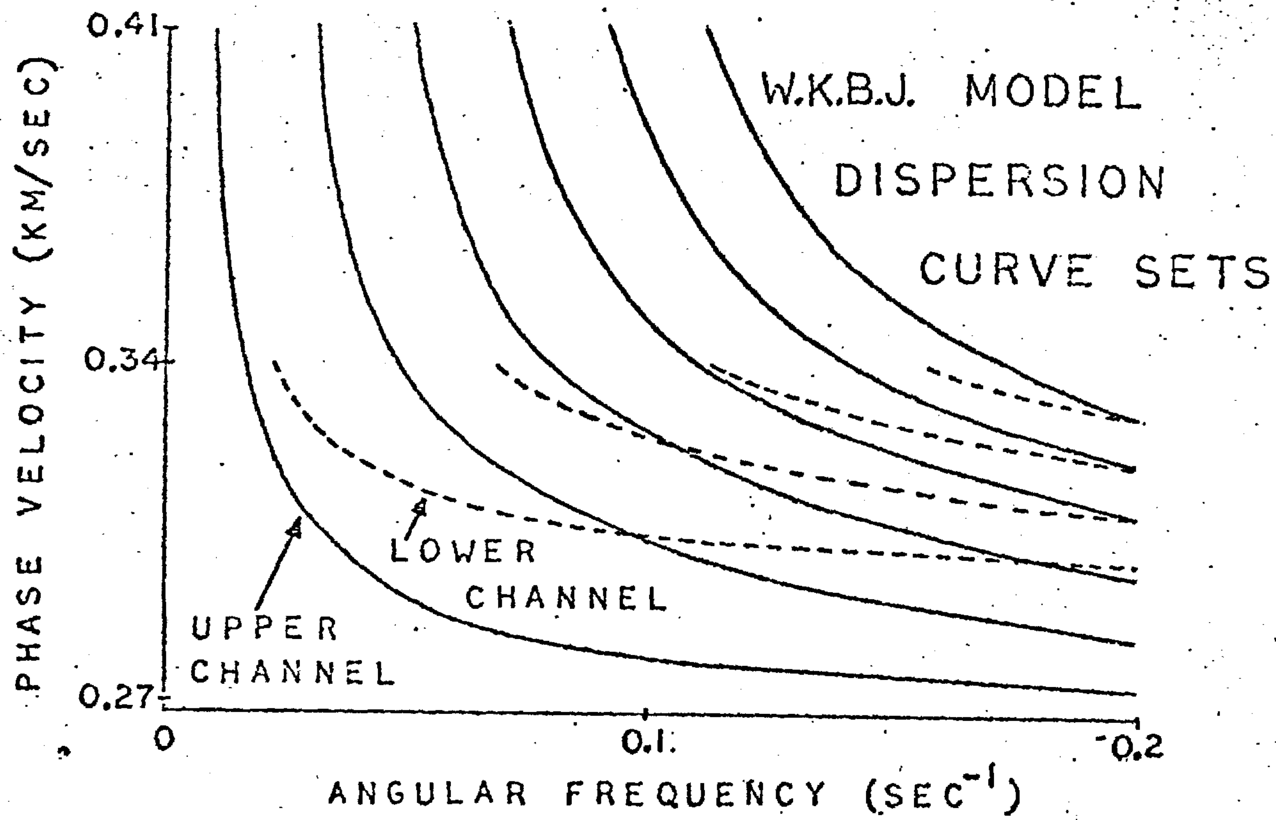

Figure 19. A comparison of theoretical guided mode dispersion curves for the U. S. Standard Atmosphere 1962. The upper set of curves were generated by full wave calculations with the multi-modal synthesis program INFRASONIC WAVEFORMS. The lower sets were obtained by applying the W.K.B.J. method to the upper sound channel (solid lines) and the lower sound channel (dashed lines), respectively.

of intersection mark regions of resonant interaction in the phase velocity-angular frequency plane between adjacent modes of the computer model. To better illustrate this observation, in the right hand portion of Fig. 20 is shown one such region of interaction with its corresponding point of intersection between two dispersion curves of the W.K.B.J. models shown to the left. It should be mentioned that the dispersion curves of the computer model never intersect with one another. An analytical explanation of this fact has previously been given by Pierce[22].

4.4 INFERENCES CONCERNING ENERGY VERSUS HEIGHT DISTRIBUTION

The above observation may be stated differently by saying that, for relatively high angular frequencies, the dispersion curve corresponding to a given mode of the computer model is comprised of portions of dispersion curves from both sets of the curves generated by the W.K.B.J. models. Two important inferences about the asymptotic high-frequency behavior of guided infrasonic modes can be drawn from this statement. First, for some frequency ranges, and depending on how dispersion curve portions match between curves of the computer model and the W.K.B.J. models, it can be inferred that the acoustic energy associated with a given mode is comprised of energy associated more with propagation of acoustic disturbances in one sound speed channel than in the other. Also, as frequency increases, this association alternates back and forth between channels. To illustrate, if, for a small range of frequencies, a portion of a dispersion curve of the computer model matches (in the phase velocity-angular frequency plane) a portion of one of the W.K.B.J. model curves for the upper channel, then that implies that, for that mode and for that small frequency range, the acoustic energy density associated with that mode is greater in the upper channel than in the lower channel. Secondly, in the standard reference atmosphere, the sound speed minimum for the upper channel is less in magnitude than the sound speed minimum for the lower channel. It can be inferred, therefore, that those acoustic disturbances for which phase velocities are less in magnitude than the sound speed minimum for the lower channel are associated more with acoustic energy trapped in the upper channel than in the lower channel, and thus, for this reason, do not contribute significantly to the acoustic energy at the ground. This inference implies that care must

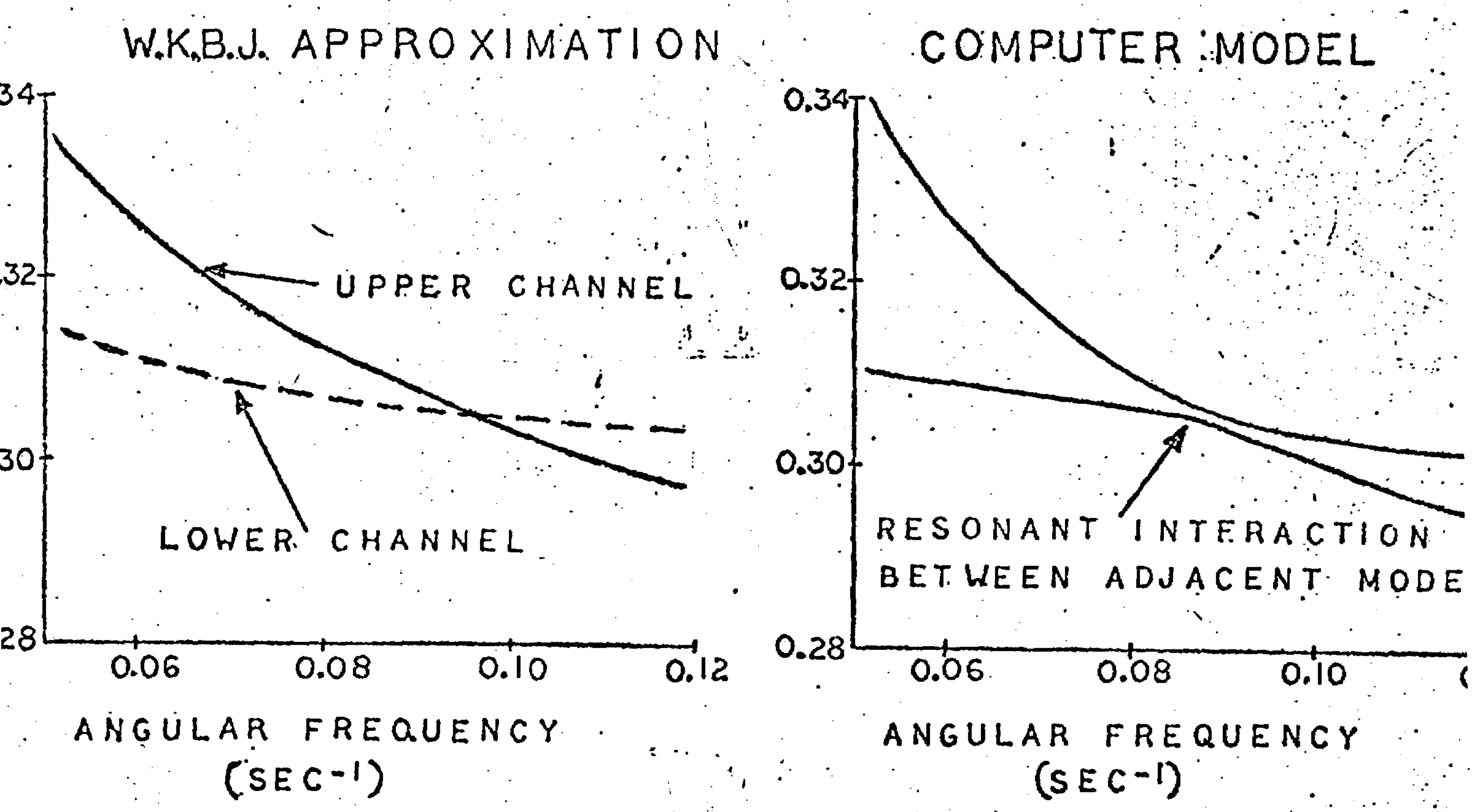

Figure 20. A detailed (blown-up) plot of a section of Fig. 19 showing a region of resonant interaction between two modes, one ducted in the upper channel, the other ducted in the lower channel. The full wave calculation (computer model) indicates that the two modes interact such that the actual dispersion curves do not cross, but indicates that the W.K.B.J. and computer model curves are nearly the same except in the region of resonant interaction.

be taken as to which modes are chosen to superpose in the attainment of the final pressure waveform at the ground, as some may not contribute.

4.5 IMPLICATIONS FOR WAVEFORM SYNTHESIS

In the previous synthesis of guided pressure waveforms at long distances, the acoustic modes were numbered in order of increasing phase velocity (i.e., S0, S1, S2,..., etc.) and the sum over modes was truncated at a finite maximum number of modes. The analysis given here indicates that this may be a very poor approximation for synthesizing high frequency portions of waveforms observed near the ground since there is always some frequency above which the first, say, N modes all correspond to channelling in the upper sound speed channel.

The preferable alternative would appear to be (for synthesis of ground level arrivals from sources below 50 km altitude) to ignore the upper sound speed channel completely for frequencies above, say, at least 0.2 rad/sec (possibly 0.1 rad/sec) corresponding to periods below at most 30 sec (possibly 1 min). The dispersion curves could then be taken as given by the W.K.B.J. approximation and the mode amplitude versus height profiles could be computed by the method outlined by Haskell. The Dispersion curves and amplitudes so computed would fit directly into the general scheme outlined by Pierce and Posey[1] which forms the theoretical basis for the current version of INFRASONIC WAVEFORMS.

Chapter V

EXTENSION OF INFRASONIC WAVEFORMS TO INCLUDE DISTANCES BEYOND THE ANTIPODE

5.1 INTRODUCTION

Previous theoretical considerations incorporated into the digital computer program INFRASONIC WAVEFORMS restricted synthesis to waves that had traveled less than one-half the distance around the earth. The purpose of this chapter is to further exemplify techniques to enable computer synthesis of acoustic-gravity pressure waveforms at points whose distances are greater than halfway around the world from a nuclear explosion. Extension of prior theory shows that for wave propagation past a point on a spherical earth, one-half the great circle distance away from the point of detonation (i.e., the antipode), a phase shift of $\pi/2$ radians to the Fourier transforms of each modal wave is incurred. Modification to the computer program necessitates the reinterpretation of the great circle distance r, the inclusion of the $\pi/2$ phase shift, and a modification to the earth curvature correction factor. Computations are presented for pre and post antipodal waveforms.

5.2 THEORETICAL CONSIDERATIONS FOR POST ANTIPODAL WAVEFORMS

In considering acoustic-gravity waves that have passed beyond the antipode, certain specific definitions for the various waveforms must be adopted. To an observer located on the surface of a spherical earth between the source and the antipode the pressure waveform that is first observed is the direct arrival or A_1 arrival. The A_1 arrival has traveled the shortest great circle distance r to reach the observation point. The next waveform observed at the above observation point is the A_2 or antipodal arrival. The A_2 arrival has traveled the longer great circle distance from the explosion point around the glove passing through the antipode to reach the observation point. The A_3 arrival is the A_1 pressure waveform that has traveled completely around the globe with respect to the observation point. Further arrivals exist but are not considered here. The distance r is measured in kilometers and is the great circle distance measured from the detonation point to the final observation point. Figure 21 shows some typical pressure waveforms recorded in suburban New York for the Russian explosion of 58 megatons at Novaya Zemlya on 30 October 1961.[23]

Previous numerical syntheses of acoustic-gravity waveforms have only considered direct arrivals. The extension of this theory to include waveform prediction for antipodal arrivals is described here. An investigation of a small region of the earth's surface in the vicinity of the antipode where prior theory breaks down yields certain waveform characteristics that enable waveform synthesis to be extended to ranges past the antipode. By taking the antipodal region small in area than say 1/100th of the earth's area as a whole we can consider this region to be flat. Then the equation governing propagation of any frequency in any guided mode near the antipode is the cylindrical wave equation in the form of

$$\partial^2 F/\partial r_A^2 + (1/r_A)\partial F/\partial r_A - (1/V_p^{\,2})\partial^2 F/\partial t^2 = 0 \qquad (5.1)$$

where F would represent the r_A and t dependent part of the integration kernal for synthesization (i.e., integration over frequency of any given modal waveform where the height dependent part is omitted here). The quantity V_p is the corresponding phase velocity. The assumed circular symmetry of the wave about the antipode is inherent in the absence of the angular derivative terms in the above equation. The distance r_A is measured positive out from the antipode. The wave solution to Eq. (5.1) for the total acoustic pressure p and small r_A can be written for time t as

$$F \cong DJ_o(kr_A)\cos(\omega t+\varepsilon) \qquad (5.2)$$

For the above, $k = \omega/V_p$ represents the horizontal wave number, ω the angular frequency, and ε some phase angle. The quantity D is some arbitrary constant while $J_o(kr_A)$ is the Bessel function of zero order.

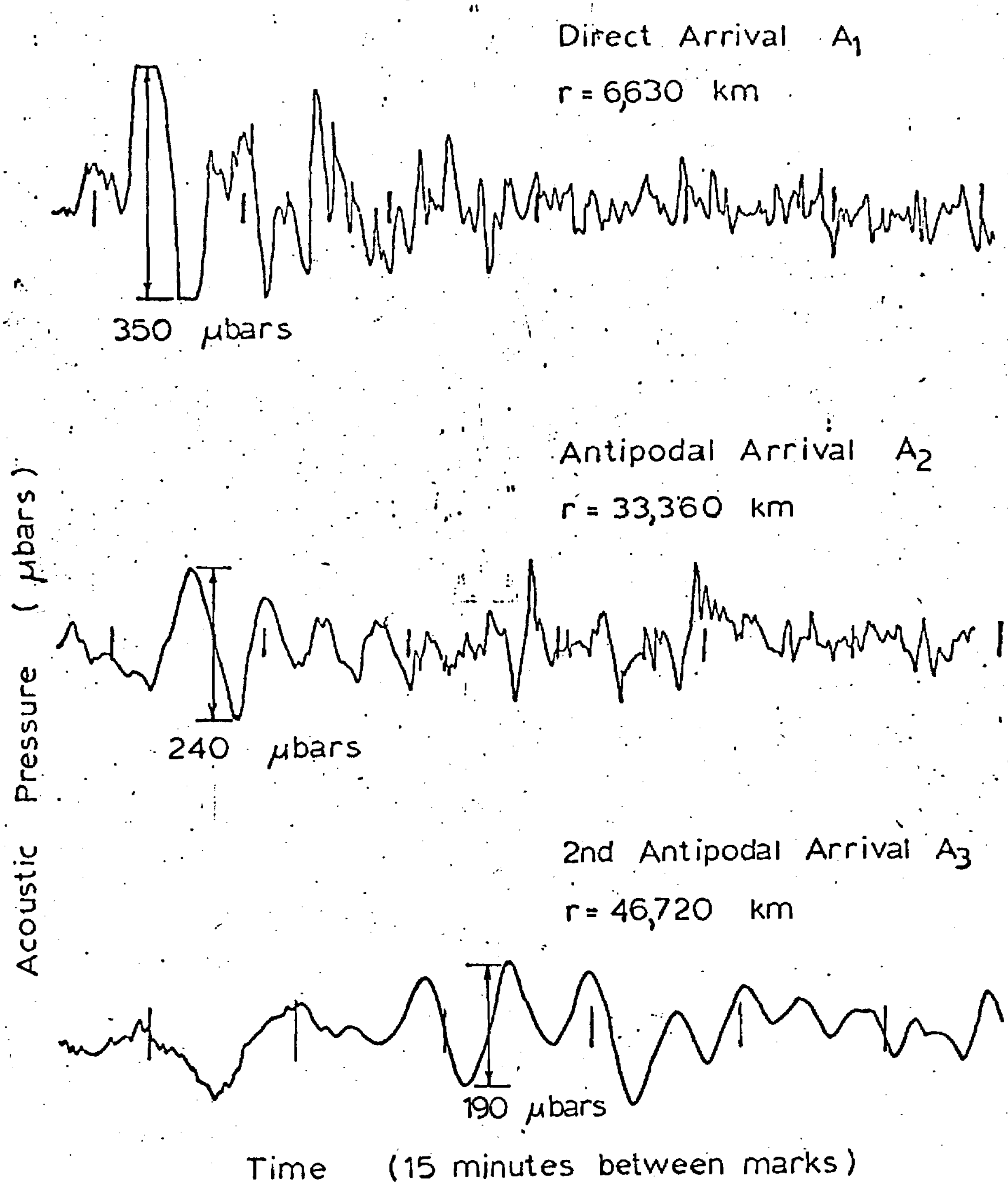

Figure 21. Infrasonic pressure waveforms recorded in suburban New York following the detonation of a 58 megaton yield nuclear device in Novaya Zemlya USSR on 30 October 1961. [Extracted from Donn and Shaw, Rev. of Geophys. 5, 53-82 (1967).]

When r_A is suffienciently large (i.e., greater than three wavelengths) a solution for the total acoustic pressure p can be considered as a sum of ingoing and outgoing waves with respect to the antipodal region. The asymptotic solution for large kr_A can be written for time t as

$$F = A(r_A)^{-1/2}\cos(\omega t+kr_A+\phi_{in}) + B(r_A)^{-1/2}\cos(\omega t-kr_A+\phi_{out}) \tag{5.3}$$

In Eq. (5.3) ϕ is some phase angle while ω and k are as previously defined. The plus sign in the argument of the cosine denotes an ingoing wave. Equation (5.3) is not defined at $r_A = 0$ and, as r_A approaches zero, wave amplification is predicted. Figure 22 illustrates waveform amplification approaching the antipode for three different values of r for a ten megaton nuclear explosion. The antipode is reached when r = 20,000 km.

Realizing that Eqs. (5.2) and (5.3) should represent the same presure waveform at large r_A we can now show the existence of a phase difference between waveforms approaching and leaving the antipode. For large r_A, the Bessel function $J_o(kr_A)$ can be represented by its asymptotic approximation such that Eq. (5.2) becomes

$$F = D(2/\pi r_A k)^{1/2}\cos(kr_A-\pi/4)\cos(\omega t+\varepsilon) \tag{5.4}$$

or with the aid of trigonometric identities as

$$F = \frac{1}{2} D(2/\pi r_A k)^{1/2} [\cos(\omega t+\varepsilon+kr_A-\pi/4) + \cos(\omega t+\varepsilon-kr_A+\pi/4)] \tag{5.5}$$

Equating (5.3) to (5.5) then requires that

$$A = B = D/(2\pi k)^{1/2} \tag{5.6a}$$

$$\phi_{in} = \varepsilon - \pi/4 \tag{5.6b}$$

$$\phi_{out} = \varepsilon + \pi/4 \tag{5.6c}$$

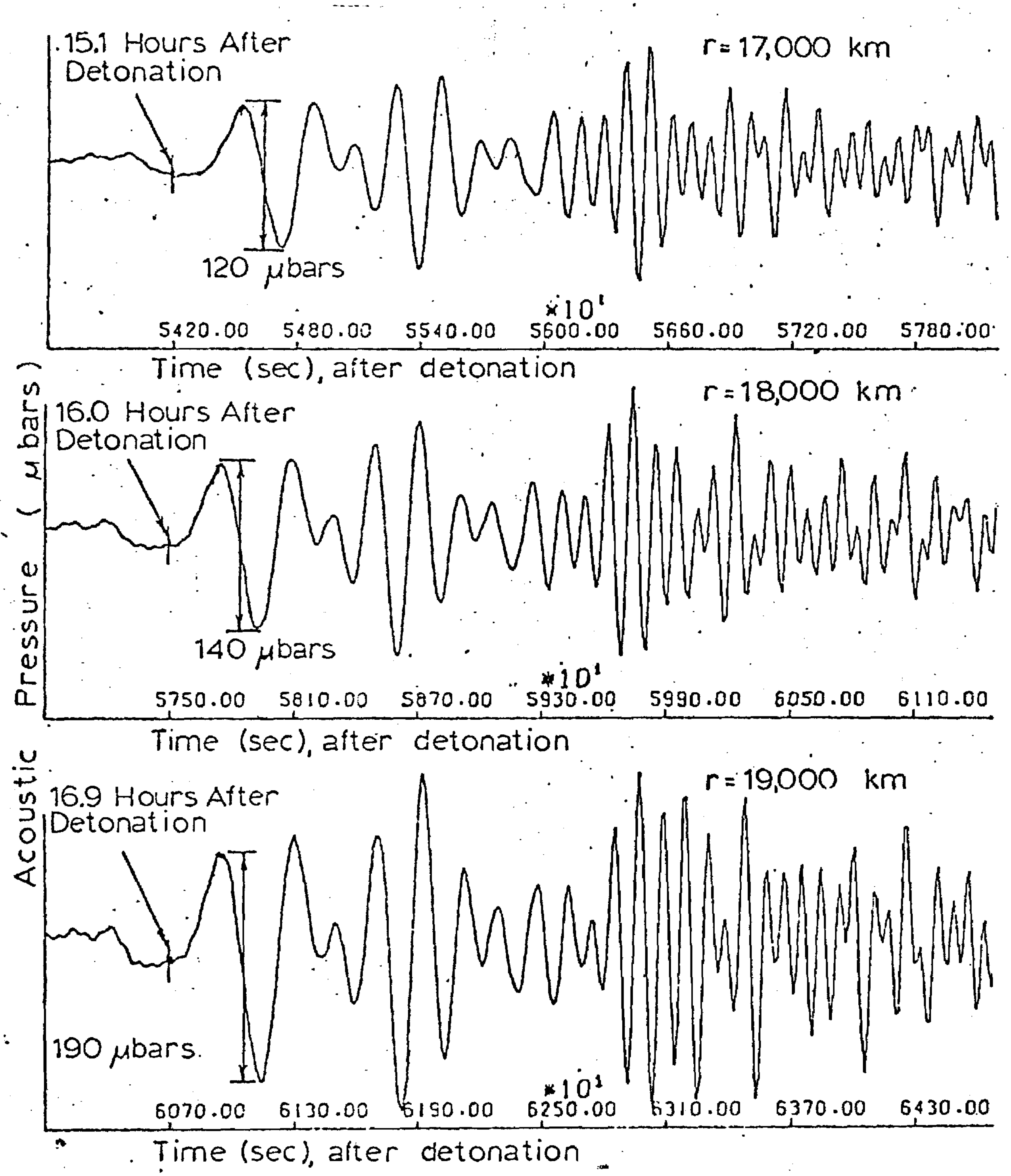

Figure 22. Theoretical pressure waveforms of a pulse propagating towards the antipode (corresponding to a great circle distance r of 20,000 km). Computations presented are for a 10 megaton burst in a standard atmosphere without winds. Note the amplification in amplitude for values of r successively closer to 20,000 km.

so

$$\phi_{out} = \phi_{in} + \pi/2 \tag{5.7}$$

The latter shows that a pressure waveform undergoes a phase shift of 90 degrees. Based on this knowledge the computer program has been altered to synthesize pressure waveforms for the A_2 arrival that passes through the antipode.

5.3 MODIFICATIONS TO INFRASONIC WAVEFORMS FOR POST ANTIPODAL WAVEFORMS

Waveform synthesis for ranges beyond the antipode necessitates only minor adjustments to the computer program. By considering the theoretical development of Brune, Nafe, and Alsop (1961)[24] for circular spreading of waves over a spherical surface of radius r_e (i.e., r_e = 6374 km for earth) the amplitude correction factor for the curvature of a spherical earth, appearing in subroutine TMPT, is altered for post antipodal waveforms by replacing the term $\sin(r/r_e)$ by its absolute magnitude, where r is interpreted as the total distance the wave has traveled from the point of detonation. For post antipodal arrivals considered here r would be between πr_e and $2\pi r_e$ kilometers. The earth curvature correction factor in subroutine TMPT appearing as

```
CF = (1./(6374. * SIN(RAD)))**0.5                                   (5.8)
```

is replaced for post antipodal waveforms by

```
CF = (1./(6374.*ABS(SIN(RAD))))**0.5                                (5.9)
```

where ROBS = r and

```
RAD = ROBS/6374.                                                    (5.10)
```

To accomodate the change in phase as the waveforms pass through the antipode two computer cards of the form

```
PH2 = PH2 + 1.570796                                                (5.11)
```

are inserted in the deck listing of subroutine TMPT after lines 160 and 177.

After incorporating the above modifications into subroutine TMPT the computer program was then utilized to synthesize various theoretical waveforms. Using the Soviet shot of 30 October 1961 as the source, a phase shift upon passing through the antipode is exhibited in Fig. 23 for two observation ranges of a synthesized pressure waveform. Further dispersion beyond the antipode of the pressure waveform is shown in Fig. 24 for a ten megaton explosion. A comparision of antipodal arrivals for a computer synthesized pressure waveform and a microbarograph recorded by Donn and Shaw in suburban New York[5] for the 58 megaton Soviet test is presented in Fig. 25. Considering the scattering in waveforms that can occur at such large arrival distances, it is not unreasonable to say that the amplitudes and typical periods of the two plots are of the same order of magnitude.

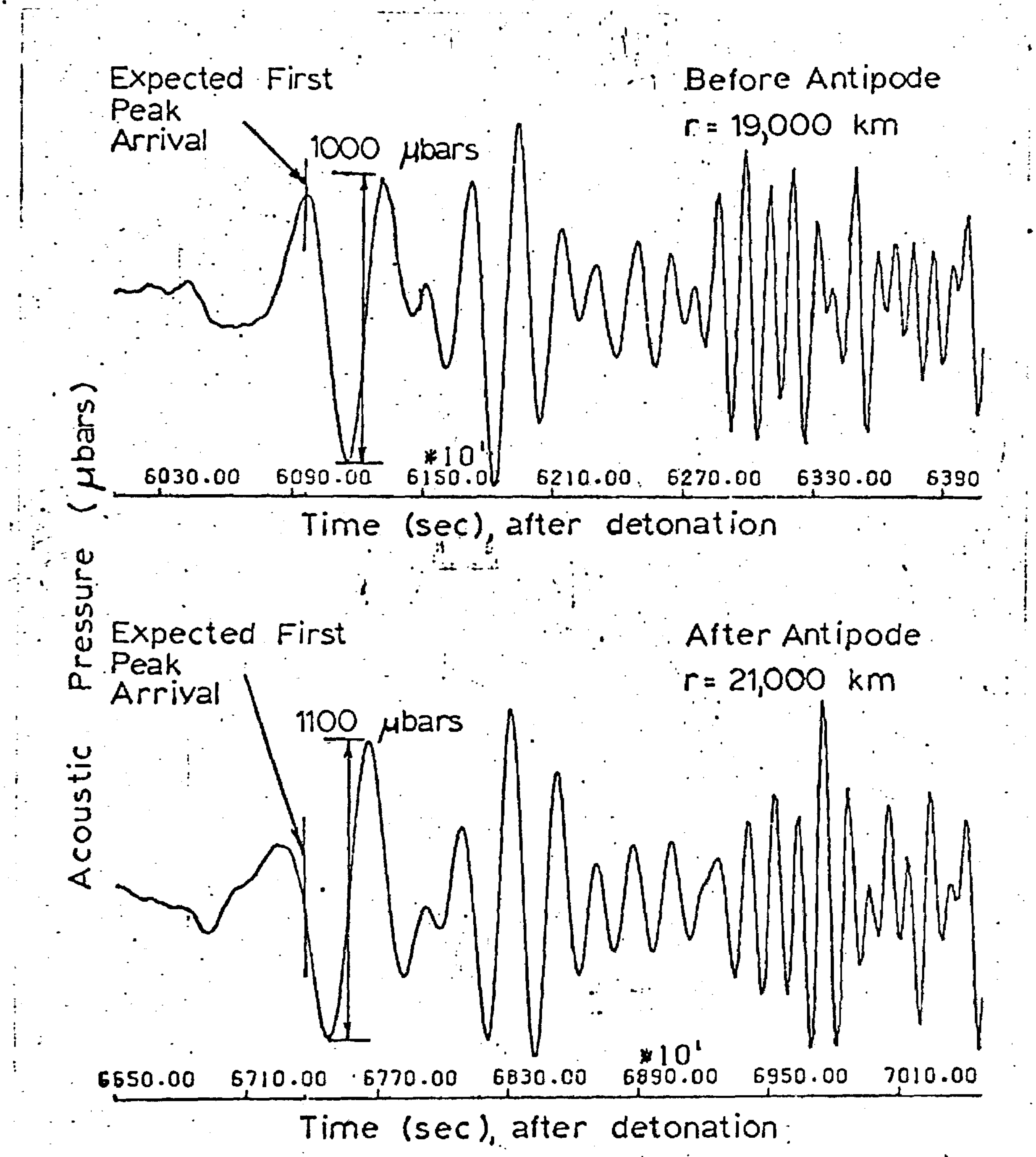

Figure 23. Theoretical pressure waveforms just before (great circle distance r of 19,000 km) and just after (r of 21,000 km) passing through the antipode (20,000 km). The $\pi/2$ phase shift after the antipodal passage is evidenced by the second figure. Time of expected first peak arrival derived from linear extrapolation of computed time of first peak arrival versus great circle distance for $r<20,000$ km to case of $r>20,000$ km. Source is the 58 megaton Soviet test in Novaya Zemlya.

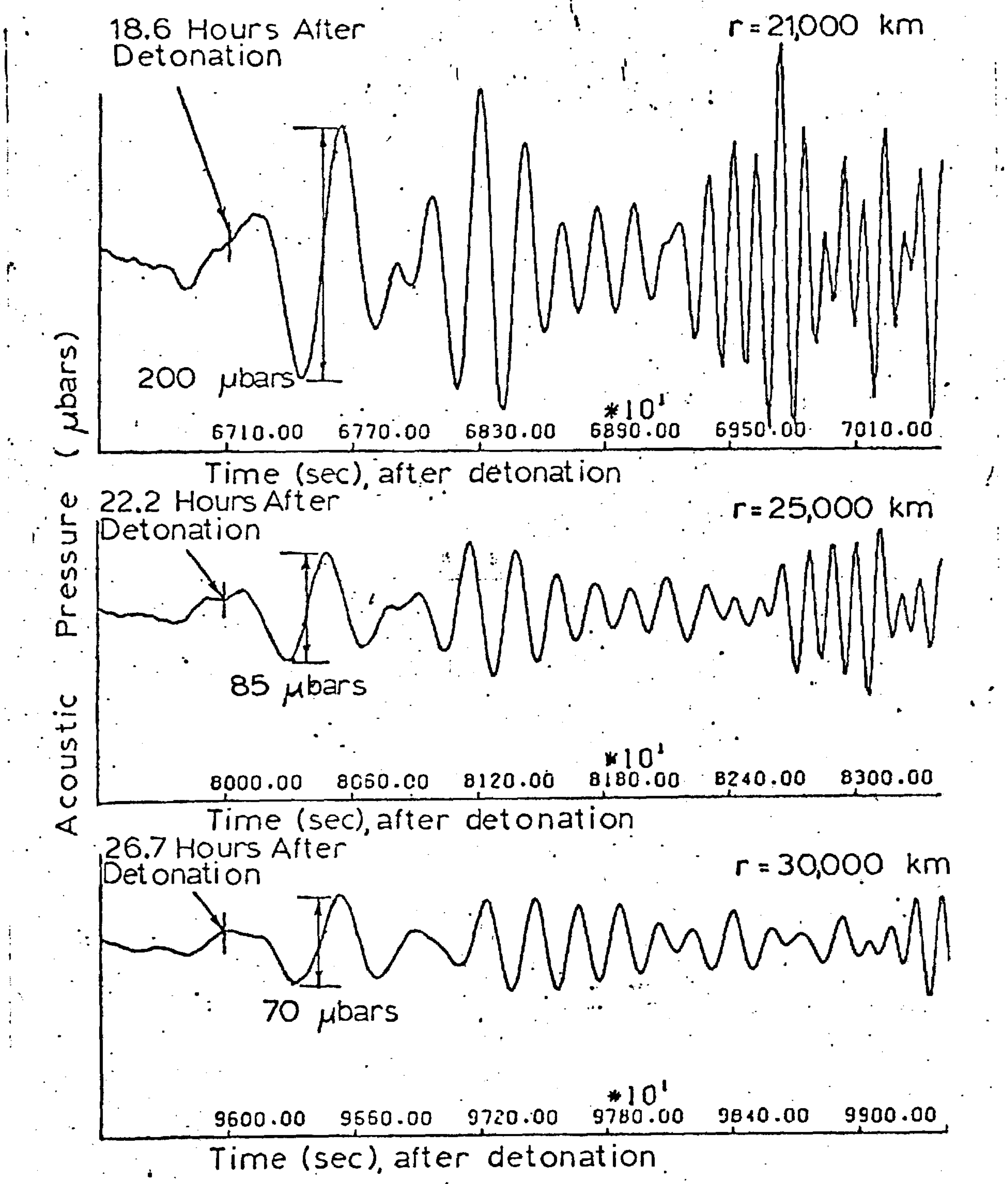

Figure 24. Theoretical pressure waveform for a pulse propagating away from the antipode. Decrease of amplitude and increased frequency dispersion occurs with increasing great circle distance r. The source is a 10 megaton nuclear explosion in a standard atmosphere without winds.

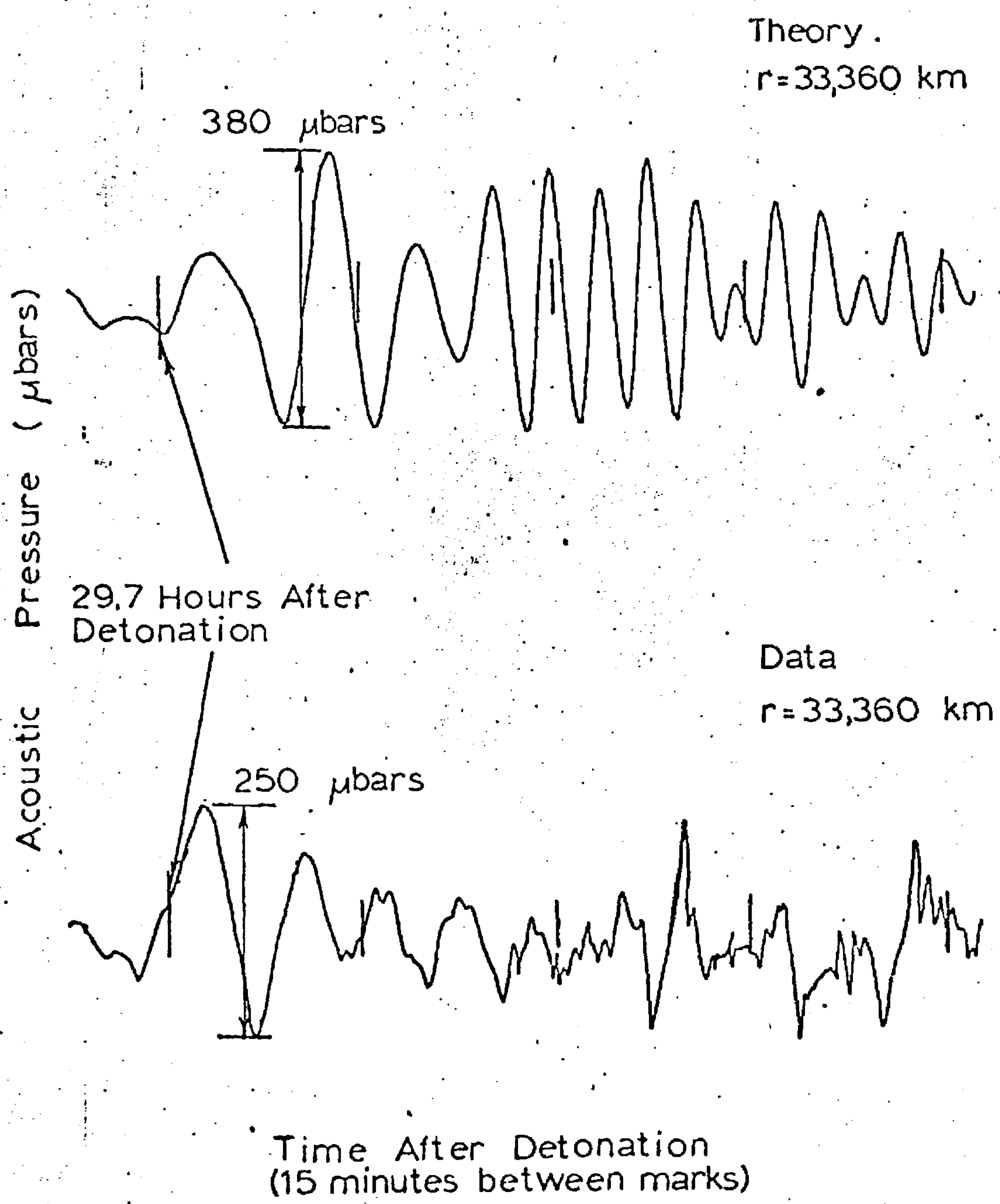

Figure 25. A comparison of theoretical and observed antipodal (A_2) arrivals for pressure wave recorded in suburban New York following the detonation of a 58 megaton yield nuclear device in Novaya Zemlya USSR on 30 October 1961. Note that the amplitude scales for the two records are not the same. Observed waveform taken from Donn and Shaw, Revs. of Geophys. 5, 53-82 (1967).

Chapter VI

CONCLUSIONS AND RECOMMENDATIONS

4.1 REMARKS CONCERNING INFRASONIC WAVEFORMS

The new version of INFRASONIC WAVEFORMS contained in this report (Appendix A) allows for the computation of waveforms which have propagated past the antipode and for the computation of waveforms including leaking modes. Our remarks here concentrate on the latter modification.

If one chooses a model atmosphere in which the sound speed is constant above some arbitrary large height, it is inevitable that the GR_0 and GR_1 modes should have lower cutoff frequencies and be leaking below that altitude. Beyond a certain point, one would expect that the computations should be independent of this choice of height, provided the analysis were carried through with some degree of exactitude. If there were a genuine sensitivity, this would indicate that these modes carry an appreciable fraction of their energies at high altitudes and this would in turn suggest that the neglect of physical dissipative mechanisms (such as viscosity and thermal conduction, Joule heating, etc.), which increase dramatically at extremely large heights for the frequencies of interest here, is not a valid approximation.

The reason we cannot take the bottom of our upper halfspace to be arbitrarily large is that some modal height-amplitudes decrease exponentially at large altitudes. This exponential decrease implies that, if one attempts to calculate the transmission matrix [R] connecting variables at the bottom of the upper halfspace to those at the ground, then the elements of [R] are going to be extremely large and the mathematical theorem that the determinant of [R] be 1, while true in principle, is not going to be satisfied for the actual numerical values computed because of the loss of significant figures. The net result is such large fluctuations in the eigenmode dispersion function due to round-off errors that it is impossible to determine its roots. This problem always arises at sufficiently high frequencies when the upper halfspace bottom is taken too high.

In Chapter III, a simple expedient for circumventing this difficulty is implicitly described. One uses one atmosphere for low frequencies, another atmosphere for higher frequencies. The atmosphere for the higher frequency calculations has its halfspace beginning at, say, 125 km altitude while the atmosphere for the lower frequency calculations has its upper halfspace beginning at, say, 225 km. Given the premise that, for the GR_0 and GR_1 modes (which appear to be the only modes for which we have problems at low frequencies), the energy is ducted below 125 km, the temperature above 225 km can be made as large as one desires without changing the answers. Thus one simply chooses this temperature to be so large that the lower cutoff frequencies for the two modes are, for all practical purposes, zero. In this manner one can construct the phase velocities and source free amplitude functions versus frequency for these modes down to arbitrarily small frequencies.

Another question is whether or not the k_I (imaginary part of wavenumber) for the leaking modes are physically meaningful. They obviously would be meaningful were the actual atmosphere terminated by an upper halfspace and were there no physical dissipation mechanisms. However, the actual atmosphere is more complicated than this model and one has to accept the fact that (1) an approximate atmosphere is going to give rise to approximate answers and (2) that the values of the k_I are going to depend on the choice of the bottom height of the upper halfspace. Thus the k_I are really somewhat arbitrary. Fortunately, the values of the k_I so derived are very small, at least for the example we have numerically carried out, that the computed waveforms are almost the same as if the k_I were identically zero.

With the above remarks in mind, it is recommended that the calculations of the k_I for the GR_0 and GR_1 modes below cutoff <u>not be carried out</u> in the synthesizing of waveforms. Rather, one should either set the k_I for frequencies below cutoff as given in our numerical example or to 2×10^{-10} (i.e., for all intents and purposes, zero). The reason the k_I

should not be set identically to zero is that the computer program uses the nonzeroness of k_I as a flag to decide whether to look for an input value of AMP (source free amplitude) or to compute the number internally (it can't do this at frequencies below cutoff and will consequently return AMP = 0). While this may seem a rather simple thing to do, considering the elaborate mathematical theory developed[2] in Scientific Report No. 1, the analysis and computations which preceded the formulations of this recommendation were necessary, if only to establish that the procedure has some rigorous mathematical basis.

In any event, it is evident that one must and should include contributions from the frequencies below the nominal low frequency cutoff (determined by the upper halfspace) if one is to adequately synthesize the initial portions of waveforms. The present report shows how this may be done. The procedure, although requiring several (three, in general) runs of the program rather than just one run to accomplish this, is relatively straightforward. It is obviously feasible to automate this so that only one run is necessary, but the time limitations of the present study precluded our doing so.

6.2 DISCREPANCY WITH LAMB EDGE MODE THEORY

It was hoped that the inclusion of leaking modes into the multimode synthesis would eliminate the discrepancy between the numerical predictions of the Lamb edge mode theory and the multi-mode theory. It is evident, however, from Fig. 16 in the present report that this was not turned out to be the case. The cause of the discrepancy has not been resolved and time limitations precluded its resolution. There is always the possibility that either program may have a mistake. However, barring this, it should be pointed out that the modified multimode theory should be the more nearly correct. The Lamb edge mode theory[15] contains a number of approximations which the multi-mode theory does not contain. Consequently, it is recommended that the multi-mode model as modified here be used in preference to the Lamb edge mode model.

The relative simplicity of the edge mode model still retains an intrinsic appeal and, consequently, it is recommended that some future effort be expended in revising the model (possibly by including higher order terms in the dispersion relation) such that the discrepancy is resolved.

6.3 GUIDED MODES AT HIGHER FREQUENCIES

The procedure outlined in Chapter IV for using a modified W.K.B.J. approximation to order the modes and to compute modal parameter at high frequencies looks eminently feasible and is recommended for inclusion into the multi-mode synthesis program INFRASONIC WAVEFORMS. Although, again, time limitations precluded this, we regret not having done so in the present study. The motivation for doing this, however, is not as strong as for the low frequency modifications because the commonly available data in the open literature is markedly poor as regards high frequency arrivals. If and when such a modification is carried out, one should ideally have appropriate data with which to compare the numerical predictions.

Another problem is that there is some question as to whether a multmodal theory with a finite number of modes (even when judiciously selected) can ever adequately synthesize higher frequency arrivals. In many respects, we believe that an appropriate modification of a geometrical acoustics theory would be preferable.

6.4 GEOMETRICAL ACOUSTICS MODEL

The geometrical acoustics model described[3] in Scientific Report No. 2, although still incompletely developed, appears to hold considerable promise for the understanding of higher frequency arrivals. We know now how to take the edge mode into account and how to handle the problem of caustics. Problems of aretes, lacunae, and wave diffusion from channel to channel still remain, but we believe these can be overcome with only a modest amount of additional theoretical effort.

The ultimate objective of the analysis should be to develop the simplest possible theory sufficient to explain and interpret available data. In this respect, we would suggest that both the multi-mode and geometrical acoustical models. While perhaps more elaborate than should be ideally required, could be used as research tools to conduct numerical experiments which test simpler models. The statistical models developed by p. Smith[25] for underwater acoustics appear especially attractive in this regard and we believe that one should be able to test his models using the geometrical acoustics model described in Scientific Report No. 2. Also, the types of numerical experiments envisioned should provide the inspiration and support required to refine Smith's models such that they be capable of a more nearly precise description of infrasonic waveforms.

REFERENCES

1. A. D. Pierce and J. W. Posey, "Theoretical Prediction of Acoustic-Gravity Waveforms generated by Large Explosions in the Atmosphere", Report No. AFCRL-70-0134, Air Force Cambridge Research Laboratories, Hanscom AFB, Mass. 01731 (30 April 1970).

2. A. D. Pierce, W. A. Kinney, and C. Y. Kapper, "Atmosphere Acoustic Gravity Modes at Frequencies near and below Low Frequency Cutoff Imposed by Upper Boundary Conditions", Report No. AFCRL-TR-75-0639, Air Force Cambridge Research Laboratories, Hanscom AFB, Mass. 01731 (1 March 1976).

3. A. D. Pierce and W. A. Kinney, "Geometrical Acoustics Techniques in Far Field Infrasonic Waveform Syntheses", Report No. AFCRL-TR-76-XXXX, Air Force Cambridge Research Laboratories, Hanscom AFB, Mass. 01731 (7 March 1976).

4. A. D. Pierce, C. A. Moo, and J. W. Posey, "Generation and Propagation of Infrasonic Waves", Report No. AFCRL-TR-73-0135, Air Force Cambridge Research Laboratories, Hanscom AFB, Mass. 01731 (30 April 1973).

5. J. E. Thomas, A. D. Pierce, E. A. Flinn, and L. B. Craine, "Bibliography on Infrasonic Waves", Geophys. J. Roy. Astron. Soc. 26, 399-426 (1971).

6. J. W. S. Rayleigh, "On the Vibrations of an Atmosphere", Phil. Mag. 29, 173-180 (1890).

7. H. Lamb, "On the Theory of Waves Propagated Vertically in the Atmosphere", Proc. London Math. Soc. 1, 122-141 (1908); "On Atmospheric Oscillations", Proc. Roy. Soc. London A84, 551-572 (1920).

8. G. I. Taylor "Waves and Tides in the Atmosphere", Proc. Roy. Soc. London A126, 169-183 (1929); "The Oscillations of the Atmosphere", Proc. Roy. Soc. London A156, 318-326 (1936).

9. C. L. Pekeris, "The Propagation of a Pulse in the Atmosphere", Proc. Roy. Soc. London A171, 434-449 (1939); "The Propagation of a Pulse in the Atmosphere, Part II", Phys. Rev. 73, 145-154 (1948).

10. R. S. Scoren, "The Dispersion of a Pressure Pulse in the Atmosphere", Proc. Roy. Soc. London A201, 137-157 (1950).

11. G. J. Symond, The Eruption of Krakatoa and Subsequent Phenomena (Trubner and Co., London, 1888).

12. F. J. W. Whipple, "On Phenomena Related to the Great Siberian Meteor", Quart. J. Roy. Meteor. Soc. 60, 505-513 (1934).

13. A. D. Pierce and C. A. Moo, "Theoretical Study of the Propagation of Infrasonic Waves in the Atmosphere", Report No. AFCRL-67-0172, Air Force Cambridge Research Laboratories, Hanscom AFB, Mass. 01731 (1967).

14. D. G. Harkrider, "Theoretical and Observed Acoustic-Gravity Waves from Explosive Sources in the Atmosphere", J. Geophys. Res. 69, 5295-5321 (1964).

15. A. D. Pierce and J. W. Posey, "Theory of the Excitation and Propagation of Lamb's Atmospheric Edge Mode from Nuclear Explosions", Geophys. J. Roy. Astron. Soc. 26, 341-368 (1971).

16. J. W. Posey, "Application of Lamb Edge Mode Theory in the Analysis of Explosively Generated Infrasound", Ph.D. Thesis, Dept. of Mech. Engrg., Mass. Inst. of Tech. (August, 1971).

17. N. A. Haskell, "Asymptotic Approximation for the Normal Modes in Sound Channel Wave Propagation", J. Appl. Phys. 22, 157-168 (1951).

18. F. Carlini, Ricerche sulla convergenza della serie che serva alla soluzione del problema di Keplero, Milan (1917).

19. G. Green, "On the Motion of Waves in a Variable Canal of Small Depth and Width", Trans. Camb. Phil. Soc. 6, 457-462 (1837).

20. C. Eckart, "Internal Waves in the Ocean", Phys. of Fluids 4, 791-799 (1961).

21. P. M. Morse and H. Feshbach, "Perturbation Methods for Scattering and Diffraction", Sec. 9.3 in Methods of Theoretical Physics, Vol. II (McGraw-Hill Book Co., New York, 1953) pp. 1092-1106.

22. A. D. Pierce, "Guided Infrasonic Modes in a Temperature and Wind-Stratified Atmosphere", J. Acoust. Soc. Amer. 41, 597-611 (1967).

23. W. L. Donn and D. M. Shaw, "Exploring the Atmosphere with Nuclear Explosions", Rev. of Geophys. 5, 53-82 (1967).

24. J. N. Brune, J. E. Nafe, and L. E. Alsop, "The Polar Phase Shift of Surface Waves on a Sphere", Bull. Seism. Soc. Amer. 51, 247-257 (1961).

25. P. W. Smith, "The Average Impulse Responses of a Shallow-Water Channel", J. Acoust. Soc. Amer. 50, 332-336 (1971); "Averaged Sound Transmission in Range-Dependent Channels", J. Acoust. Soc. Amer. 55, 1197-1204 (1974).

APPENDIX A

SOURCE DECK LISTING OF THE PRESENT VERSION OF INFRASONIC WAVEFORMS

This supercedes the source deck listing originally given by Pierce and Posey in AFCRL-70-0134. Changes incorporated include those described by Pierce, Moo, and Posey in AFCRL-TR-73-0135 and those described in the present report.

APPENDIX B

SOURCE DECK LISTING OF
AN ALTERNATE VERSION OF SUBROUTINE TABLE

This version of SUBROUTINE TABLE is used, as described in Chapter III of the present report, to tabulate listings of R_{11} and R_{12} versus angular frequency OMEGA and phase velocity VPHSE which are used in calculating the parameter α and β for the GR_0 and GR_1 modes which in turn are used in calculating the values of the imaginary component k_I of horizontal wave-number for these modes at frequencies below cutoff. This version of TABLE should replace the version in Appendix A when a tabulation of R_{11} and R_{12} is desired.

```
      SUBROUTINE TABLE(OM1,OM2,V1,V2,NOM,NVP,THETK,OM,V,INMODE,NOPT)
C     TABLE (SUBROUTINE)                        7/19/68   LAST CARD IN DECK IS NO.
C
C
C                ----ABSTRACT----
C
C TITLE - TABLE
C        GENERATION OF SUSPICIONLESS TABLE OF NORMAL MODE DISPERSION
C        FUNCTION SIGNS
C
C               TABLE CALLS SUBROUTINE MPOUT TO CONSTRUCT THE MATRIX OF
C               NORMAL MODE DISPERSION FUNCTION SIGNS INMODE (STORED IN
C               VECTOR FORM COLUMN AFTER COLUMN) FOR REGION IN FREQUENCY-
C               PHASE VELOCITY PLANE (OM1.LE.OMEGA.LE.OM2.AND.V1.LE.VP.LE
C               .V2).  SUBROUTINE SUSPCT IS CALLED TO EVALUATE THE SUSPI-
C               CION INDEX ,ISUS, OF EACH INTERIOR ELEMENT IN THE MATRIX
C               SCANNING FROM LEFT TO RIGHT, TOP TO BOTTOM. IF ISUS .NE.
C               0 , INMODE IS ALTERED AS FOLLOWS.
C                   ISUS=1 ROW ADDED ABOVE SUSPICIOUS ELEMENT AND COLUMN
C                          ADDED TO ITS LEFT
C                       =2 COLUMN ADDED TO RIGHT OF SUSPICIOUS ELEMENT
C                          AND ROW ADDED ABOVE IT
C                       =3 ROW ADDED BELOW SUSPICIOUS ELEMENT AND COLUMN
C                          ADDED TO ITS RIGHT
C                       =4 COLUMN ADDED TO LEFT OF SUSPICIOUS ELEMENT
C                          AND ROW ADDED BELOW IT
C               HOWEVER, NEITHER THE NUMBER OF ROWS NVP NOR THE NUMBER OF
C               COLUMNS NOM WILL BE INCREASED BEYOND 100.  IF ISUS CALLS
C               FOR AN ADDITIONAL ROW WHEN NVP = 100 , THE MESSAGE
C               (NVP = 100            N = XX      M = XX) WILL BE PRINTED.
C               N IS ROW NO. OF SUSPICIOUS ELEMENT.  M IS COLUMN NO.  IF
C               ISUS CALLS FOR ADDITION OF A COLUMN WHEN NOM = 100, THE
C               MESSAGE (NOM = 100            N = XX      M = XX) IS PRINTED.
C               WHEN INMODE HAS BEEN EXPANDED SCANNING IS RESUMED AT THE
C               ELEMENT IN NEW MATRIX WITH SAME ROW AND COLUMN NOS. AS
C               THOSE OF SUSPICIOUS ELEMENT IN OLD MATRIX.  IF NOPT IS
C               POSITIVE INMODE WILL BE PRINTED AS IT IS RETURNED FROM
C               MPOUT AND IN ITS FINAL FORM.
C
C LANGUAGE    - FORTRAN IV (360, REFERENCE MANUAL - C28-6515-4)
C
C AUTHOR      - J.H.POSEY, M.I.T., JUNE,1968
C
C
C                    ----USAGE----
C
C     SUBROUTINES MPOUT,SUSPCT,LNGTHN,WIDEN,NMDFN ARE CALLED IN TABLE.
C
C FORTRAN USAGE
C     CALL TABLE(OM1,OM2,V1,V2,NOM,NVP,THETK,OM,V,INMODE,NOPT)
C
C INPUTS
C
C    OM1        MINIMUM VALUE OF FREQUENCY TO BE CONSIDERED.
C      R*4
C    OM2        MAXIMUM VALUE OF FREQUENY TO BE CONSIDERED
C      R*4
```

```
C     V1          MINIMUM VALUE OF PHASE VELOCITY TO BE CONSIDERED
C       R*4
C     V2          MAXIMUM VALUE OF PHASE VELOCITY TO BE CONSIDERED
C       R*4
C     NOM         INITIAL NO. OF FREQUENCIES TO BE CONSIDERED
C       I*4
C     NVP         INITIAL NO. OF PHASE VELOCITIES TO BE CONSIDERED
C       I*4
C     THETK       PHASE VELOCITY DIRECTION (RADIANS)
C       R*4
C     NOPT        PRINT OUT OPTION.  IF NOPT = -1, NO PRINT.  IF NOPT = 1,
C       I*4       INMODE IS PRINTED IN ITS INITIAL FORM (GENERATED BY MPOUT)
C                 AND IN ITS FINAL FORM.
C
C OUTPUTS
C
C     NOM         TOTAL NO. OF FREQUENCIES CONSIDERED
C       I*4
C     NVP         TOTAL NO. OF PHASE VELOCITIES CONSIDERED
C       I*4
C     OM          VECTOR WHOSE ELEMENTS ARE THE VALUES OF ANGULAR FREQUENCY
C       R*4(D)    CORRESPONDING TO THE COLUMNS OF THE INMODE MATRIX
C
C     V           VECTOR WHOSE ELEMENTS ARE THE VALUES OF PHASE VELOCITY
C       R*4(D)    CORRESPONDING TO THE ROWS OF THE INMODE MATRIX
C
C     INMODE      EACH ELEMENT OF THIS MATRIX CORRESPONDS TO A POINT IN THE
C       I*4(D)    FREQUENCY (OM) - PHASE VELOCITY (V) PLANE.  IF THE NORMAL
C                 MODE DISPERSION FUNCTION (FPP) IS POSITIVE AT THAT POINT,
C                 THE ELEMENT IS +1, IF FPP IS NEGATIVE, THE ELEMENT IS -1,
C                 IF FPP DOES NOT EXIST, THE ELEMENT IS 5.  INMODE HAS NVP
C                 ROWS AND NOM COLUMNS.  MATRIX IS STORED AS A VECTOR,
C                 COLUMN AFTER COLUMN.
C
C
C                     ----EXAMPLE----
C
C LET INMODE = -1,5,5,5,1,-1,-1,-1,1,1,-1,-1,1,1,1,1
C    WITH NOM = NVP = 4
C    AND OM = 1.0,1.5,2.0,2.5           THETK = 3.14159
C        V = 1.0,2.0,3.0,4.0
C (VALUES NOT CORRECT, FOR ILLUSTRATION ONLY)
C
C THEN THE TABLE WILL BE PRINTED AS FOLLOWS.
C
C VPHASE        NORMAL MODE DISPERSION FUNCTION SIGN
C  1.00000    -+++
C  2.00000    X-++
C  3.00000    X--+
C  4.00000    X--+
C
C       OMEGA 1234
C             PHASE VELOCITY DIRECTION IS   90.000DEGREES
C
C OMEGA =
C    0.10000E 01   0.15000E 01   0.20000E 01   0.25000E 01
C
```

```
C
C                    ----PROGRAM FOLLOWS BELOW----
C
C
C
      DIMENSION OM(100),V(100),INMODE(10000),DORN(100),KORN(100)
      DIMENSION EPP(2,2)
      COMMON IMAX,CI(100),VXI(100),VYI(100),HI(100)
C
C MPOUT IS CALLED TO PRODUCE INMODE MATRIX AND OM AND V VECTORS.
      CALL MPOUT(OM1,OM2,V1,V2,NOM,NVP,INMODE,OM,V,THETK)
C
C IFLAG = 1 INDICATES FIRST TIME THROUGH WRITE PROCEDURE
      IFLAG = 1
C
C INMODE IS PRINTED IF NOPT IS POSITIVE
      IF (NOPT.GE.0) GO TO 123
    5 IFLAG = 0
      NOPER=0
C NOPER IS THE NUMBER OF EXPANSION OPERATIONS PERFORMED IN THE PRESENT
C SCAN OF THE MATRIX.  THUS, NOPER IS THE NUMBER OF SUSPICIOUS POINTS
C FOUND IN THE PRESENT SCAN.
C
C BEGIN SCANNING OF INTERIOR ELEMENTS OF INMODE IN UPPER LEFT CORNER
      N = 2
      M = 2
   10 CALL SUSPCT(N,M,NVP,INMODE,ISUS)
C
C POINT (N,M) IS SUSPICIOUS IF ISUS.NE.0
      IF(ISUS.NE.0) GO TO 60
C
C CHECK FOR END OF ROW
   20 IF (M.LT.(NOM-1)) GO TO 30
C
C CHECK FOR LAST ROW
      IF (N.LT.(NVP-1)) GO TO 40
      GO TO 121
C
C MOVE ONE COLUMN TO RIGHT
   30 M = M+1
      GO TO 10
C
C ADVANCE ONE ROW AND START AT COLUMN TWO
   40 N = N+1
      M = 2
      GO TO 10
C
C CHECK FOR MAXIMUM VALUE OF NVP
   60 IF(NVP.LT.100) GO TO 62
   61 FORMAT (24H NVP = 100            N =,I3,8H      M =,I3)
      WRITE (6,61) N,M
      GO TO 20
   62 IF(NOM .LT. 100) GO TO 70
   63 FORMAT(24HNOM = 100              N=,I3, 8H      M=,I3)
   64 WRITE(6,63) N,M
      GO TO 20
   70 IF(ISUS .NE. 1) GO TO 75
```

```
C
C  ADD ROW ABOVE SUSPICIOUS POINT
      N1=N-1
C
C  ADD A COLUMN TO LEFT OF SUSPICIOUS POINT
      M1=M-1
      GO TO 100
   75 IF(ISUS .NE. 2) GO TO 80
C
C  ADD A COLUMN TO RIGHT OF SUSPICIOUS POINT
      M1=M
C
C  ADD ROW ABOVE SUSPICIOUS POINT
      N1=N-1
      GO TO 100
   80 IF(ISUS .NE. 3) GO TO 85
C
C  ADD A COLUMN TO RIGHT OF SUSPICIOUS POINT
      M1=M
C
C  ADD ROW BELOW SUSPICIOUS POINT
      N1=N
      GO TO 100
C
C  ADD ROW BELOW SUSPICIOUS POINT
   85 N1=N
C
C  ADD A COLUMN TO LEFT OF SUSPICIOUS POINT
      M1=M-1
  100 CONTINUE
      CALL LNGTHN(OM,V,INMODE,NOM,NVF,NVPP,N1,1,THETK)
      CALL WIDEN(OM,V,INMODE,NOM,NOMP,NVPP,M1,1,THETK)
      NVP=NVPP
      NOM=NOMP
      NOPER=NOPER+1
      GO TO 10
  121 CONTINUE
      IF(NOPER .GT. 0 .AND. NVP .LT. 100 .AND. NOM .LT. 100) GO TO 5
C
C DO NOT PRINT INMODE IF NOPT IS NEGATIVE
      IF(NOPT .LT. 0) RETURN
C
C LABELING
  122 FORMAT (6H1VPHSE,6X,36HNORMAL MODE DISPERSION FUNCTION SIGN/)
  123 WRITE (6,122)
      DO 133 I=1,NVP
      DO 128 J=1,NOM
      J88=(J-1)*NVP+I
      J89=INMODE(J88)-1
      IF (J89) 126,125,124
  124 CONTINUE
C
C IF INMODE = 5, DORN = 1HX
      DATA O1/1HX/
      DORN(J) = O1
      GO TO 127
  125 CONTINUE
```

```
C
C IF INMODE = 1, DORN = 1H+
      DATA Q2/1H+/
      DORN(J) = Q2
      GO TO 127
  126 CONTINUE
C
C IF INMODE = -1, DORN = 1H-
      DATA Q3/1H-/
      DORN(J) = Q3
  127 CONTINUE
  128 CONTINUE
C
C PRINT ROW I OF TABLE
      WRITE (6,130)V(I),(DORN(J), J=1,NOM)
  130 FORMAT(1H ,F8.5,3X,100A1)
  133 CONTINUE.
      J10 = 10
      DO 150 J=1,NOM
C
C NUMBER COLUMNS
  150 KORN(J) = MOD(J,J10)
      WRITE (6,213) (KORN(J), J=1,NOM)
  213 FORMAT (6HOOMEGA,6X,100I1)
C
C CONVERT THETK FROM RADIANS TO DEGREES
      X = THETK*180/3.14159
      WRITE (6,413) X
  413 FORMAT (1H ,11X,27HPHASE VELOCITY DIRECTION IS,F9.3,
     1    8HDEGREES )
      WRITE (6,513)
  513 FORMAT ( 8HOOMEGA =)
C
C LIST VALUES OF OMEGA WHICH CORRESPOND TO COLUMNS OF TABLE
      WRITE (6,613) (OM(I),I=1,NOM)
  613 FORMAT ( 1H ,5E14.5)
C
C IF SUSPICION ELIMINATION HAS NOT BEEN PERFORMED, BEGIN IT AT THIS TIME
      IF(IFLAG.EQ.1) GO TO 5
      DOLVP=(V2-V1)/(NVP-1)
      OMEGK=OM1
      DELOM=(OM2-OM1)/(NOM-1)
      DO 988 IAA=1,NOM
      WRITE (6,933) OMEGK
 933  FORMAT (1H ,3X,6HOMEGA=,E14.5)
      DO 977 JAA=1,NVP
      VE=V1+(JAA-1)*DOLVP
      AKX=OMEGK/VE
      AKY=0.0
      CALL RRRR(OMEGK,AKX,AKY,RPP,KY)
      WRITE (6,944) VE,RPP(1,1),RPP(1,2)
 944  FORMAT (1H ,E12.5,6X,E12.5,3X,E12.5)
 977  CONTINUE
      OMEGK=OMEGK+DELOM
 988  CONTINUE
      RETURN
      END
```